THE UNIVERSITY OF ALBERTA

Studies of Electrostatic, Salt, and Metal-Binding Interactions in the α-Helical Coiled-Coil: a Model Protein System

By

Wayne David Kohn ©

A THESIS
SUBMITTED TO THE FACULTY OF GRADUATE STUDIES AND RESEARCH IN
PARTIAL FULFILLMENT OF THE REQUIREMENTS FOR THE DEGREE OF
DOCTOR OF PHILOSOPHY

DEPARTMENT OF BIOCHEMISTRY

EDMONTON, ALBERTA

FALL 1998

National Library
of Canada

Acquisitions and
Bibliographic Services

395 Wellington Street
Ottawa ON K1A 0N4
Canada

Bibliothèque nationale
du Canada

Acquisitions et
services bibliographiques

395, rue Wellington
Ottawa ON K1A 0N4
Canada

Your file Votre référence

Our file Notre référence

The author has granted a non-exclusive licence allowing the National Library of Canada to reproduce, loan, distribute or sell copies of this thesis in microform, paper or electronic formats.

The author retains ownership of the copyright in this thesis. Neither the thesis nor substantial extracts from it may be printed or otherwise reproduced without the author's permission.

L'auteur a accordé une licence non exclusive permettant à la Bibliothèque nationale du Canada de reproduire, prêter, distribuer ou vendre des copies de cette thèse sous la forme de microfiche/film, de reproduction sur papier ou sur format électronique.

L'auteur conserve la propriété du droit d'auteur qui protège cette thèse. Ni la thèse ni des extraits substantiels de celle-ci ne doivent être imprimés ou autrement reproduits sans son autorisation.

0-612-34790-7

Canada

THE UNIVERSITY OF ALBERTA

LIBRARY RELEASE FORM

NAME OF AUTHOR: Wayne David Kohn

TITLE OF THESIS: Studies of Electrostatic, Salt, and Metal-Binding Interactions in the α-Helical Coiled-Coil: a Model Protein System

DEGREE: Doctor of Philosophy

YEAR THIS DEGREE GRANTED: 1998

Permission is hereby granted to the University of Alberta Library to reproduce single copies of this thesis and to lend or sell such copies for private, scholarly, or scientific research purposes only.

The author reserves all other publication and other rights in association with the copyright in the thesis, and except as hereinbefore provided neither the thesis nor any substantial portion thereof may be printed or otherwise reproduced in any material form whatever without the author's prior written permission.

Wayne Kohn

PERMANENT ADDRESS:
4620 - 51 Ave.
Vermilion, Alberta, Canada
T9X 1S1

DATE: August 7 1998

THE UNIVERSITY OF ALBERTA

FACULTY OF GRADUATE STUDIES AND RESEARCH

The undersigned certify that they have read, and recommend to the Faculty of Graduate Studies and Research for acceptance, a thesis entitled Studies of Electrostatic, Salt, and Metal-Binding Interactions in the α-Helical Coiled-Coil: a Model Protein System submitted by Wayne David Kohn in partial fulfillment of the requirements for the degree of Doctor of Philosophy.

Dr. Robert S. Hodges
(Supervisor)

Brian D Sykes
Dr. Brian D. Sykes

Charles F B Holmes
Dr. Charles F. B. Holmes

David Bundle
Dr. David R. Bundle

Dr. Tomi K. Sawyer
(External Examiner)

Date: July 24, 1998

ABSTRACT

The α-helical coiled-coil is a common assembly motif found in a diverse array of structural and regulatory proteins in nature. Coiled-coils are comprised of two, three, or four right-handed amphipathic α-helices, which associate in aqueous solution through burial of their hydrophobic faces in the subunit interface. Due to its structural simplicity, the coiled-coil has proven to be a very useful model protein system for studying the fundamentals of noncovalent interactions in protein folding. Information from these studies will help guide the *de novo* design of synthetic proteins with improved or novel properties and activities for industrial or medical applications, and contribute to a better understanding of coiled-coil containing proteins in nature.

Coiled-coils are characterized by a seven residue (heptad) sequence repeat commonly denoted $(\mathbf{abcdefg})_n$ where positions **a** and **d** are primarily occupied by hydrophobic amino acids that are sequestered in the interface. The **e** and **g** positions flank the hydrophobic face formed by the **a** and **d** positions and can also participate in interhelical interactions. The studies in this thesis are aimed at providing a better characterization of interhelical interactions between charged residues at the **e** and **g** positions.

Synthetic 35-residue peptides, based on the heptad sequence $Q_\mathbf{g}V_\mathbf{a}G_\mathbf{b}A_\mathbf{c}L_\mathbf{d}Q_\mathbf{e}K_\mathbf{f}$ were used for studies of the effects on folding and stability of charged residue substitutions at the **e** and **g** positions. A number of important results which highlight this work are summarized here. First, it was demonstrated that the interhelical interactions between negatively charged Glu residues at positions **e** and **g** occur preferentially in the **g-e'** (i to i'+5) rather than the **e-g'** (i to i'+2) orientation (where the prime indicates a position on the other helix). These **g-e'** interactions were found to be destabilizing by about 0.5 kcal/mol. The effects of an increasing number of these Glu-Glu repulsions on coiled-coil folding and stability were found to be approximately additive. Both specific charge-charge repulsions and general interhelical charge repulsions play roles in the destabilization of a coiled-coil, but the relative roles of each may vary. End effects were also found to be important, as

charged residues could interact with the helix macrodipole to significantly affect coiled-coil stability.

The effect of salts on the interhelical electrostatics (both attractions and repulsions) was probed. Monovalent salt was inefficient at screening the interhelical **g-e'** interactions in the model coiled-coil, which may be a result of the synergy between **g-e'** electrostatics and the hydrophobic packing interactions of the side chains with the hydrophobic core of the coiled-coil. An observed orientation preference for interhelical Lys-Glu interhelical ion pairs was also consistent with the hypothesis that a synergy exists between packing and **g-e'** interactions. Further, **g-e'** interactions were found to influence the oligomerization properties, with Lys-Glu interactions in either orientation promoting trimer formation and Gln-Gln interactions promoting dimer formation.

A salt containing a trivalent metal ion, $LaCl_3$, affected the stability of coiled-coils containing interhelical attractions and repulsions, likely due to binding of La^{3+} ions to negatively charged Glu residues on the peptide. The stabilization of peptides containing interhelical Glu-Glu repulsions by $LaCl_3$ was predicted to be via 'bridging' of the repelling Glu residues by the La^{3+} ions. This hypothesis was supported by subsequent experiments comparing the effects of $LaCl_3$ on the stabilities of coiled-coils containing potential i to i'+5 and i to i'+2 Glu-Glu interactions. These studies led to the design of a coiled-coil in which La^{3+} binding at specific sites was used as a reversible control on coiled-coil folding. A higher affinity metal-chelating residue γ-carboxyglutamic acid (Gla) was incorporated in the successful design.

In summary, these experiments represent a step towards the design of environmentally sensitive proteins in which the folding, stability and function can be controlled by buffer conditions including pH, salt conditions and specific metal binding.

Dedicated to my parents

ACKNOWLEDGEMENTS

I would like to thank the following people for their contributions to the success of my research over the course of my graduate studies.

First, I thank my supervisor, Bob Hodges, who has been an inspiring force in my intellectual and scientific development as a PhD student. He has allowed me the chance to work in the exciting field of *de novo* design in a first-class, well-equipped, and well-funded laboratory, which has greatly aided my research success and productivity. His wise advice and genuine concern for the progress of those in his lab is much appreciated.

I also thank Drs. Cyril Kay and Brian Sykes for their kind advice and the use of equipment in their laboratories.

I wish to thank all the graduate students, post-doctoral fellows, research associates, and technical staff associated with the Hodges group past and present. Oscar Monera helped me in my early days of coiled-coil research. Pierre Lavigne has offered much advice and help with learning about computer modelling. Mike Houston has also offered some very good advice on peptide design ideas. I thank Colin Mant and Paul Cachia for editing of manuscripts and technical advice. I also thank other members of both the PENCE and MRC labs including Brian Tripet, Stanley Kwok, Jennifer Litowski, Bruce Yu, Kurt Wagschal, Rob Hodgins, Les Kondejewski, Heman Chao, and Jenny Van Eyk. Everyone has helped make this an enjoyable and stimulating atmosphere in which to work.

I also want to thank a lot of people whose technical assistance contributed greatly to my research. I thank Paul Semchuk, Len Daniels, Iain Wilson, Jason Moses, Cindy Gannon, and Marc Genest in the PENCE peptide chemistry lab; Les Hicks for ultracentrifugation; Bob Luty and Kim Oikawa for CD spectroscopy; Bruce Lix and Linda Golden for NMR spectroscopy; Jack Moore, Terri Keown and others at the Alberta Peptide Institute for amino acid analysis and other assistance; and Lorne Burke for help with various things including HPLC, computer problems, making figures and slides, etc.

A number of organizations contributed financially to this work. The research has been supported by the NCE program of the Federal Government through the Protein Engineering Network of Centres of Excellence and by the Medical Research Council through the MRC Group in Protein Structure and Function. I also thank the Natural Sciences and Engineering Research Council and the Izaak Walton Killam Memorial Fund for graduate student fellowships and the American Peptide Society for travel grants to two APS symposia.

Lastly, I thank my family, particularly my parents, for their support and encouragement throughout this endeavor and my beautiful wife Teresa for her love and support.

TABLE OF CONTENTS

Page

Chapter I. Introduction

1. General introduction to protein folding........................ 1
2. Noncovalent interactions in protein folding........................ 3
    i. Hydrophobic interactions........................ 4
    ii. Polar (hydrogen bond) interactions........................ 6
    iii. Electrostatic interactions........................ 7
3. Effects of additives on protein stability........................ 12
    A. Salt effects on proteins........................ 12
        i. Dielectric effects........................ 12
        ii. ion binding........................ 13
        iii. effects of salt on water structure/properties........................ 14
    B. Other additives........................ 15
4. Model protein systems for studying protein folding........................ 17
5. α-helical coiled-coils........................ 18
6. Details of coiled-coil structure........................ 20
    i. hydrophobic core........................ 20
    ii. **e** and **g** positions........................ 22
    iii. **b**, **c**, and **f** positions........................ 24
    iv. secondary structural propensities........................ 24
    v. supercoiling........................ 25
    vi. X-ray and NMR structural data........................ 25
7. Questions dealt with and aims of this investigation........................ 26

Chapter II. Materials and Methods

A. Materials........................ 34
    1. Chemicals and reagents........................ 34

B. Methods

    1. Peptide synthesis........................ 35
    2. Peptide purification........................ 44
    3. Peptide oxidation........................ 44
    4. Peptide primary structure characterization........................ 45

5. Size-exclusion chromatography ... 49
6. Sedimentation-equilibrium ultracentrifugation ... 49
7. Laser light-scattering experiments ... 52
8. Circular dichroism measurements ... 53
9. Fitting of metal titration curves ... 55
10. Proton NMR experiments ... 56
11. Calculation of free energy of unfolding from chemical denaturation ... 56
12. Computer modelling ... 59
13. Design of the model coiled-coil and peptide nomenclature ... 60

Chapter III. Elucidation of the specificity of interhelical ionic interactions between the ***e*** and ***g*** positions of a two-stranded α-helical coiled-coil: destabilization by Glu-Glu repulsions

A. Introduction ... 64
B. Results and Discussion ... 65
  a) Peptide design and nomenclature ... 65
  b) Structural characterization of the model coiled-coils ... 68
  c) Stabilities of disulfide-bridged coiled-coils at pH 7 and pH 3 ... 73
  d) Stabilities of reduced coiled-coils at pH 7 and pH 3 ... 82
  e) Reversed-phase HPLC behavior ... 84
C. Conclusions ... 88

Chapter IV. Effects of interhelical electrostatic repulsions between glutamic acid residues on the dimerization and stability of two-stranded α-helical coiled-coils

A. Introduction ... 91
B. Results and Discussion ... 92
  a) Peptide design and nomenclature ... 92
  b) Structural characterization of the model coiled-coils ... 95
    i) CD spectra ... 95
    ii) Effects of pH on coiled-coil formation ... 100
    iii) Studies of oligomerization state ... 104
  c) Denaturation studies with urea and GdnHCl ... 106
  d) Effects of GdnHCl on electrostatic interactions ... 111
  e) Effects of different chloride salts on electrostatic interactions ... 116
  f) Summary of the effects of Glu substitutions on stability ... 117

g) Effects of N-terminal Gln to Glu substitutions 119
h) General Discussion 121

Chapter V. Positional dependence of the effect of a negatively-charged Glu side chain on the stability of an α-helical coiled-coil
A. Introduction 127
B. Results and Discussion.. 129
a) Peptide design and nomenclature 129
b) Structural characterization of the model coiled-coils 131
c) Stability studies
i) Single Glu substitutions at the N terminus, C terminus and middle of the helix 131
ii) Salt effects on the stability of Glu substituted coiled-coils . . . 139
iii) Effects of Glu substitutions on coiled-coil stability at low pH 142
iv) Charge-helix dipole interactions versus side chain to main chain hydrogen bonding 145
C. Conclusions 146

Chapter VI. Salt effects on protein stability: two-stranded α-helical coiled-coils containing inter- or intrahelical ion pairs
A. Introduction 150
B. Results 151
a) Peptide design and nomenclature....................... 151
b) Structural characterization of the model coiled-coils 153
c) Stability studies by chemical denaturation 155
i) Effects of increasing KCl concentration on coiled-coil stability 155
ii) Effects of different salts on coiled-coil stability 159
C. Discussion 168

Chapter VII. Orientation, positional, additivity, and oligomerization-state effects of interhelical ion pairs in α-helical coiled-coils
A. Introduction 177

B. Results 178
  a) Peptide design and nomenclature 178
  b) Structural characterization of the model coiled-coils 180
  c) Stability studies 180
    i) Substitution of Lys or Glu at position **e** or **g** - pH 7 180
    ii) Substitution of Lys or Glu at position **e** or **g** - pH 3.2 183
    iii) Substitution of Lys and Glu at positions **e** and **g** - interhelical ionic attractions at pH 7 186
    iv) Substitution of Lys and Glu at positions **e** and **g** - at pH 3.2 192
    v) Role of ionic strength in the stability of the coiled-coil 194
    vi) Effects of substitutions at positions **e** and **g** on the stability and oligomerization of reduced coiled-coils 196

C. Discussion

  a) Origins of the destabilizing effects of charged residue substitutions at positions **e** and **g** 202
  b) Context may play a role in the effects of positions **e** and **g** on stability 204
  c) A Lys-Glu ion pair is more stabilizing in the E_e-K_g orientation than the K_e-E_g orientation 205
  d) Double mutant cycles versus pK_a shifts for measurement of ionic interactions 208
  e) Effects of the **e** and **g** positions on coiled-coil oligomerization state . 211
  f) Additivity of **g-e'** ionic interactions in coiled-coil 213

Chapter VIII. Effects of lanthanide binding to glutamic acid residues on the stability of α-helical coiled-coils: the La^{3+}-bridging model

A. Introduction 215
B. Results and Discussion 216
  a) Peptide design and nomenclature 216
  b) Structural characterization of the model coiled-coils 219
  c) Stability studies 220
    i) Urea denaturation, oxidized peptides 220
    ii) Urea denaturation, reduced peptides 230
    iii) Effects of 1 M $MgCl_2$ and $CaCl_2$ on urea denaturation behavior 233

C. Conclusions 235

Chapter IX. Metal ion induced folding of a *de novo* designed coiled-coil peptide

A. Introduction 238
B. Results 240
  a) Peptide design 240
  b) Structural charactérics of Gla_2Nx 246
  c) pH dependence 251
  d) Stability 254
  e) Metal ion titration monitored by CD spectroscopy 256
  f) Metal ion titration monitored by NMR spectroscopy 258
C. Discussion 259

Chapter X. General Discussion

1) Specificity of **g-e'** interactions 266
2) General versus specific ionic repulsions/attractions and effects of salts on interhelical electrostatics 267
3) Additivity of **g-e'** interactions 271
4) Dynamics of coiled-coil structure and mutational effects on stability 273
5) Manipulation of protein stability and folding with buffer conditions - pH, salt, and metal binding 275
6) Roles of charged residues in coiled-coils - an overview 277
7) Future research directions 279

Bibliography 285

Appendix I. *De novo* design of α-helical coiled-coils and bundles: models for development of protein-design principles 314

LIST OF TABLES

Table **Page**

II.1 List of reagents used and suppliers 34

III.1 CD molar ellipticities and reversed-phase HPLC retention times 70

III.2 Stability data from urea and GdnHCl denaturation 75

IV.1 Molar ellipticities and % helix of N-E10 under various buffer conditions 97

IV.2 Stabilities of Nx-E10x under different conditions 108

V.1 Urea denaturation stability data at pH 7 134

V.2 Urea denaturation stability data at pH 3 144

VI.1 Effects of varying KCl concentration on coiled-coil stability 158

VI.2 Effects of 50 mM $LaCl_3$ on stability at pH 7; urea denaturation. 163

VI.3 Effects of 50 mM $LaCl_3$ on stability at pH 7; GdnHCl denaturation 165

VI.4 Effects of $LaCl_3$, $MgCl_2$, and KCl on coiled-coil stability at pH 7 167

VII.1 Urea denaturation results at pH 7 - Lys or Glu substitution 181

VII.2 Urea denaturation results at pH 3.2 - Lys or Glu substitution. 184

VII.3 GdnHCl denaturation results at pH 3.2 - Lys or Glu substitution. 185

VII.4 Urea denaturation results at pH 7 - ion pair peptides 189

VII.5 Urea denaturation results at pH 3.2 - ion pair peptides 193

VII.6 Urea denaturation results at pH 7 - reduced coiled-coils 201

VIII.1 Effects of $LaCl_3$ on the stability of the disulfide-bridged coiled-coils from urea denaturation 221

VIII.2 Effects of $LaCl_3$ on the stability of the reduced coiled-coils from urea denaturation 231

VIII.3 Combined effects of $LaCl_3$ and $MgCl_2$ on the stability of the disulfide-bridged coiled-coils from urea denaturation 234

LIST OF FIGURES

Figure **Page**

I.1 Schematic representation of the folding of a globular protein in water 2

I.2 Patterns of polar and nonpolar residues promoting different secondary structures 21

I.3 Schematic helical wheel and helical rod diagrams of a parallel two-stranded α-helical coiled-coil 23

I.4 Helical ribbon illustration of a coiled-coil structure 27

I.5 Helical-wheel representations of Fos and Jun homodimers and Fos/Jun heterodimer 30

II.1 A general outline of solid-phase peptide synthesis 36

II.2 Example of deprotection and activation reactions involved in SPPS 38

II.3 Side-chain protecting groups used in peptide synthesis 42

II.4 Reversed-phase chromatograms of crude and purified oxidized peptides 46

II.5 Electrospray mass spectral results for a reduced and oxidized peptide 47

II.6 Standard curve for size-exclusion chromatography 50

II.7 Sequence and helical wheel representation of the native (control) coiled-coil . . 61

III.1 Sequences of the peptide analogs studied in Chapter III (determining specificity of interhelical Glu-Glu repulsions) 66

III.2 Helical rod diagrams of $E_2(15,20)$, $E_2(20,22)$, and $E_2(13,22)$ 67

III.3 CD spectra of Nr, Nx, E_2(15,20)r and E_2(15,20)x at pH 7 69

III.4 Urea and GdnHCl denaturation profiles of Nx, E_1(20)x, E_2(15,20)x, E_2(20,22)x, and E_2(13,22)x at pH 7 74

III.5 Urea and GdnHCl denaturation profiles of Nx, E_1(20)x, E_2(15,20)x, E_2(20,22)x, and E_2(13,22)x at pH 3 80

III.6 Urea denaturation profiles of Nr, E_1(20)r, E_2(15,20)r, E_2(20,22)r, and E_2(13,22)r at pH 7 and pH 3 83

III.7 Reversed-phase HPLC profiles of Nr, E_1(20)r, E_2(15,20)r, E_2(20,22)r, and E_2(13,22)r at pH 7 and pH 2 85

IV.1 Sequences of the peptide analogs studied in Chapter IV (determining effects of varying numbers of repulsions on folding and stability) 93

IV.2 Helical wheel diagram of E10x depicting interhelical Glu-Glu repulsions 94

IV.3 CD spectra of Nx-E10x and Nr-E6r at pH 7 96

IV.4 pH dependence of the helicity of E10x and E10r 101

IV.5 Effect of pH on the dimerization of E8r, monitored by size-exclusion chromatography 103

IV.6 Sedimentation-equilibrium results for Nr and E8r 105

IV.7 Denaturation profiles for Nx-E10x (urea at pH 7; GdnHCl at pH 7 and 3) 107

IV.8 Effects of KCl and GdnHCl on the helicity of E10x 112

IV.9 Effects of KCl, $MgCl_2$, and $LaCl_3$ on the interhelical Glu-Glu repulsions - urea denaturation profiles 115

IV.10 Effects of KCl, $MgCl_2$, and $LaCl_3$ on the helicity of E10x 118

IV.11 Summary of the effects of Glu substitutions on coiled-coil stability measured under different conditions 120

IV.12 Net charge versus specific charge repulsion effects: KE-EKx heterodimer stability 124

V.1 Sequences of the peptide analogs studied in Chapter V (Glu substitutions at different **e** and **g** positions along the peptide chain) 130

V.2 Urea and GdnHCl denaturation profiles of Nr, Nx, E1r, E1x, E6r, E6x, E15r, and E15x at pH 7 132

V.3 Effect of salt on the urea denaturation midpoints of Nx, E1x, and E15x 140

VI.1 Sequences of the peptide analogs studied in Chapter VI (effects of salts on coiled-coils containing intra- or interhelical ion pairs) 152

VI.2 Helical wheel diagrams of QQx, KEx, and KQEx 154

VI.3 Sedimentation-equilibrium results for KEx at 100 mM and 1 M KCl 156

VI.4 Dependence of KEx and QQx stability on KCl concentration at pH 7 and 3 . . . 157

VI.5 Dependence on KCl concentration of the difference in $[\text{urea}]_{1/2}$ values between KEx and QQx and the stability change upon acidification for EQx and KEx 160

VI.6 Effect of $LaCl_3$ on the urea denaturation profiles of QQx and KEx at pH 7 and pH 3 162

VI.7 Proposed model for the destabilization of the folded state of KEx by $LaCl_3$ . . 173

VII.1 Sequences of peptide analogs studied in Chapter VII (double mutant cycle analyses of Lys-Glu ion pairs) 179

VII.2 Urea and GdnHCl denaturation profiles of Nx, EK(VL)x, and KE(VL)x at pH 7 187

VII.3 Illustration of a double mutant cycle analysis for determination of Lys-Glu interaction energy 190

VII.4 Effect of KCl concentration on the stability of KE(VL)x and QK(VL)x at pH 7 and pH 3.2 195

VII.5 Sedimentation-equilibrium results for Nr, EK(VL)r, KE(VL)r, E15K20r, and K15E20r 197

VII.6 Urea and GdnHCl denaturation profiles for EK(VL)r and KE(VL)r at pH 7 . . 200

VIII.1 Helical rod diagrams depicting the coiled-coils $E_2(13,22)$, $E_2(20,22)$, $E_2(15,20)$, $E_3(13,15,20)$, and $E_3(15,20,22)$ 217

VIII.2 Urea denaturation profiles of Nx and $E_2(15,20)$x at pH 7 - effect of $LaCl_3$ . . . 222

VIII.3 Effect of $LaCl_3$ on the temperature denaturation of $E_2(15,20)$x 225

VIII.4 Dependence of urea denaturation properties of $E_2(15,20)$x and $E_3(13,15,20)$x on $LaCl_3$ concentration 228

VIII.5 Schematic representation of the orientations of Val and Leu side chains at positions **a** and **d**, respectively, of a dimeric coiled-coil 229

VIII.6 Urea denaturation profiles of $E_2(15,20)$r and $E_3(13,15,20)$r at pH 7 - effect of $LaCl_3$ 232

IX.1 Sequence and helical wheel diagram of Gla_2Nx 241

IX.2 Effect of $LaCl_3$ on the CD spectrum of Gla_2Nx 247

IX.3 Sedimentation-equilibrium results for Gla_2Nx with and without $LaCl_3$ 249

IX.4 Effect of $LaCl_3$ on the one-dimensional ^1H NMR spectrum of Gla_2Nx 250

IX.5 Effect of $YbCl_3$ on the one-dimensional ^1H NMR spectrum of Gla_2Nx 252

IX.6 Effect of pH on the helicity of Gla_2Nx 253

IX.7 Effect of $LaCl_3$ on the urea denaturation of Gla_2Nx 255

IX.8 Metal-titration curves of Gla_2Nx ($LaCl_3$, $YbCl_3$, $ZnCl_2$, and $CaCl_2$) 257

IX.9 Schematic of metal-binding equilibria and proposed application for metal-dependent subunit assembly 263

X.1 Summary of the effect of increasing Glu substitutions on coiled-coil stability at pH 7 at low and high ionic strength 268

LIST OF ABBREVIATIONS

Amino acids:

Ala, A	Alanine
Arg, R	Arginine
Asn, N	Asparagine
Asp, D	Aspartic acid
Cys, C	Cysteine
Gla	γ-carboxy glutamic acid
Gln, Q	Glutamine
Glu, E	Glutamic acid
Gly, G	Glycine
His, H	Histidine
Ile, I	Isoleucine
Leu, L	Leucine
Lys, K	Lysine
Met, M	Methionine
Nle	Norleucine
Phe, F	Phenylalanine
Pro, P	Proline
Ser, S	Serine
Thr, T	Threonine
Trp, W	Tryptophan
Tyr, Y	Tyrosine
Val, V	Valine

Boc or t-Boc	*tert*- Butyloxycarbonyl
CD	Circular dichroism

DCC	N,N'-Dicyclohexylcarbodiimide
DCM	Dichloromethane
DCU	N,N'-Dicyclohexyl urea
DIEA	N,N-Diisopropylethylamine
DMF	N,N-Dimethylformamide
DMSO	Dimethylsulfoxide
DSS	2,2-Dimethyl-2-silapentane-5-sulfonic acid
DTT	Dithiothreitol
EDT	1,2-Ethanedithiol
EDTA	Ethylenediaminetetraacetic acid
Fmoc	9-Fluorenylmethoxycarbonyl
GdnHCl	Guanidine hydrochloride
$[\mathrm{GdnHCl}]_{1/2}$	Guanidine hydrochloride denaturation midpoint
HBTU	2-(1H-Benzotriazol-1-yl)-1,1,3,3-tetramethyluronium hexafluorophosphate
HF	hydrofluoric acid
HOBt	1-Hydroxybenzotriazole
HPLC	High performance liquid chromatography
I.D.	Internal diameter
K_d	Apparent dissociation constant
m	slope of free energy versus denaturant concentration plots
MW	molecular weight
MOPS	3-(N-morpholino)propanesulfonic acid
NEM	N-Ethylmaleimide
NMP	N-Methylpyrrolidinone
NMR	nuclear magnetic resonance
SEC	size-exclusion chromatography

SPPS	Solid-phase peptide synthesis
TFA	Trifluoroacetic acid
TFE	2,2,2-Trifluoroethanol
Tris	Tris(hydroxymethyl)amino methane
T_m	Temperature denaturation midpoint
$[\text{urea}]_{1/2}$	urea denaturation midpoint
ΔG_u	free energy of unfolding
$\Delta\Delta G_u$	change or difference in free energy of unfolding

CHAPTER I

INTRODUCTION

This thesis deals with studies of the folding and stability of model coiled-coil proteins, therefore the first part of this introductory chapter comprises a general overview of the current understanding of the effects of various noncovalent forces on protein folding in aqueous solution. A description of the effects of various cosolvents on protein stability in aqueous solution comes next. The introductory chapter then moves on to a discussion of the role for simple model systems in studying protein structure, stability, and design as well as more specific information about the coiled-coil motif (its occurrence in nature and structural details). Finally, the introduction describes the particular issues dealt with in the experiments that follow.

1) General introduction to protein folding

Proteins are the most important functional molecules in biology and fulfill diverse roles as structural molecules, signalling molecules, receptors, carriers, regulatory molecules, and catalysts of biochemical reactions. The folding of polypeptide chains, consisting of the 20 naturally-occurring amino acids, into distinct three-dimensional structures serves as the key to conversion of the one-dimensional genetic code into life by creating recognition surfaces and active sites which allow proteins to efficiently carry out their unique functions. There are two broad structural classes of proteins. The fibrous proteins, such as keratin and collagen, are generally extended and primarily play roles in structural rigidity of cells and tissues. The globular proteins, which include the majority of the functional proteins in aqueous intracellular conditions, are compact and usually roughly spherical with tightly folded polypeptide chains, in which the nonpolar residues are buried in the core of the folded structure (Fig. I.1). Before the experimental determination of any three-dimensional structures of proteins, it was theorized that all proteins may fold into

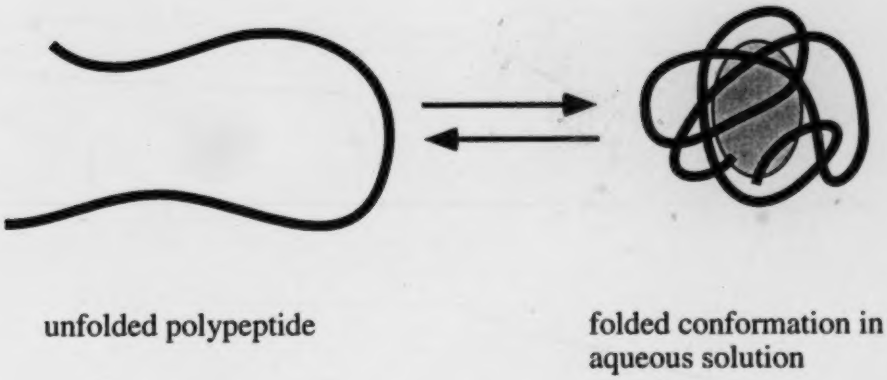
unfolded polypeptide
folded conformation in aqueous solution

Figure I.1 Schematic representation of the folding of a globular protein in water. The nonpolar amino acid side chains are directed toward the inside of the folded structure to form a "hydrophobic core" buried from water (shown shaded), and the polar side chains are primarily exposed.

highly-symmetric structures and that general, simple principles for their folding and function could be determined. The first X-ray crystallographic determination of a globular protein structure was the low-resolution structure of myoglobin (Kendrew *et al.*, 1958), which suggested that, contrary to expectations, proteins adopt complex, asymmetric structures. The complexity and diversity of protein structure observed in nature is a likely result of the need for exact recognition amongst thousands of molecules in the biological context.

While earlier work hinted at the reversibility of denaturation of the 'native' structure of proteins, it was the pioneering work of Anfinsen's group which clearly demonstrated what came to be known as the thermodynamic hypothesis: the three-dimensional structure of a protein in its normal physiological environment is that in which the free energy of the system is the lowest, and is determined by all the interatomic noncovalent interactions within the protein and between the protein and its surroundings (solvent, ions, etc.), and thus, by the primary amino acid sequence of the protein (Anfinsen, 1973). It is therefore theoretically possible to predict the structure of a given protein from its amino acid sequence, but the absence of a simple set of principles for protein folding makes this a difficult task, leading to the so-called 'protein-folding problem'. Obtaining a better understanding of the protein folding puzzle has been the ultimate goal of much protein research in recent decades.

2) Noncovalent interactions in protein folding

The net stability of the folded conformation of a protein versus the unfolded, biologically inactive state is generally only 5 to 10 kcal/mol and represents a balance between stabilizing and destabilizing noncovalent forces that are much larger in magnitude (Creighton, 1990; Dill, 1990; Makhatadze & Privalov, 1995; Pace *et al.*, 1996). These forces result from interactions within the protein, interactions with other protein subunits, and interactions between the protein and its environment (usually water but also may include a hydrophobic lipid environment in the case of transmembrane proteins). Entropy also plays an important role in the thermodynamics of protein folding. For example, the major force that opposes protein folding is loss of conformational entropy of the protein, which has been estimated to be about 1.2 kcal/mol per residue at 25°C (Pace *et al.*, 1996).

i) Hydrophobic interactions

For the past several decades, the most popular view has been that the dominant effect promoting protein folding in water is also primarily entropy-driven. This driving force is the 'hydrophobic effect', which is thought to occur because water arranges around the hydrophobic side chains of an unfolded protein in a cage-like or clathrate structure with much higher order than bulk water (Pertsemlidis *et al.*, 1996). The solvent entropy is therefore severely reduced by the presence of the unfolded protein, and protein folding is promoted by a gain in solvent entropy that is even larger than the folding-induced entropy loss of the protein itself. The hydrophobic effect, first popularized by Kauzmann for protein folding (Kauzmann, 1959), also is thought to drive the formation of micelles, vesicles, and lipid bilayer membranes by amphipathic lipids in an aqueous environment.

The effect of ordering water molecules around the surface of protein molecules on the thermodynamics (enthalpy (ΔH) and entropy (ΔS)) of unfolding is temperature dependent and the large, positive partial heat capacity, ΔC_p, observed for protein unfolding (heat capacity is greater in the unfolded state) is a measure of this temperature dependence (Creighton, 1990; Makhatadze & Privalov, 1995). The ΔC_p of unfolding is affected by exposure of both hydrophobic and hydrophilic groups (Makhatadze & Privalov, 1995) but is generally believed to be dominated by the exposure of hydrophobic surface area, due to the observation of unusually large heat capacities for small hydrophobic compounds dissolved in water (Baldwin, 1986; Murphy *et al.*, 1990). Studies have shown a direct correspondence between the increase in solvent-accessible nonpolar surface area and the ΔC_p for protein unfolding (Livingstone *et al.*, 1991; Spolar *et al.*, 1989) and suggested that the value of ΔC_p could be a measure of the contribution of nonpolar surface area to protein stability (Baldwin, 1986; Livingstone *et al.*, 1991; Spolar *et al.*, 1989). Interestingly, examination of a form of the Gibbs-Helmholtz equation in which the free energy of unfolding can be expressed as a function of temperature, led Creighton to suggest that a greater value for the ΔC_p of unfolding (resulting from a more hydrophobic protein interior) could actually be destabilizing to the folded conformation of a protein, thereby challenging the hydrophobic effect dogma (Creighton, 1993, p. 300). Similarly, Makhatadze and Privalov pointed out that the heat induced denaturation of proteins is testimonial to the enthalpic factors prevailing over entropic factors in stabilizing protein structure, particularly at higher temperatures (Makhatadze & Privalov, 1995). Indeed, it had previously been suggested that the 'hydrophobic effect' changes from being entropy-driven at low temperature to enthalpy-driven at high temperature (Baldwin, 1986).

Interactions between the buried hydrophobic core side chains play an important role in the actual stabilization of the folded state by the hydrophobic core. Indeed, the traditional view of the hydrophobic effect neglects the role of interactions between buried hydrophobic side chains, but mutagenesis experiments reveal these close packing interactions play as significant a role as the burial of hydrophobicity (Eriksson *et al.*, 1992; Kellis *et al.*, 1989; Matthews, 1995a; Pace *et al.*, 1996), possibly even more significant (Makhatadze & Privalov, 1995). These enthalpically stabilizing interactions between the aliphatic side chains are the so-called van der Waals interactions, originating from the London dispersion forces that are a result of momentary uneven distributions in electron density (induced dipole interactions) (Schulz & Schirmer, 1979). Although its role in protein folding is currently not universally believed to be as important as it once was, the hydrophobic effect (both solvation effects and van der Waals interactions) is still held to be the largest (Creighton, 1990; Dill, 1990; Honig & Yang, 1995; Lazaridis *et al.*, 1995) or one of the largest (Makhatadze & Privalov, 1995; Pace *et al.*, 1996) stabilizing forces in protein folding.

ii) Polar (hydrogen bond) interactions

The uncertainty over the relative role of hydrophobic residues in protein folding exists in conjunction with a similar debate regarding the effects of polar backbone and side chain groups on protein folding. Approximately 70% of the polar amide backbone groups in the average protein are buried in the interior out of contact with solvent (Pace *et al.*, 1996). These buried polar backbone groups are mostly involved in formation of α-helix or β-sheet secondary structure, in which short range and long range hydrogen bonds, respectively, are formed between the NH of one amide group and the CO of another amide group. In the early days of protein chemistry, hydrogen bonding between these polar groups was believed to be the critical force in promoting protein folding, but its perceived role was diminished almost completely as the hydrophobic effect model became prominent (Makhatadze & Privalov, 1995; Pace *et al.*, 1996).

A common conclusion among many in the protein folding field today is that the polar groups contribute nothing to the stabilization of protein folding and complex formation because the energetic cost of their desolvation upon folding more than offsets the energy of interaction between these groups. It is also thought that because buried polar groups are able to interact with water in the unfolded state, there is not likely to be any significant net increase in favorable interactions upon folding (Honig & Yang, 1995; Lazaridis *et al.*, 1995). Under this theory, protein backbone hydrogen bonds involved in secondary structure formation are required to compensate (at least partially) for the loss of hydrogen bonds to water. Others contend, mostly based on experimental results, that hydrogen bonding, particularly the hydrogen bonding between backbone NH and CO groups seen in regular secondary structure but also between polar side chains, can stabilize protein structure (Huyghues-Despointes *et al.*, 1995; Makhatadze & Privalov, 1995; Myers & Pace, 1996; Pace *et al.*, 1996). Creighton suggested the possibility that hydrogen bonds in a folded protein could in fact be much stronger than hydrogen bonds between the unfolded protein and water because the hydrogen bonds within the protein: (1) are intramolecular and thus may have a higher stability for simple entropic reasons; (2) may comprise a cooperative system giving a greater contribution to stability than could individual interactions; (3) are present essentially all the time rather than only a fraction of the time (such as the case for transient water-protein interactions) (Creighton, 1993, p. 301). Additionally, the stabilization of protein structure by internal hydrogen bonds has been suggested to have a significant entropic component because exposed polar groups order water around themselves similarly to nonpolar groups (Makhatadze & Privalov, 1995). Therefore, a number of researchers now believe that hydrogen bonding plays a roughly equal role in stabilizing protein folding as does hydrophobic burial and packing (Creighton, 1990; Makhatadze & Privalov, 1995; Pace *et al.*, 1996).

iii) Electrostatic interactions

Even more controversial than the role of hydrogen bonding in protein folding and complex formation is the contribution of electrostatic interactions. Electrostatics can be described fundamentally by Coulomb's Law, where the energy of interaction, E, between two charges is approximated by:

$$E = CQ_1Q_2/Dr$$

where Q_1 and Q_2 are the charges of the interacting atoms, r is the distance between the charges and D is the dielectric constant of the medium, which acts to screen the electrostatic interaction by orienting its dipoles around the charges. A highly polar solvent like water has a high dielectric constant (about 78 at 25°C) while nonpolar hydrocarbons have dielectric constants as low as 2. The dielectric constant of water decreases with increasing temperature since thermal motion overcomes the orienting effects of the water dipoles. As a result, electrostatic interactions in water are stronger at higher temperatures. C is a constant with a value of 331 for energies expressed in kcal/mol and r in units of angstroms. Thus, the interaction between an Na^+ ion and a Cl^- ion that are 3.0 Å apart in water at 25°C has an energy of -1.4 kcal/mol (assuming an infinitely low effect of ionic strength - see below).

Coulomb's law describes interactions between point charges, so its applicability is complicated unless the distance between charges is significantly greater than the atomic dimensions. In proteins, the complication is even greater since the charges are distributed over two or more atoms. In addition, the interaction of oppositely charged groups in proteins at short distances consist of an electrostatic attraction as well as a hydrogen-bond component. For example, the positively charged $-NH_3$ group of a Lys side chain can form a hydrogen bond with the negatively charged $-CO_2$ group of a Glu or Asp side chain. Such ion pairs in proteins occur with a preferred distance between the hydrogen bond acceptor and donor atoms of about 3 Å (Barlow & Thornton, 1983) and are also commonly referred to as salt bridges.

Electrostatic interactions are long range (proportional to1/r), in contrast to van der Waals interactions (proportional to $1/r^6$ where r is the distance between two atoms). Thus, while other types of interactions can usually be described in molecular mechanics potential energy algorithms by simple mathematical functions involving only a few atoms at a time, electrostatics in macromolecules in solution are difficult to model (Harvey, 1989). The earliest model for protein electrostatics derived by Linderstrom-Lang in 1924 treated a globular protein as an impenetrable sphere with a continuous (uniform) charge distribution on the surface, for which the electrostatic free energy is proportional to the square of the net surface charge and is destabilizing at all pH values except the isoelectric point (pH at which the protein has zero net charge) (Linderstrom-Lang, 1924). More advanced continuum computational techniques (Tanford-Kirkwood theory and various modifications), in which individual atoms can be specified in terms of their positions, solvent accessibilities, and interactions with other charged and polar parts of the protein, have been developed and used for simulating protein electrostatics with increasing success (Harvey, 1989; Nakamura, 1996). High-speed computational techniques have allowed continuum analysis by numerical solutions to the Poisson-Boltzmann equation, in which the exact shapes of proteins can be included (Harvey, 1989; Nakamura, 1996).

Several problems remain in the modelling of electrostatics, such as the difficulty of choosing the correct dielectric constant for the interior of a protein. With the majority of the buried side chains being hydrophobic, this value is generally taken to be quite low (in the range 2-4) but considerable controversy has arisen, and the choice of the dielectric constant is critical to the results of computer simulations, particularly molecular mechanics simulations (Harvey, 1989). Complicating the matter is the fact that the dielectric constant is a macroscopic property of homogeneous environments, but the interior of a protein is heterogeneous with some portions being more polar than others. Even more complicated is the interface between regions with different dielectric constants, such as between a protein and water. Both molecular mechanics (microscopic) and continuum (macroscopic) types of computer simulations are used currently, each having its advantages (Harvey, 1989; Nakamura, 1996). Combination of the continuum model with molecular mechanics simulations has proven difficult (Nakamura, 1996). The difficulty in accurately simulating protein electrostatics makes it particularly important to study these interactions experimentally.

While electrostatic interactions, in particular ion pairs between opposite charges, play important roles in functions such as catalysis and allosteric conformational changes that affect substrate binding and enzyme activation (Barlow & Thornton, 1983; Lounnas & Wade, 1997; Nakamura, 1996; Perutz, 1978), their role in protein folding and formation of protein-protein complexes is less clear. Proteins generally display a significant pH dependence for their folding and stability, which clearly demonstrates that ionizable side chains contribute to protein stability. In many cases, the maximum stability is observed at or near the isoelectric point, in agreement with Linderstrom-Lang. In other cases, the pH at which maximum stability occurs can differ quite significantly from the isoelectric point (such as bacteriophage T4 lysozyme, which has maximum stability at pH 5 and an isoelectric point of pH 10 (Anderson *et al.*, 1990)). In such cases, specific ionic interactions between a small number of buried residues with large pK_a shifts in the folded state (versus the unfolded state) substantially affect protein stability by 3-5 kcal/mol (Anderson *et al.*, 1990; Fersht, 1972; Friend & Gurd, 1979). Ion pairs on the surface of proteins appear to contribute only 0.2-0.5 kcal/mol of net stabilization (Dao-pin *et al.*, 1991; Horovitz *et al.*, 1990; Lyu *et al.*, 1992; Sali *et al.*, 1991; Serrano *et al.*, 1990; Zhou *et al.*, 1994b), presumably due to screening by the solvent. Recent experimental (Waldburger *et al.*, 1995; Wimley *et al.*, 1996) and theoretical (Froloff *et al.*, 1997; Hendsch & Tidor, 1994; Honig & Nicholls, 1995; Honig & Yang, 1995) studies indicate that the energetically unfavorable desolvation of charged residues upon protein folding or complexation is generally larger than the stabilization due to ionic attractions, so a buried ion pair contributes less to the stability of a protein than an interaction between hydrophobic residues. It was further suggested that surface charges also destabilize proteins overall because of desolvation resulting from putting them at the surface of a low dielectric object such as a protein (Yang & Honig, 1993).

Although electrostatic interactions may not in general contribute substantially to stability of the folded state or binding affinity of a complex, they are likely to confer conformational specificity in folding (Bryson *et al.*, 1995; Handel *et al.*, 1993; Lumb & Kim, 1995a) and binding (Antosiewicz *et al.*, 1996; Muegge *et al.*, 1998; Nakamura, 1996) due to the requirement for compensation of buried polar groups through specific hydrogen-bond and electrostatic interactions and the desire of a folded protein to arrange charges on its surface in order to maximize electrostatic attractions and minimize electrostatic repulsions (Yang & Honig, 1993). Statistically, short-range ionic attractions outnumber repulsions by a 3:1 ratio in globular proteins, suggesting again that electrostatics do help direct protein folding (Barlow & Thornton, 1983).

There is other evidence that suggests a greater importance for ion pairs in stabilizing proteins and protein complexes in certain cases. For example, networks of ion pairs where charged residues participate in more than one attraction have been identified in a number of proteins (a statistical analysis showed 37% of ion pairs occur as part of such networks (Barlow & Thornton, 1983)), and may be able to significantly stabilize a protein due to cooperativity between the ion pairs (Horovitz *et al.*, 1990; Lounnas & Wade, 1997). In particular, a number of studies of proteins from thermophilic bacteria indicate that ion-pair networks play a critical role in their extreme thermostability (Nakamura, 1996; Yip *et al.*, 1995). Several recent computational studies also suggest that electrostatic interactions can contribute to binding energy for protein-protein interactions if the binding interface is hydrophilic enough that desolvation upon complex formation is not too high (Chong *et al.*, 1998; Muegge *et al.*, 1998; Xu *et al.*, 1997).

Because of the potential long-range nature of electrostatic interactions, it is sometimes useful to categorize electrostatics into two broad classes. The first is nonspecific, long-range (or general) charge effects, such as those described by the Linderstrom-Lang model, in which the overall charge on the protein is involved in determining stability or interactions with other molecules. The second type is short-range or specific interactions between charged residues, such as in salt bridges, and between charged residues and the immediate surrounding protein environment.

Long-range electrostatic effects become particularly important in dealing with repulsion between like charges. This is readily apparent in the idea that a protein is most stable at the isoelectric point. For example, it is a general phenomenon that proteins denature at very low pH where the acidic side chains become protonated and the protein takes on a significant positive net charge. Under these conditions, denaturation generally is thought to allow a decrease in electrostatic free energy (decrease in repulsive effects) by expansion of the molecule that occurs upon unfolding (Goto & Nishikiori, 1991; Stigter & Dill, 1990). However, acid-induced denaturation may also be just as much a result of the loss of ionic attractions upon protonation of acidic residues, ultimately leading to uncompensated buried or partly buried positive charges that are highly destabilizing to the folded state (Yang & Honig, 1993). Acetylation of lysine side chain amino groups in horse ferricytochrome c resulted in destabilization of the native state at pH 7, as a result of increased local repulsion between negative charged residues rather than an increase in net charge (Hagihara *et al.*, 1994). Thus, both short- and long-range electrostatics can affect protein folding and stability, but the relative roles are not clear and may vary widely between proteins.

Protein electrostatic interactions are far from being understood completely. In fact, the relative roles of all noncovalent interactions on both folding and binding processes are not well-defined to this point in terms of specific rules that apply in all cases. The research presented in this dissertation is aimed at contributing to the understanding of noncovalent interactions in proteins, particularly focussing on electrostatics, employing the α-helical coiled-coil (see below) as a model system.

3) Effects of additives on protein stability

The stability of a protein in aqueous solution is subject to the effects of various cosolvents, particularly salts. These additives also have effects on the solubility of proteins and their interactions with other proteins and other molecules like DNA.

A) Salt effects on proteins

i) dielectric effects

The most commonly recognized effect of salt in aqueous solution is to increase the dielectric constant of the solution. Small ions such as Na^+ and Cl^- can diffuse in solution and concentrate in the vicinity of charges of the opposite sign, thus adding to the ability of water itself to screen the energy of interaction between charges. This screening of electrostatics by salt, referred to as Debye-Hückel screening, can be described by an effective dielectric constant:

$$D_{eff} = D_{H_2O} \cdot \exp(\kappa r)$$

where D_{H_2O} is the dielectric constant of pure water, r is the distance between the charges, and κ is a parameter that is proportional to the square root of the ionic strength. Thus, as ionic strength is increased, the D_{eff} at a particular distance is increased and ionic interactions are squelched. The existence of stabilizing or destabilizing electrostatic interactions in proteins is therefore commonly probed by varying salt concentration with the idea that salt will screen the interactions.

ii) Ion binding

Proteins in nature commonly bind to cations or anions in solution, which can enhance protein stability (Strynadka & James, 1989; Findlay *et al.*, 1992), and play a role in modulating protein function and protein-protein interactions. For example, Ca^{2+} binding at specific sites is a common regulatory mechanism through its effects on protein structure in molecules such as calmodulin, troponin C, and parvalbumin (Findlay *et al.*, 1992; Ikura, 1996; Strynadka & James, 1989), and bound metal ions can play important roles in enzyme catalysis (Nakamura, 1996; Volbeda *et al.*, 1996; Williams, 1995). In addition to a number of cases where specific metal-binding sites have been structurally characterized, there are many proteins for which metal binding modulates stability or function but the binding sites are not determined or the binding is nonspecific. For example, a number of salts including $MgCl_2$ and $CaCl_2$ can be destabilizing to protein structure under certain circumstances, which originates from specific binding of the metal ions to the peptide backbone, more of which is exposed in the unfolded state (Arakawa *et al.*, 1990a). Conversely, ion binding to regions of high net charge density can favor the folded state of the protein; for example, while acidic conditions can cause denaturation due to buildup of positive charge, anion binding to positive charges on the protein can promote the folded or partially folded molten-globule state of proteins (Goto *et al.*, 1990) and α-helical peptides like melittin (Goto & Hagihara, 1992) and coiled-coils (Hoshino *et al.*, 1997; Yu *et al.*, 1996). In all cases of nonspecific binding, the preferential binding of the ion to one conformational state of the protein will increase the relative stability of that state simply due to the law of mass action (Creighton, 1993, Chapter 8).

iii) Effects of salt on water structure/properties

While salt ions can have direct interactions with proteins and other biological macromolecules, they also have interactions with the bulk solvent that affect the structure/properties of the solvent to varying degrees and ultimately affect the behavior of proteins in aqueous solution. Generally, inorganic salts may be described by the Hofmeister series (Baldwin, 1996) for their effects on protein stability and solubility. The effects of anions and cations are generally additive. A representative sample includes:

cations: $NH_4^+ > K^+ > Na^+ > Mg^{2+} > Ca^{2+}$

anions: $SO_4^{2-} > HPO_4^{2-} >$ acetate $>$ citrate $> ClO_4^- > SCN^-$

where the first ion in each series increases the surface tension of water and results in a decrease in solubility of nonpolar groups, and the last ion in each series has less effect on surface tension and increases solubility. $(NH_4)_2SO_4$ is therefore the strongest stabilizer of protein structure and can precipitate (salt out) proteins from solution. The increased surface tension observed upon addition of most salts is proportional to the salting-out effect of the salt and is a result of exclusion of the salt ions from the air-water (or protein-water) interface, which leads to preferential hydration of the protein and generally stabilization (Arakawa *et al.*, 1990a, 1990b; Baldwin, 1996; Leberman & Soper, 1995; Lin & Timasheff, 1996). However, there is often competition between general effects of the salt on solvent structure and preferential binding of the ions to the protein (Arakawa *et al.*, 1990a, 1990b; Lin & Timasheff, 1996). Thus, while $MgCl_2$ may cause some preferential hydration, it generally is not stabilizing due to the stronger direct binding effects of the magnesium ion (Arakawa *et al.*, 1990a, 1990b). Early studies with model peptides showed that salts in general make transfer of nonpolar groups into water less favorable (Nandi & Robinson, 1972a) and transfer of the polar backbone groups more favorable (Nandi &

Robinson, 1972b). Comparison of the two studies indicated that the effects were additive, and in general one will be dominant depending on the circumstances.

The stabilizing effect of salt on protein structure that results from preferential hydration/increased surface tension may be due to increased water structure around the protein (and therefore the loss of solvent entropy upon protein unfolding may be enhanced by salt). In particular, it has been suggested to occur due to electrostriction, which makes formation of a cavity for solute more unfavorable and 'squeezes' the protein into its most compact, folded form (Leberman & Soper, 1995; McDevit & Long, 1952). In addition, 'repulsive' effects between the salt ions and the nonpolar protein interior is a potential factor favoring protein folding (the enthalpy of interactions between polar solvent molecules and nonpolar groups is weaker than the enthalpy of hydrogen-bond interactions between the polar solvent molecules themselves or the van der Waals interactions between nonpolar groups, and this would be even more pronounced for ions and nonpolar groups). The latter effect is probably more relevant at higher temperatures where the ordering effects (preferential hydration) of the solvent would be lower and ions would be more likely to come into contact with the protein. In both cases, the result is generally explained as an increase in the apparent hydrophobic effect.

B) Other additives

A variety of other compounds besides inorganic salts have profound effects on protein stability and solubility when present as cosolvents in aqueous solution (Creighton, 1993, Chapter 7). For example, compounds such as polyethylene glycol increase the surface tension of water (causing preferential hydration and decreasing the solubility of proteins) and are therefore used for protein crystallization. Organic solvents, which are miscible with water, such as acetonitrile and methanol decrease the overall solvent polarity and interact more strongly with the nonpolar core of proteins than does water, thus destabilizing globular protein structure. Detergents such as sodium dodecyl sulfate have similar denaturing effects. Two chemical denaturants commonly used to probe protein stability are the polar molecules urea and guanidine hydrochloride (or guanidinium chloride) (Pace, 1986):

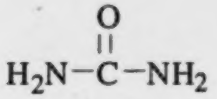

$$H_2N-\overset{\overset{\displaystyle O}{||}}{C}-NH_2$$

urea

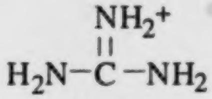

$$H_2N-\overset{\overset{\displaystyle NH_2^+}{||}}{C}-NH_2$$

guanidinium ion

The mechanism of action of these denaturants has been difficult to explain. It was previously attributed to their ability to hydrogen bond to the protein backbone (later it was suggested these denaturants likely do not hydrogen bond to the peptide backbone better than water) or their possible 'chaotropic' effects on the solvent structure (but experiments have suggested that urea does not affect water structure (Zou *et al.*, 1998)). In addition, urea and guanidine increase the surface tension of water (Breslow & Guo, 1990), which usually increases protein stability. Currently, these denaturants are believed to promote protein unfolding primarily via preferential binding to both polar and nonpolar portions of the protein, more of which is exposed in the unfolded state (Breslow & Guo, 1990; Makhatadze & Privalov, 1992; Zou *et al.*, 1998). The physical basis for the interaction of these polar denaturants with nonpolar surface area is unclear but almost certainly must be more favorable than interactions between nonpolar groups and water. Recent experiments with dipeptides indicate that the interaction of nonpolar portions of a protein with urea in aqueous solution is enthalpically unfavorable but is highly favored entropically (water molecules ordered around the exposed nonpolar groups are released by urea and the bulk solvent entropy is increased - urea decreases the hydrophobic effect) (Zou *et al.*, 1998). The same study suggested that the enthalpy of hydrogen bonding between urea and the peptide backbone is higher than previously predicted and supported the original explanation that strong denaturant hydrogen bonding to the peptide backbone is a cause of protein unfolding (Zou *et al.*, 1998).

Denaturants can have unexpected effects on protein stability if there are specific denaturant binding sites on the protein. For example, the enzyme urease has a specific binding site for urea and is not denatured by urea (Andrews *et al.*, 1984). Results presented in this thesis also emphasize the effects of preferential denaturant binding to particular parts of a protein on the resulting protein stability data.

4) Model protein systems for studying protein folding

A number of native globular proteins have served as models for studies of protein folding and protein-protein interactions (see for example Alber, 1989; Matthews, 1995a, 1996). The advent of site-directed mutagenesis has allowed the creation of mutants that can be used to probe the importance of specific residues in folding, stability and function (Alber, 1989; Knowles, 1987). While studies on natural proteins have met with considerable success, they are limited by the fact that the proteins are often large and contain complex networks of intramolecular noncovalent interactions. A mutation made to study one interaction can inadvertantly change other interactions. This limitation has led to the development of simpler model protein systems that contain fewer noncovalent interactions but have sufficient information encoded in their sequences to result in a well-defined structure. Such 'minimalist' models make it easier to isolate and study the effects of particular noncovalent interactions on folding and stability while still maintaining a protein-like context, thus increasing the likelihood that the results are applicable to native proteins (DeGrado *et al.*, 1989).

The *de novo* design (from scratch) of model proteins directly tests the designer's knowledge of the fundamental principles that control protein folding, which is apparent in the level of success in achieving a design goal (Betz *et al.*, 1995; Betz & DeGrado, 1996; Bryson *et al.*, 1995; Cordes *et al.*, 1996). *De novo* design is often referred to as addressing the reverse-protein-folding problem; i.e. predicting a peptide sequence that leads to a desired structure rather than predicting the structure for a given sequence. It is also hoped that the knowledge gained from *de novo* design studies will eventually lead to the ability to design proteins with totally new activities not present in nature, which will have medical and industrial applications (Bryson *et al.*, 1995; Hodges, 1996; Kohn & Hodges, 1998, Appendix I; Voyer & Lamothe, 1995). In particular, a quantitative understanding of the relative and absolute contributions of various types of noncovalent interactions to protein folding and stability, gained from studies of model systems, may be of great value in the design of totally *de novo* proteins with the desired activities (Hodges, 1996).

5) α-helical coiled-coils

α-helical coiled-coils and α-helical assemblies in general have been the most common target of model protein *de novo* design efforts (Bryson *et al.*, 1995; DeGrado *et al.*, 1989; Hodges, 1996; Kohn & Hodges, 1998, Appendix I). These molecules have several advantages, which make them attractive for protein design (DeGrado *et al.*, 1989; Hodges, 1996; Talbot & Hodges, 1982). First, the α-helix is structurally simple and is internally hydrogen bonded, giving it the ability to form autonomous folding units. β strands, in contrast, require hydrogen bonds to other strands in order to form. Second, proteins with only one type of secondary structure, particularly α-helical, are easier to study with techniques like circular dichroism spectroscopy. In addition, α-helical coiled-coils and bundles are the simplest molecules that contain tertiary (and/or quaternary) long range folding interactions. These α-helical proteins can be simplified by incorporation of a high degree of symmetry in the design process but can accurately represent the various types of short- and long-range noncovalent interactions that control the folding of proteins in general.

The two-stranded coiled-coil, which contains just two interacting helices, is the simplest (most minimalist) model protein possible, making it the ideal model system for studying protein-folding principles and developing *de novo* design capabilities. The two-stranded coiled-coil motif serves as a universal dimerization domain in a diverse group of proteins in nature (Adamson *et al.*, 1993; Kohn *et al.*, 1997a; Lupas, 1996). Therefore, studying the coiled-coil is also relevant from the standpoint of understanding the structure-function relationship for these proteins.

Two-stranded coiled-coils have long been known to play structural roles in α-fibrous proteins, such as the kmef (keratin, myosin, epidermis, fibrinogen) class (Coulombe, 1993; Titus, 1993) and intermediate filament proteins (Stewart, 1993). Crick first proposed the two-stranded coiled-coil in 1953 for α-keratin, based on the protein's X-ray diffraction pattern (Crick, 1953). Pauling and Corey independently made the same prediction (Pauling & Corey, 1953). In contrast to the two-stranded coiled-coils observed in intracellular proteins, extracellular α-fibrous proteins, including laminin, tenascin, fibrinogen, and the macrophage scavenger receptor, generally contain three-stranded coiled-coils (Conway & Parry, 1991). A number of other examples of two- and three-stranded coiled-coils in a structural role have been identified in recent years (Adamson *et al.*, 1993; Cohen & Parry, 1990; Lupas, 1996); for example, in receptor subunit assembly (Beavil *et al.*, 1992).

Perhaps, more interesting is the involvement of coiled-coil domains in a number of regulatory roles. For example, the two-stranded coiled-coil protein tropomyosin mediates the calcium-dependent interaction of thin filaments with thick filaments in the process of muscle contraction (Phillips *et al.*, 1986; Smillie, 1979). The most prominent example of regulation by the coiled-coil motif is control of dimerization of a large number of transcription factors, particularly the basic leucine zipper (bZIP) class (Busch & Sassone-Corsi, 1990; McKnight, 1991), in which the dimerization-mediating leucine zipper region was shown to form a coiled-coil (O'Shea *et al.*, 1989a, 1991). The coiled-coil motif also mediates the dimerization and DNA binding of other transcription factors in conjunction with the basic-helix-loop-helix (Murre *et al.*, 1989) or zinc-finger (Reddy *et al.*, 1992) motifs and in a variety of other cases (Marmorstein *et al.*, 1992; Marmorstein & Harrison, 1994; Sessa *et al.*, 1993). Several of the transcription factors in which the leucine zipper is involved in dimerization, including Myc, Fos, and Jun, have been implicated as protooncogenes (Busch & Sassone-Corsi, 1990; McKnight, 1991; Murre *et al.*, 1989). Conformational changes involving three-stranded coiled-coils have been shown to mediate membrane fusion and cell entry by influenza and HIV through the hemagglutinin (Carr & Kim, 1993) and gp41 (Chan *et al.*, 1997) proteins, respectively.

6) Details of coiled-coil structure

All the noncovalent interactions that control protein folding (hydrophobic, hydrogen bond and ionic) are readily apparent in the structure of the α-helical coiled-coil.

i) hydrophobic core

The major requirement for formation of α-helical proteins is the correct periodicity of hydrophobic and hydrophilic residues, which will control the type(s) of secondary structure present in such a way as to maximize the burial of hydrophobic side chains in the core of the protein (DeGrado *et al.*, 1989; Kaiser & Kezdy, 1983; Kamtekar *et al.*, 1993; Xiong *et al.*, 1995). If hydrophilic and hydrophobic side chains alternate, amphipathic β strand structure is preferentially formed (Fig. I.2, top) because the β strands are able to associate in water through their hydrophobic faces. A spacing of hydrophobic residues 3 or 4 residues apart leads to an amphipathic α-helix (Fig. I.2, bottom), which can then form dimers or higher order complexes through interaction of the hydrophobic faces. These amphipathic helices can be characterized by a seven residue (heptad) repeat designated **abcdefg** where positions **a** and **d** contain hydrophobic residues. The 3-4 hydrophobic repeat (HXXHXXXHXXH....... where H is a hydrophobic residue) was experimentally demonstrated in the 284-residue coiled-coil tropomyosin, in which 71 of 82 **a** and **d** positions contained hydrophobic residues (Hodges *et al.*, 1972). This and subsequent studies have shown that hydrophobicity at the **a** and **d** positions is critical to coiled-coil

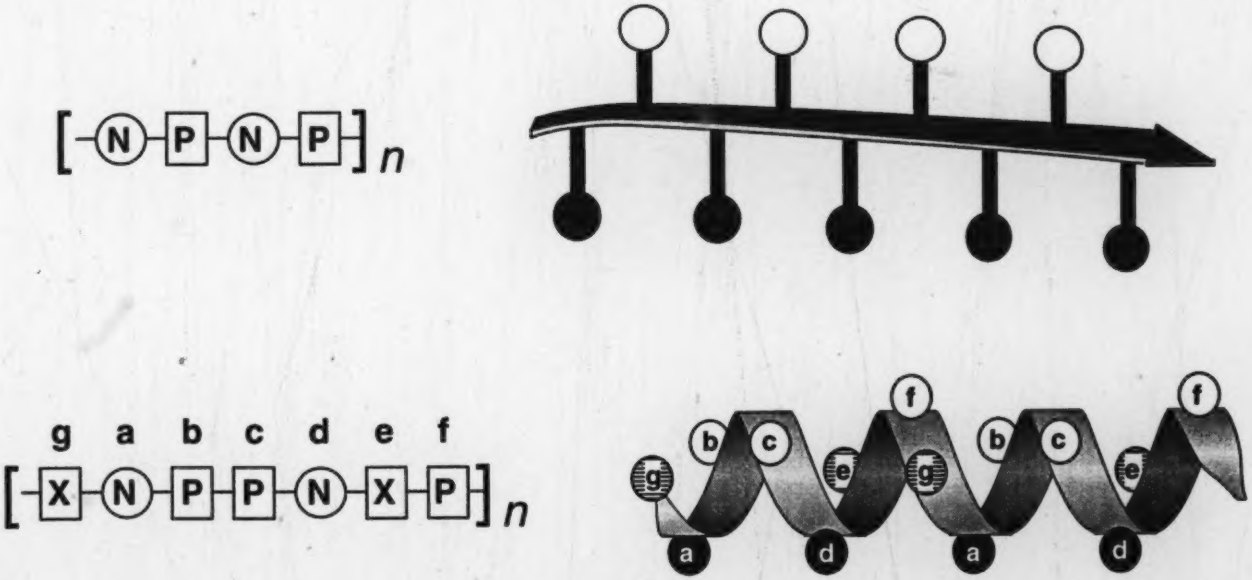

Figure I.2 Patterns of polar (P) and nonpolar (N) amino acid residues that promote amphipathic β-sheet (top) or α-helical (bottom) secondary structure. Open balls represent polar side chains, closed balls represent nonpolar side chains and hatched balls represent side chains that could be polar or nonpolar. In an amphipathic α-helix, the **[g-a-b-c-d-e-f]***n* nomenclature is used to label the various positions of the seven-residue sequence repeat, as explained in the text. Placement of hydrophobic residues only at positions **a** and **d** leads to the so-called 3-4 (or 4-3) hydrophobic repeat, in which the spacing between hydrophobes is three (**d** is three positions down from **a**) followed by four (**a** is four positions down from **d**). The **e** and **g** positions (hatched balls) are able to contribute to either the polar or the nonpolar face of the helix and may contain polar or nonpolar residues. In general, the position at which the heptad sequence starts is arbitrary since it is a repeating sequence, but in *de novo* designed coiled coils it is generally started at position **g**, which allows the N-terminal **g** residue to participate in a stabilizing **g-e'** interhelical interaction (Lumb & Kim, 1994) . (adapted from Figure 2 of Kohn & Hodges (1998), Appendix I)

folding (Cohen & Parry, 1990; Hu *et al.*, 1990; Zhou *et al.*, 1992b) although some polar residues at those positions are allowed and in some cases necessary for specifying the structure (Gonzalez *et al.*, 1996b; Lumb & Kim, 1995a; Potekhin *et al.*, 1994). The other positions of the heptad repeat are more solvent exposed and generally contain a high proportion of polar residues (Hu & Sauer, 1992). Extensive studies on the role of the **a** and **d** positions in coiled-coil folding and stability have been reviewed (Adamson *et al.*, 1993; Betz *et al.*, 1995; Cohen & Parry, 1994; Hodges, 1992, 1996; Kohn & Hodges, 1998, Appendix I).

ii) e and g positions

The **e** and **g** positions of an amphipathic α-helix flank the hydrophobic face formed by positions **a** and **d** (Fig. I.2, bottom). It is often convenient to represent a coiled-coil in a cross-sectional helical wheel diagram, in which the molecule is viewed from one end (Fig. I.3A) or a side view where the helices are represented as cylinders (Fig. I.3B). These diagrams illustrate the interaction of the **a** and **d** residues at the helix interface and the potential for interactions across the interface involving positions **e** and **g** is also apparent. Thus, positions **a**, **d**, **e**, and **g** of each helix are all involved in the dimerization interface. The two-stranded coiled-coil undergoes "knobs into holes" packing where a residue at position **a** of one helix packs into a hole between residues at position **a**, **d**, and **g** of the other helix, and similarly for position **d** (Fig. I.3B), as originally predicted by Crick (1953).

In a parallel coiled-coil, residues at position **g** of one helix are opposite residues at position **e** of the other helix, allowing for interactions between these residues across the dimer interface (Fig. I.3). Concomitant with their interhelical interactions, the **e** and **g** residues also can help shield the hydrophobic core from solvent and make direct van der Waals contacts with the core side chains through the aliphatic portion of the side chain. The **e** and **g** positions contain a high proportion of charged residues allowing for interhelical electrostatic interactions that have long been predicted to be important in controlling in-

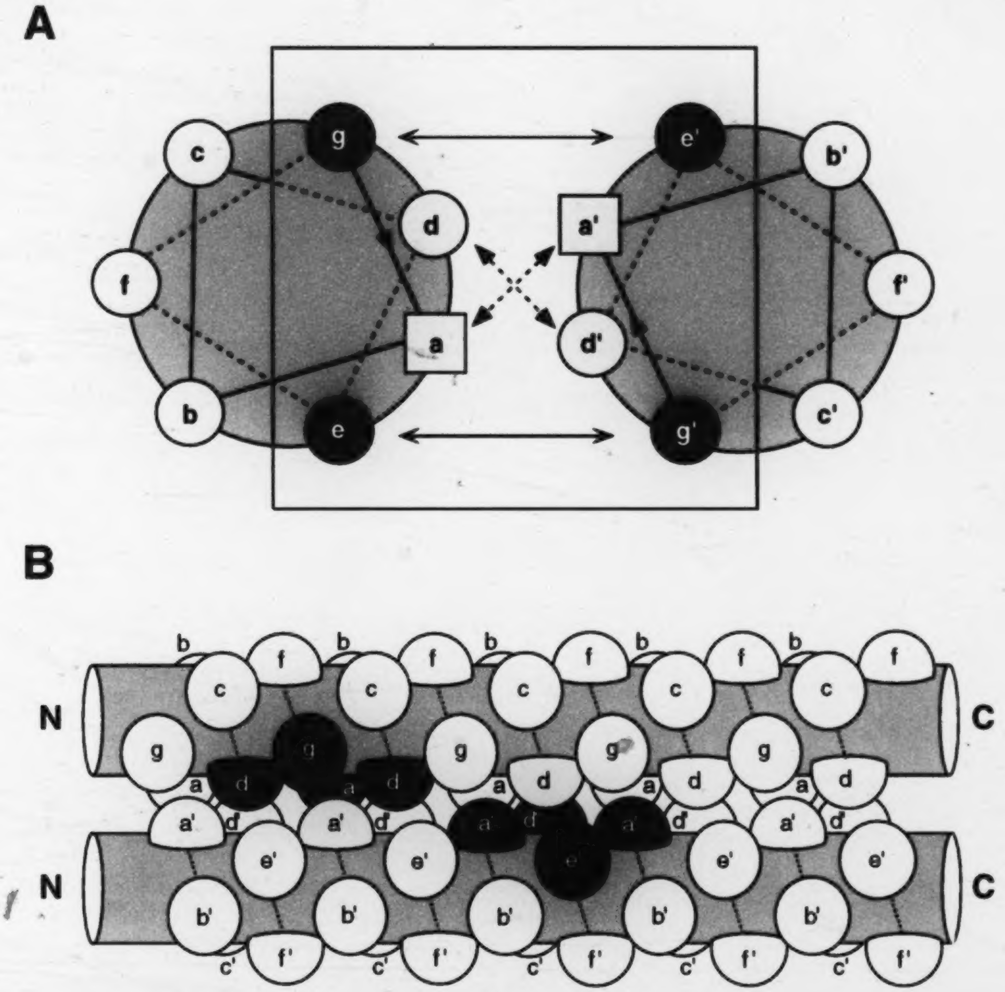

Figure I.3 Schematic illustrations of a parallel two-stranded α-helical coiled-coil. In (**A**), the coiled-coil is viewed in a cross-sectional helical-wheel representation where the direction of polypeptide chain propagation is into the page from N to C terminus. Interchain **a-a'** and **d-d'** (prime indicating a position on the other helix) van der Waals packing interactions between side chains (colored yellow) in the hydrophobic core are depicted with arrows. Potential interhelical interactions between residues at position **g** of one helix (in this case colored red to signify a negatively-charged side chain) and position **e'** of the other helix (colored blue to signify a positively-charged side chain) are also depicted with arrows. Residues that make up the entire dimerization interface are included in the box. In (**B**), the coiled-coil is viewed from the side. N and C refer to the N and C termini, respectively. The "knobs into holes" packing at the dimer interface is depicted. For example, the side chain at position **a'** (colored yellow on the bottom helix) packs into the hole between four residues (colored green) on the upper helix. Similarly, a side chain at position **d** (colored yellow on the upper helix) packs into the hole between four residues (colored green) on the lower helix.

register helix association and stability of coiled-coils (McLachlan & Stewart, 1975; Stone *et al.*, 1975; Talbot & Hodges, 1982). The research in this thesis focusses on interhelical ionic interactions involving positions **e** and **g**.

iii) ***b, c, and f*** *positions*

These heptad positions are solvent exposed and primarily uninvolved in interhelical contacts in two- and three-stranded coiled-coils (Fig I.3) but can have effects on stability due to intrahelical side chain interactions (Scholtz *et al.*, 1993; Zhou *et al.*, 1993c) and intrinsic helical propensities (see below). In a four-stranded coiled-coil, the **b** and **c** residues can contribute to interactions across the subunit interface (Fairman *et al.*, 1996; Harbury *et al.*, 1993). From a functional standpoint, the **b**, **c**, and **f** positions are probably most important in coiled-coils for contributions to interactions with other molecules, such as in tropomyosin, which must interact with troponin-T and actin through its exposed surface (McLachlan & Stewart, 1976; Phillips *et al.*, 1986; Smillie, 1979). In addition, the exposed positions **b**, **c**, and **f** (along with the positions **e** and **g**) also play an important role in maintaining aqueous solubility.

iv) Secondary structural propensities

Secondary structure in proteins is influenced by intrinsic propensities of the amino acid side chains (Chou & Fasman, 1978; Munoz & Serrano, 1994). However, these propensities have modest effects on protein stability. For example, a substitution in the solvent exposed face of a coiled-coil (O'Neil & DeGrado, 1990) or a monomeric amphipathic α-helix (Zhou *et al.*, 1994d) affected stability by less than 1 kcal/mol, suggesting that intrinsic secondary structural propensities only control structure when summed over a significant stretch of residues. Long-range forces often overcome the effects of intrinsic propensities because the burial of hydrophobic surface area generally will be the greatest contributor to the stability of the folded protein (Kuroda *et al.*, 1996; Xiong *et al.*, 1995). Thus, the prediction of secondary structure from statistically-observed secondary-structural preferences of amino acids is generally only correct for at most 60 to

70% of the sequence of an unknown protein structure (Defay & Cohen, 1995). Intrinsic propensities will certainly modulate the stability of a particular secondary structural unit in the context of a folded protein. For example, substitution of a residue with low/high helical propensity into a helical portion of a protein will generally decrease/increase the overall protein stability (Blaber *et al.*, 1994; Myers *et al.*, 1997).

v) supercoiling

The α-helix has a periodicity of about 3.6 residues per turn or 7.2 residues per two turns of the helix. Thus, in a standard α-helix the 3-4 hydrophobic repeat would yield a hydrophobic face that gradually winds around the helix circumference, and dimerization of two such helices would result in divergence of the hydrophobic strips from the interface. Crick (1953) predicted that the helices of a coiled-coil would twist around one another like the strands of a rope in a left-handed fashion to maintain contact between the hydrophobic faces. The twisting (or supercoiling) results in a periodicity of 3.5 residues per turn (along the supercoil axis). The helices of a coiled-coil were also predicted by Crick to cross at about 18°, which is similar to crossing angles found in other helical proteins (Kamtekar & Hecht, 1995). The supercoil pitch varies depending on the oligomerization state from around 150 Å for a dimer to 200 Å for a tetramer (Seo & Cohen, 1993). For example, a low resolution X-ray structure of tropomyosin (Phillips *et al.*, 1986) indicated a pitch of about 140 Å, so that the entire 284 residue coiled-coil makes approximately three complete turns (assuming a 1.5 Å rise per residue along the coiled-coil axis). The curvature of the helices of a coiled-coil results in hydrogen bonds that are shorter in the hydrophobic face and longer in the hydrophilic face, as observed by NMR (Oas *et al.*, 1990). Amphipathic α-helices have been shown to have intrinsic curvature (Zhou *et al.*, 1992d), which favors coiled-coil formation.

vi) X-ray and NMR structural data

A number of X-ray and NMR structures of α-helical coiled-coils have been obtained in recent years. The high resolution (1.8 Å) structure of the 33-residue GCN4 leucine zipper (a short coiled-coil which controls dimerization of the GCN4 bZIP transcription factor) confirmed essentially all of the structural predictions of Crick and subsequent researchers, including "knobs into holes" packing, the 18° crossing angle, the left-handed supercoiling, and the ability of **e** and **g** residues to form interhelical ion pairs (O'Shea *et al.*, 1991). Interestingly, the original paper reported a supercoil pitch of 180 Å, but it was later recalculated to be about 140 Å (Phillips, 1992). A schematic representation of the GCN4 leucine zipper structure is given in Figure I.4.

Subsequent X-ray structures have elucidated the nature of leucine zipper transcription factor-DNA complexes (Ellenberger *et al.*, 1992; Glover & Harrison, 1995; König & Richmond, 1993) and further supported the previous conclusions on coiled-coil structure. A number of synthetic coiled-coil structures have also been determined crystallographically (Gonzalez *et al.*, 1996a, 1996b; Harbury *et al.*, 1993, 1994; Lovejoy *et al.*, 1993; Ogihara *et al.*, 1997), and these have shed further light on the principles of coiled-coil folding and stability, such as the important role of the **a** and **d** positions in determining the oligomerization state (Betz *et al.*, 1995; Harbury *et al.*, 1993). NMR structures of the GCN4 (Saudek *et al.*, 1991) and c-Jun (Junius *et al.*, 1996) leucine zippers were in general agreement with the X-ray structures but emphasized the dynamic nature of the coiled-coil (King, 1996; Mackay *et al.*, 1996).

7) Questions dealt with and aims of the investigation

As mentioned already, interhelical ionic interactions between positions **e** and **g** have been traditionally assumed to play a role in coiled-coil folding and stability. Such interactions could affect coiled-coil stability in two potential ways: (1) specific ionic interactions between **g** and **e'** positions (where the prime indicates a position on the opposing helix) and (2) general long-range electrostatic effects involving the net charge density on the dimerization interface (including all of positions **a**, **d**, **e**, and **g**). Charged residues, which occasionally occur at the **a** and **d** positions, also can contribute to

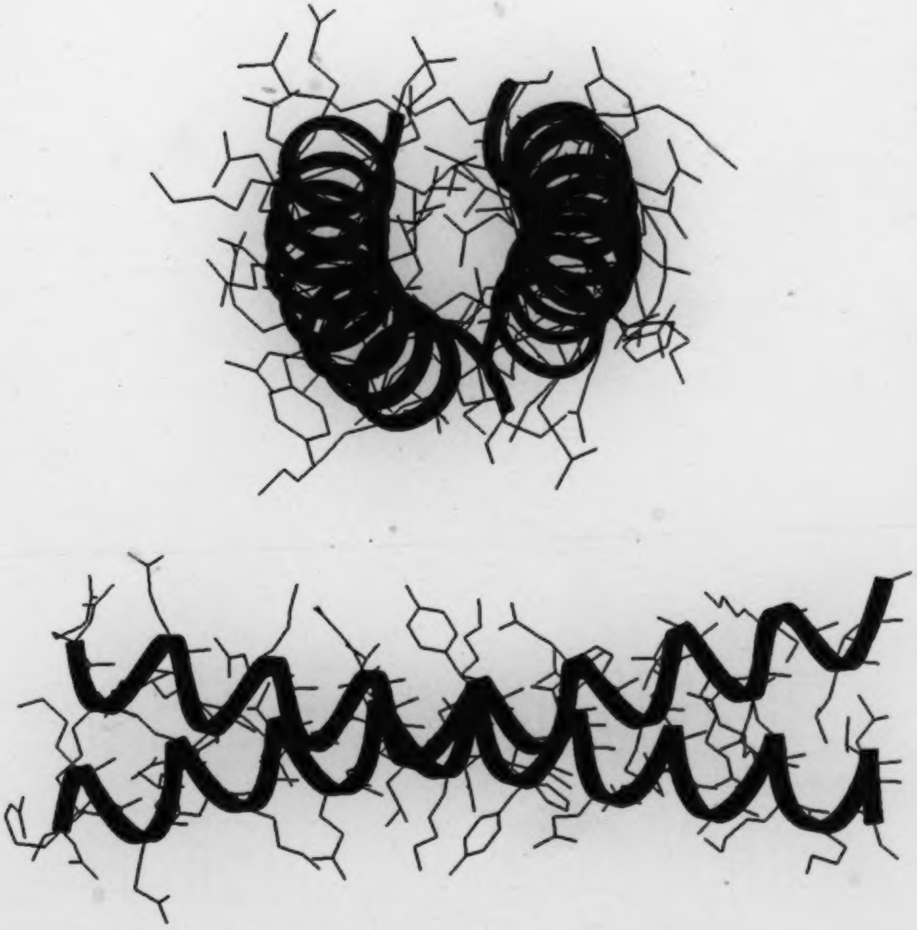

Figure I.4 The 33-residue GCN4 leucine zipper (a two-stranded α-helical coiled-coil) is illustrated in two views in which the helical peptide backbone is highlighted by a ribbon. A view along the superhelix axis from the N terminus (top) illustrates the curved nature and left-handed supercoiling of the helices. The pitch of the superhelical twist of a two-stranded coiled-coil is generally 140-150 Å (there are about 100 residues per repeat of the superhelix). The side view (bottom) clearly shows the approximate 18° crossing angle of the helices. (adapted from the crystal structure coordinates of the GCN4 leucine zipper (O'Shea *et al.*, 1991))

interhelical ionic interactions, both specific and general (Glover & Harrison, 1995; Hu & Sauer, 1992; Lavigne *et al.*, 1995; Schneider *et al.*, 1997).

The role of these electrostatic interactions (both general and specific) has been the subject of a number of studies in recent years of both naturally-occurring coiled-coils and simplified model coiled-coils. It was recently shown that the number of electrostatic attractions and repulsions (both inter- and intrahelical) are correlated with coiled-coil stability (Monera *et al.*, 1994b). From mutational studies the contributions of ionic interactions to coiled-coil stability have been estimated in the range 0.1 to 1 kcal/mol (Krylov *et al.*, 1994; Zhou *et al.*, 1994b, 1993c). Thus, these solvent exposed ion pairs contribute a similarly small energetic effect to that of surface-exposed ion pairs on proteins in general (Dao-pin *et al.*, 1991; Lyu *et al.*, 1992; Sali *et al.*, 1991; Scholtz *et al.*, 1993; Serrano *et al.*, 1990), but a large number of such interactions can potentially add up to exert a large effect on stability.

On the other hand, a number of results have brought the role of ionic interactions in coiled-coils, particularly interhelical attractions, into a great deal of uncertainty. For example, the stabilities of a number of naturally-occurring and synthetic coiled-coils have been observed to be anomalously higher at low pH, where protonation of acidic residues prevents ion pair formation, than at neutral pH (Lowey, 1965; Lumb & Kim, 1995b; O'Shea *et al.*, 1992; Zhou *et al.*, 1994b). The net charge on the molecule also becomes higher at low pH, which should decrease the stability according to classical electrostatic theory. Substitution of hydrophobic residues at the **e** and **g** positions resulted in mutants of increased stability (Hu & Sauer, 1992; Pu & Struhl, 1993; Schmidt-Dörr *et al.*, 1991) proving that ion pairs are not required for maximum stability, and a GCN4 mutant containing Ala and Thr at all **e** and **g** positions was fully transcriptionally functional (Hu *et al.*, 1993), proving the ion pairs play no special *in vivo* functional role. Furthermore, acidic residues (Glu20 and Glu22) were found to be involved in ion pairs to Lys15 and Lys27, respectively, in the X-ray structure of GCN4 (O'Shea *et al.*, 1991), but they did not display the decreased pK_a characteristic of ion pair participation (Lumb & Kim, 1995b).

Other studies have demonstrated an apparent important role for the **e** and **g** positions in coiled-coil dimerization specificity. For example, transcription factors which dimerize through the leucine zipper type of coiled-coil must be able to to choose efficiently from a large variety of potential partners (Baxevanis & Vinson, 1993; Jones, 1990). The Fos and Jun proteins have been shown to preferentially form a heterodimer over either of the respective homodimers by about 1000-fold, apparently due in large part to electrostatic repulsions in the homodimers and attractions in the heterodimer, as well as differences in the interhelical hydrophobic interactions (O'Shea *et al.*, 1992, 1989b; Schuermann *et al.*, 1991). In particular, the dimerization faces (positions **a**, **d**, **e**, and **g**) of the Fos and Jun leucine zippers have charges of -4 and +4, respectively, meaning that either homodimer would incur a penalty due to general charge repulsion while a heterodimer would benefit from an attraction between the opposite net charges (Fig. I.5). Thus, studies of Fos/Jun heterodimerization suggest that general electrostatic effects, as well as specific interactions, are important for allowing two charged helices to associate. Other coiled-coils, such as tropomyosin, have been shown to preferentially heterodimerize, and it seems likely that interhelical electrostatics play a role in those as well (Lehrer *et al.*, 1989; Lehrer & Stafford, 1991).

The formation of ionic attractions versus repulsions has been clearly demonstrated to control hetero- versus homodimerization specificity in synthetic two-stranded coiled-coils where other parts of the molecule, including the hydrophobic core, are kept constant (Graddis *et al.*, 1993; O'Shea *et al.*, 1993; Zhou *et al.*, 1994c). This design concept has been taken advantage of in various applications (Hodges, 1996; Tripet *et al.*, 1996) and has been extended to control heterotrimer (Nautiyal *et al.*, 1995) and heterotetramer (Fairman *et al.*, 1996) formation (although formation of the heterotetramer was controlled by ionic interactions involving positions **b** and **c** rather than **e** and **g**). Interhelical ionic interactions

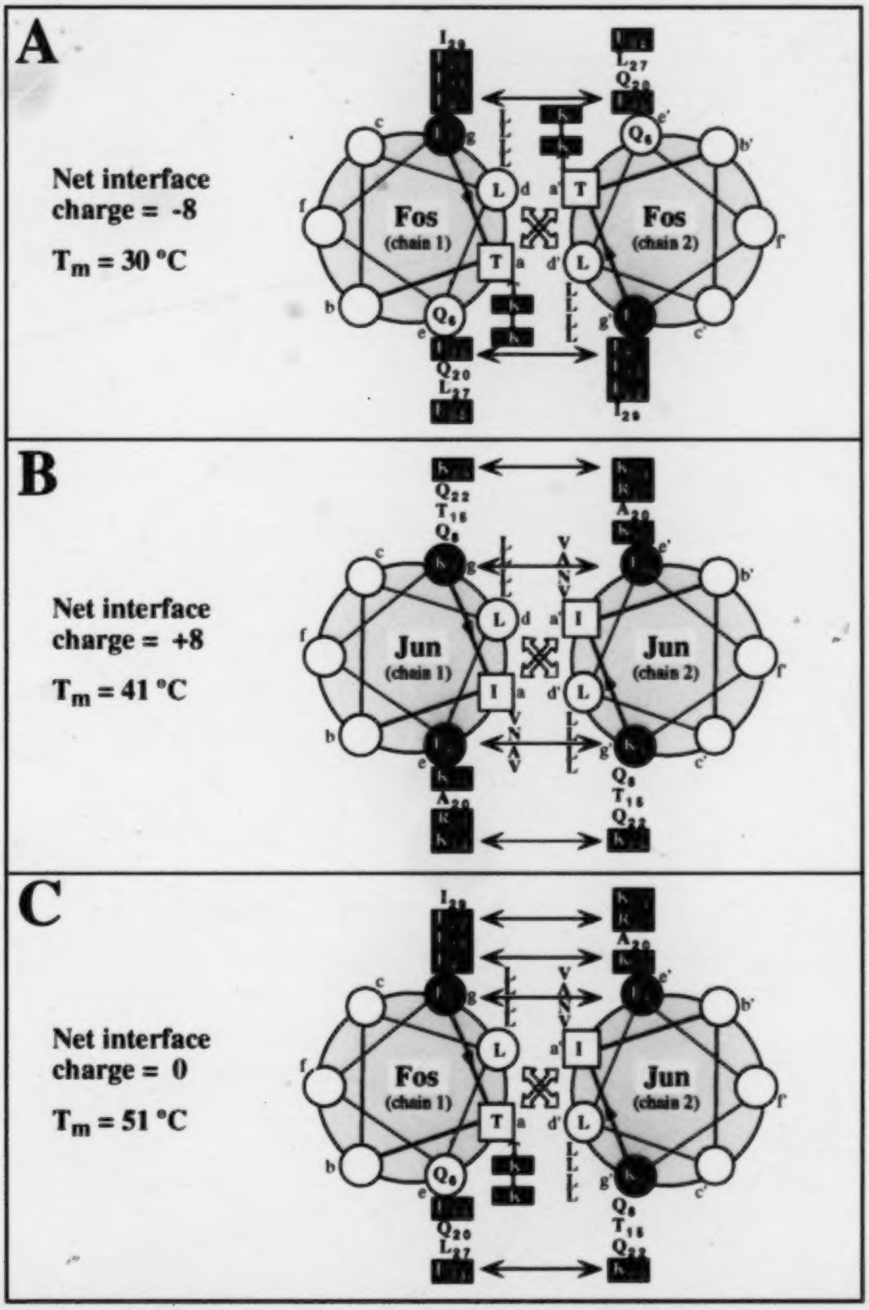
A
Net interface charge = -8
T_m = 30 °C
Fos (chain 1)
Fos (chain 2)
I_{28}
L_{27}
Q_{20}
Q_6
L
T
c
g
d
a
f
b
e
a'
d'
e'
b'
f'
c'
g'
B
Net interface charge = +8
T_m = 41 °C
Jun (chain 1)
Jun (chain 2)
Q_{22}
T_{15}
Q_8
A_{20}
V
A
N
L
I
C
Net interface charge = 0
T_m = 51 °C
Fos (chain 1)
Jun (chain 2)

Figure I.5 Helical wheel representations of the Fos (**A**) and Jun (**B**) homodimeric coiled-coils and the Fos/Jun heterodimer (**C**). Glu (red) and Arg + Lys (blue) residues at the dimer interface are highlighted, and predicted specific **g-e'** ionic attractions and repulsions are indicated with arrows. The temperature denaturation midpoint (T_m) values were obtained on synthetic peptides that were disulfide-bridged at the N terminus (via a Cys-Gly-Gly extension) in a pH 7, 10 mM phosphate, 50 mM NaCl buffer (O'Shea *et al.*, 1992).

have also been shown to potentially control antiparallel versus parallel chain alignment (Monera *et al.*, 1994a). It has been suggested that repulsions in the homodimer rather than attractions in the heterodimer are the dominant force in determining specificity (O'Shea *et al.*, 1992, 1993; Vinson *et al.*, 1993) although other results suggest a direct stabilizing role for the attractions is important (Fairman *et al.*, 1996). Thus, the exact mechanism by which these interhelical ionic interactions control folding and the relative contributions of attractions and repulsions is still not completely established.

Computer modelling (Cregut *et al.*, 1993; McLachlan & Stewart, 1975; Nilges & Brunger, 1993), X-ray structure (Ellenberger *et al.*, 1992; O'Shea *et al.*, 1991) and mutagenesis (Hu *et al.*, 1993; Schmidt-Dörr *et al.*, 1991) studies all suggest that specific interactions occur preferentially in one of two possible directions (**g-e'** rather than **e-g'**). In Chapter III of this thesis (Kohn *et al.*, 1995a), strong evidence is shown to support the conclusion that specific **g-e'** interactions occur and control coiled-coil stability, but **e-g'** interactions are absent. In this case, the destabilization resulting from Glu-Glu electrostatic repulsions was probed and quantified.

Heterodimerization of Fos/Jun and other coiled-coils has suggested that both general electrostatic effects and specific interactions are important for allowing folding to occur. One possible implication is that zero net charge at the coiled-coil interface will lead to optimum stability. However, these native sequences are not ideal for studying the effects of interhelical interactions on folding due to the complexity of interactions present. In Chapter IV of this report (Kohn *et al.*, 1995b), the role of net negative charge and specific Glu-Glu repulsion on coiled-coil folding is probed in a systematic fashion in our model coiled-coil. The question to be answered is how much net charge or how much charge repulsion is allowed before coiled-coil structure is abolished. Some qualitative experiments regarding the relative roles of the general and specific components of the charge repulsions in the resulting stability were also carried out. The ability to modulate the electrostatic effects with buffer conditions (pH and salt) was another important aspect of the study presented in Chapter IV.

In Chapter V (Kohn *et al.*, 1997b), a Gln to Glu substitution was 'walked' along the coiled-coil **e** and **g** positions, in order to probe for structural differences between the **e** and **g** positions and between the different heptads of the coiled-coil as well as to probe for interactions between charged residues and the helix macrodipole (see introduction to Chapter V), which previous results (Chaper IV) had suggested could play a significant role in coiled-coil stability.

The controversial issue of the role of interhelical ion pairs in coiled-coil stability is explored in Chapters VI (Kohn *et al.*, 1997c) and VII (Kohn *et al.*, 1998c). In Chapter VI, a variety of salts were used to perturb the stability of coiled-coils containing interhelical, intrahelical, or no ion pairs (the last as a control for the intrinsic changes in stability caused by the salt). The specific effects of certain salt ions on stability and their proposed mechanism of action help to give insight into the nature of ion pairs in coiled-coils. The origin of the anomalous increase observed in coiled-coil stability at low pH despite the loss of ion pairs is also addressed. In depth double mutant cycle analyses in Chapter VII, in which the effect of orientation on Lys-Glu interhelical ion pairs was probed, were aimed at gaining further insight into the mechanism of stabilization and destabilization of coiled-coils by **g-e'** ionic interactions. An observation of the degree of positional dependence and additivity that occurs for **g-e'** ion pairs was also sought.

The last two chapters (Chapters VIII and IX, Kohn *et al.*, 1998a, 1998b) deal with the engineering of specific metal ion binding sites in proteins. The regulation of structure, stability, and activity by metal ion binding is common in native proteins (Findlay *et al.*, 1992; Ikura, 1996; Nakamura, 1996; Strynadka & James, 1989; Volbeda *et al.*, 1996; Williams, 1995) and has been actively pursued in the engineering of both native and *de novo* designed proteins and peptides (Hellinga, 1996; Lu & Valentine, 1997; Matthews, 1995b; Regan, 1993, 1995). The goal here was to alter the stability (Chapter VIII, Kohn *et* *al.*, 1998a) and structure (Chapter IX, Kohn *et al.*, 1998b) of a synthetic *de novo* designed coiled-coil peptide by binding of a metal ion at specific sites. Such design studies will help set a foundation for applications of synthetic proteins with desired spectroscopic and chemical properties, based on the unique characteristics of the bound metal that can be modulated by the protein environment.

It is useful at this point to reemphasize the goals, in general terms, of the coiled-coil research. In other words, what do we hope to accomplish in the long run from detailed studies of coiled-coil stability:

1) A quantitative understanding of the contributions of various noncovalent forces to protein folding and stability. The studies presented here add to other studies on coiled-coil stability to generate a wealth of information on protein folding that can be applied along with information from other protein folding studies to *de novo* design.
2) The ability to design coiled-coils with desired stability characteristics under given solution conditions for particular novel applications
3) A better understanding of the structure-function relationship for the myriad of naturally-occurring coiled-coils many of which control important cellular processes and could be potential drug targets.
4) The development of synthetic proteins whose stabilities and structures can be modulated by the conditions (pH, salt, or metal binding) is a step toward the design of synthetic proteins which can be regulated or optimized to operate under a desired condition.

The work presented in this thesis adds to the overall goals listed above through its dissection of the role of the **e** and **g** positions in coiled-coil folding and stability.

CHAPTER II

MATERIALS AND METHODS

A. Materials

1. Chemicals and reagents

Unless otherwise stated, all chemicals and solvents used were analytical grade. Most of the chemicals used in this project are available from common sources, so suppliers are listed below only for uncommon and some other reagents that were used (Table II.1). All solutions were prepared in water that was run through a Milligen Milli-Q or Corning Mega-Pure distillation-deionization purification system. DIEA, DCM, and TFA were distilled prior to use in peptide synthesis.

Table II.1 List of reagents

Reagent	**Supplier(s)**
Amino acids (protected for peptide synthesis)	Advanced Chemtech, Louisville, KY Bachem, Torrance, CA Novabiochem, San Diego, CA Peninsula Laboratories Inc., Belmont, CA
DCC	Advanced Chemtech, Louisville, KY
DCM	BDH Inc., Toronto, ON
DIEA	Caledon Laboratories, Georgetown, ON
DMF	General Intermediates of Canada, Edmonton, AB
Fmoc-Gla(OtBu)-OH	Peninsula Laboratories Inc., Belmont, CA
GdnHCl (ultra pure)	ICN Biomedicals Inc., Aurora, OH
HF	Matheson Gas Products, Edmonton, AB
HOBt	Advanced Chemtech, Louisville, KY

Reagent	**Supplier(s)**
$LaCl_3 \cdot 6H_2O$	Fisher Scientific, Fairlawn, NJ
MBHA resin	Bachem, Torrance, CA
NMP	General Intermediates of Canada, Edmonton, AB
Rink amide resin	Novabiochem, San Diego, CA
TFA	General Intermediates of Canada, Edmonton, AB
TFE	Aldrich Chemical Co., Milwaukee, WI
Urea (ultra pure)	Life Technologies Inc., Gaithersburg, MD
$YbCl_3 \cdot XH_2O$	Ventron Alfa Division, Danvers, MA

B. Methods

1. Peptide synthesis

Peptide synthesis can be performed by two general types of procedures: the classical solution-phase method and solid-phase peptide synthesis (SPPS), based upon the method developed by Merrifield (1963). In SPPS, the growing peptide chain is attached to an insoluble support matrix (polymeric resin bead), which allows easy washing away of excess reagents and reaction byproducts at each synthesis step. SPPS is convenient for most peptide synthesis because of its efficiency, speed, and successful automation. Solution-phase synthesis is still used, however, in large-scale synthesis and specialized applications. Some good general references for solid-phase peptide synthesis include (Bodanszky, 1988; Fields, 1997; Novabiochem, 1997; Stewart & Young, 1984).

A general outline of the SPPS procedure is given in Figure II.1. SPPS always is carried out in the C- to N-terminal direction and consists of four major steps: anchoring, deprotection, coupling, and cleavage (release). The amino acids used in SPPS are

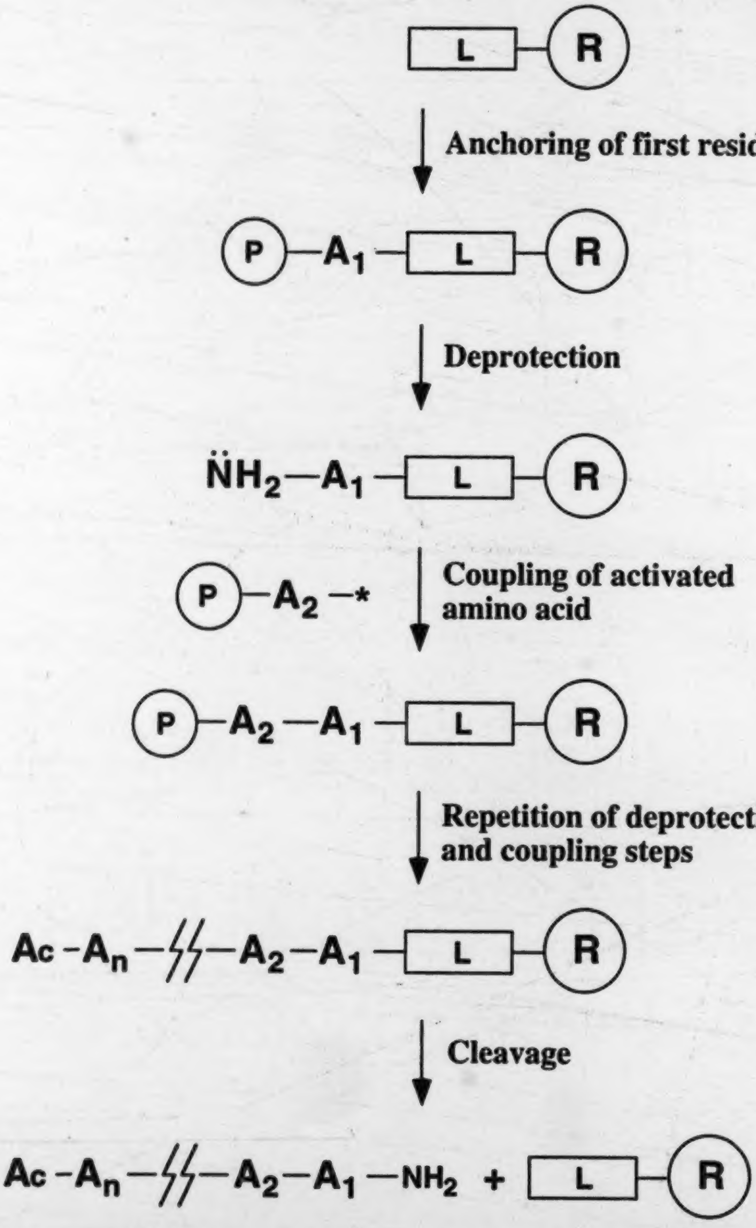
L
R
Anchoring of first residue
P
A1
Deprotection
NH2
Coupling of activated amino acid
A2
*
Repetition of deprotection and coupling steps
Ac
An
Cleavage
NH2
+

Figure II.1 A general outline of solid-phase peptide synthesis. The insoluble polymeric resin support is labelled **R**, the chemical linker or handle between the resin and peptide is labelled **L**, amino acids are labelled $\mathbf{A_1}$, $\mathbf{A_2}$, ... , $\mathbf{A_n}$, and the N^{α}-protecting group is labelled **P**. The C-terminal group after cleavage is shown here as an amide but can also be a carboxylate depending on the linker used. The asterisk (*) denotes preactivation of the C^{α}-carboxylate group. The N-terminal group after cleavage is shown here as an N^{α}-acetyl group but can also be left as a free amino group or otherwise functionalized.

derivatized at the N^{α} group and any reactive side chain functionalities to prevent side reactions during formation of the peptide bond.

The first step is anchoring of the first (C-terminal) amino acid to the resin through a linker moiety that is preattached to the resin. The type of linker used will determine the final C-terminal group after release (cleavage) from the resin (either a free carboxylate or amide C terminus can be readily generated) and the conditions required for cleavage (Songster & Barany, 1997). The peptides in the current study were all synthesized with a C-terminal amide, which required the use of a linker that presents an amino moiety that can be directly reacted (coupled) with the carboxylate group of the first amino acid to form an amide bond.

The next step in peptide synthesis is deprotection of the N^{α} group of the amino acid anchored to the resin to allow peptide bond formation with the subsequent amino acid residue. Currently, two types of N^{α}-protecting strategies are commonly used. These employ the t-Boc (tert-butyloxycarbonyl) and Fmoc (9-fluorenylmethoxycarbonyl) groups, which are acid and base labile, respectively. t-Boc is removed with TFA, followed by neutralization with a tertiary amine, usually DIEA; Fmoc is removed with a secondary amine, usually piperidine (Fig. II.2).

Coupling involves amide bond formation with the newly deprotected N^{α} group on the resin and the activated carboxylate group of the next N^{α}-protected amino acid to be attached. A number of reagents are currently available for both *in situ*- and preactivation of the amino acid (Albericio & Carpino, 1997; Novabiochem, 1997). In the current study, the amino acids were all preactivated to form either symmetric anhydrides or activated HOBt-esters. Formation of both activated species involved the use of the activating agent DCC (dicyclohexylcarbodiimide), as shown in Figure II.2.

Repetition of the deprotection and coupling steps, with washing away of excess reagent and byproducts after each step, allows for stepwise peptide chain elongation. The key to a successful peptide synthesis is very efficient coupling at each step. With an average coupling efficiency of X% and n amino acid residues, the final purity would be

a) TFA deprotection of t-Boc group

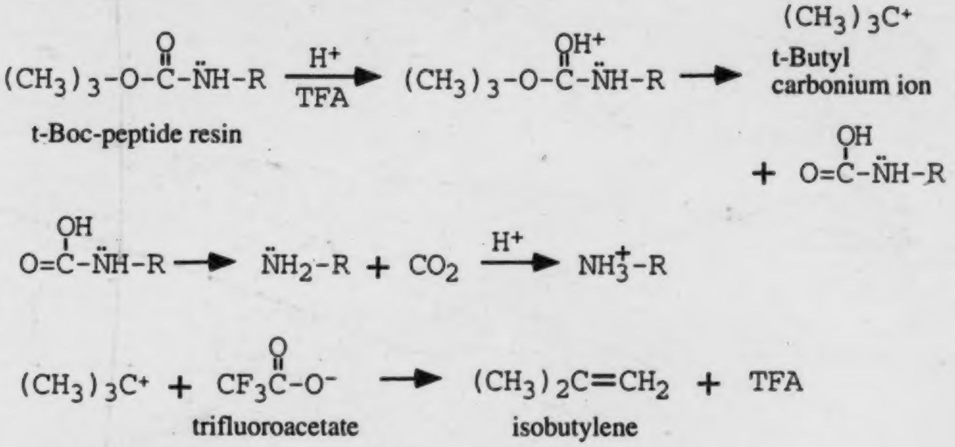

$$(CH_3)_3\text{-O-}\overset{O}{\overset{\|}{C}}\text{-}\ddot{N}H\text{-R} \xrightarrow[TFA]{H^+} (CH_3)_3\text{-O-}\overset{OH^+}{\overset{\|}{C}}\text{-}\ddot{N}H\text{-R} \longrightarrow (CH_3)_3C^+ + O{=}\overset{OH}{\overset{|}{C}}\text{-}\ddot{N}H\text{-R}$$

$$O{=}\overset{OH}{\overset{|}{C}}\text{-}\ddot{N}H\text{-R} \longrightarrow \ddot{N}H_2\text{-R} + CO_2 \xrightarrow{H^+} NH_3^+\text{-R}$$

$$(CH_3)_3C^+ + CF_3\overset{O}{\overset{\|}{C}}\text{-}O^- \longrightarrow (CH_3)_2C{=}CH_2 + TFA$$

t-Boc-peptide resin
t-Butyl carbonium ion
trifluoroacetate
isobutylene

b) piperidine deprotection of Fmoc group

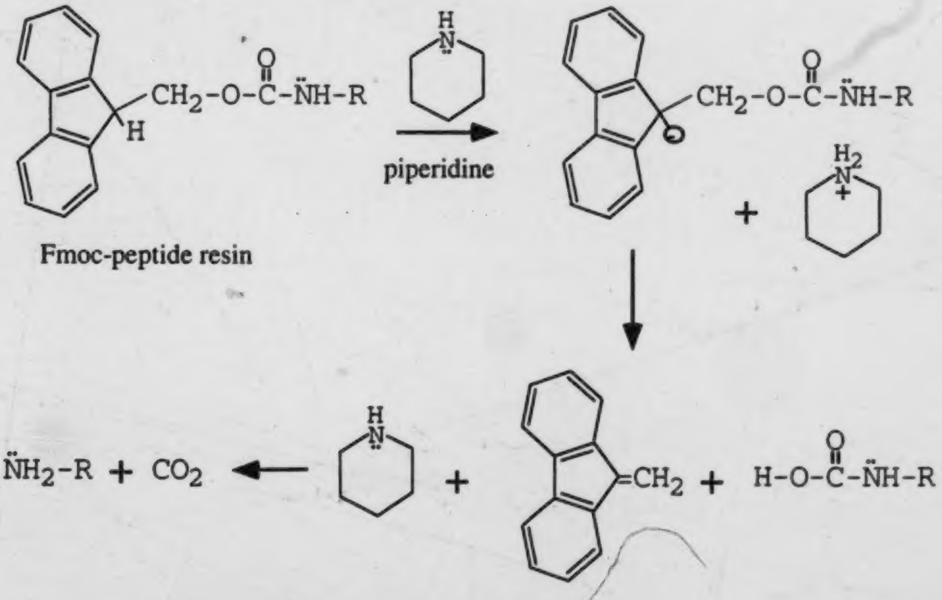

piperidine
Fmoc-peptide resin
$\ddot{N}H_2$-R + CO_2
=CH_2
H-O-C-NH-R

Figure II.2 **(continued on next page)**

c) amino acid activation

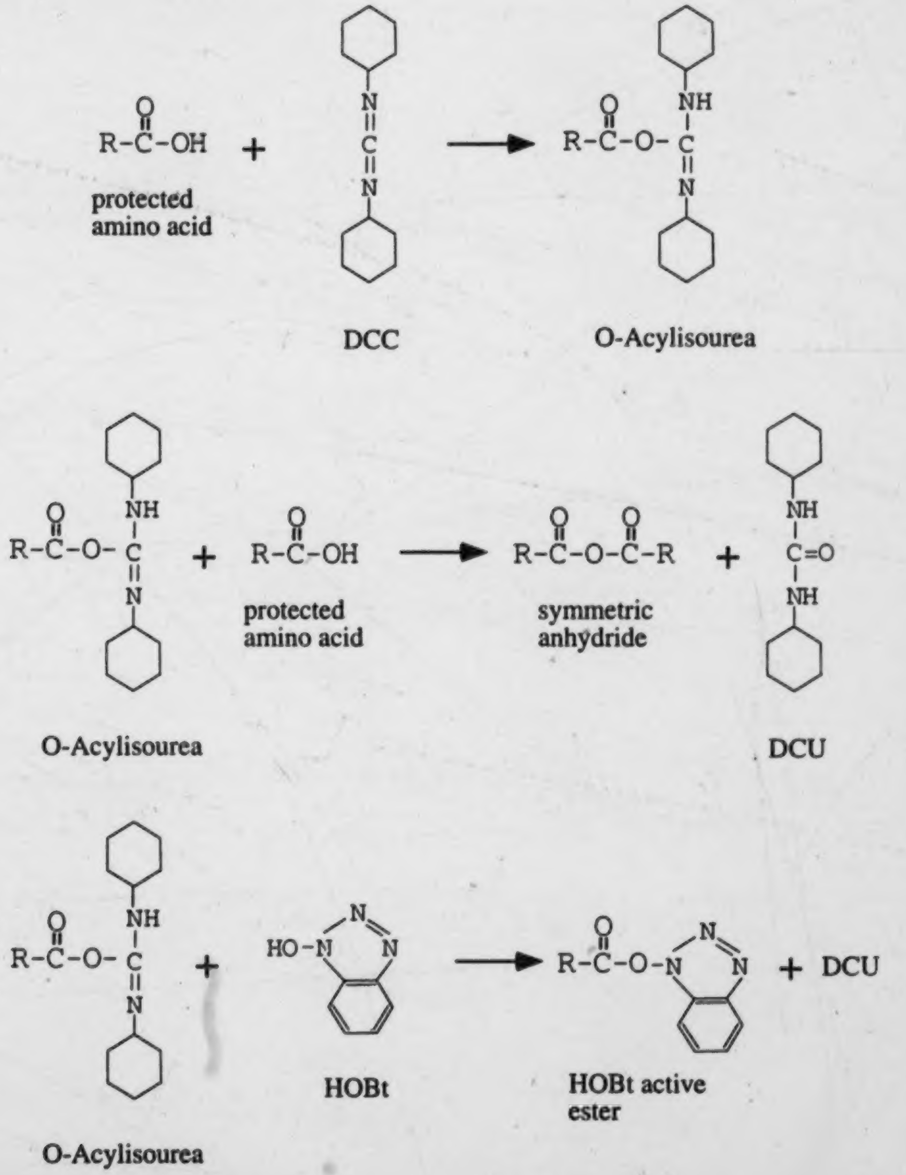
R-C(=O)-OH
+
protected amino acid
DCC
O-Acylisourea
R-C(=O)-O-C(=N)-NH
symmetric anhydride
R-C(=O)-O-C(=O)-R
DCU
C=O
HO-N
HOBt
HOBt active ester
+ DCU

Figure II.2 Examples of reactions involved in SPPS. **a)** acid catalyzed removal of the t-Boc group. **b)** base-catalyzed removal of the Fmoc group. **c)** DCC activation of the amino acid to a symmetric anhydride or HOBt active ester.

$(X/100)^n$ x 100%. For example, 95% coupling over 20 residues would yield a final purity of only 36%. To improve the success of the synthesis, the peptides in this study were double-coupled at each step to maximize the reaction completion and the remaining unreacted amino groups were capped with acetic anhydride at each reaction cycle. This latter procedure eases the purification of the final product because the truncated peptides that result are generally more easily separated from the product of interest than are the deletion peptides that often result when capping is not employed.

Once the peptide chain is synthesized, the final N-terminal group can be determined. This is often left as a free amine but in the current study was acetylated once again by reaction with acetic anhydride. The peptide is then cleaved from the resin with the procedure used depending on the type of synthesis strategy (t-Boc or Fmoc). t-Boc synthesis requires a linkage to the resin that is stable to TFA and must be cleaved with the strong acid anhydrous HF in a specially-designed sealed apparatus. Fmoc synthesis allows use of linkers that are conveniently cleavable with moderate strength acid (TFA) under atmospheric conditions. In both cases, the protecting groups on functionalized amino acid side chains are removed simultaneously with cleavage from the resin. These protecting groups are released as carbonium ions which must be trapped by a 'scavenger' added to the cleavage mixture to prevent irreversible reattachment to the peptide. Anisole is most commonly used for this purpose. A reducing agent, such as 1,2-ethanedithiol (EDT), is also added to the cleavage to prevent thiol oxidation in peptides containing Cys (as do the peptides in the current study).

All the peptides in this study were synthesized by the solid-phase method (Erickson & Merrifield, 1976) on an Applied Biosystems automated peptide synthesizer model 430A or 431A (Foster City, CA) using small scale 0.1 mmol cycles. For each peptide that was prepared, either the t-Boc or Fmoc strategies was used, with double coupling at each step. t-Boc synthesis was performed starting with 4-methylbenzhydrylamine (MBHA) copoly-(styrene-1% divinyl benzene) resin (0.74 mmol of NH_2/g of resin) (Bachem, Torrance, CA), and Fmoc synthesis was carried out using Rink amide [4-(2',4'-dimethoxyphenylaminomethyl)phenoxy] copoly-(styrene-1% divinyl benzene) resin (0.6 mmol of NH_2/g of resin) (Novabiochem, San Diego, CA). For t-Boc synthesis, side chain protecting groups were 2-ClZ for Lys, Bzl for Glu, and 4-MeBzl for Cys. For Fmoc synthesis, side chain protecting groups were t-Boc for Lys, t-Bu for Glu, and Trt for Cys and Gln (Fig. II.3).

t-Boc deprotection was carried out in 30% trifluoroacetic acid - 70% dichloromethane (DCM) for 20 min, and neutralization was done in 25% diisopropylethylamine (DIEA) - 75% N-methylpyrrolidinone (NMP) or dimethylformamide (DMF) for 5 min. Fmoc deprotection was carried out in 20% piperidine - 80% NMP for 15 min.

Amino acids to be coupled were activated by one of two methods. The formation of symmetric anhydrides was accomplished by the reaction of 1 mmol of t-Boc protected amino acid with 0.5 mmol of DCC, resulting in 0.5 mmol of symmetric anhydride (a five-fold excess) while HOBt esters were generated from 1 mmol each of amino acid, DCC, and HOBt, resulting in 1.0 mmol of HOBt ester (a ten-fold excess). In both cases, the activation procedure is complete in about 30 min. The DCU precipitate from the activation process is filtered out in the activation compartment and dissolved and washed away with methanol. The symmetric anhydride is generally more reactive but HOBt-esters are necessary with Gln and Asn that are unprotected on the side chain to prevent dehydration. In both cases, the activation is performed on the ABI synthesizer in a separate activation compartment, and the mixture is then added to the reaction vessel containing the peptide resin.

Coupling was generally allowed to proceed for 35 to 50 min on the standard cycles (these can be modified to extend the time). In the longer coupling times, 15% DMSO was present for the last 15 min to increase coupling efficiency because DMSO acts as a structure breaker to prevent aggregation of the growing peptide chains on the solid support

A) t-Boc chemistry

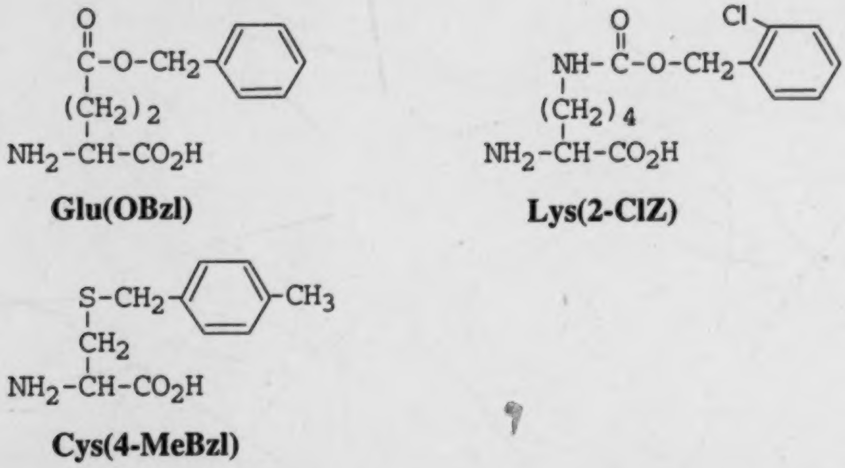
Glu(OBzl)
Lys(2-ClZ)
Cys(4-MeBzl)

B) Fmoc chemistry

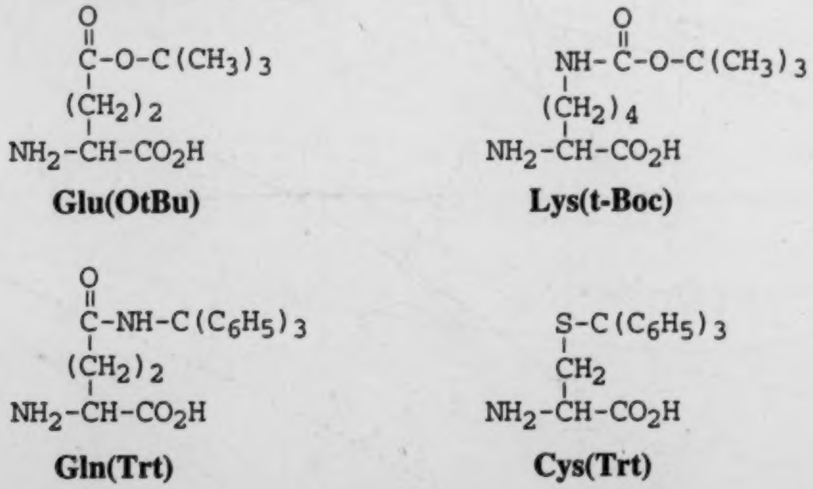
Glu(OtBu)
Lys(t-Boc)
Gln(Trt)
Cys(Trt)

Figure II.3 Side-chain protecting groups used in t-Boc (A) and Fmoc (B) synthesis strategies are shown attached to the amino acid structures. Abbreviations are: Bzl, benzyl; 2-ClZ, 2-chlorobenzyloxycarbonyl; 4-MeBzl, 4-methylbenzyl; tBu, *tert*-butyl; t-Boc, *tert*- butyloxycarbonyl; Trt, trityl (triphenylmethyl)

(particularly due to hydrogen bonds), which could block interaction of the deprotected amino terminus with activated amino acid. Double coupling was performed at each step with the second amino acid activation occurring concurrently with coupling of the first activated amino acid batch. Coupling was performed in either NMP or DMF as the primary solvent. Both are polar, aprotic hydrogen-bonding solvents that are used in SPPS primarily because of their ability to solvate peptides, and both have their advantages. DMF is slightly better for peptide chain solvation, while NMP appears to have slighly better ability to swell most peptide synthesis resins to maximize accessibility of the immobilized peptide chains to reagents. For coupling of HOBt-esters 5% DIEA was added for the last 5 min of coupling (free HOBt released during the coupling reaction is a weak acid that can protonate unreacted amino groups). After coupling, acetic anhydride capping of unreacted chains was employed at each cycle (10% acetic anhydride / 5% DIEA / 85% DMF or NMP for 5 min). Difficult coupling steps or coupling of specialty amino acids (in particular Gla in Chapter IX) was assessed by a quantitative ninhydrin test (Kaiser *et al.*, 1970) in which a purple color results from reaction between free amino groups and ninhydrin.

The peptides synthesized by t-Boc strategy were cleaved from the resin by reaction with HF (20ml/g resin) containing 10% anisole and 2% EDT for 1.5 hours at -5°C (in an ice bath containing NaCl to depress the freezing point) on a type 1B HF-Reaction Apparatus (Peninsula Laboratories Inc., Belmont, CA). The HF was removed under vacuum, and the resin was washed with diethyl ether to remove the cleaved side-chain protecting groups and other nonpolar byproducts of the cleavage (the cleaved peptide being polar remains noncovalently-associated with the resin). Peptides were extracted from the resin with glacial acetic acid and the extract was lyophilized. Peptides synthesized via Fmoc strategy were cleaved in a mixture of 95% TFA, 2.5% distilled-deionized water and 2.5% EDT at room temperature for 1.5 hours (10 mL of reaction mixture per 0.1 to 1.0 g of peptide-resin) in a round-bottomed flask. The peptide-resin and cleavage mixture were cooled to 0°C before mixing. The reaction mixture was filtered from the resin and the resin was washed with an additional 2 mL TFA and 10 mL DCM. The combined filtrate was then concentrated on a rotary evaporator to less than 2 mL. The peptide was precipitated by addition of 50 mL of cold anhydrous diethyl ether and filtered out on a fine-porosity sintered-glass funnel. The peptide was then dissolved in glacial acetic acid and lyophilized.

2. *Peptide purification*

The crude peptides were purified by reversed-phase HPLC on a Varian 5000 (Varian, Walnut Creek, CA) or a Waters Deltaprep 4000 (Millipore, Milford, MA) liquid chromatograph system using a Synchropak RP-4 preparative C8 column (250 X 21.2 mm internal diameter (I.D.), 6.5 µm particle size, 300 Å pore size) (Synchrom, Lafayette, IN). Flow rate was 5 ml/min with a linear AB gradient of 1% B/min from 0 to 25% B followed by a linear AB gradient of 0.2% B/min thereafter for elution of the peptide, where solvent A was 0.05% TFA/water and solvent B was 0.05% TFA/ acetonitrile (see Burke *et al.*, 1991). The major product was generally eluted between 50 and 60 min after starting the gradient program. Purity of the peptides was verified by analytical RP-HPLC on a Zorbax SB 300 C8 column (250 X 4.6 mm I.D., 5 µm particle size, 300 Å pore size) (Rockland Technologies, Wilmington, DE) on a Hewlett Packard HP1090 Series II chromatograph (Avondale, PA) with a linear AB gradient of 2% B/min and 1 ml/min flowrate and with solvents A and B the same as described for the preparative HPLC.

3. *Peptide oxidation*

The peptides were subjected to air oxidation in 0.1 M NH_4HCO_3 pH 8.5 at room temperature, with stirring, in an open vial to form the disulfide-bridged two-stranded peptides. The reaction typically was complete in 10-12 hours as determined by a reduction of the retention time on reversed-phase HPLC of 4-5 min (with a gradient rate of 2% B/min) (Lee *et al.*, 1991). In the rare case where the oxidized and reduced peptides elute at the same time, the presence of oxidized peptide can be determined by reaction of the free sulfhydryl group of the reduced form with N-ethyl maleimide (NEM), which increases the retention time; the oxidation is complete when there is no reaction with NEM (Lee et al., 1991). Peptides containing many interhelical ionic repulsions were slow to oxidize and were oxidized in the presence of 6 M GdnHCl, which screened the electrostatic effects. It was found that the standard air oxidation technique at pH 8.5 resulted in decarboxylation of Gla residues (used in peptides in Chapter IX). Thus for these peptides, disulfide-bridged peptides were formed from purified reduced peptide by oxidation in a mixture containing 30% DMSO, 67% water, and 3% acetic acid at pH 4, stirred under nitrogen overnight (18-20 hrs) (Tam *et al.*, 1991).

Oxidized two-stranded peptides were further purified to > 95% purity on a Zorbax 300-SB C8 semipreparative column (250 X 9.4 mm I.D., 5 μm particle size, 300 Å pore size) (Rockland Technologies, Wilmington, DE) using a linear AB gradient of 1% B/min from 0 to 20% B and a 0.2% B/min gradient rate thereafter with the same 0.05% TFA in water/acetonitrile solvent system as above and a flow rate of 2 ml/min. Chromatograms of a typical crude product and final purified, oxidized peptide are shown in Figure II.4

4. Peptide primary structure characterization

In addition to analytical HPLC, the purified peptides were characterized by amino acid analysis: peptides were hydrolyzed in 6 N HCl containing 0.1% (v/v) phenol at 160°C for 1.5 hours in sealed evacuated tubes. Amino acid analyses were performed on a Beckman Model 6300 amino acid analyzer (Beckman, San Ramon, CA). The correct molecular weights of the peptides were confirmed by plasma-desorption time-of-flight mass spectrometry on a BIOION-20 Nordic (BIOION, Uppsala, Sweden) or by electrospray quadrupole mass spectrometry on a Fisons VG Quattro (VG Biotech, Cheshire, England). Electrospray mass spectra of the reduced and oxidized (disulfide-bridged) forms of a peptide are shown in Figure II.5 (note the presence of additional peaks in the spectrum of the oxidized form).

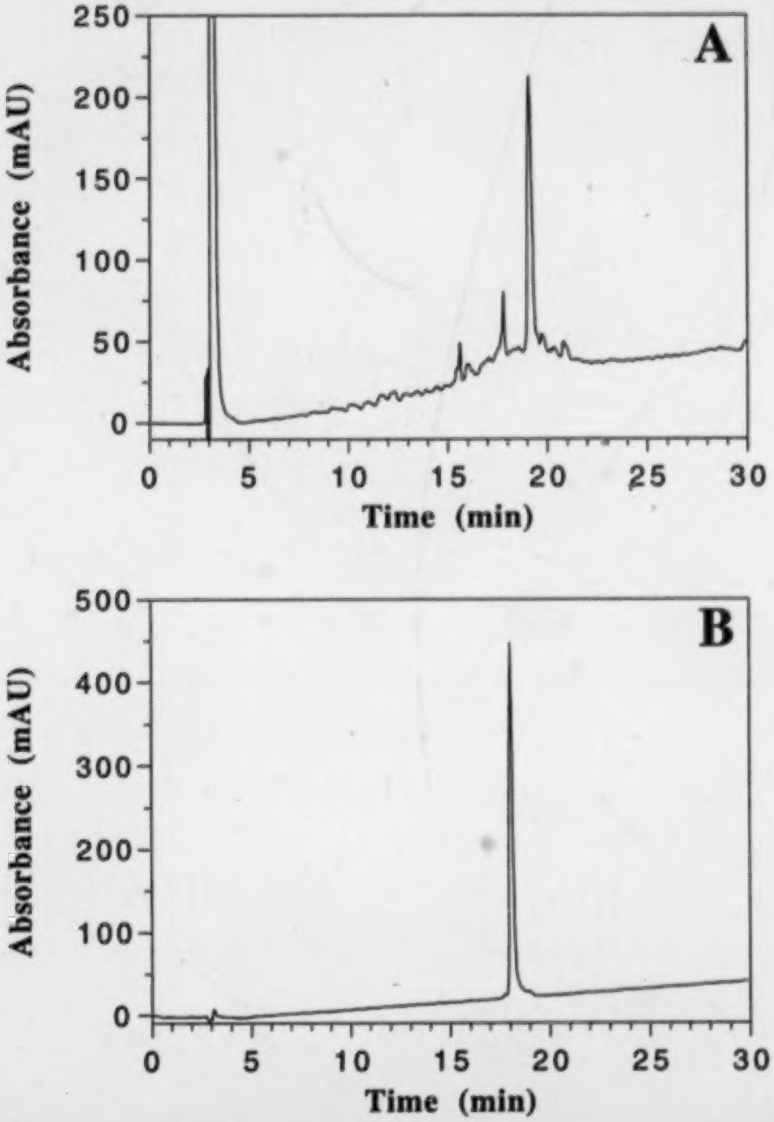

Figure II.4 Reversed-phase chromatograms of a crude 35-residue coiled-coil peptide after lyophilization (**A**) and the final oxidized peptide after purification (**B**). Note the oxidized peptide has a lower retention time than the reduced form. Eluting peptides were detected at 210 nm on a Hewlett-Packard HP1090 Series II chromatograph (Avondale, PA) using a Zorbax SB-300 C8 column (250 X 4.6 mm I. D., 5 µm particle size, 300 Å pore size; Rockland Technologies, Newport, DE). Run conditions were: linear AB gradient (2% B/min), where eluent A is 0.05% aqueous TFA (pH 2) and eluent B is 0.05% TFA in acetonitrile; flow rate, 1 ml/min; room temperature. The sequence of the peptide is: Ac-QCGALKK-(QVGALKK)$_4$-amide.

Figure II.5 Electrospray mass spectra of the 35-residue native peptide in the reduced (**top**) and oxidized, disulfide-bridged (**bottom**) forms. Spectra were collected in positive mode from an eluent solution of 50:50 (v/v) water and acetonitrile containing 0.1% TFA. The mass spectrum (shown on the right) contains several peaks at different mass to charge ratios (the mass spectrometer measures the mass to charge ratio rather than the absolute mass). The polypeptide chain contains five Lys residues and each can pick up a proton. For Nr (**top**) the +5 peak (at 738.5 due to the ion with five positive charges) is most abundant, followed by the +4 peak (at 922.9), and a small +3 peak (at 1230.3). The data is transformed to deconvolute the mass/charge axis to absolute mass, as shown on the left. The calculated mass is an average based on all the peaks present in the mass spectrum. The deconvoluted mass of 3687.79 for Nr is very close to the theoretical value of 3687.38. For the disulfide-bridged peptide Nx (**bottom**), the mass is approximately doubled, so the peaks at roughly 738, 922, and 1230 are the +10, +8, and +6 peaks (rather than the +5, +4, and +3 peaks, as for Nr). In addition, the spectrum of Nx contains peaks not present in that of the reduced peptide at odd charges (+5, +7 and +9 charges yielding mass/charge ratios of 1475.98, 1054.3 and 820.3, respectively). These peaks are therefore characteristic to Nx *versus* Nr. Note also the mass of Nx, 7373.4, is twice the mass of Nr, 3787.79, less two mass units due to the loss of two protons upon disulfide bond formation.

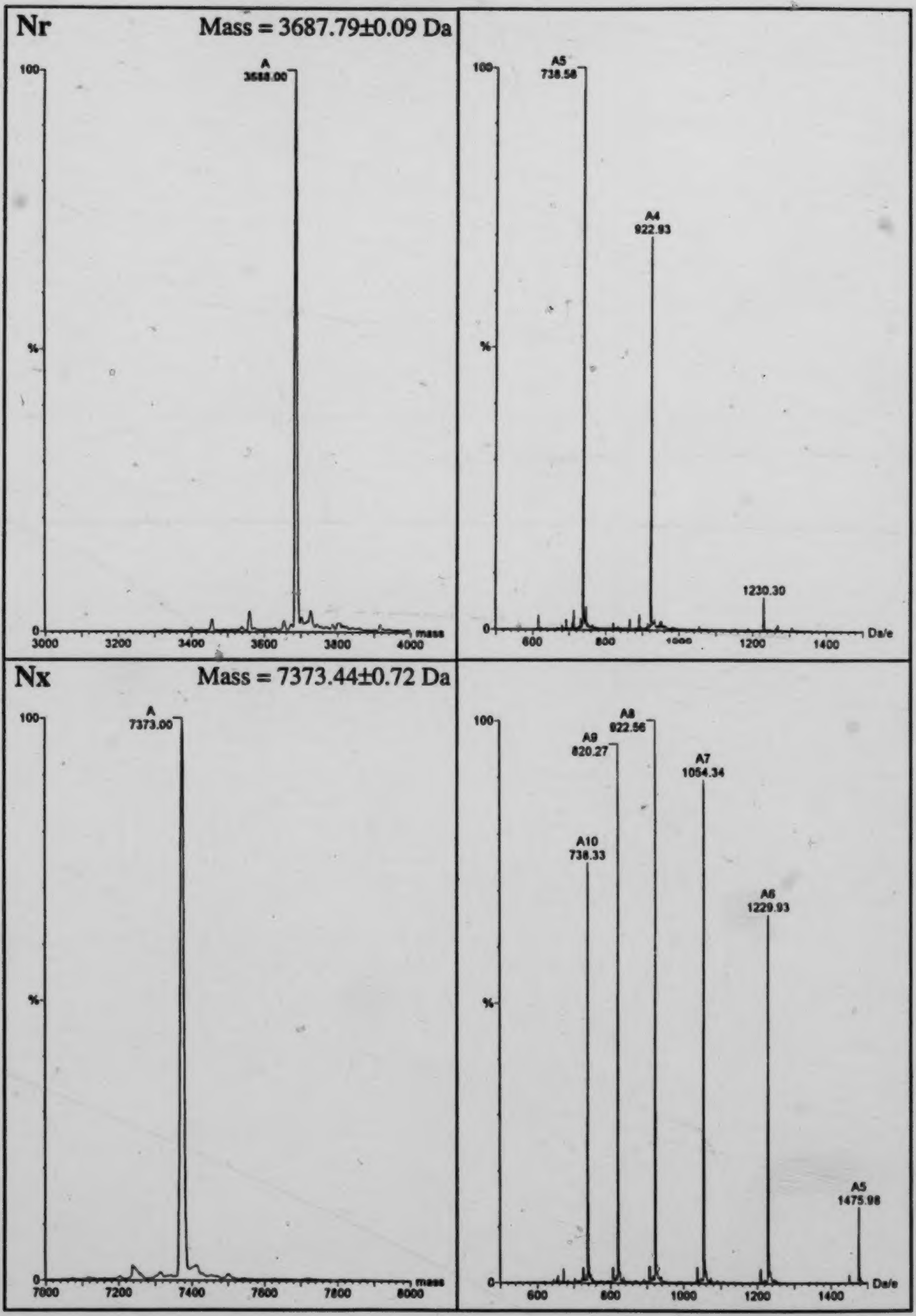
Nr
Mass = 3687.79±0.09 Da
100
%
0
A
3688.00
3000
3200
3400
3600
3800
4000
mass
A5
738.56
A4
922.93
1230.30
600
800
1000
1200
1400
Da/e
Nx
Mass = 7373.44±0.72 Da
A
7373.00
7000
7200
7400
7600
7800
8000
mass
A8
922.56
A9
820.27
A7
1054.34
A10
738.33
A6
1229.93
A5
1475.98
Da/e

5. Size-exclusion chromatography

The effective molecular weights of the disulfide-bridged two-stranded peptides and the reduced peptides were determined by size-exclusion chromatography (SEC). SEC was carried out on a Superdex 75 FPLC size-exclusion column (290 mm X 13 mm I.D., 10 µm particle size, 125 Å pore size) (Pharmacia LKB Biotechnology, Uppsala, Sweden) with a Varian Series 5000 liquid chromatograph coupled to a Hewlett Packard (Avondale, PA) HP1040A detection system and a HP9000 series 300 computer. Unless otherwise specified, the samples were eluted with 50 mM PO_4 or 50 mM Tris, 1 M KCl, pH 7 buffer at a flow rate of 0.5 ml/min. The high salt concentration was used to minimize nonspecific electrostatic interactions with the column matrix and to prevent nonspecific aggregation. Reduced peptides were dissolved in buffer containing DTT to prevent oxidation. Peptide retention times were compared with a standard curve (Fig. II.6) constructed with two-stranded disulfide-bridged coiled-coil standards of 16, 19, 23, 26, 30, 33, and 35 residues per polypeptide chain giving molecular weights ranging from 3514 to 7642, respectively (Su *et al.*, 1994), in order to estimate the apparent molecular weights and detect aggregation tendency.

6. Sedimentation-equilibrium ultracentrifugation

Sedimentation-equilibrium experiments were carried out at 20°C with a Beckman Model E analytical ultracentrifuge equipped with a Raleigh interference optical system, a titanium rotor, and 12 mm double-sector charcoal-filled Epon centerpieces, as described previously (Kay *et al.*, 1991; Zhu *et al.*, 1993). Samples were run under a number of different buffer conditions, as outlined in the respective chapters (Chapters IV, VI, VII, and IX). In each case, the peptide solution (at a concentration of approximately 1 to 2 mg/mL) was dialyzed to equilibrate against the reference buffer (1 to 2 L) for 2 to 3 days. This is essential because the interference pattern generated by the optics is dependent on very small changes between the solution in the sample and reference sectors of the cell. For

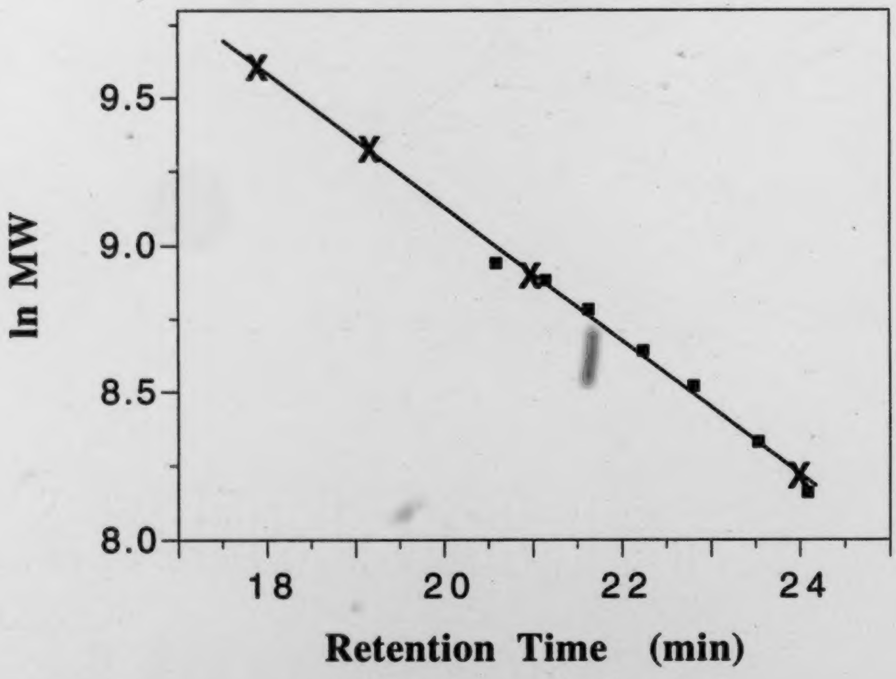

Figure II.6 A standard curve for size-exclusion chromatography constructed with two-stranded disulfide-bridged coiled-coil standards of 16, 19, 23, 26, 30, 33, and 35 residues per polypeptide chain giving molecular weights ranging from 3514 to 7642, respectively (marked with squares). These peptides were previously used in a study of the effect of chain length on coiled-coil stability (Su *et al.*, 1994). The standard peptides were run on a Superdex 75 FPLC size-exclusion column (290 mm X 13 mm I.D., 10 µm particle size, 125 Å pore size) (Pharmacia LKB Biotechnology, Uppsala, Sweden) at 0.5 mL/min with a 50 mM phosphate, 1 M KCl, pH 7 buffer. The retention times of the 35-residue analogs in the current study were compared to the standard curve to estimate the extent of oligomerization occurring for each. The expected positions of a one-, two-, three, and four-stranded species are marked on the standard curve with "X". Based on the retention behavior of the standard peptides, retention times observed in the range 20 to 22 min for the peptides in this study suggested the peptides were in the two-stranded form. Monomeric species eluted slightly before the time expected from the standard curve, suggesting the unfolded 35-residue peptide is more expanded than the disulfide-bridged version of the 16-residue standard.

reduced peptides (in 5 mM DTT solution), dialysis tubing with a cutoff of 1000 MW was used. For oxidized (disulfide-bridged) peptides, dialysis tubing with a cutoff of 3500 MW was used. Initial peptide concentration was determined by sedimenting at 8000 rpm for 15 min in a synthetic boundary cell and counting the resulting fringe displacement that occurs at the protein-buffer interface due to the refractive index change. A value of 4.1 fringes per 1 mg/mL was used based on the results of Babul and Stellwagen (1969). Equilibrium photographs were taken after 24 to 48 h at each rotor speed. The equilibrium photographs were manually measured on a Nikon model 6 microcomparator at 50-fold magnification. A number of data points at different distances, r, from the top of the centrifuge cell were obtained at which the fringe displacement, Y, which is a function of optical density, was directly measured. This was converted to an apparent concentration at that position in the centrifuge cell, based on the initial concentration and the observed optical density gradient. The raw data at each measured r value was converted using the equation for sedimentation equilibrium (see below) to an apparent molecular weight (the molecular weight of a species which would yield the measured optical density at that r value under the specified conditions assuming ideal behavior). This procedure was done using a program written in the APL language. Briefly, sedimentation equilibium is described by the following equation (Freifelder, 1982; McRorie & Voelker, 1993):

$$\ln(c_r) = [M(1-v\rho)\omega^2/2RT]r^2$$

where c_r is the concentration (optical density) at distance r from the axis of rotation, v is the partial specific volume of the sample, ρ is the solution density, and ω is the angular velocity (R and T are the gas constant and temperature, respectively). The partial specific volume used in all calculations was based on the weight average of the partial specific volumes of the individual amino acids (Cohn & Edsall, 1943). Densities of the salt solutions were determined from standard physical tables (Weast, 1971).

For an ideal, single-species system, the sedimentation-equilibrium data represented as a graph of ln Y (or $\ln(c_r)$) versus r^2 yields a linear plot (from the above equation), in which the slope is proportional to the molecular weight of the molecule or complex (see Fig. IV.6). An upward curved plot is indicative of a multi-species system, in which a mixture of oligomeric states is present (see Fig. VII.5). In such a multi-species system, the increase in total peptide concentration toward the bottom of the centrifuge cell (at larger r) results in an increase in the apparent oligomeric state. Data plotted as concentration versus r were also fit using non-linear least squares analysis to models for single species or associating systems using the program Table Curve as outlined (McRorie & Voelker, 1993). The most sensitive representation of goodness of fit is the residual plot. The residuals are the difference between the data points and the corresponding points on the calculated line of best fit, and a plot of residuals should have a random distribution about the zero point (see Fig. VI.3).

7. Laser light scattering experiments

Molecular weight determinations using laser light scattering techniques were performed on a Dawn F multiangle laser light scattering photometer (Wyatt Technology Corporation, Santa Barbara) connected in series with an Optilab 903 refractometer according to methodology described by Farrow *et al.* (1994). Apparent molecular weight determinations at relatively low concentration were made by injecting samples onto a gel filtration column and laser light scattering detection of the peaks that eluted from the column. (Injection of samples at a concentration of approximately 1 mg/ml led to an approximate final concentration of 0.1 mg/mL at the end of the SEC column). A Superose 12 size-exclusion column (300 mm X 10 mm I.D., 10 μm particle size, 125 Å pore size) (Pharmacia LKB Biotechnology, Uppsala, Sweden) was used at room temperature with a flow rate of 0.5 mL/min. The buffer was 50 mM K_2HPO_4, 100 mM KCl, 2 mM DTT, pH 7. Concentrations for the eluting peaks from the column were measured on the basis of the differential refractive index increment of the sample (dn/dc), for which a value of 0.185

was used. Apparent weight-averaged molecular weights were calculated for each peak using Debye plots by extrapolation to 0° angle of scattering.

8. Circular dichroism measurements

Circular dichroism spectra were recorded at 20°C (unless otherwise stated) on a Jasco J-500C spectropolarimeter (Jasco Inc., Easton, MD) equipped with a Jasco IF500II interface, an IBM PS/2 computer running the Jasco DP- 500PS2 system version 1.33a software and a Lauda model RMS water bath (Brinkmann Instruments, Rexdale, ON, Canada) to control the cuvette temperature. The spectropolarimeter was routinely calibrated with an aqueous solution of recrystallized *d* -10-(+)-camphorsulfonic acid at 290.5 nm. The results are expressed as mean residue molar ellipticity [θ] with units of deg•cm^2•dmol^{-1} and calculated from the following equation:

$$[\theta]=([\theta]_{obs} \times MRW)/(10 \times l \times c)$$

where $[\theta]_{obs}$ is the observed ellipticity measured in millidegrees, MRW is the mean residue molecular weight (molecular weight of the peptide divided by the number of amino acid residues), c is the peptide concentration in mg/ml, and l is the optical path length of the cell in cm. CD spectra were the average of four scans obtained by collecting data at 0.1 nm intervals from 255 nm to 190 nm (or to the lowest wavelength possible limited by the photomultiplier voltage which should not exceed 800).

Urea and GdnHCl denaturation studies were carried out at 20°C by monitoring the ellipticity at 222 nm as a function of denaturant concentration. Each ellipticity reading involved the averaging of eight 1.0 sec readings. This was repeated five times at each data point and the resulting average was taken (a total of forty 1.0 sec readings at each data point). Mixtures were prepared from stock peptide solution in buffer (various buffer conditions were employed as indicated in the individual results), buffer alone, and a solution of 10 M urea or 8 M GdnHCl in buffer. The ratios of buffer and denaturant solution added were varied to give the appropriate final denaturant concentrations, and 10 μl of peptide stock solution was added to each. A total of 120 μL (urea) or 128 μL (GdnHCl) was made up at each data point using a digital micropipetter. The samples were allowed to equilibrate at room temperature for 1 hour (urea) or 2 hours (GdnHCl) prior to reading the ellipticities. Urea solution can be accurately made up from simply weighing out the urea on an accurate analytical balance and dissolving in an accurate volume of solution in a volumetric flask, but GdnHCl is hygroscopic and accurate concentrations require measurement of the refractive index of the solution (Pace, 1986). In the current study, most of the measurements were done with urea, and those with GdnHCl were not corrected by reading the refractive index of the stock solution, although the important result was relative stabilites, which will not be greatly affected.

pH titrations followed by CD spectroscopy were done by making up separate buffer solutions at the required pH values using Na_2HPO_4 and NaH_2PO_4 (50 mM total) adjusted with 6 N HCl for buffering and adding 10 μL of peptide stock solution to 110 μL of the buffer at each pH. The pH of the final solutions for CD measurements were verified with a digital pH meter.

Salt titrations were carried out similarly to the chemical denaturations (the ratios of buffer alone and buffer containing a high concentration of the salt to be added were varied to give the appropriate final salt concentrations, and 10 μl of peptide stock solution was added to each). For most cases, it was sufficient that the salt concentration was estimated from the dry weight measured out on a digital analytical balance and made up accurately in a volumetric flask. For the higher affinity binding titration experiments (Chapter IX, Kohn *et al.*, 1998b). Lanthanum, ytterbium and zinc concentrations in stock solutions were determined by EDTA titration using xylenol orange as the end point indicator (Gariepy *et al.*, 1983). A stock solution of 0.01 M EDTA•2Na•$2H_2O$, which was dried in a dessicator under vacuum prior to use, was made up in a 100 mL volumetric flask and titrated against a 100 μL aliquot of the metal stock solution (made up to about 0.1 M). 100 μL of a 0.1% (w/v) xylenol orange solution was added to the aliquot of metal solution in about 4 mL of

0.02 M MES buffer solution at pH 6. The titration was performed by additions with a micropipetter, calibrated by measuring the distilled-deionized water delivered on an analytical balance when the pipetter is set to a particular volume (100 µL of water weighs 0.1 g). The concentration was taken as the average of five titration results. Metal stock solutions were diluted to 0.5 mM using a calibrated 1 mL micropipetter and a Hamilton syringe prior to titrations.

In general, cell path lengths used were 0.05 cm for the data points in the denaturation studies and other experiments where the ellipticity at 222 nm only was monitored and 0.02 cm for the CD spectral scans. Exceptions were occasionally adapted (for example, a 0.01 cm cell could be used for CD scans to achieve more spectral data at lower wavelength where solvent cutoff was a problem but the CD signal was also reduced in half). The concentration of peptide in the stock solutions was determined by amino acid analysis as described above, and an internal norleucine standard was added to each sample to correct for handling losses or instrument variation.

9. Fitting of metal titration curves (Chapter IX)

Metal titration data were analyzed by least squares fitting to the equation: $Y = \{(M_o + P_o + K_d)-[(M_o + P_o + K_d)^2 - 4M_oP_o]^{1/2}\}/ 2P_o$ (Gariepy *et al.*, 1983) where M_o is the total metal ion concentration, P_o is the total peptide concentration, and K_d is the metal dissociation constant to be determined. Because Gla_2Nx is assumed to contain two metal binding sites, the value used for P_o in the curve fitting procedure was twice the concentration of the disulfide-bridged two-stranded coiled-coil, which equals the expected total number of binding sites present. The use of this equation assumes that the binding sites in Gla_2Nx behave independently. In this case, Y (fraction folded) = $(\theta_o-\theta_f)/(\theta_s-\theta_f)$ where θ_o is the molar ellipticity value at 222 nm (θ_{222}) at a particular point in the titration, and θ_f and θ_s are the θ_{222} values of the metal-free and metal-saturated forms of the peptide, respectively. The data was fit by inputting the equation into the program Kaleidograph

(Synergy Software, Reading, PA) which does a non-linear least squares analysis using the Levenberg-Marquardt algorithm.

10. Proton NMR experiments

Proton NMR experiments were performed on a Varian Unity 300 MHz spectrometer at 24.9°C with presaturation of the water resonance (Gariepy *et al.*, 1983). Spectrum parameters for the $LaCl_3$ titration were as follows: 256 aquisitions with 8 steady-state preparation scans, sweep width of 4000 Hz, 1.5 s aquisition time with a 2 s delay, pulse width of 7.6 µs (90°), and spectral line broadening value of 0.5 Hz. The respective values for the $YbCl_3$ titration were: 720 aquisitions with 8 steady-state preparation scans, sweep width of 16,000 Hz, 1.5 s aquisition time with a 2 s delay, pulse width of 7.7 µs (90°), and spectral line broadening value of 5 Hz. The sample was dissolved in a 50 mM deuterated-imidazole, 50 mM KCl buffer at pH 6.9 containing 10% D_2O / 90% H_2O and 0.1 mM DSS as a chemical shift standard. Peptide concentration was determined by amino acid analysis. Small aliquots of $LaCl_3$ or $YbCl_3$ solution were added to the peptide solution with the total volume changing less than 5% over the titration. The sample was allowed 10-15 min equilibration time after each addition before spectral aquisition.

11. Calculation of free energy of unfolding from chemical denaturation

The unfolding process for coiled-coils is not completely understood, but the most commonly accepted model is the two-state transition model, as judged by the appearance of a monophasic denaturation curve. The two-state model requires that a coiled-coil unfolds in one cooperative step to denatured monomers, in which chain dissociation and loss of helix are presumed to be simultaneous events (Engel *et al.*, 1991; Monera *et al.*, 1994b; Skolnick & Holtzer, 1985; Thompson *et al.*, 1993). This is consistent with the observation that isolated α-helices are generally unstable in solution (Cohen & Parry, 1990; Dyson *et al.*, 1988; Thompson *et al.*, 1993). However, the two-state model does not require an all or none helix-coil transition, meaning that the folded state can have a variation of helical content (Qian, 1994). For a two-state transition, all that is required is that the fluctuation within each state is small relative to the average structural difference between the two states. For example, a coiled-coil can have less than 100% helix in the 'folded state' due to fraying of the helix ends, and this fraying will increase with temperature.

Not all coiled-coils have been found to follow a two-state transition. In some cases, biphasic denaturation has been observed, particularly in long coiled-coils like tropomyosin (Greenfield & Hitchcock-DeGregori, 1993; Lehrer *et al.*, 1989; Lehrer & Stafford, 1991). Formation of an interchain disulfide bridge in tropomyosin at position 190 (out of 284) led to two domains on either side of the bridge that unfold separately (Skolnick & Holtzer, 1986). Such results show that folding intermediates can occur, as previously suggested by the "continuum of states" theory (Skolnick & Holtzer, 1986), in which a broad spectrum of partially folded intermediates may occur in the unfolding process (this model is particularly relevant to longer coiled-coils). Also, it was recently observed in a 33-residue GCN4-like coiled-coil that different residues monitored by NMR gave slightly different unfolding curves (Holtzer *et al.*, 1997). Other recent results from calorimetry (Jelesarov & Bosshard, 1996; Thompson-Kenar *et al.*, 1995) and stopped-flow spectroscopy (both fluorescence and CD) measurements of coiled-coil folding kinetics (Sosnick *et al.*, 1996; Wendt *et al.*, 1997; Zitzewitz *et al.*, 1995), all on short coiled-coils, are consistent with a two-state model. While the two-state theory adequately explains the unfolding process of most coiled-coils, it is not necessarily a universally correct description for the process, but is generally appropriate for short coiled-coils, such as the ones studied in this work.

With the assumption that coiled-coil denaturation is a two state process (based on the above considerations), the molar fraction of folded peptide (f_f) was calculated from the equation $f_f = ([\theta]_o - [\theta]_u)/([\theta]_f - [\theta]_u)$, in which $[\theta]_o$ represents the observed mean residue ellipticity at any particular denaturant concentration and $[\theta]_f$ and $[\theta]_u$ are the mean residue ellipticities of the folded and unfolded states, respectively. The free energy of unfolding

(ΔG_u) at each denaturant concentration was calculated from $\Delta G_u = - RT\ln(K_u)$, where K_u is the equilibrium constant of the unfolding process. In the case of the disulfide-bridged peptides (which unfold via a unimolecular process), this is simply given by $K_u = f_u/f_f = (1-f_f)/f_f$. For noncovalently-linked coiled-coils, folding is dependent on the total concentration of peptide monomer, Pt, in mol/l (Zhou *et al.*, 1992c). In this case, $K_u= 2P_t f_u^2/f_f$ for a dimer and $K_u= 3P_t^2 f_u^3/f_f$ for a trimer.

There are three techniques used for estimating the free energy of unfolding in the absence of denaturant ($\Delta G_u^{H_2O}$): Tanford's Model, the denaturant binding model, and the linear extrapolation method (LEM) (Pace, 1986). Of these, the LEM is by far the most commonly used approach, primarily because it is the easiest to employ and because different denaturants often (but not always) give very similar extrapolated $\Delta G_u^{H_2O}$ values (with the other techniques a higher $\Delta G_u^{H_2O}$ value is always observed for GdnHCl than for urea). Recently, measurements of the energetics of dissolution of a series of cyclic dipeptides in aqueous urea solution showed that both the ΔH° and ΔS° of dissolution had a linear dependence on urea concentration, which suggests an underlying physical basis in support of the LEM (Zou *et al.*, 1998). In the LEM technique, $\Delta G_u^{H_2O}$ is obtained simply by linear extrapolation according to the equation:

$$\Delta G_u = \Delta G_u^{H_2O} - m\,[\text{denaturant}]$$

Plots of ΔG_u versus denaturant concentration were made incorporating only data points near the transition midpoint where the greatest linearity was displayed, and a linear least squares analysis was performed (not shown). However, small errors in the slope term, *m* , lead to large errors in the extrapolated value of $\Delta G_u^{H_2O}$ (Green *et al.*, 1992; Pace, 1986). The main interest of this study was to determine the difference in free energy of unfolding between analogs ($\Delta\Delta G_u$), specifically the difference in stability between the native sequence and an analog or the change in stability for an analog upon a change in buffer conditions. Therefore, despite the large uncertainty of the extrapolated $\Delta G_u^{H_2O}$

values, $\Delta\Delta G_u$ can be determined accurately by use of the equation given by Serrano *et al.* (1990):

$$\Delta\Delta G_u = ([\text{denaturant}]_{1/2,A} - [\text{denaturant}]_{1/2,B})(m_A + m_B)/2$$

where $[\text{denaturant}]_{1/2}$ is the denaturant concentration at which the protein is 50% unfolded. This approach gives the value of $\Delta\Delta G_u$ at the denaturant concentration half-way between the $[\text{denaturant}]_{1/2}$ values of the peptides being compared and is much more accurate for determining small differences in protein stability since errors from long extrapolations are avoided and linearity between ΔG_u and denaturant concentration is assumed over a small range of denaturant concentration. For reduced coiled-coils, the $[\text{denaturant}]_{1/2}$ increases with the peptide concentration (Zhou *et al.*, 1992c). The $\Delta\Delta G_u$ values for the reduced coiled-coils were in some cases (Chapter III, Kohn *et al.*, 1995a) calculated by subtracting the ΔG_u value (on the line of best fit) of the native coiled-coil from that of the mutant coiled-coils at the urea concentration equal to the $[\text{urea}]_{1/2}$ value of the native coiled-coil (at 2.5 M urea for the pH 7 results and 2.4 M urea for the pH 3 results), similarly to previous papers (Zhou *et al.*, 1992b; Zhu *et al.*, 1993). In other cases, the above equation of Serrano *et al.* (1990) was used.

The precision of the stability measurements from urea denaturation is quite high. Run to run reproducibility for the denaturation midpoint was found to be ± 0.02 to 0.05 M (approximately 1%) and the *m* value varied within ± 5%. Thus, the $\Delta\Delta G_u$ values calculated were reliable to approximately ± 0.05 kcal/mol, as previously suggested by Serrano and Fersht (1989) for urea denaturation of barnase mutants.

12. Computer modelling

Modelling of the side chain interactions and metal ion binding were carried out with the program Insight II (Biosym Technologies Inc., San Diego, CA) in Biopolymer mode on a Silicon Graphics Personal Iris workstation. A dimeric coiled-coil polypeptide backbone was created from the crystal structure coordinates of the GCN4 leucine zipper

(O'Shea *et al.*, 1991). The side chains of the peptides studied were substituted in the appropriate positions maintaining the side chain conformational angles observed in the crystal structure, particularly for the hydrophobic core Val, Asn, and Leu residues.

13. Design of the model coiled-coil and peptide nomenclature

i) Design of the coiled-coil model system

The studies of synthetic coiled-coil peptides leading up to the present work established several guidelines for coiled-coil design (Adamson *et al.*, 1993; Hodges, 1992; Zhou *et al.*, 1993a, 1992c). For example, a chain length of 28 residues (four heptads) was shown to allow for stable coiled-coil formation (Lau *et al.*, 1984b; Su *et al.*, 1994), which is consistent with the prevalence of 30-35 residue coiled-coils in nature. All the peptides in this thesis consisted of 35 residues (five heptads), allowing enough flexibility of sequence and stability to measure a variety of interactions in a single peptide model.

Because the objective was to study electrostatic effects, it was important to base these studies on a control sequence in which no inter- or intrahelical ionic interactions were present. This peptide could therefore act as a reference point for all the measurements of the effects of electrostatic, salt, and metal binding interactions on coiled-coil folding and stability. All the subsequent peptides that were studied were versions of the control (native) peptide incorporating substitutions of charged residues.

The control (native) coiled-coil consists of five repeats of the heptad sequence $\mathbf{Q_gV_aG_bA_cL_dQ_eK_f}$ (Fig. II.7). With Val and Leu at the **a** and **d** positions, respectively, this sequence resembles the naturally-occurring leucine zipper coiled-coils, in which Leu is highly conserved at position **d** (hence, the origin of the term leucine zipper) and β-branched amino acids are prevalent at position **a** (Hu & Sauer, 1992). Rather than the common interhelical **g-e'** ionic attractions, the design incorporates neutral Gln residues at positions **e** and **g**. Previously, the replacement of **g-e'** Lys-Glu ion pairs with Gln residues actually was found to slightly increase stability (Zhou *et al.*, 1994b). Computer modelling using the

1 5 10 15 20 25 30 35

g a b c d e f g a b c d e f g a b c d e f g a b c d e f g a b c d e f

Ac-**Q**-C-G-A-L-**Q**-K-**Q**-V-G-A-L-**Q**-K-**Q**-V-G-A-L-**Q**-K-**Q**-V-G-A-L-**Q**-K-**Q**-V-G-A-L-**Q**-K-amide

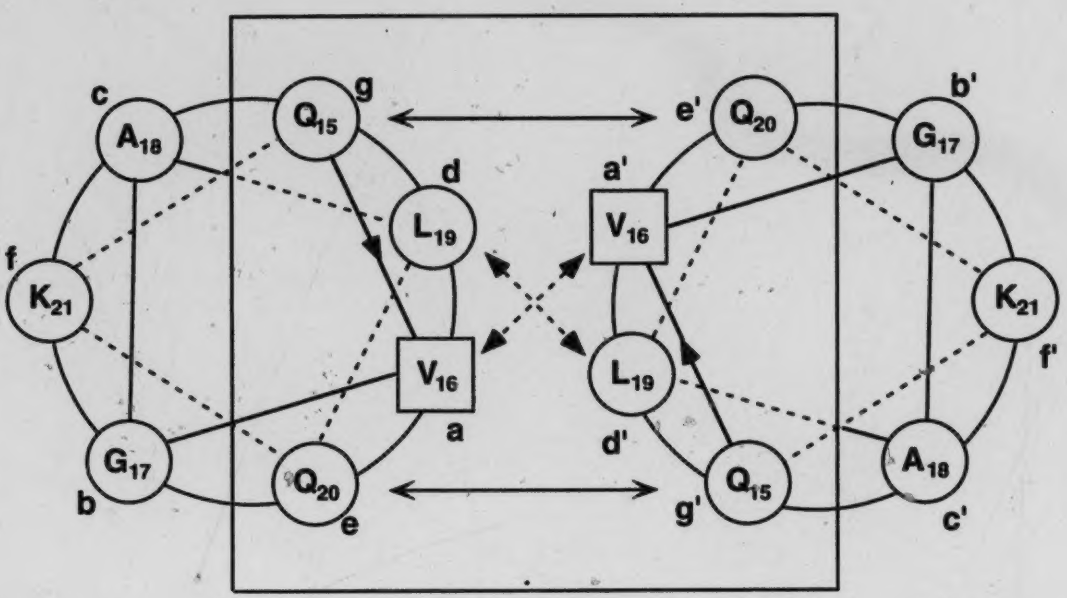
c
A18
Q15
g
d
L19
f
K21
V16
a
G17
b
Q20
e
e'
Q20
b'
G17
a'
V16
K21
f'
L19
d'
Q15
g'
A18
c'

Figure II.7 Sequence (top) and helical wheel diagram of the central heptad (bottom) of the native (control) peptide used in the studies in this thesis. All peptides studied were based on this sequence (or a similar control sequence in Chapter VI). The box includes all residues involved in interhelical interactions. Ac represents an N-terminal acetyl group.

high resolution GCN4 crystal structure (O'Shea *et al.*, 1991) for the backbone coordinates indicated that Gln residues can effectively participate in an interhelical **g-e'** hydrogen bond between the amide hydrogen of one Gln side chain and the carboxy oxygen of the other Gln side chain with a proton-oxygen distance of approximately 2.8 Å. This is similar to the proton-oxygen distance of 3.0 Å observed for the Lys15-Glu20 ion pair in the GCN4 crystal structure (O'Shea *et al.*, 1991). In opposition to the precise folding of the side chains at the **e** and **g** positions of the coiled-coil are the loss of side chain entropy involved in fixing their conformation (Doig & Sternberg, 1995) and the partial desolvation involved in bringing the polar side chain carboxamide groups into the partially hydrophobic microenvironment of the dimer interface.

In order to clarify the effect of interhelical interactions on coiled-coil stability, the control sequence contains small, neutral Gly and Ala residues at positions **b** and **c**, respectively. Thus, i to i+3 (**b-e** or **g-c**) and i to i+4 (**c-g** or **e-b**) intrahelical interactions with the **e** and **g** heptad positions are minimized. The Ala and Gly residues have opposite modulating effects on stability, owing to high and low intrinsic helical propensities, respectively (Chakrabartty *et al.*, 1991, 1994; O'Neil & DeGrado, 1990; Zhou *et al.*, 1994d). The helical wheel diagram (Fig. II.7) illustrates the positioning of positions **e** and **g**, in which charged residue substitutions are to be studied, away from the positively-charged Lys residues at position **f**, which were included to aid water solubility and to discourage nonspecific aggregation. The N and C termini of the peptides were capped with an acetyl and amide moiety, respectively, to remove possible effects of charges at these positions on the electrostatic interactions being studied and on overall coiled-coil stability.

The coiled-coils in this study all contain a substitution of Cys for Val at position 2 (position **a** of the heptad). This allows interhelical disulfide bridge formation, such that the disulfide bridge is in the hydrophobic interface of the coiled-coil. Such a disulfide bridge ensures parallel, in-register coiled-coil formation and also makes coiled-coil unfolding a unimolecular rather than a bimolecular process, thereby removing the dependence of coiled-coil formation on total peptide monomer concentration (Zhou *et al.*, 1992c). A disulfide bridge at position 2 of a similar coiled-coil was shown to be stabilizing (increased the denaturation midpoint) and did not introduce unreasonable strain on the molecule (Zhou *et al.*, 1993a). The peptides could be studied in the oxidized disulfide-bridged form or in the reduced form after treatment with the disulfide-reducing agent dithiothreitol (DTT).

Further details of the design process for the individual analogs studied are given in the specific chapters in which the results are presented (Chapters III to IX).

ii) Peptide nomenclature

The control sequence with Gln residues at positions **e** and **g** is referred to throughout this thesis as 'N', 'native', and in Chapter VI (Kohn *et al.*, 1997c) as QQ (where the hydrophobic core is slightly different). In all the work comprising this thesis, the substitutions were primarily at the **e** and **g** positions, and analogs are named based on the positions and numbers of mutations, as well as the types of amino acids substituted (one letter code for amino acids). For example, the peptide E_2(20,22) discussed in Chapter III (Kohn *et al.*, 1995a) contains two substitutions of Glu at positions 20 and 22. Further details on the nomenclature of the peptides studied in each section are given along with the peptide sequences in the individual chapters in which those peptides appear. Each peptide is further designated with "x" if it is present in the disulfide-bridged (oxidized) form or "r" if it is present in the nondisulfide-bridged (reduced) form.

CHAPTER III

ELUCIDATION OF THE SPECIFICITY OF INTERHELICAL IONIC INTERACTIONS BETWEEN THE *e* AND *g* POSITIONS OF A TWO-STRANDED α-HELICAL COILED-COIL: DESTABILIZATION BY GLU-GLU REPULSIONS[1]

A. Introduction

Specific interhelical ionic interactions between positions **g** and **e'** of a two-stranded coiled-coil could potentially occur in two ways: (1) between position **e** and position **g'** of the same heptad (designated i to i'+2 or **e-g'**) and (2) between position **g** and position **e'** of the following heptad (designated i to i'+5 or **g-e'**). Although the distances between the C^{α} atoms are closer for the **e-g'** interaction, modelling of tropomyosin (Cregut *et al.*, 1993; McLachlan & Stewart, 1975) and the GCN4 leucine zipper (Nilges & Brunger, 1993), indicated that these interactions would be sterically blocked by bulky aliphatic side chains at position **d**. The X-ray structure of GCN4 (Ellenberger *et al.*, 1992; O'Shea *et al.*, 1991) supported this conclusion and showed several **g-e'** side chain contacts. Results of mutagenesis studies also indicated that the **g-e'** interactions are more significant than **e-g'** interactions in two-stranded coiled-coils (Hu *et al.*, 1993; Schmidt-Dörr *et al.*, 1991).

The objective of this study was to experimentally measure the potential destabilizing effect of specific ionic repulsions between Glu residues at the **e** and **g** positions of a two-stranded coiled-coil. Two peptides were designed with either a single **g-e'** or **e-g'** potential Glu-Glu interaction on each side of the coiled-coil, where all other **e** and **g** positions contained neutral Gln residues. These peptides were compared to control peptides containing Glu substitutions that were not able to interact specifically to determine the intrinsic effect of a Gln to Glu substitution. This intrinsic effect could then be subtracted from the overall destabilization to determine any specific destabilizing effect of **g-e'** or e-g' interhelical Glu-Glu repulsions in the former peptides. In all cases, the net charge at the coiled-coil interface was low, so effects of general charge effects were expected to be minimized.

---

[1] A version of this chapter has been published: Kohn, W. D., Kay, C. M., and Hodges, R. S. (1995). *Protein Science* **4**, 237-250.

B. Results and Discussion

a) Peptide design and nomenclature

The amino acid sequences and nomenclature of the peptides used are displayed in Figure III.1. The native sequence, designated 'N', provided a stable reference coiled-coil containing no interhelical electrostatic interactions to which the mutant peptides could be compared (as described in Chapter II, p. 59). There were four mutant peptides synthesized with either 1 or 2 Gln to Glu substitutions as shown in Figure III.1 and named according to the number and positions of the Glu substitutions as well as the presence or absence of a disulfide bridge. Oxidized (disulfide-bridged) peptides are indicated with a "x" while reduced peptides are designated with "r". The analog $E_1(20)$ contains a single Gln to Glu substitution near the center of the polypeptide chain (position 20) in order to determine the minimum (intrinsic) effect of a charged Glu residue substitution for Gln (in the absence of interchain Glu-Glu interactions). Peptide $E_2(13,22)$ was designed to have 2 Glu substitutions but no interchain Glu-Glu interactions since the Glu residues are separated by a full heptad repeat and close interactions between their charged termini would be unlikely (Fig. III.2). The other two analogs $E_2(20,22)$ and $E_2(15,20)$ contain 2 potential i to i'+2 or i to i'+5 Glu-Glu interactions, respectively, as depicted in Figure III.2. By comparison of these peptides with $E_2(13,22)$, it was predicted that a measure of any specific coiled-coil destabilization due to Glu-Glu interactions could be discerned.

Peptide Name	**Amino Acid Sequence**
	1 5 10 15 20 25 30 35
	g a b c d e f g a b c d e f g a b c d e f g a b c d e f g a b c d e f
native	**Ac**-**Q**-C-G-A-L-**Q**-K-**Q**-V-G-A-L-**Q**-K-**Q**-V-G-A-L-**Q**-K-**Q**-V-G-A-L-**Q**-K-**Q**-V-G-A-L-**Q**-K-**amide**
E_1(20)	**Ac**-**Q**-C-G-A-L-**Q**-K-**Q**-V-G-A-L-**Q**-K-**Q**-V-G-A-L-$\boxed{E}$-K-**Q**-V-G-A-L-**Q**-K-**Q**-V-G-A-L-**Q**-K-**amide**
E_2(13,22)	**Ac**-**Q**-C-G-A-L-**Q**-K-**Q**-V-G-A-L-$\boxed{E}$-K-**Q**-V-G-A-L-**Q**-K-$\boxed{E}$-V-G-A-L-**Q**-K-**Q**-V-G-A-L-**Q**-K-**amide**
E_2(20,22)	**Ac**-**Q**-C-G-A-L-**Q**-K-**Q**-V-G-A-L-**Q**-K-**Q**-V-G-A-L-$\boxed{E}$-K-$\boxed{E}$-V-G-A-L-**Q**-K-**Q**-V-G-A-L-**Q**-K-**amide**
E_2(15,20)	**Ac**-**Q**-C-G-A-L-**Q**-K-**Q**-V-G-A-L-**Q**-K-$\boxed{E}$-V-G-A-L-$\boxed{E}$-K-**Q**-V-G-A-L-**Q**-K-**Q**-V-G-A-L-**Q**-K-**amide**

Figure III.1 Amino acid sequences of the peptides studied to determine the specificity of interhelical Glu-Glu repulsions involving residues at positions **e** and **g** (shown in bold type) of the heptad repeat. Substitutions of Glu (E) for Gln (Q) are highlighted by boxes. A cysteine at position 2 allows formation of an interchain disulfide bridge. Peptide nomenclature is based on the number and positions of Glu substitutions. For example, E_2(15,20) contains two Glu substitutions at positions 15 and 20.

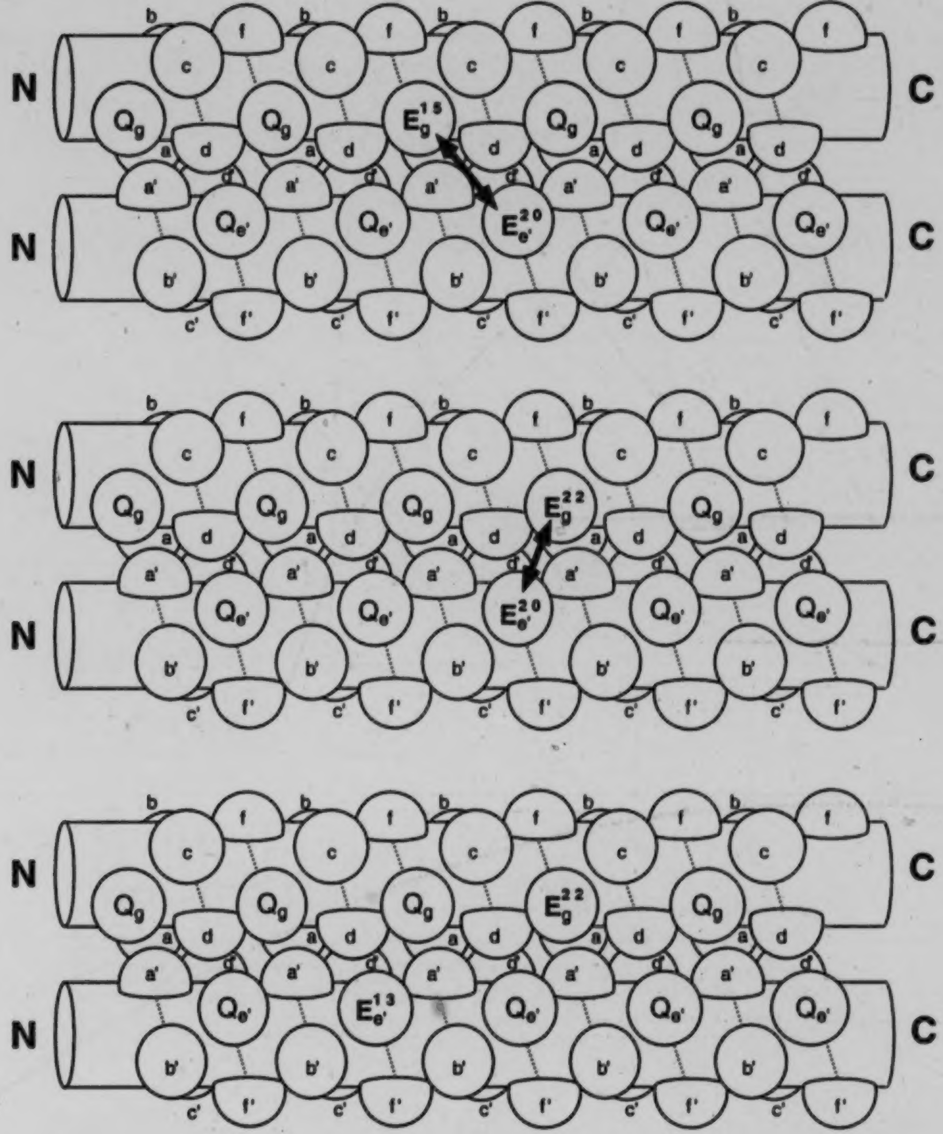

Figure III.2 Helical rod diagrams illustrating the positioning of Glu substitutions at the dimer interface. E_2(15,20) (top) contains potential **g-e'** (i to i'+5) repulsions. E_2(20,22) (middle) contains potential **e-g'** (i to i'+2) repulsions. In both cases, one potential repulsion is indicated with an arrow and the other potential repulsion is on the other side of the molecule out of view. In contrast, no interactions between Glu 13 and Glu22' are expected to occur.

b) Structural characterization of the model coiled-coils

The far-ultraviolet CD spectra of peptides Nr, Nx, $E_2(15,20)r$, and $E_2(15,20)x$ in the absence and presence of 50% trifluoroethanol (TFE) are shown in Figure III.3. The double minima at 222 nm and 209 nm as well as the high positive ellipticity at 195 nm in benign medium (50 mM KCl, 25 mM phosphate, pH 7) indicate that the peptides are all predominantly α-helical. The mean residue ellipticities as reported in Table III.1 show a high degree of helical content. The predicted molar ellipticity for a 100% α-helical 35 residue polypeptide was calculated as $[\theta]_{222,max} = -33,600\ \mathrm{deg \cdot cm^2 \cdot dmol^{-1}}$ (Hodges *et al.*, 1988) based on the theoretical equation described previously (Chen *et al.*, 1974). The native sequence is essentially 100% helical in benign conditions in both the disulfide bridged (Fig. III.3C) and reduced (Fig. III.3A) forms (see Table III.1). $E_2(15,20)$ is approximately 100% helical in the oxidized form (Fig. III.3D) but is significantly less helical in the reduced form (Fig. III.3B) with a $[\theta]_{222}$ value equal to only about 75% of $[\theta]_{222,max}$. This suggests a destabilization of the coiled-coil by interhelical repulsions between Glu residues at the **e** and **g** positions in the reduced coiled-coil, which is not observed in terms of helical content in the disulfide-bridged coiled-coil, likely as a result of the increased stability from the contribution of the disulfide bridge.

The ratios of the mean residue ellipticities at 222 nm and 209 nm $[\theta]_{222}/[\theta]_{209}$ were in the range 1.01-1.08 for the spectra in Figure III.3, which were run under benign conditions (shown in Table III.1). These are similar to $[\theta]_{222}/[\theta]_{209}$ ratios obtained for similar coiled-coil models (Graddis *et al.*, 1993; Hodges *et al.*, 1988; Lau *et al.*, 1984b) and distinctly different from those of noninteracting monomeric α-helices, in which the ellipticity at 209 nm is generally more negative than that at 222 nm, and the $[\theta]_{222}/[\theta]_{209}$ ratio is therefore less than 1.0 (Cooper & Woody, 1990; Zhou *et al.*, 1993b, 1992c). In the presence of 50% TFE, all four peptides showed $[\theta]_{222}/[\theta]_{209}$ ratios of 0.86-0.94 (Table III.1) suggestive of dissociated helices. This follows the established behavior of TFE in disrupting interhelical hydrophobic interactions and stabilizing unassociated helices

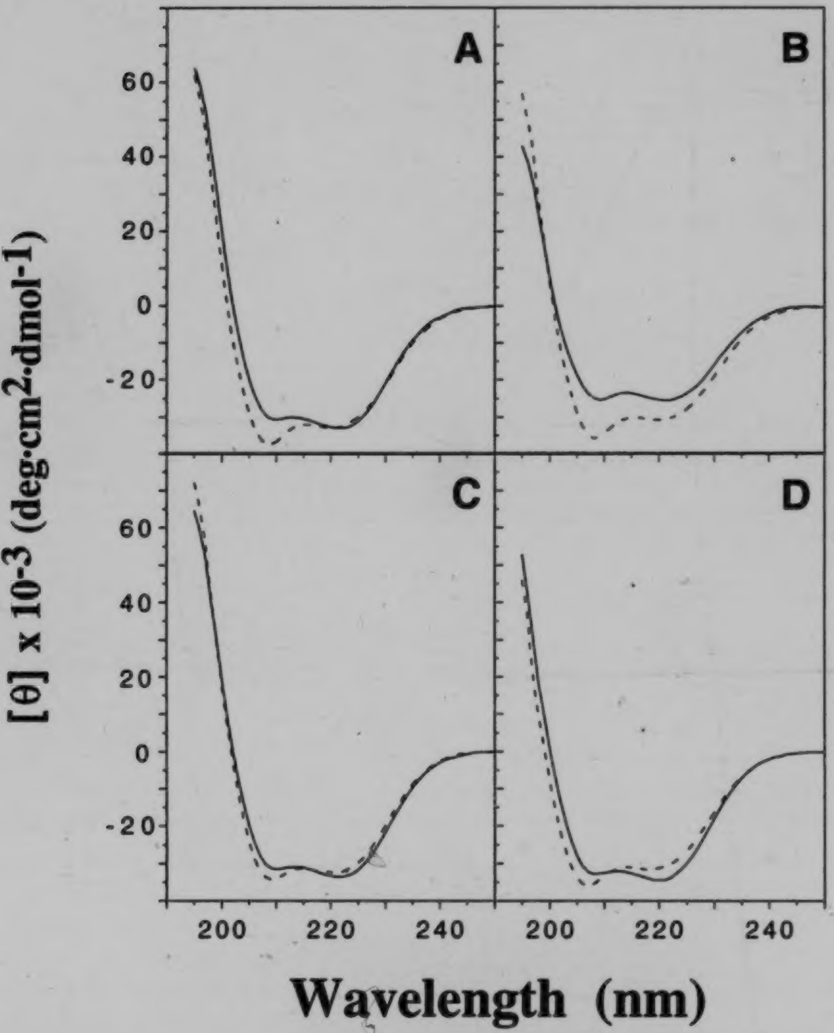

Figure III.3 Circular dichroism spectra of the reduced coiled coils Nr (A) and E_2(15,20)r (B); and the oxidized coiled coils Nx (C) and E_2(15,20)x (D). Spectra were recorded at 20°C in a 0.05 M KCl, 0.025 M phosphate, pH 7 buffer in the absence (solid line) and presence (dotted line) of 50% TFE (v/v). The buffer also contained 2 mM DTT for the reduced peptides. The peptide concentrations are given in Table III.1.

[a] The sequences of the peptides are shown in Figure III.1.

[b] The mean residue molar ellipticities at 222 nm in units of deg·cm^2·dmol^{-1}, measured at 20°C in benign buffer (0.1 M KCl, 0.05 M PO_4) at pH 7 diluted 1:1 (v:v) with water or trifluoroethanol, TFE.

[c] $[\theta]_{222}/[\theta]_{209}$ is the ratio of the mean residue ellipticity at 222 nm to the mean residue ellipticity at 209 nm.

[d] Concentration of peptide for CD scans as determined by amino acid analysis on the peptide stock solution.

[e] t_r is the retention time on reversed-phase high performance liquid chromatography at pH 7 or pH 2 under the conditions described in the legend to Figure III.7.

[f] Δt_r is the difference between the retention time of the peptide and the native peptide under the same HPLC conditions. A positive number indicates that the peptide elutes later than the native sequence and a negative number indicates that the peptide elutes before the native sequence.

[g] $\Delta\Delta t_r$ is the difference in absolute value between Δt_r at pH 7 and at pH 2 (a measure of the difference in the retention time relative to the native peptide in going from pH 7 to pH 2).

Table III.1: Circular dichroism molar ellipticities and reversed-phase HPLC retention times

Peptide [a]	$[\theta]_{222}$ [b]		$[\theta]_{222}/[\theta]_{209}$ [c]		Peptide Conc. (μM) [d]	Retention Time, t_r (min) [e]		Δt_r (min) [f]		$\Delta\Delta t_r$ pH 7-2 (min) [g]
	benign	50% TFE	benign	50% TFE		pH 7	pH 2	pH 7	pH 2	
Nx	-33,500	-32,200	1.07	0.94	180	38.2	33.2	0.0	0.0	0.0
E_1(20)x	-32,600	-30,500	1.08	0.91	195	35.8	33.5	-2.4	+0.3	+2.7
E_2(13,22)x	-33,400	-31,800	1.08	0.90	173	34.1	33.4	-4.1	+0.2	+4.3
E_2(20,22)x	-33,600	-31,700	1.07	0.92	186	34.1	33.4	-4.1	+0.2	+4.3
E_2(15,20)x	-33,800	-30,100	1.03	0.88	188	34.7	33.8	-3.5	+0.6	+4.1
Nr	-32,990	-32,500	1.08	0.87	202	44.9	38.9	0.0	0.0	0.0
E_1(20)r	-31,500	-30,200	1.07	0.86	187	40.9	41.0	-4.0	+2.1	+6.1
E_2(13,22)r	-30,800	-30,200	1.07	0.85	234	38.0	42.3	-6.9	+3.4	+10.3
E_2(20,22)r	-32,900	-31,000	1.06	0.87	174	37.6	42.4	-7.3	+3.5	+10.8
E_2(15,20)r	-25,500	-30,300	1.01	0.86	150	37.5	42.5	-7.4	+3.6	+11.0

in solution (Lau *et al.*, 1984a; Zhou *et al.*, 1992d). Nr, Nx, and E_2(15,20)x did not show any increase in helicity, as determined by the ellipticity at 222 nm, upon addition of the helix inducing solvent TFE (in fact the ellipticity at 222 nm is slightly decreased), showing that they had already reached their maximum potential helicity in benign buffer conditions. E_2(15,20)r was significantly increased in its helical content (a 19% increase) by the addition of TFE, indicating that it had not achieved its maximum potential helicity under benign conditions, possibly due to the inhibition of chain association by interchain Glu-Glu repulsions. An increase in helicity could be obtained in 50% TFE since the helices are monomeric in this medium and independent of interchain repulsions. In both the oxidized and reduced states, the analogs E_1(20), E_2(13,22) and E_2(20,22) show behavior similar to that of the native peptide (spectra not shown) with very high ellipticities in benign buffer and no increase in $[\theta]_{222}$ upon addition of 50% TFE (Table III.1), suggesting they too have already attained their maximum potential helicity (near 100%) under benign conditions. As well, the $[\theta]_{222}/[\theta]_{209}$ ratios are similar to those for the peptides shown in Figure III.3, again consistent with a coiled-coil structure in benign conditions and monomeric helices in 50% TFE. The fact that E_2(20,22)r is more helical than E_2(15,20)r in benign buffer (Table III.1) gives preliminary evidence that if there is a destabilization of this coiled-coil by i to i'+2 interchain Glu-Glu repulsions its effect is smaller than that due to i to i'+5 repulsions.

The apparent molecular weights of all the five sequences in both the reduced (without an interchain disulfide bridge) and oxidized (with an interchain disulfide bridge) forms were determined by size-exclusion chromatography (SEC). Both the reduced and oxidized peptides have essentially the same retention times (data not shown).The disulfide-bridged peptides show the presence of small amounts of aggregate, but they are predominantly in the two-stranded form. The reduced peptides show small amounts of monomeric species in their chromatograms (broad peaks due to a monomer-dimer equilibrium) but are predominantly two-stranded. Therefore the SEC results suggest that these sequences preferentially form a two-stranded coiled-coil rather than a three or four helix structure in both their reduced and oxidized forms. This result was expected due to the nature of the residues at the hydrophobic **a** and **d** positions (Val and Leu, respectively), which were shown to favor helix association to the two-stranded form (Harbury *et al.*, 1993; Lovejoy *et al.*, 1993; Lupas *et al.*, 1991). Further analysis of the state of association is given in Chapter IV (Kohn *et al.*, 1995b).

c) Stabilities of disulfide-bridged coiled-coils at pH 7 and pH 3

The stabilities of the disulfide-bridged coiled-coils were determined by both urea and guanidine hydrochloride (GdnHCl) denaturation at pH 7 and pH 3 where Glu side chains were expected to be fully ionized and mostly protonated, respectively. Stabilities were determined by measuring the ellipticities at 222 nm as a function of denaturant concentration at 20°C, assuming a two-state coiled-coil to random coil transition as described in Chapter II. The stability of the peptides is expressed as the urea or GdnHCl concentration at which the coiled-coil is half unfolded, designated $[\text{urea}]_{1/2}$ or $[\text{GdnHCl}]_{1/2}$. The $[\text{urea}]_{1/2}$ of Nx at pH 7 was 6.1 M, demonstrating high stability without the presence of any interchain electrostatic effects (Fig. III.4A). Linear extrapolation leads to a $\Delta G_u^{H_2O}$ of about 5 kcal/mol. For peptide $E_1(20)$x the $[\text{urea}]_{1/2}$ was reduced to 5.8 M, representing a difference in the free energy of unfolding, (denoted $\Delta\Delta G_u$) of -0.3 kcal/mol (Table III.2). Since there are two Glu residues per $E_1(20)$x molecule, the $\Delta\Delta G_u$ per Glu is -0.15 kcal/mol. This corresponds quite well to the value of -0.22 kcal/mol per Gln to Glu substitution found by Zhou *et al.* (1994b) in a similar study. The $[\text{urea}]_{1/2}$ values for peptides $E_2(13,22)$x and $E_2(20,22)$x under the same pH 7 conditions and 20°C temperature were both 5.4 M, representing a $\Delta\Delta G_u$ of -0.5 kcal/mol relative to Nx. Since these coiled-coils both have four Glu residues per molecule, the $\Delta\Delta G_u$ per Glu was -0.13 kcal/mol, similar to the result obtained from $E_1(20)$x. The destabilization of these peptides with respect to Nx therefore appears to be due to effects that are additive in going from 0 to 2 to

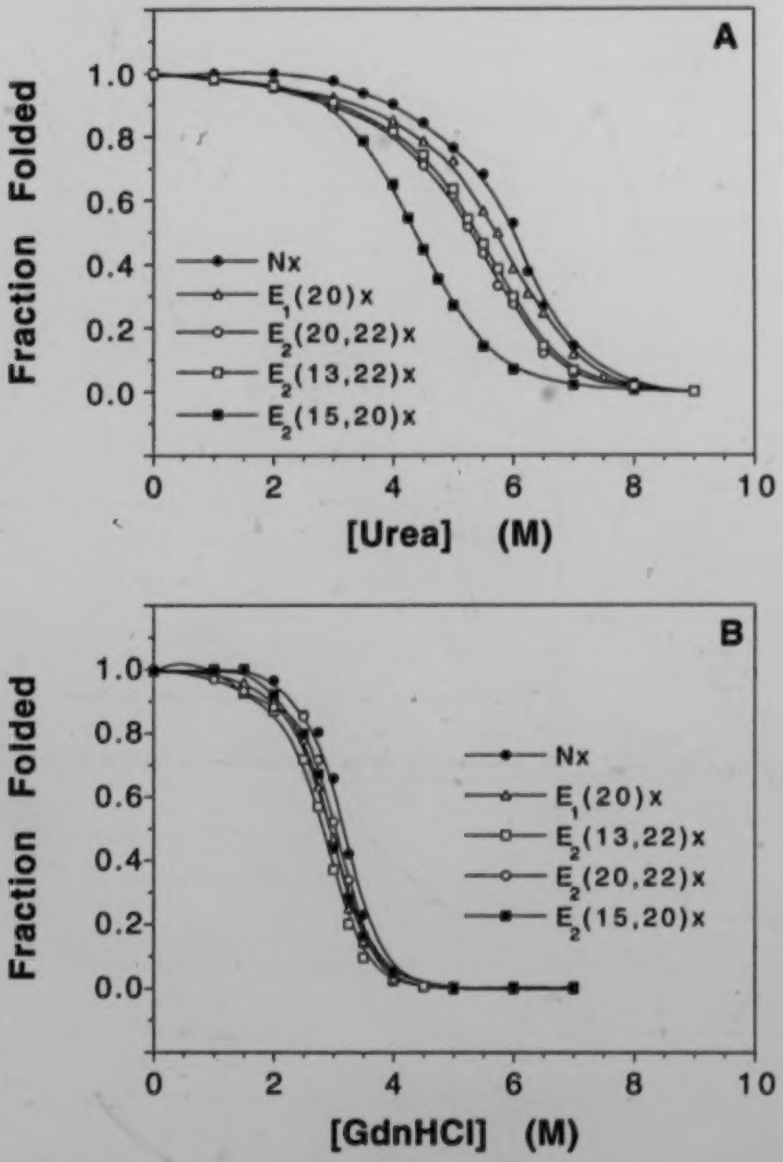

Figure III.4 Denaturation profiles of the disulfide-bridged coiled-coils at 20°C in a 0.1 M KCl, 0.05 M PO_4, pH 7 buffer with urea as denaturant in Panel A and GdnHCl as denaturant in Panel B. The fraction folded peptide was calculated from the observed mean residue molar ellipticity at 222 nm as described in Chapter II, p. 57. Peptide concentrations were: Panel A: Nx, 108 μM; E_1(20)x, 76 μM; E_2(13,22)x, 84 μM; E_2(20,22)x, 96 μM; E_2(15,20)x, 84 μM. Panel B: Nx, 94 μM; E_1(20)x, 67 μM; E_2(13,22)x, 68 μM; E_2(20,22)x, 79 μM; E_2(15,20)x, 99 μM.

[a] $[D]_{1/2}$ is the concentration of denaturant (GdnHCl or urea) at which the peptide is 50% folded, as determined by comparing its molar ellipticity at 222 nm to that of the native peptide in the absence of denaturant (the fully folded state).

[b] $\Delta[D]_{1/2}$ is the change in $[D]_{1/2}$ in going from pH 7 to pH 3.

[c] m is the slope of the assumed linear relationship between ΔG_u and denaturant concentration as discussed in Chapter II.

[d] $\Delta\Delta G_u$ is the difference in the free energy of unfolding between native peptide and the mutant peptide. For oxidized peptides this was calculated from $\Delta\Delta G_u = ([D]_{1/2(\text{mutant})}-[D]_{1/2(\text{native})})*(m_{\text{native}}+m_{\text{mutant}})/2$ as discussed in Chapter II (pp. 56-59, see Serrano *et al.*, 1990; Pace, 1986). A positive $\Delta\Delta G_u$ indicates the mutant coiled-coil is more stable than the native coiled-coil. For reduced coiled-coils the $[D]_{1/2}$ is concentration dependent, so the $\Delta\Delta G_u$ values were calculated by subtracting the ΔG_u value of the native coiled-coil from that of the mutant coiled-coil at the $[\text{urea}]_{1/2}$ of the native coiled-coil (2.5 M urea).

[e] $\Delta\Delta G_{u,\text{ ox-red}}$ is the change in the free energy of unfolding of the specified coiled-coil in going from the disulfide bridged to the reduced form calculated with the equation described in *d* above.

Table III.2: Stability data from urea and GdnHCl denaturation

Peptide	Denaturant	$[D]_{1/2}$, (M)[a]		$\Delta[D]_{1/2}$[b]	slope, m[c]		$\Delta\Delta G_u$[d] (kcal/mol)		$\Delta\Delta G_{u,ox\text{-}red}$[e]	
		pH 7	pH 3		pH 7	pH 3	pH 7	pH 3	pH 7	pH 3
Nx	GdnHCl	3.1	3.2	+0.1	1.8	1.8	0.0	0.0	-	-
	Urea	6.1	5.9	-0.2	0.8	0.9	0.0	0.0	-	-
E_1(20)x	GdnHCl	3.0	3.6	+0.6	1.7	1.7	-0.2	1.0	-	-
	Urea	5.8	6.8	+1.0	1.0	0.9	-0.3	0.8	-	-
E_2(13,22)x	GdnHCl	3.0	4.3	+1.3	1.5	2.0	-0.2	2.1	-	-
	Urea	5.4	8.4	+3.0	0.7	0.6	-0.5	1.9	-	-
E_2(20,22)x	GdnHCl	3.0	4.3	+1.3	1.3	1.8	-0.2	2.0	-	-
	Urea	5.4	8.5	+3.1	0.7	0.6	-0.5	2.0	-	-
E_2(15,20)x	GdnHCl	3.0	4.4	+1.4	1.6	2.1	-0.2	2.3	-	-
	Urea	4.4	8.5	+4.1	0.8	0.5	-1.4	1.8	-	-
Nr	Urea	2.5	2.4	-0.1	1.4	1.6	0.0	0.0	3.1	3.2
E_1(20)r	Urea	2.3	2.5	+0.2	1.3	1.3	-0.1	0.4	3.3	2.6
E_2(13,22)r	Urea	2.1	4.1	+2.0	1.4	1.1	-0.6	2.1	2.9	2.8
E_2(20,22)r	Urea	2.0	4.2	+2.2	1.3	1.2	-0.6	2.3	2.7	2.8
E_2(15,20)r	Urea	0.9	4.3	+3.4	1.1	1.2	-1.6	2.4	2.6	2.7

4 Glu substitutions. There are likely two main effects contributing to the reduction in stability of these coiled-coils. First, Gln has a higher helical propensity value than an ionized Glu residue, for example 0.61 versus 0.32, respectively, (Zhou *et al.*, 1994d) and other studies (Chakrabartty *et al.*, 1994; O'Neil & DeGrado, 1990; Scholtz *et al.*, 1993). It was previously shown (Hodges *et al.*, 1981) that replacement of Ala by Ser (helical propensity values of 0.96 and 0.33, respectively, from Zhou *et al.* (1994d)) in positions **c** and **f** of a coiled-coil greatly reduced the stability, presumably due to the lower helical propensity of the Ser side chain. Similar results were observed at position **f** of a coiled-coil (O'Neil & DeGrado, 1990). Also, the apparent hydrophobicity of the Gln side chain is higher than that of an ionized Glu at pH 7 (Guo *et al.*, 1986). Higher hydrophobicity of the side chains present at positions **e** and **g** likely results in increased stabilization of the coiled-coil because they can extend across the hydrophobic interface reducing solvent accessibility to the hydrophobic core as observed in the X-ray structure of the GCN4 leucine zipper coiled-coil (O'Shea *et al.*, 1991). The more hydrophobic these side chains are, the better they will be able to interact with the hydrophobic core and exclude solvent. Previous studies demonstrated the stabilizing effects of hydrophobic residues at positions **e** and **g** (Schmidt-Dörr *et al.*, 1991). Therefore, the combined effects of the lower helical propensity and lower hydrophobicity of an ionized Glu side chain versus a Gln side chain would be expected to contribute to the observed decrease in the stability of the coiled-coil.

The fact that E_2(13,22)x and E_2(20,22)x have the same stability strongly suggests that there are no electrostatic repulsions between the Glu residues at position 20 of one chain and position 22 of the other. This supports the conclusion (O'Shea *et al.*, 1991) that bulky hydrophobes at position **d** hinder the side chains in the i to i'+2 orientation from interacting to form Lys-Glu salt bridges, and we can now extend this observation to include Glu-Glu repulsions. In E_2(13,22)x the Glu residues are separated by two full turns of the helix (a full heptad) and are therefore unlikely to interact. In both E_2(13,22)x and

E_2(20,22)x the entire destabilization with respect to Nx can therefore be explained by the above described hydrophobicity and helical propensity effects.

E_2(15,20)x is significantly less stable than all the other disulfide-bridged analogs with a $[\text{urea}]_{1/2}$ of only 4.4 M (Fig. III.4A, Table III.2). This $[\text{urea}]_{1/2}$ value is 1 M less than was obtained for E_2(13,22)x and E_2(20,22)x and corresponds to a $\Delta\Delta G_u$ of -1.4 kcal/mol relative to Nx. This coiled-coil is therefore 0.9 kcal/mol less stable than E_2(13,22)x and E_2(20,22)x, which suggests that there are specific charge effects between the residues at positions 15 and 20' of the opposing chains (of which there are two present in the molecule), which destabilize the coiled-coil by 0.45 kcal/mol each.

All five oxidized peptides were also submitted to GdnHCl denaturation at pH 7 and 20°C. The denaturation profiles (Fig. III.4B) show a striking difference with the urea denaturation profiles (Fig. III.4A). The GdnHCl denaturation curves for all five coiled-coils are similar, with a range of only 0.2 M in the $[\text{GdnHCl}]_{1/2}$ values and -0.2 kcal/mol for the $\Delta\Delta G_u$ values with respect to Nx (Table III.2). This suggests that GdnHCl is suppressing the charge-charge repulsions ($\Delta\Delta G_u$ for E_2(15,20)x is -1.4 kcal/mol from urea denaturation but only -0.2 kcal/mol from the GdnHCl results). These observations agree with the results of Monera *et al.* (1993, 1994a, 1994b), which suggested that the ionic nature of GdnHCl causes ionic interactions to be screened and gives a measure of the coiled-coil stability based on the strength of the interchain hydrophobic interactions while urea provides a measure of overall stability including both electrostatics and hydrophobic interactions (Monera *et al.*, 1994b). Similar results were obtained with denaturation studies on horse cytochrome c (Hagihara *et al.*, 1994). In addition, it is possible that binding of the positively charged guanidinium ion to the carboxylate of an ionized Glu neutralizes the side chain and allows it to interact more closely with the hydrophobic interface, thus reducing the observed intrinsic destabilization resulting from ionized Glu substitution. The effects of GdnHCl are further studied in Chapter IV (Kohn *et al.*, 1995b).

Coiled-coils have long been known to increase in stability as pH decreases, a phenomenon observed with tropomyosin (Lowey, 1965; Noelken & Holtzer, 1964), the Fos-Jun leucine zipper heterodimer (O'Shea *et al.*, 1992), and synthetic model coiled-coils (Hodges *et al.*, 1988; Zhou *et al.*, 1992c; Zhu *et al.*, 1993) despite the loss of interhelical salt bridges as Glu residues are protonated. The peptides in this study also follow this pattern, as shown in Figure III.5. The oxidized peptides were subjected to denaturation at 20°C and pH 3 with urea (Fig. III.5A) and GdnHCl (Fig. III.5B). Unlike at pH 7 (see Fig. III.4), the relative stabilities observed in the urea and GdnHCl profiles are similar. Because at pH 3 there are no charged residues present in the positions **a**, **d**, **e**, and **g** that may affect interchain interactions, it appears the two denaturants are both giving a measure only of the hydrophobic stability. The peptides require much lower concentrations of GdnHCl than urea to denature, suggesting GdnHCl is a stronger denaturant for disrupting hydrophobic interactions, as previously observed with globular proteins (Greene & Pace, 1974; Pace, 1986). For Nx, the $[\text{urea}]_{1/2}$ and $[\text{GdnHCl}]_{1/2}$ values both appear to be essentially pH independent over the range 3 to 7, consistent with the fact that this coiled-coil has no residues which change their ionization state in going from pH 7 to pH 3 (the pK_a of Lys is around 10.5). However, the stabilities of the peptides containing Glu residues increased dramatically upon lowering the pH to 3, indicating that protonation of the Glu side chains at low pH greatly enhances coiled-coil stability relative to that of Nx. In addition, the three peptides containing two Glu substitutions per chain all have equal stability in the protonated form, so the exact position of the protonated Glu residue is not a factor in its effect on stability. The large increases in $[\text{urea}]_{1/2}$ and $[\text{GdnHCl}]_{1/2}$ at pH 3 versus pH 7 (denoted $\Delta[D]_{1/2}$) are given in Table III.2. The most significant of these is +4.1 M for $E_2(15,20)x$ in urea denaturation due to the fact that the (i to i'+5) ionic interactions greatly decrease the coiled-coil stability observed by urea denaturation at pH 7.

In a recent study it was shown that one protonated Glu residue makes a greater contribution to coiled-coil stability of 0.46 kcal/mol over a Gln residue and 0.65 kcal/mol

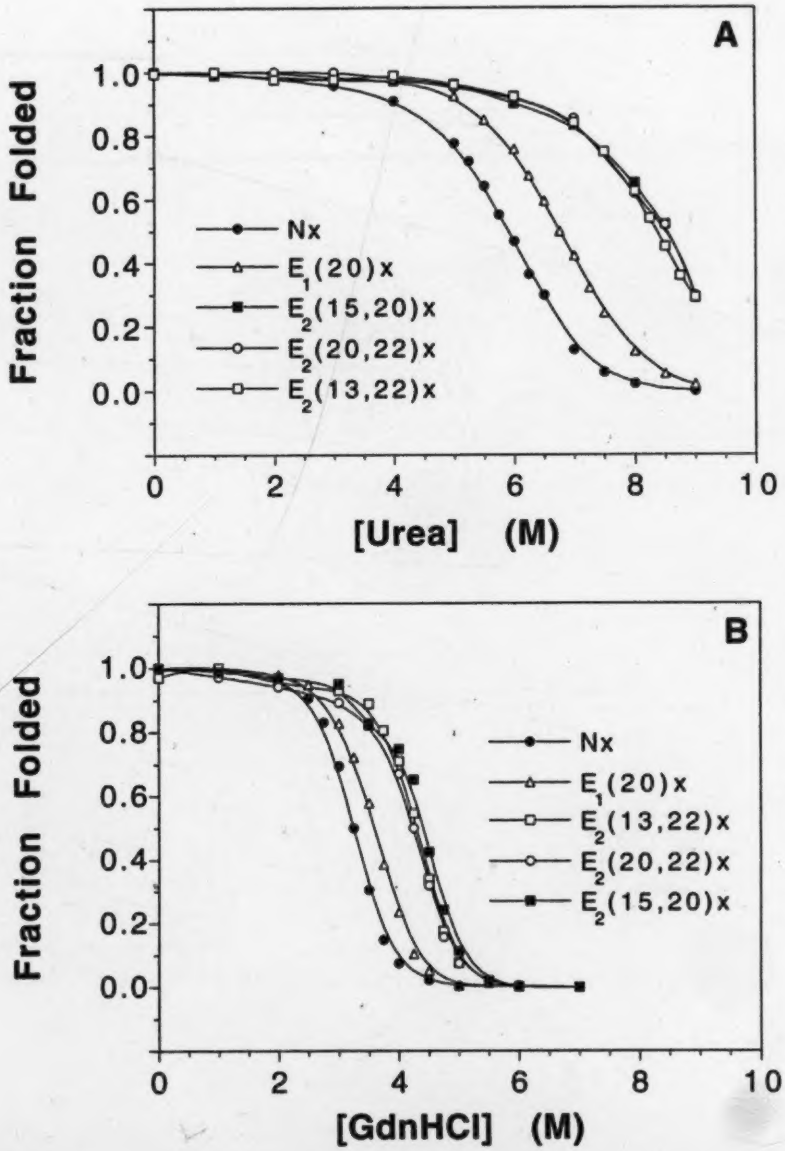

Figure III.5 Denaturation profiles of the disulfide-bridged coiled-coils at 20°C in a 0.1 M KCl, 0.05 M PO$_4$, pH 3 buffer with urea as denaturant in Panel A and GdnHCl as denaturant in Panel B. The fraction folded was calculated from the observed mean residue molar ellipticity at 222 nm as described in Chapter II, p. 57. Peptide concentrations were: Panel A: Nx, 81µM; E$_1$(20)x, 76µM; E$_2$(13,22)x, 90µM; E$_2$(20,22)x, 84µM; E$_2$(15,20)x, 101µM. Panel B: Nx, 76µM; E$_1$(20)x, 63µM; E$_2$(13,22)x, 75µM; E$_2$(20,22)x, 73µM; E$_2$(15,20)x, 70µM.

over an ionized Glu residue (Zhou *et al.*, 1994b). For $E_2(20,22)x$ the $\Delta\Delta G_u$ at pH 3 is +2.0 kcal/mol as determined from both the GdnHCl and the urea results (Table III.2). This finding corresponds to +0.5 kcal/mol per Gln to Glu substitution, which correlates well with Zhou's value of +0.46 kcal/mol. Similarly, $E_2(15,20)x$ and $E_2(13,22)x$ give average $\Delta\Delta G_u$ values (average of the GdnHCl and urea obtained values) of about +0.5 kcal/mol per Glu. For $E_1(20)x$ the average $\Delta\Delta G_u$ is +0.9 kcal/mol or +0.45 kcal/mol per Glu. The effect is additive in going from zero to two to four Glu residues at pH 3 as it was at pH 7, except the $\Delta\Delta G_u$ is in the opposite direction (stabilizing rather than destabilizing). The difference between the $\Delta\Delta G_u$ value at pH 7 and pH 3 is a measure of the change in stability of the peptide in changing from an ionized Glu to a protonated Glu. For $E_2(13,22)x$ and $E_2(20,22)x$ the urea data give $\Delta\Delta G_u$ values of +2.4 and +2.5 kcal/mol, respectively, corresponding to +0.6 and +0.63 kcal/mol per Glu residue. These correlate well with the value of +0.65 kcal/mol determined by the previous study (Zhou *et al.*, 1994b), also obtained from urea denaturation data. For $E_2(15,20)x$ the change in $\Delta\Delta G_u$ is +3.2 kcal/mol or +0.8 kcal/mol per Glu residue, which is higher due to the added destabilization of this peptide at pH 7 by i to i'+5 Glu-Glu repulsions. For $E_1(20)x$ the difference between the $\Delta\Delta G_u$ values at pH 3 and at pH 7 obtained from urea denaturation is +1.2 kcal/ mol (or +0.6 kcal/mol per Glu), in agreement with the other results.

The observed increase in stability at pH 3 with increasing number of Glu residues at **e** and **g** positions can be explained similarly to the decrease in stability observed at pH 7 upon substitution of Glu residues at the **e** and **g** positions. The helical propensity of a protonated Glu residue is higher than that of a Gln residue, 0.66 versus 0.56 respectively (Chakrabartty *et al.*, 1994; Scholtz *et al.*, 1993). As well, the apparent hydrophobicity of a protonated Glu side chain is higher than that of a Gln side chain (Guo *et al.*, 1986; Sereda *et al.*, 1994), and as described above, the two effects should combine to increase coiled-coil stability. It should be noted that although the increase in helical propensity correlates with an increase in hydrophobicity in the order: ionized Glu < Gln < protonated Glu, this is not always the case. For example, the Lys and Arg side chains have higher helical propensities than the Phe and Ile side chains (Chakrabartty *et al.*, 1994; O'Neil & DeGrado, 1990; Zhou *et al.*, 1994d), but Arg and Lys have lower apparent hydrophobicities than Phe and Ile (Guo *et al.*, 1986; Sereda *et al.*, 1994). In general, increasing side chain hydrophobicity does not correlate with increasing helical propensity (Monera *et al.*, 1995).

d) Stabilities of the reduced coiled-coils at pH 3 and pH 7

All five analogs were subjected to urea denaturation at 20°C in the reduced form. It was found that the denaturation profiles at pH 7 (Fig. III.6A) were similar to those for the disulfide-bridged coiled-coils, except the curves for all five peptides have shifted so that the $[\text{urea}]_{1/2}$ values are all about 3.5 M less. $E_2(15,20)r$ is only about 80% folded in benign buffer, as demonstrated in its CD scan (Fig. III.3B), and it unfolds very rapidly as urea is added. The $\Delta\Delta G_u$ values for the reduced mutant peptides with respect to Nr (Table III.2) are similar to those observed for the oxidized peptides, showing that loss of the disulfide bridge has destabilized all the peptides to the same extent (approximately 3 kcal/mol). The value obtained for the destabilizing effect of the i to i'+5 repulsion in $E_2(15,20)r$ is -0.5 kcal/mol, very similar to the value of 0.45 kcal/mol obtained for $E_2(15,20)x$.

The urea denaturation profiles for the reduced coiled-coils at pH 3 are shown in Figure III.6B. Unlike at pH 7, $E_2(15,20)r$ is fully helical in the absence of urea, as a result of protonation of the Glu residues and removal of the interhelical i to i'+5 repulsions. It showed a molar ellipticity of -34,300 $\text{deg}\cdot\text{cm}^2\cdot\text{dmol}^{-1}$, equal to that of Nr (-33,000 $\text{deg}\cdot\text{cm}^2\cdot\text{dmol}^{-1}$) within experimental error. As was the case with Nx, the $[\text{urea}]_{1/2}$ of Nr did not change significantly with pH. At pH 3 the reduced peptides containing two Glu substitutions are all of similar stability and have much higher stability than Nr, as in the disulfide-bridged form. In terms of $\Delta\Delta G_u$, the average value of all three peptides is +2.3 kcal/mol, which is similar to the average $\Delta\Delta G_u$ of +1.9 kcal/mol obtained from the three

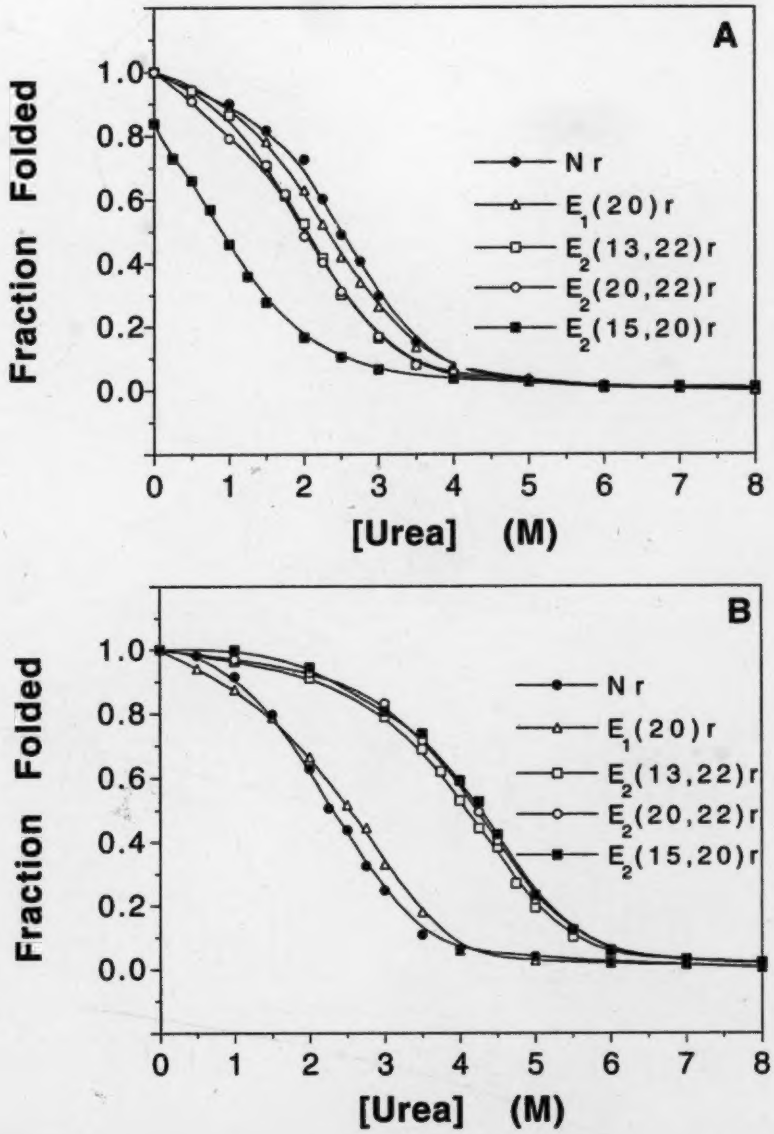

Figure III.6 Urea denaturation profiles of the reduced coiled-coils at 20 C in 0.05 M PO$_4$, 0.1 M KCl buffer containing 5 mM DTT at pH 7 (Panel A) and pH 3 (Panel B). The fraction folded was calculated from the observed mean residue molar ellipticity at 222 nm as described in Chapter II. Note that for $E_2(15,20)$r the fraction folded at 0 M urea is less than 1.0 because this peptide is not as helical as the other peptides in benign conditions. Therefore, $[\theta]_n$ (ellipticity of the fully folded state) is taken as the mean residue ellipticity of Nr in benign conditions. Peptide concentrations were Panel A: Nr ,171 μM; $E_1(20)$r,134 μM; $E_2(13,22)$r,152 μM; $E_2(20,22)$r, 173 μM; $E_2(15,20)$r,151 μM. Panel B: Nr, 143 μM; $E_1(20)$r, 116 μM; $E_2(13,22)$r, 110 μM; $E_2(20,22)$r, 108 μM; $E_2(15,20)$r, 104 μM.

oxidized peptides. The $\Delta\Delta G_u$ value for $E_1(20)r$ is only +0.4 kcal/mol; 0.4 kcal/mol less than for the oxidized peptide.

At both pH 7 and pH 3, the $\Delta\Delta G_u$ between the oxidized and reduced forms of the five sequences, denoted as $\Delta\Delta G_{u,ox-red}$ (see Table III.2) is around -3 kcal/mol, which compares quite closely to the values obtained for similar 35 residue coiled-coils with a disulfide bridge at position 2 (Hodges *et al.*, 1990).

e) Reversed-phase HPLC behavior

The behavior of the reduced and oxidized coiled-coils on reversed-phase chromatography at pH 2 and pH 7 can explain the stability data obtained from denaturation studies. As was previously reported by Zhu *et al.* (1992) and Hodges *et al.* (1994), the 70 residue disulfide-bridged peptides elute significantly sooner than their 35 residue reduced counterparts (Table III.1), suggesting that they are retaining a large portion of their coiled-coil structure. This keeps the hydrophobic faces from interacting with the stationary phase and makes their apparent hydrophobicity lower than that of the reduced coiled-coils, which are generally denatured under reversed-phase conditions (Ingraham *et al.*, 1985; Lau *et al.*, 1984a). This would be expected considering the significant stability difference between reduced and oxidized coiled-coils (Table III.2).

In terms of the difference in retention time between the native and mutant peptides (denoted Δt_r; see Table III.1) the clearest results are for the reduced peptides (shown in Fig. III.7). The chromatograms at pH 7 of mixtures of Nr with each of the mutant peptides show a definite correlation between increasing number of Glu residues at **e** and **g** positions and decreasing retention time (Fig. III.7A). At pH 2 (Fig. III.7B) the opposite trend is obtained; increasing the number of Glu residues increases the retention time. This is consistent with the study of Hodges and co-workers, who observed a large increase in retention time upon protonation of Glu residues at the **g** position of a 35-residue coiled-coil peptide and concluded that the surface area of the peptide which interacts substantially with

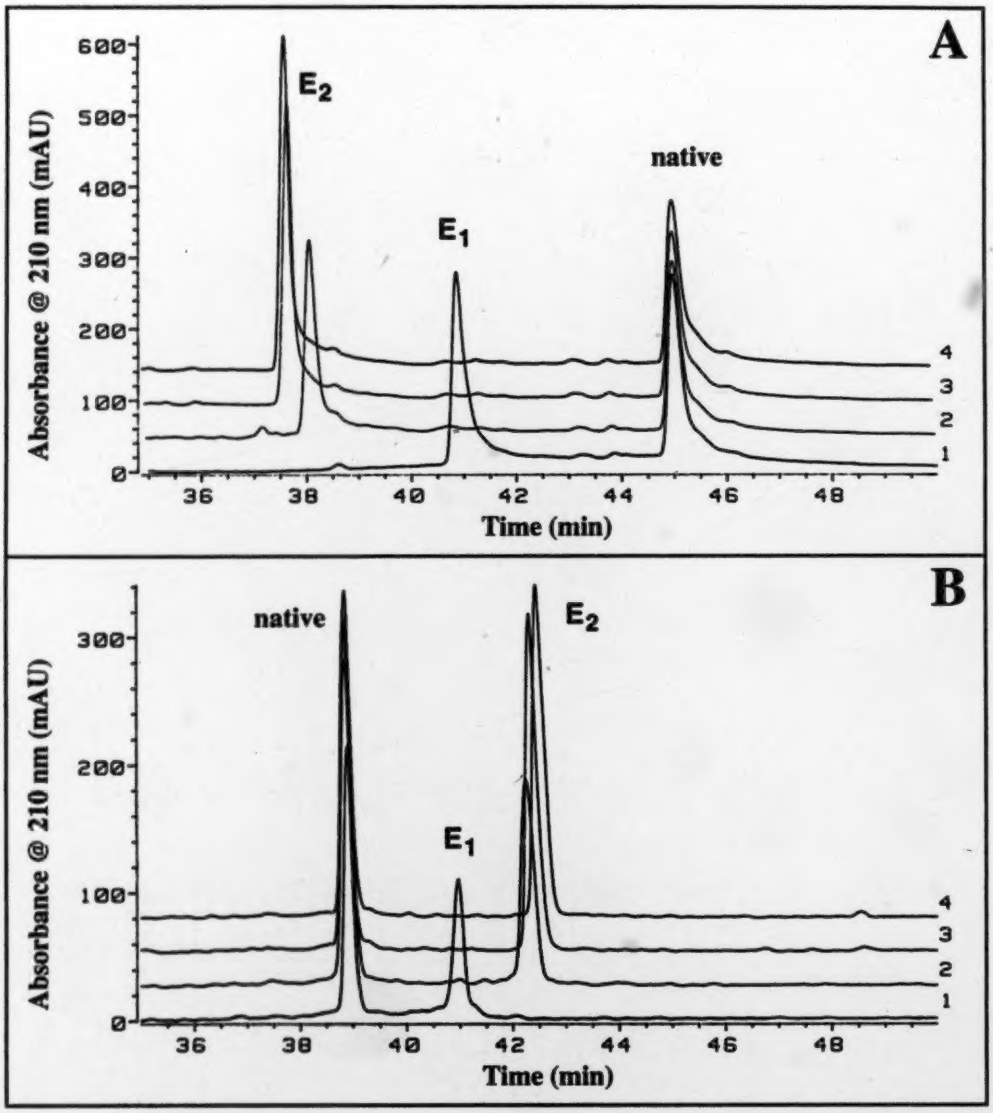

Figure III.7 Reversed-phase HPLC profiles of the reduced peptides at pH 7 (Panel A) and pH 2 (Panel B). Column: Aquapore RP-300 C8 column (220 X 4.6 mm I.D., 7 µm particle size, 300Å pore size) (Brownlee Labs, Santa Clara, CA). Mobile phase: Panel A: linear AB gradient 2% B/min (equivalent to 1% CH_3CN/min) where A = 0.01 M $(NH_4)_2HPO_4$, 0.1 M $NaClO_4$ in H_2O, pH 7 and B= 0.01 M $(NH_4)_2HPO_4$, 0.1 M $NaClO_4$ in CH_3CN:H_2O (1:1,v:v), pH 7. Panel B: linear AB gradient 1% B/min where A = 0.05% TFA/H_2O and B = 0.05% TFA/CH_3CN. Flow rate was 1.0 ml/min. In both panels run 1 contains Nr + E_1(20)r, run 2 contains Nr + E_2(13,22)r, run 3 contains Nr + E_2(20,22)r, and run 4 contains Nr + E_2(15,20)r

the stationary phase includes the side chains of positions **e** and **g** as well as the hydrophobes at positions **a** and **d** (Hodges *et al.*, 1994). Previous results had illustrated the concept of a preferred binding domain in amphipathic helical peptides, where the peptides remain helical and bind preferentially through their hydrophobic faces (Zhou *et al.*, 1990). The positions inside the box in Figure I.3A (p. 23) are included in the preferred binding domain for interaction of the helix with the hydrophobic stationary phase surface of the column. Therefore, protonation of the Glu side chains increases hydrophobicity of the binding domain, which in turn increases the retention time.

At pH 7, $E_1(20)r$ elutes 4.0 min before Nr, a very large decrease in retention time for a single Gln to ionized Glu substitution. The reduced peptides containing two Glu substitutions elute 6.9-7.3 min before Nr, an average reduction in retention time of 3.6 min per ionized Glu. At pH 2 there is an increase of 2.1 min in the retention time of $E_1(20)r$ and 3.4-3.6 min for the reduced peptides containing two Glu substitutions (an average of 1.75 min per protonated Glu). Thus, at both pH values, the Δt_r with two Glu residues present is almost twice what it is with one Glu residue present, suggesting the effect is additive, but the magnitude of the Δt_r is about two-fold higher at pH 7. This laboratory has determined retention coefficients for amino acid residues on reversed-phase HPLC based on substitutions in a model 8 residue peptide with Gln as the reference amino acid at the substitution site (Guo *et al.*, 1986). Relative coefficients for an ionized Glu at pH 7 and a protonated Glu at pH 2 were -1.3 min and +1.1 min respectively. While these results do not correlate exactly in magnitude to the results obtained here (-3.6 to 4.0 min for ionized Glu and +1.75 to 2.1 min for protonated Glu) the relative order of the hydrophobicity for these side chains is: protonated Glu > Gln > ionized Glu in both peptide systems. The differences between the results obtained here and in the previous study may be due to the nature of the host peptide; in this study there is a preferred binding domain in an amphipathic helix with the substitution site(s) within the hydrophobic face while Guo's model was a short peptide lacking any secondary structure. Recently, Sereda *et al.* (1994)

determined the effect on hydrophobicity of substitution of all 20 amino acids in the center of the hydrophobic face of an amphipathic α-helix, as measured by reversed-phase HPLC at pH 2. Their results for the relative difference in retention time of a Glu substituted peptide over a Gln substituted peptide was +2.2 min in an Ala face and +1.9 min in a Leu face, in much closer agreement with the results obtained in this study.

The results from the reduced peptides therefore support the conclusion that there is increased hydrophobicity of the Glu side chain at low pH and this leads not only to stronger hydrophobic interactions of a single helix with the reversed-phase matrix but also to increased hydrophobic interactions between the helices of a two-stranded α-helical coiled-coil.

The data obtained on the oxidized peptides is much less clear because, as stated above, they are retaining some degree of tertiary and quaternary structure.The Δt_r values are much smaller than for the reduced peptides at both pH 7 and 3. At pH 7, the trend in retention times is still clear (a decrease with each additional Glu residue) with an overall range of elution times of 4.1 min (Table III.1). At pH 2 the oxidized peptides elute much closer together over a range of only 0.6 min. Since the coiled-coils were most stable in the oxidized form at low pH, it follows that the retention times under these conditions in reversed-phase HPLC would show the least variation since the hydrophobic faces, where the differences in sequence exist, are least dissociated and unavailable to interact with the stationary phase.

The Δt_r values at pH 7 were subtracted from those at pH 2 for each peptide to give $\Delta\Delta t_r$ (Table III.1), a measure of the change in retention time in going from pH 7 to pH 2 (with respect to native peptide as an internal standard to correct for changes in retention times due to the buffer conditions). The results show that the retention times of the reduced peptides are more than twice as sensitive to pH as the retention times of the oxidized peptides. This again indicates that the reduced peptides have their hydrophobic faces completely exposed and able to interact with the stationary phase, making the retention time more sensitive to changes in residues at the hydrophobic face.

Nr and Nx both elute significantly later at pH 7 than pH 2 even though there is no difference in their ionization state. In the pH 7 buffer, ammonium phosphate and sodium perchlorate are present in much higher concentrations (10 mM and 100 mM, respectively) than the 0.05% (5 mM) trifluoroacetic acid present in the pH 2 buffers . Therefore, at pH 7 there may be more complete ion pairing with the Lys^+ side chains, decreasing the hydrophilicity of the peptides by neutralizing their charge and increasing retention time. Alternatively, the higher salt concentration could increase retention time by enhancing hydrophobic interactions between the peptide and stationary phase (salting-out effects) as discussed in Chapter I.

C. Conclusions

The main goal of this study was to determine the destabilizing effects of possible interchain Glu-Glu electrostatic interactions. It was clearly shown that in the i to i'+5 orientation of Glu residues, there was a definite destabilization that was not seen when the orientation of opposing Glu residues was i to i'+2. The magnitude of the destabilizing i to i'+5 Glu-Glu repulsion was determined to be 0.45 kcal/mol per interaction, and there were two of these interactions in the E_2(15,20) coiled-coil. A double mutant analysis as performed previously by Zhou *et al.* (1994b) was not necessary since the effects on helical propensity and hydrophobicity of a Gln to Glu substitution were determined in E_2(13,22) and subtracted from the overall destabilization of E_2(15,20). The magnitude for the Glu-Glu repulsion is close to what was found for the charge repulsive destabilization of the melittin tetramer of 0.6 kcal/charge•mole of tetramer (Hagihara *et al.*, 1992) and for the molten globule state of horse cytochrome c (Goto & Nishikiori, 1991) which was determined to be 0.45 kcal/mol•charge. It is also comparable to the destabilizing effect of

0.2 kcal/mol found for an interhelical i to i+4 Lys-Lys repulsion in a monomeric α-helical peptide (Stellwagen *et al.*, 1992).

The average stabilizing effect for an interhelical Glu-Lys salt bridge was found to be 0.38 kcal/mol (Zhou *et al.*, 1994b) in a two-stranded α-helical coiled-coil model similar to the one employed here. These electrostatic interactions in α-helical two-stranded coiled-coils are in a hydrophobic microenvironment since they cross the hydrophobic interface (Talbot & Hodges, 1982). However, this value is within the range 0.2-0.5 kcal/mol in which surface-exposed ion pairs contribute to the stability of folded proteins (Dao-pin *et al.*, 1991; Horovitz *et al.*, 1990; Sali *et al.*, 1991; Serrano *et al.*, 1990) and also in the range 0.4-0.5 kcal/mol determined for the stabilization of intrahelical i to i+3 and i to i+4 Glu-Lys ion pairs on isolated α-helical peptides (Lyu *et al.*, 1992; Scholtz *et al.*, 1993; Stellwagen *et al.*, 1992). Therefore, it appears that all these interactions have very similar quantitative effects on stability.

It was noted by Vinson *et al.* (1993) that increasing the number of interchain ionic attractions between **e** and **g** positions of opposing helices has a small effect on dimerization specificity, but the addition of one repulsive interaction to a heterodimeric leucine zipper drove formation of the respective homodimers instead. This finding also supports the conclusion of O'Shea *et al.* (1992, 1993) that electrostatic repulsions in the homodimers rather than attractions in the heterodimer are the major driving force for heterodimer formation. These conclusions and the fact that very stable coiled-coils form without the need for interchain salt bridges have caused the relevance of interchain salt bridges to be questioned. However, based on the studies that have demonstrated the influence of interchain ionic attractions and repulsions between residues at the **e** and **g** positions of the heptad repeat on homodimer versus heterodimer coiled-coil formation (Graddis *et al.*, 1993; O'Shea *et al.*, 1993; Zhou *et al.*, 1994c), it was important to determine the relative energetic effects of stabilizing salt bridges versus destabilizing repulsions. The results of this study and those of Zhou *et al.* (1994b) indicate that the effects are similar in magnitude, and the stabilizing effect of one Glu-Lys attraction should nearly offset the destabilizing effect of one Glu-Glu repulsion.

The present study clearly demonstrates the quantitative importance of electrostatic repulsions in protein stability. Questions that remain to be answered concerning electrostatics are the additivity of salt bridge and charge repulsion effects, and the relative roles of net charge in the hydrophobic interface versus specific ionic interactions in determining the stability and folding of α-helical chains in coiled-coils and proteins in general.

CHAPTER IV

EFFECTS OF INTERHELICAL ELECTROSTATIC REPULSIONS BETWEEN GLUTAMIC ACID RESIDUES ON THE DIMERIZATION AND STABILITY OF TWO-STRANDED α-HELICAL COILED-COILS[2]

A. Introduction

A detailed, systematic analysis of the regulation of coiled-coil formation and stability by electrostatic repulsions was carried out, to obtain more information on the importance of these interactions in regulating the dimerization specificity of various coiled-coil containing proteins in nature and to understand how such interactions can be used to manipulate the folding of *de novo* designed proteins under various buffer conditions.

Previous studies (Graddis *et al.*, 1993; O'Shea *et al.*, 1993; Zhou *et al.*, 1994c) showed that incorporation of glutamic acid residues at all the **e** and **g** positions of model coiled-coil proteins completely prevented coiled-coil formation, presumably due to the effects of interhelical charge repulsion. Each specific **g-e'** Glu-Glu repulsion has been estimated to destabilize a two-stranded coiled-coil by 0.45 kcal/mol (Chapter III, Kohn *et al.*, 1995a) and 0.78 kcal/mol (Krylov *et al.*, 1994). These repulsive destabilizing effects are over and above the intrinsic destabilization of the Gln to Glu substitutions resulting from differences in helical propensity and hydrophobic packing interactions at the dimer interface and are the dominating effect (Chapter III, Kohn *et al.*, 1995a).

As the number of Glu residues in the **e** and **g** positions is varied, the degree of coiled-coil formation should be altered significantly, which may be a function of the overall net charge at the dimer interface (general charge repulsions between like-charged helical faces) as well as the effects of specific electrostatic repulsions. In this study, the net interface charge as well as the number of potential specific charge-charge repulsions were systematically increased by the substitution of Glu for Gln residues, and the effects on coiled-coil formation and stability were measured. Particular interest was in determining the degree of negative charge repulsion allowed before coiled-coil formation is completely abolished, thus giving a qualitative measure of the relative roles of electrostatic and other contributions to coiled-coil stability. Further experiments were also carried out in order to investigate the relative roles of the general and specific components of the charge repulsions in the control of coiled-coil folding and stability. Finally, the ability of salt and changes in pH to modulate the structure and stability of the coiled-coil analogs is addressed.

---

[2] A version of this chapter has been published: Kohn, W. D., Monera, O. D., Kay, C. M., and Hodges, R. S. (1995). *J. Biol. Chem.* **270**, 25495-25506.

B. Results and Discussion

a) Peptide design and nomenclature

Figure IV.1 shows the amino acid sequences of the synthetic peptides that were used in this study. Each consisted of a 35-residue peptide chain with an acetylated N-terminus and an amide group at the C-terminus. The native sequence, designated 'N', provided a stable reference coiled-coil containing no interhelical electrostatic interactions to which the mutant peptides could be compared (as discussed under Methods in Chapter II).

Substitutions of glutamic acid for glutamine were made in a systematic fashion from the N terminus towards the C terminus as shown in Figure IV.1. The resulting analogs were designated E2, E4, E6, E8 and E10 according to the number of Glu residues at positions **e** and **g** in the 35 residue polypeptide chain (Figure IV.1). The peptides with reduced cysteine at position 2 were designated with an "r" while those with an interchain disulfide bridge between cysteines at positions 2 and 2' were designated with an "x".

Shown in Figure IV.2 is a helical wheel diagram of the potential coiled-coil formed by E10. The diagram depicts with arrows the van der Waals interactions between residues at the **a** and **d** positions on opposing chains as they pack together in the hydrophobic core and the potential electrostatic repulsions between glutamic acid residues at position **e** of one helix and at position **g** of the opposing helix. Although charged groups do not interact

Peptide Name	Net Interface Charge	Amino Acid Sequence
		1 5 10 15 20 25 30 35
		g a b c d e f g a b c d e f g a b c d e f g a b c d e f g a b c d e f
native	0	Ac-Q-C-G-A-L-Q-K-Q-V-G-A-L-Q-K-Q-V-G-A-L-Q-K-Q-V-G-A-L-Q-K-Q-V-G-A-L-Q-K-amide
E2	-4	Ac-E-C-G-A-L-E-K-Q-V-G-A-L-Q-K-Q-V-G-A-L-Q-K-Q-V-G-A-L-Q-K-Q-V-G-A-L-Q-K-amide
E4	-8	Ac-E-C-G-A-L-E-K-E-V-G-A-L-E-K-Q-V-G-A-L-Q-K-Q-V-G-A-L-Q-K-Q-V-G-A-L-Q-K-amide
E6	-12	Ac-E-C-G-A-L-E-K-E-V-G-A-L-E-K-E-V-G-A-L-E-K-Q-V-G-A-L-Q-K-Q-V-G-A-L-Q-K-amide
E8	-16	Ac-E-C-G-A-L-E-K-E-V-G-A-L-E-K-E-V-G-A-L-E-K-E-V-G-A-L-E-K-Q-V-G-A-L-Q-K-amide
E10	-20	Ac-E-C-G-A-L-E-K-E-V-G-A-L-E-K-E-V-G-A-L-E-K-E-V-G-A-L-E-K-E-V-G-A-L-E-K-amide

Figure IV.1 Amino acid sequences of the peptides studied to determine the effect of an increasing number of interhelical Glu-Glu repulsions involving residues at positions **e** and **g** of the heptad repeat (in bold type) on the folding and stability of a two-stranded coiled-coil. Substitutions of Glu (E) for Gln (Q) are highlighted by boxes. A cysteine at position 2 allows formation of an interchain disulfide bridge. Peptide nomenclature is based on the number of Glu substitutions.

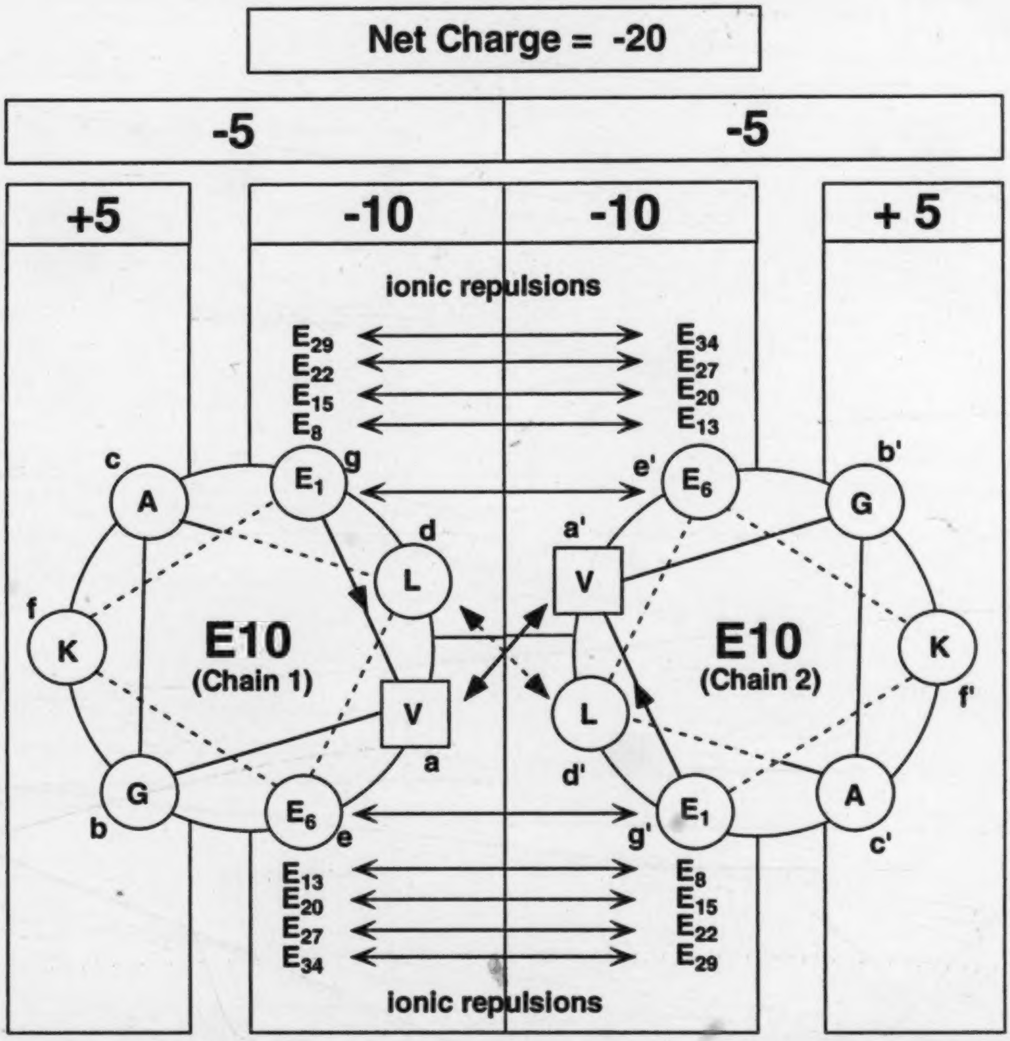
Net Charge = -20
-5
-5
+5
-10
-10
+ 5
ionic repulsions
E29
E22
E15
E8
E34
E27
E20
E13
c
A
E1
g
e'
E6
b'
G
d
L
a'
V
f
K
E10
(Chain 1)
E10
(Chain 2)
K
f'
V
a
L
d'
G
b
E6
e
E1
g'
A
c'
E13
E20
E27
E34
E8
E15
E22
E29
ionic repulsions

Figure IV.2 Cross-sectional helical wheel diagram of coiled-coil E10. The direction of propagation of the polypeptide chain is into the page from N to C terminus with the chains parallel and in-register. This diagram depicts interchain **a-a'** and **d-d'** van der Waals interactions between the hydrophobic side chains, which pack in a knobs into holes fashion (the prime indicates the corresponding position on the opposing helix). Also indicated are **g - e'** (i to i'+5) interchain repulsions between glutamic acid residues at position g of the heptad repeat on one helix and position e' of the following heptad on the other helix. The residues which comprise the entire dimerization interface at positions **a, d, e, g, a', d', e'**, and **g'** are within the central boxes. Also given are the net charge on the nonpolar and polar faces of each helix (-10 and +5, respectively) as well as the net charge on each helix (-5) and on the dimer interface of the coiled-coil (-20).

significantly in an aqueous environment due to solvent screening (Chapter I), these residues are in a partially hydrophobic microenvironment due to their being partially surrounded by hydrophobic residues. Therefore, despite being solvent exposed, charged interactions between these residues can contribute to coiled-coil stability (Cantor & Schimmel, 1980; Krylov *et al.*, 1994; Talbot & Hodges, 1982; Zhou *et al.*, 1994b). The central boxes in Figure IV.2 containing the **a**, **d**, **e** and **g** positions on chain 1 and the **a'**, **d'**, **e'** and **g'** positions on chain 2 signify the complete dimerization interface (Adamson *et al.*, 1993; Hodges *et al.*, 1994; O'Shea *et al.*, 1991) where any potential interhelical contacts are made.

The net charge at the dimer interface in this series of peptides ranges from zero in the native coiled-coil to -20 in the E10 coiled-coil, as shown in Figure IV.1.

b) Structural characterization of the model coiled-coils

The peptides were evaluated by several techniques to determine the extent of two-stranded α-helical coiled-coil formation. These techniques included circular dichroism spectroscopy, ultracentrifugation, laser light scattering, and high performance size-exclusion liquid chromatography.

i) CD spectra of coiled-coil analogs. The CD spectra of the peptides are shown in Figure IV.3. In Panel A are the spectra for the disulfide-bridged analogs Nx, E4x, E6x, E8x and E10x in benign 25 mM PO_4, 50 mM KCl buffer at pH 7. The double minima at 208 nm and 220 nm are characteristic of helical structure. The CD band at 220 nm is due to the n-π* transition and is responsive to the amount of helical content. The predicted molar ellipticity for a 100% α-helical 35 residue polypeptide was calculated as $[\theta]_{220,\max} = -33{,}600\ \mathrm{deg{\bullet}cm^2{\bullet}dmol^{-1}}$ (Hodges *et al.*, 1988) based on the theoretical equation of (Chen *et al.*, 1974). Therefore, Nx, with a $[\theta]_{220}$ of -31,900 is highly α-helical (Table IV.1). Addition of the helix enhancing solvent TFE (Sonnichsen *et al.*, 1992) did not increase the helical content of Nx as indicated by the molar ellipticity at 220 nm (Table IV.1).

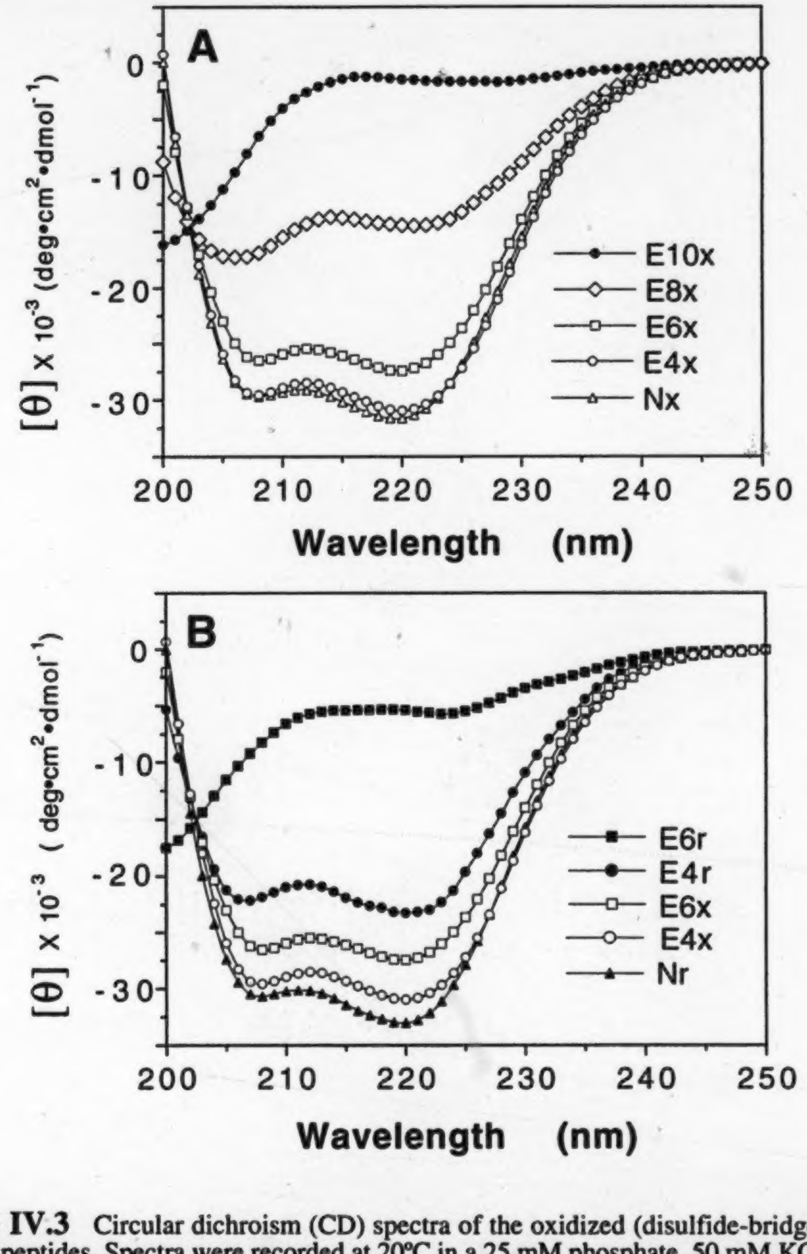

Figure IV.3 Circular dichroism (CD) spectra of the oxidized (disulfide-bridged) and reduced peptides. Spectra were recorded at 20°C in a 25 mM phosphate, 50 mM KCl, pH 7 buffer. **A**, spectra for the oxidized peptides. **B**, comparison of reduced and oxidized peptides. Peptide concentrations: Panel A: Nx, 201 μM; E4x, 122 μM; E6x, 208 μM; E8x, 145 μM; E10x, 165 μM. Panel B: Nr, 203 μM; E4r, 243 μM; E6r, 306 μM; E4x and E6x same as Panel A. Concentrations are given as the concentration of single stranded monomer for the reduced and two-stranded monomer for the oxidized peptides.

a The sequences and nomenclature for the peptides are shown in Figure IV.1.

b $[\theta]_{220}$, the mean residue molar elipticity at 220 nm in units of deg·cm^2·dmol^{-1}, was measured at 20°C and pH 7 in 50 mM PO_4 buffer and the salt conditions listed.

c The $[\theta]_{220}$ value of -33,600 deg•cm^2•dmol^{-1} was used for 100% α-helical content based on the equation:

$$X_H^n = X_H^\infty(1-k/n)$$

where X_H^∞ is -36,300 degree•cm^2•dmol^{-1} for a helix of infinite length, n is the number of residues per helix, and k is a wavelength dependent constant (2.6 at 220 nm) (see Chen *et al.*, 1974).

d Benign medium conditions (50 mM KCl concentration) combined 1:1 (v/v) with trifluoroethanol.

Table IV.1: Molar ellipticities and % helix of the coiled-coil analogs N-E10 under different buffer conditions

Peptide [a] Name	Benign, 50 mM KCl		Benign, 3 M KCl		1 M GdnHCl		50 % TFE [d]	
	$[\theta]_{220}$[b]	% Helix [c]	$[\theta]_{220}$	% Helix	$[\theta]_{220}$	% Helix	$[\theta]_{220}$	% Helix
Nx	-31,900	95	-32,100	96	-32,000	95	-30,600	91
E2x	-32,900	98	-32,300	96	-31,500	94	-32,200	96
E4x	-31,000	92	-31,900	95	-31,500	94	-30,700	91
E6x	-27,500	82	-31,800	95	-27,400	82	-23,600	70
E8x	-14,500	43	-31,500	94	-29,400	88	-25,100	75
E10x	-1,500	4	-29,900	89	-29,000	86	-21,800	65
Nr	-32,900	98	---	--	---	--	-32,600	97
E2r	-31,500	94	---	--	---	--	-30,800	92
E4r	-23,100	69	---	--	---	--	-26,500	79
E6r	-5,400	16	---	--	---	--	-26,600	79
E8r	-3,200	10	---	--	---	--	-24,800	74
E10r	-1,200	4	---	--	---	--	-22,200	66

As shown in both Figure IV.3A and Table IV.1, an increase in the number of glutamic acid residues per chain from 0 to 10, corresponding to an increase in the net charge at the dimer interface from 0 to -20 and an increase in the number of interhelical i to i'+5 Glu-Glu repulsions from 0 to 10, results in a gradual decrease in the amount of helical content from approximately 100% to 4%, the latter indicative of a mostly random coil structure. As mentioned above, the native coiled-coil Nx contains a high degree of helical content in benign conditions of low salt. E4x contains nearly the same helical content as Nx, so a net charge of -8 in the dimer interface has not significantly affected the coiled-coil structure. As the number of glutamic acid residues per chain is further increased to 6, 8, and 10 a progressive loss in helical content is observed until with 10 Glu residues per chain the amount of helical content is only about 4%. Therefore, the helical content has been systematically reduced through the effects of a gradual increase in the net negative charge at the dimer interface and specific charge repulsions. This result is likely due to a shift in the equilibrium between folded and unfolded protein rather than a decrease in helicity of the folded state; consistent with the assumption that the unfolding of all the coiled-coils in this study follows a two-state transition (see Chapter II, p. 56), and the peptides are present only in the fully folded or fully unfolded states.

The increase in net negative charge prevents dimerization primarily through interchain electrostatic repulsions. However, this increase in negative charge has a much smaller effect on the formation of monomeric α-helices in 50% TFE. TFE has been shown to disrupt tertiary and quaternary structure (Lau *et al.*, 1984a). For example, the molar ellipticity of E10x at 220 nm is increased from -1,500 deg•cm^2•dmol^{-1} in benign buffer to -21,800 deg•cm^2•dmol^{-1} in 50% TFE (Table IV.1). The low helicity of E10x relative to Nx in 50% TFE indicates that the high negative charge density on the helix is inherently destabilizing, even though the net charge has not changed (overall net charge on Nx is +10 and on E10x is -10).

In Figure IV.3B and Table IV.1, the effect of reducing the interhelical disulfide bridge is illustrated. While the reduced native coiled-coil, Nr, is fully helical, the helical contents of E4r, E6r and E8r are substantially decreased compared to their oxidized counterparts. A disulfide bridge between positions 2 and 2' has been shown to significantly stabilize model 35-residue coiled-coils against denaturing conditions (Hodges *et al.*, 1990; Zhou *et al.*, 1993a; Zhu *et al.*, 1992). The increased stability of the coiled-coil resulting from the disulfide bridge is able to overcome the destabilizing effects of the interhelical charge-charge repulsions to a significant extent.

ii) Effects of pH on coiled-coil formation. Because the loss of helical content upon the substitution of glutamic acid for glutamine appears to be due to interhelical electrostatic repulsions, protonation of the glutamic acid residues should promote a recovery in helical content by removing the repulsions. This is evident in Figure IV.4A where the CD spectrum of E10x is shown at three different pH values. At pH 7 the spectrum is essentially that of a random coil peptide, at pH 6.25 the peptide is approximately 50% helical, and at pH 5.4 the peptide is fully helical. The isodichroic point at around 203 nm suggests a two-state transition (Engel *et al.*, 1991; Thompson *et al.*, 1993). The pH titration profile (Fig. IV.4B) shows that both E10x and E10r are random coils at pH 7. As the pH is decreased, there is a sharp transition to helical structure within a range of one pH unit as indicated by the large increase in negative ellipticity at 220 nm. Interestingly, the transition for E10x is shifted to higher pH relative to that for E10r, which suggests that E10x can form a coiled-coil with a lower degree of glutamic acid residue protonation (a higher net negative charge at the interface). These results are consistent with those of Figure IV.3, both showing that the destabilizing effects of the negatively charged glutamate residues can be partially overcome by the stabilizing presence of a disulfide bridge. It may be inferred that, in general, the more inherently stable the coiled-coil, due to factors such as the presence of an interhelical disulfide bridge or stronger packing of the

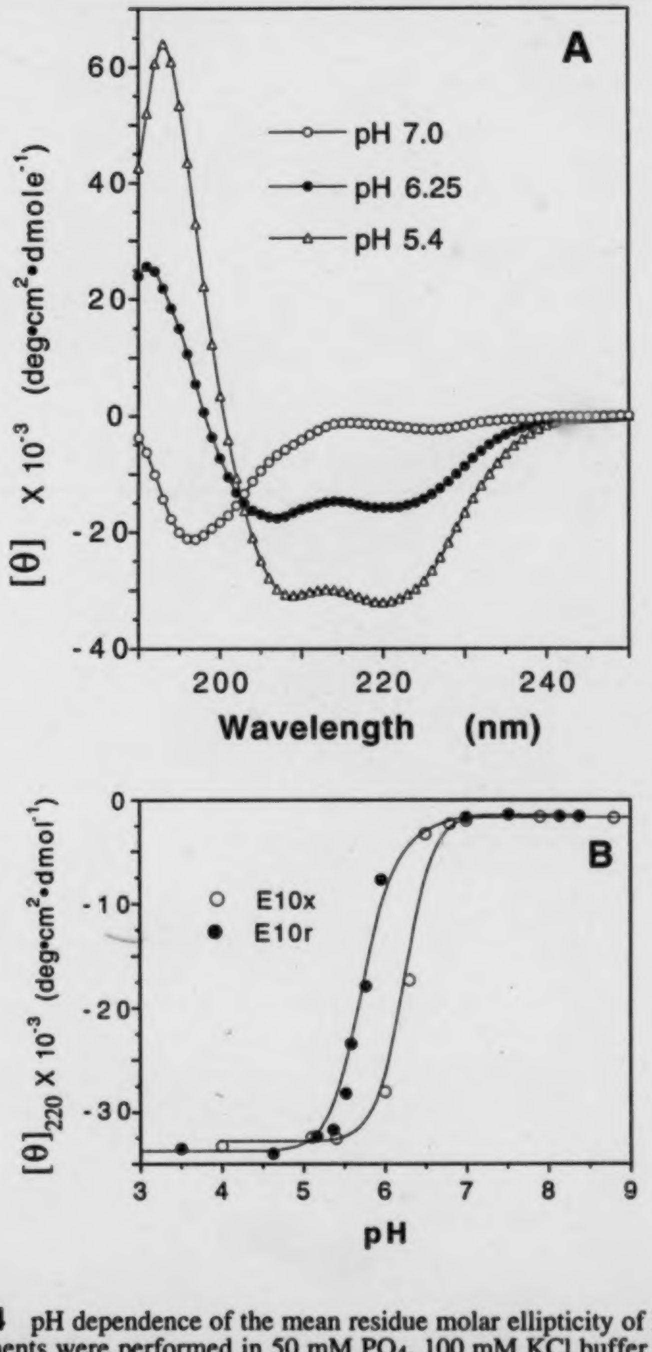

Figure IV.4 pH dependence of the mean residue molar ellipticity of E10x and E10r. All measurements were performed in 50 mM PO_4, 100 mM KCl buffer at 20°C. **A**, CD spectra of E10x at pH 7, 6.25, and 5.4. **B**, mean residue molar ellipticity at 220 nm versus pH for E10x and E10r. Peptide concentrations were 43 μM and 156 μM for E10x and E10r, respectively.

hydrophobic residues in the dimer interface, the more interhelical charge repulsion the coiled-coil can tolerate and still be folded.

It is important to realize that the midpoint of the folding transition curve is not the pK_a of the glutamate side-chain carboxylate groups. In fact, the pK_a values of the glutamate side chains, which appear to influence the folding, will not be constant but should be different in the folded and unfolded states. If this were not the case, they would have little or no effect on the pH dependence of stability (Yang & Honig, 1993). Therefore, if an unfolding transition takes place over a certain pH range, the pK_a value(s) of the group(s) responsible for causing the transition do(es) not correspond to the pH at the transition midpoint, but instead the pK_a of these groups is shifted from one value that corresponds to the titration start point (pK_a in the folded protein) to another value that corresponds to the titration endpoint (pK_a in the unfolded protein) (Yang & Honig, 1993). The correlation between the transition endpoints and the pK_a values will not be exact, especially when more than one ionizable residue is responsible for the pH dependence.

The pH-induced conversion from random coil monomer to coiled-coil dimer is also shown by the size-exclusion chromatograms of E8r (at a flow rate of 0.2 mL/min for increased resolution) at different pH values ranging from 7 to 5 (Fig. IV.5). At pH 7, E8r elutes at about 56 min, corresponding to the monomer. As the pH is reduced, a peak at about 51 min corresponding to the coiled-coil dimer begins to appear by pH 6. At pH 5.87, there are two approximately equal peaks in the chromatogram indicating that this is the midpoint of the conversion. As the pH is further reduced, the dimerization becomes complete by pH 5.5. This pH-induced folding is very similar to that observed by circular dichroism in Figure IV.4. In both cases, the folding transition is rapid, taking place within one pH unit, and the midpoints are similar (for E10r the apparent pH transition midpoint was 5.6 using CD while for E8r the apparent pH transition midpoint was 5.87 using SEC). Thus, there is a correlation between the transition in helicity as measured by CD and

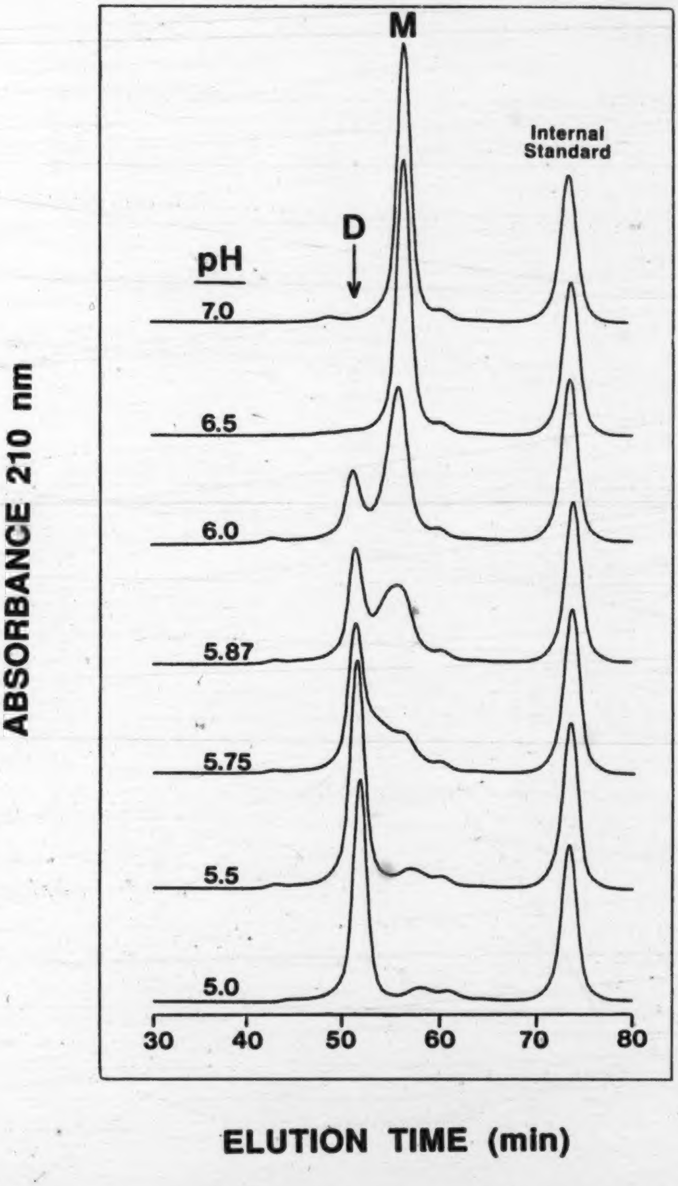

Figure IV.5 Effects of pH on the conformation of E8r as monitored by size-exclusion chromatography. All runs were carried out in 50 mM PO_4, 100 mM KCl buffer with a flow rate of 0.2 ml/min on a Pharmacia Superdex 75 column. The peptide was dissolved in running buffer containing 10 mM DTT to keep it reduced. An internal standard 10 residue unstructured peptide with the sequence Ac-RGAGGLGLGK-NH_2 was included in each run to confirm run to run reproducibility. M and D represent the monomeric and dimeric forms of peptide E8r, respectively.

subunit association as measured by SEC, which supports a two-state transition from helical dimer to random coil monomers or *vice versa.*

iii) Studies of oligomerization state The preference for the order of association (oligomerization state) of a coiled-coil has been shown to be dependent mainly on the residues in the **a** and **d** positions of the heptad repeat. Val at position **a** and Leu at position **d**, as in the peptides in this work, has been shown to favor dimer and/or trimer formation over tetramer formation (Harbury *et al.*, 1993; Lovejoy *et al.*, 1993; Lupas *et al.*, 1991). Recent studies with the GCN4 leucine zipper showed that a mutant with Val at all **a** positions and Leu at all **d** positions formed a mixture of dimer and trimer (Harbury *et al.*, 1993). Another study where the asparagine at position 16 (position **a** of the heptad repeat) of the 33-residue leucine zipper of GCN4 was substituted with valine yielded a triple-stranded α-helical coiled-coil with a temperature denaturation midpoint 40°C higher than the dimeric native sequence (Potekhin *et al.*, 1994). Their conclusion was that having Val at position **a** and Leu at position **d** favors trimer structure but that the presence of a polar group such as asparagine in the **a** and **d** positions directed two-stranded coiled-coil formation instead.

Size-exclusion chromatography of the series of coiled-coil analogs in both the reduced and oxidized forms were carried out (data not shown). In the case of the oxidized peptides, all six eluted in a narrow range of retention times predicted from the standard curve (Fig. II.6) to correspond to the two-stranded 70-residue monomer. In the case of the reduced analogs, Nr, E2r and E4r were predicted by SEC to be present as dimers while E6r, E8r and E10r were predicted by SEC to be present mostly as monomers, corresponding with the results of the CD spectral analysis.

Sedimentation-equilibrium experiments in the analytical ultracentrifuge were carried out as previously described (Kay *et al.*, 1991; Zhu *et al.*, 1993) to confirm the assignment of monomeric and dimeric species. The E8r peptide gave an apparent MW of 3600 (Fig IV.6), which closely matches the calculated MW of 3696 for the monomer. This confirms

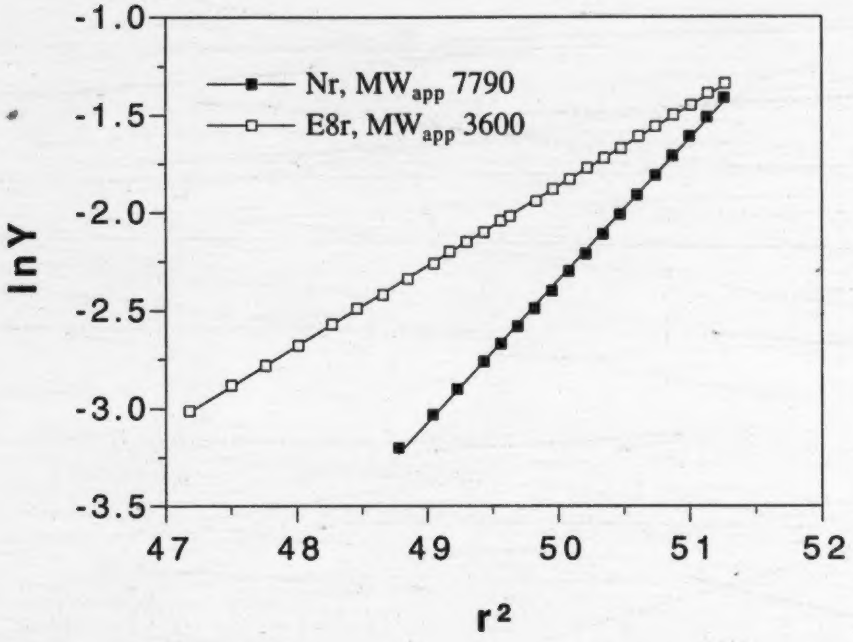

Figure IV.6 lnY versus r^2 plot from sedimentation-equilibrium experiments on Nr and E8r. Samples were run in 50 mM PO_4, pH 7 buffer with 10 mM DTT. The buffer contained 100 mM KCl for E8r and 1M KCl for Nr. Both samples were brought into equilibrium at a rotor speed of 44,000 RPM in a Beckman Model E analytical ultracentrifuge. Concentrations were 1.08 mg/ml (290 µM) and 0.80 mg/ml (216 µM) for E8r and Nr, respectively.

our assignment of E6r, E8r, and E10r, which coeluted in SEC, as monomers. Similarly, an apparent MW of 7790 was determined for Nr (Fig. IV.6), which closely agrees with the expected dimer MW of 7376. The linearity of the data in Figure IV.6 is consistent with the presence of a single species.

Further evidence for the association state was obtained by use of a low angle laser light scattering detector (Arakawa *et al.*, 1992) to estimate molecular weights of the peptides eluted from a Superose 12 size-exclusion column. The results gave a molecular weight for E4r twice that for E6r, which indicates that E6r is present as the monomer and E4r is present as the dimer (data not shown), in agreement with the assignment of association state by retention time on SEC.

We conclude from size-exclusion chromatography, ultracentrifugation, and laser light scattering that our sequence preferentially forms a two-stranded coiled-coil. Thus, either the cysteine at position **a** in the reduced coiled-coils or sequence differences at other positions could be destabilizing trimers, analogous to the effect of the buried Asn in GCN4. Recent studies by Krylov *et al.* (1994) and Alberti *et al.* (1993) have shown that residues in the **e** and **g** positions of the heptad repeat can greatly affect the order of association (see also Chapter VII, Kohn *et al.*, 1998c).

c) Denaturation of coiled-coil analogs in urea and GdnHCl

The stabilities of the disulfide-bridged coiled-coils at 20°C were determined by urea denaturation at pH 7 and GdnHCl denaturation at pH 7 and pH 3 (Fig. IV.7). The stability of the coiled-coils is expressed as the urea or GdnHCl concentration at which the coiled-coil is 50% unfolded, designated $[\text{urea}]_{1/2}$ or $[\text{GdnHCl}]_{1/2}$, as well as by the difference in free energy of unfolding with respect to the native coiled-coil, designated $\Delta\Delta G_u$ (Table IV.2). The $[\text{urea}]_{1/2}$ for Nx in a 50 mM phosphate, 100 mM KCl, pH 7 buffer is 6.1 M (see also Chapter III), indicating significant stability in the absence of interhelical electrostatic interactions and making this coiled-coil a good control with which to compare

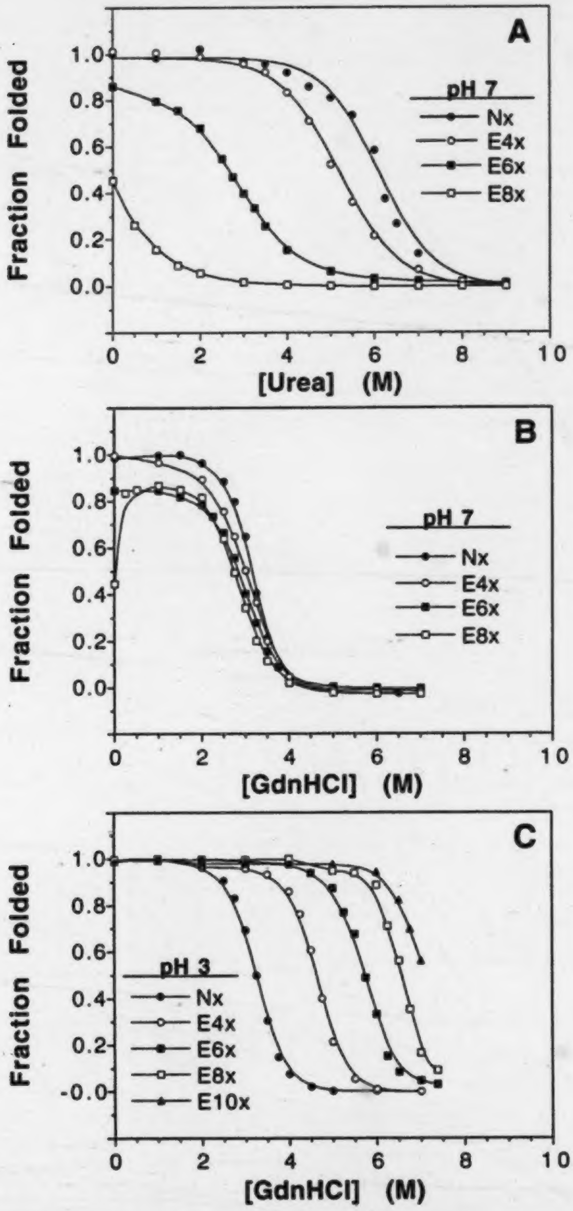

Figure IV.7 Denaturation profiles of the disulfide-bridged coiled-coils at 20°C in 50 mM PO_4, 100 mM KCl buffer using: urea at pH 7 (**A**), GdnHCl at pH 7 (**B**), and GdnHCl at pH 3 (**C**). The fraction of folded peptide was calculated from the observed mean residue molar ellipticity at 220 nm, as described under Materials and Methods (Chapter II, p. 57). For those analogs which are not fully helical, the fraction folded was calculated based on the ellipticity of Nx in benign conditions. The peptide concentrations in the final solutions for CD measurements ranged from 70 to 100 μM.

Table IV.2: Stabilities of the disulfide-bridged coiled coils Nx-E10x under different conditions

Peptide [a] Name	pH 3, 0.1 M KCl		pH 7, 0.1 M KCl		pH 7, 0.1 M KCl		pH 7, 3 M KCl	
	$[\mathrm{GdnHCl}]_{1/2}$ [b]	$\Delta\Delta G_u$ [c]	$[\mathrm{GdnHCl}]_{1/2}$	$\Delta\Delta G_u$	$[\mathrm{Urea}]_{1/2}$	$\Delta\Delta G_u$	$[\mathrm{Urea}]_{1/2}$	$\Delta\Delta G_u$
Nx	3.2	----	3.1	----	6.1	---	8.4	----
E2x	3.6	+0.6	3.1	0.00	6.8	+0.6	8.3	-0.1
E4x	4.6	+2.4	3.0	-0.16	5.1	-0.79	6.6	-1.6
E6x	5.8	+4.1	2.9	-0.32	2.8	-2.3	5.5	-2.5
E8x	6.6	+5.9	2.8	-0.50	0.0	-4.4	4.2	-3.7
E10x	7.2	+6.5	2.7	-0.64	---	---	3.7	-4.4

[a] The sequences of the peptides are shown in Figure IV.1.

[b] $[\mathrm{GdnHCl}]_{1/2}$ or $[\mathrm{Urea}]_{1/2}$ is the concentration of GdnHCl or urea (M) at which the peptide is 50% folded, as determined by comparing its molar ellipticity at 220 nm to that of the native coiled coil, Nx, in the absence of denaturant (the fully folded state).

[c] $\Delta\Delta G_u$ is the difference in the free energy of unfolding between the native coiled coil and the specified analog. This was calculated from the equation: $\Delta\Delta G_u=([D]_{1/2(\mathrm{mutant})}-[D]_{1/2(\mathrm{native})})*(m_{\mathrm{native}}+m_{\mathrm{mutant}})/2$ where $[D]_{1/2}$ is the $[\mathrm{Urea}]_{1/2}$ or $[\mathrm{GdnHCl}]_{1/2}$ and m is the slope of the assumed linear relationship between ΔG_u and denaturant concentration. A positive $\Delta\Delta G_u$ indicates the mutant coiled coil is more stable than Nx. Details of the procedures for calculating $\Delta\Delta G_u$ are given under Materials and Methods (pp. 56-59).

the mutant analogs (Fig. IV.7A, Table IV.2). E4x has a $[\text{urea}]_{1/2}$ of 5.1 M, and a $\Delta\Delta G_u$ value of -0.8 kcal/mol. The addition of another two Glu residues per chain in E6x leads to a more pronounced decrease in stability, with a $[\text{urea}]_{1/2}$ of 2.8 M and a $\Delta\Delta G_u$ of -2.3 kcal/mol. E8x is only about 50% folded under benign conditions, so its $[\text{urea}]_{1/2}$ by definition is about 0 M and it has a $\Delta\Delta G_u$ of approximately -4.5 to 5 kcal/mol. Finally, the stability of E10x cannot be determined under these benign pH 7 buffer conditions at 20°C since it is too unstable to show appreciable helical content. As was observed for the amount of helical content (Fig IV.3), the increased charge repulsion at the coiled-coil interface has substantially decreased the $[\text{urea}]_{1/2}$ in a progressive fashion.

The GdnHCl denaturation profiles in benign buffer at pH 7 (Fig. VI.7B) show a much different result from those obtained with urea (Fig. VI.7A). The $[\text{GdnHCl}]_{1/2}$ values for Nx, E4x, E6x and E8x are all very similar, in the range 3.1 M to 2.8 M (Table IV.2). The results with GdnHCl do not reflect the large systematic decrease in the stability of the coiled-coils that was observed with urea denaturation as the net interface charge and degree of interhelical charge repulsion is increased. These observations support previous results from this laboratory (Monera *et al.*, 1994a, 1994b, 1993) and the results in Chapter III (Kohn *et al.*, 1995a), which showed that GdnHCl appears to mask electrostatic repulsions and attractions in two-stranded coiled-coils; giving the same measure of stability whether the residues at positions **e** and **g** were arranged to form interhelical attractions or repulsions as long as the hydrophobic packing at the dimer interface was the same. Similarly, Hagihara *et al.* (1994) have also recently illustrated this same phenomenon where urea denaturation at pH 7 showed progressively lower apparent stability as the degree of acetylation of horse heart cytochrome c was increased while GdnHCl denaturation yielded the same apparent stability regardless of the extent of acetylation. This indicates an ability of GdnHCl to mask the negatively charged residues and their interactions with other charged residues which contribute to stability. The ionic nature of GdnHCl is the probable reason for its ability to disrupt the effects of charged residues on protein stability. The positively charged guanidinium ion, which is responsible for binding to the protein surface and subsequent denaturation (Greene & Pace, 1974; Pace, 1986; Tanford, 1970) may initially bind specifically at the negatively charged Glu carboxylate groups when present at low concentrations, thereby neutralizing the charge repulsions and removing their effects on stability. The GdnHCl denaturation, however, still shows a small apparent destabilization resulting from the glutamic acid substitutions, as was the case in Chapter III, of about 0.05 kcal/mol per Glu residue (see Tables IV.2 and III.2). However, this is much smaller than the apparent intrinsic destabilization of a Glu substitution obtained via urea denaturation (0.1 to 0.2 kcal/mol per Glu substitution - Chapters III and VII, Kohn *et al.*, 1995a, 1998c). Binding of the positively charged guanidinium ion to the carboxylate of an ionized Glu therefore is also the most likely explanation for this reduction in the observed intrinsic destabilization resulting from ionized Glu substitution.

At low pH, the stabilities of many coiled-coils have been observed to be higher than at pH 7 as shown for example in the muscle protein tropomyosin (Lowey, 1965; Noelken & Holtzer, 1964), the Fos-Jun heterodimeric leucine zipper (O'Shea *et al.*, 1992) and synthetic model coiled-coils (Hodges *et al.*, 1994; Zhou *et al.*, 1992c; Zhu *et al.*, 1993). Zhou *et al.* (1994b) demonstrated that a protonated Glu residue (at pH 3) at the **e** position of the heptad repeat in a coiled-coil makes a 0.65 kcal/mol greater contribution to coiled-coil stability than an ionized Glu residue (at pH 7) and a 0.45 kcal/mol greater contribution to stability than a Gln residue in the absence of interhelical or intrahelical charge-charge interactions. Recently, Lumb and Kim (1995b) found that the pK_a of a Glu residue at position 20 of the GCN4 leucine zipper (position **e** of the heptad repeat) is slightly higher in the folded state than in the unfolded state, also indicating that the protonated form is energetically favorable. The current study supports these previous results, as shown in Figure IV.7C. As the number of protonated Glu residues is increased, the stability of the coiled-coil is increased (determined by GdnHCl denaturation at pH 3) with Nx being least stable and E10x the most stable at pH 3. Nx has the same stability as at pH 7 (Table IV.2), as one would expect, since there are no residues which change their ionization state over the pH range 3 to 7. E10x is so stable at pH 3 that it is only about 50% unfolded in 7.4 M GdnHCl (the maximum experimentally possible concentration). This peptide is fully folded in 9 M urea (data not shown) indicating a greater efficiency of GdnHCl as a denaturant versus urea, as previously described (Greene & Pace, 1974). The results of Figure IV.7C are consistent with the observation in Chapter III (Kohn *et al.*, 1995a) of a large enhancement of stability for a protonated Glu substitution (as measured by either urea or GdnHCl denaturation). As suggested in Chapter III, this enhanced stability is probably a result of the greater helical propensity and apparent hydrophobicity characteristics of the protonated Glu side chain. In particular, positions **e** and **g** extend across the hydrophobic interface, thereby reducing solvent accessibility to the hydrophobic core. More hydrophobic residues in these positions have therefore been shown to lead to higher coiled-coil stability (Hodges *et al.*, 1994; Schmidt-Dörr *et al.*, 1991).

d) Effects of GdnHCl on the electrostatic interactions in the coiled-coils

GdnHCl titrations of Nx and E10x had dramatically different results (Fig. IV.8A). While Nx displays a typical two-state denaturation curve, E10x is initially unfolded in benign medium but is actually induced to a helical state by small concentrations of GdnHCl and achieves about 90% as much helical structure as Nx at 1 M GdnHCl. Upon further increase of the GdnHCl concentration, the coiled-coil is subsequently unfolded. E8x behaves similarly, increasing from ~ 43% folded in benign buffer to 90% folded in 1 M GdnHCl and then unfolding with further increase in GdnHCl concentration (Fig. IV.7B). The ability of GdnHCl to act as a stabilizer or inducer of protein structure when present at low concentration has been previously suggested (Hagihara *et al.*, 1993, 1994; Mayr & Schmid, 1993; Morjana *et al.*, 1993; Tsong, 1975) either through the masking of positive charge repulsions by the Cl^- ions or negative charges by the guanidinium$^+$ ions. The binding of guanidinium ions to the negatively-charged glutamate groups in E10x or E8x at

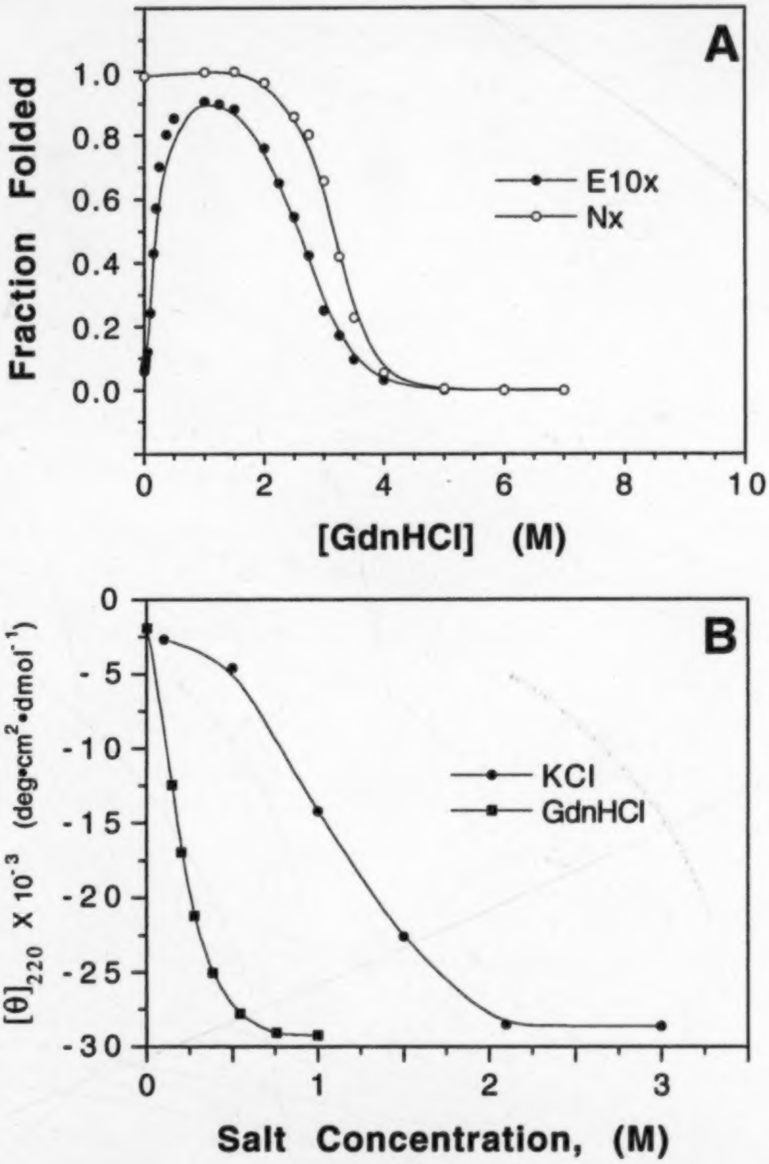

Figure IV.8 Effects of KCl and GdnHCl on the helicity of peptides Nx and E10x. **A,** Comparison of the effects of GdnHCl on the structures of peptides Nx and E10x in 50 mM PO_4, 100 mM KCl, pH 7 buffer at 20°C. The fraction folded peptide was calculated from the mean residue molar ellipticity as described in Chapter II (p. 57). Peptide concentrations were 89 µM for Nx and 82 µM for E10x. **B,** Effects of KCl and GdnHCl concentration on the mean residue molar ellipticity of E10x. All measurements were performed in a 50 mM PO_4, pH 7 buffer at 20°C. Peptide concentration was 73 µM in the GdnHCl titration and 67 µM in the KCl titration.

low GdnHCl concentration would neutralize the Glu-Glu charge repulsion, thereby inducing the coiled-coil structure. Alternatively, GdnHCl could promote dimerization through general electrostatic charge screening (Debye-Hückel screening). Goto and co-workers proposed these two possible mechanisms for the salt-induced folding transition of melittin and the acid-unfolded states of cytochrome c and apomyoglobin. Experiments with different anions indicated that the ion-binding effect was more important in all of these salt-induced transitions (Goto & Hagihara, 1992; Goto *et al.*, 1990).

The abilities of GdnHCl and KCl to induce helical structure in the E10x peptide are compared in Figure IV.8B. In the case of GdnHCl, the maximum inducible helix (-29,000 deg•cm^2•dmol^{-1}) is achieved at a concentration of 0.75 M and is about 90% of the maximum helical content of Nx. KCl is able to induce the same degree of helical structure but requires a concentration of over 2 M to do so. The potassium ion has the same plus one charge as the guanidinium ion but does not have the same apparent binding affinity for the glutamate groups. We propose that the guanidinium ion can bind to the glutamate groups via an electrostatic interaction and through hydrogen bonding, while potassium ion can only bind to the Glu carboxylate group through an electrostatic attraction. Therefore, the added effect of hydrogen bonding may increase the overall affinity of the guanidinium ion for the Glu carboxylate groups and thereby increase its ability to mask the charge repulsions. The ability of salts to have general Debye-Hückel charge screening effects should depend on the ionic strength and therefore be the same for equal concentrations of GdnHCl and KCl. Consequently, general charge screening appears not to be the major contribution to the induction of helix in E10x by GdnHCl.

As outlined in Chapter I, it has long been accepted that salts can affect hydrophobic interactions in proteins. Thus, a high concentration of KCl could promote protein stability mainly through its effect on the structure of water, leading to preferential hydration. The different apparent abilities of KCl and GdnHCl to promote the E10x coiled-coil structure may therefore be due to different mechanisms of action by the two salts: GdnHCl potentially operates mainly by masking charge repulsions through direct ion binding while KCl may act primarily through promoting a stronger hydrophobic effect which can override the effects of the charge repulsions on the coiled-coil folding (*i.e.* it is able to force the coiled-coil to form even in the presence of the charge-charge repulsions). Debye-Hückel charge screening may be involved as an additional stabilizing effect, although its relative contribution is difficult to assess.

Possible evidence for this line of reasoning is given by the results of urea denaturation of the disulfide-bridged coiled-coils at pH 7 in the presence of 3 M KCl (Fig. IV.9A). The large KCl concentration shifts the stabilities of the entire series of analogs significantly to higher $[\text{urea}]_{1/2}$ values. As a result, the stabilities are now such that even the lowest stability analogs, E10x and E8x, are almost fully helical in the absence of urea (Table IV.1), and their entire denaturation with urea can be observed and compared with that of the other analogs. The shifting of all of these denaturation curves by the presence of 3 M KCl supports the suggestion that the high KCl concentration acts to increase the apparent hydrophobic effect. This effect on stability should be the same for all the analogs since they share the same hydrophobic core residues and is seen clearly from the increase in the $[\text{urea}]_{1/2}$ of Nx (which is not affected by electrostatic interactions) from 6.1 M to 8.4 M (Table IV.2) as the KCl concentration is increased from 0.1 M to 3 M. This corresponds to an increase in the ΔG_u of 1.8 kcal/mol, which counteracts the destabilizing effects of the interchain repulsions enough to promote full coiled-coil formation. Another potential effect of the salt could be anion binding to the Lys residues along the solvent exposed face at position **f** of the helices (Figs. IV.1 and IV.2), which has also been proposed previously as a stabilizing effect of salt on coiled-coils (Thompson-Kenar *et al.*, 1995; Yu *et al.*, 1996). Privalov and co-workers suggested that due to higher charge density in the folded form of the coiled-coil, anions preferentially bind to the folded form versus the unfolded form (Thompson-Kenar *et al.*, 1995; Yu *et al.*, 1996). This phenomenon has been well documented in explaining the effects of cation binding on dsDNA stability (Manning, 1972;

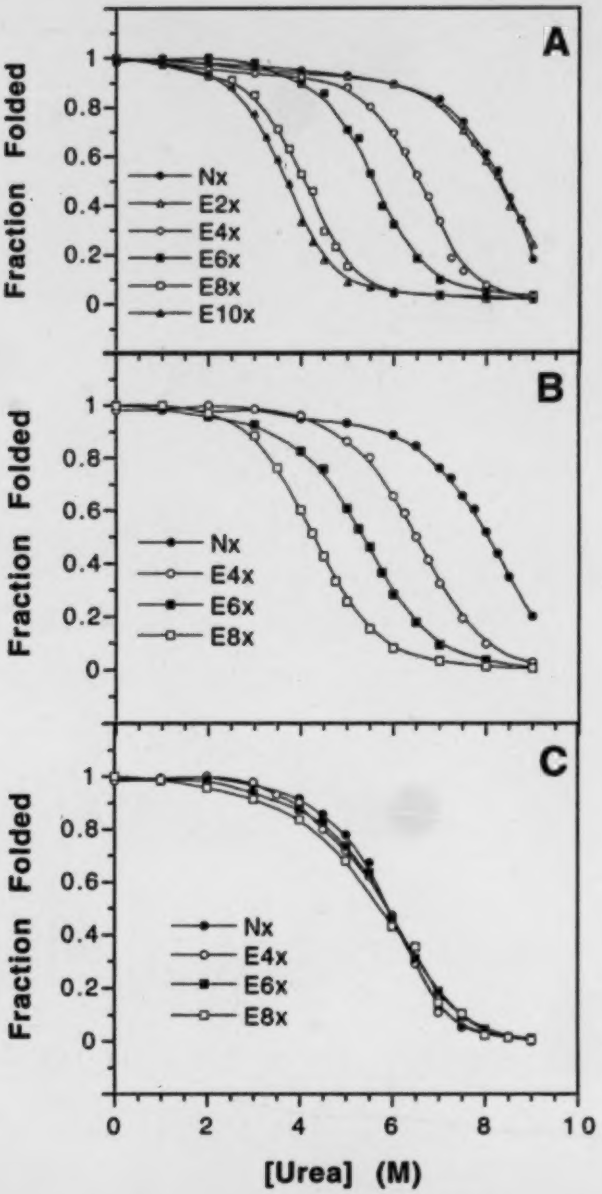

Figure IV.9 Effects of salt on the urea denautration profiles of the disulfide-bridged coiled-coils. Experiments were carried out at pH 7 and 20°C under the following buffer conditions: **A,** 50 mM phosphate, 3 M KCl (total ionic strength approximately 3.3); **B,** 50 mM tris, 100 mM KCl, 1 M $MgCl_2$ (total ionic strength approximately 3.2); and **C,** 20 mM imidazole, 100 mM KCl, 50 mM $LaCl_3$ (total ionic strength approximately 0.5). The fraction of folded peptide was calculated from the observed mean residue molar ellipticity at 220 nm, as described in Chapter II (p. 57). The peptide concentrations in the final solutions for CD measurements ranged from 60 to 100 μM.

Privalov *et al.*, 1969). There may also be some degree of charge screening by the KCl contributing to the increased coiled-coil formation and stability of the analogs with repulsions, but this effect is not large since a wide range of stabilities (range in $[\text{urea}]_{1/2}$ from 3.7 to 8.4 M; see Table IV.2) is obtained in the high KCl concentration. If KCl were very effective at screening the charge-charge repulsions, all the analogs should have similar $[\text{urea}]_{1/2}$ values. Similar results were obtained by Monera *et al.* (1993) where the inability of KCl to screen electrostatic interactions was also observed.

In contrast to KCl, GdnHCl does not increase protein stability through promoting stronger hydrophobic interactions. For example, the urea denaturation of Nx in the presence of 1 M GdnHCl gave a $[\text{urea}]_{1/2}$ of 4.8 M (data not shown) versus 6.1 M without the GdnHCl present. This corresponds to the known effects of GdnHCl on decreasing the temperature stability (T_m) of proteins (Von Hippel & Wong, 1965).

e) Effects of different chloride salts on the electrostatic interactions in the coiled-coils

The effects of salts on stability were further investigated by urea denaturation in the presence of 1 M $MgCl_2$ and 50 mM $LaCl_3$. The results with $MgCl_2$ (Fig. IV.9B) were very similar to those obtained in the presence of 3 M KCl (in both cases the additional salt represents an ionic strength of about 3.0). For example, in both buffer conditions, the $[\text{urea}]_{1/2}$ value for Nx is over 8 M. In contrast, 50 mM $LaCl_3$ (ionic strength of about 0.3) appears to effectively screen the destabilizing effects of Glu substitutions (Fig. IV.9C). At this lower ionic strength, all the peptides have $[\text{urea}]_{1/2}$ values around 6 M, which is the same as that of Nx under standard buffer conditions. The results indicate that the La^{3+} ion may be able to bind to the negatively-charged Glu side chains due to its higher charge and stabilize the folded peptide, while Mg^{2+} and K^+ ions do not to a significant extent. In particular, the metal ion may be complexed (bridged) by Glu side chains that would normally repel one another across the dimer interface. This possibility was further investigated in Chapter VIII (Kohn *et al.*, 1998a).

Comparison of the salt-induced folding of E10x for the three salts KCl, $MgCl_2$, and $LaCl_3$ (Fig. IV.10) further supports the conclusion that general charge screening is not the main mechanism of action. While a large concentration of KCl was required to induce the helical structure, smaller concentrations of $MgCl_2$ and $LaCl_3$ were required, and higher maximum molar ellipticities were obtained. The data is plotted as the ionic strength of salt added, which as mentioned earlier corrects for general screening (if general charge screening were dominant, all three salts would have a similar effect at a particular ionic strength). Thus, the much greater induction of helicity by $LaCl_3$ is likely due primarily to the high cation charge promoting direct binding to the peptide. This effect would be expected to be decreased with Mg^{2+} and very weak with K^+, so that the induction of peptide structure by $MgCl_2$ and KCl would be expected to occur more so through other mechanisms that become prevalent at the higher salt concentrations and increase the stability of all the analogs.

f) Effects of Gln to Glu substitutions on stability

The $\Delta\Delta G_u$ values for the disulfide-bridged analogs with respect to the native coiled-coil, Nx, as obtained by GdnHCl denaturation at pH 7 and pH 3 in 50 mM phosphate buffer containing 100 mM KCl and by urea denaturation at pH 7 in 50 mM phosphate buffer containing 3 M KCl are compared in Table IV.2. These data were plotted as $\Delta\Delta G_u$ versus the number of Glu residues per chain in Figure IV.11. The urea denaturation shows negligible destabilization for the Glu residues in the first two positions (two Glu/chain). For the middle three heptads (increasing to 4, 6 and 8 Glu per chain) there is an approximately linear decrease in stability (a negative $\Delta\Delta G_u$) with respect to Nx of about 1.2 kcal/mol for each additional two Glu residues substituted per chain (four in the dimer). Since we have previously determined a destabilization of about 0.15 kcal/mol per Gln to

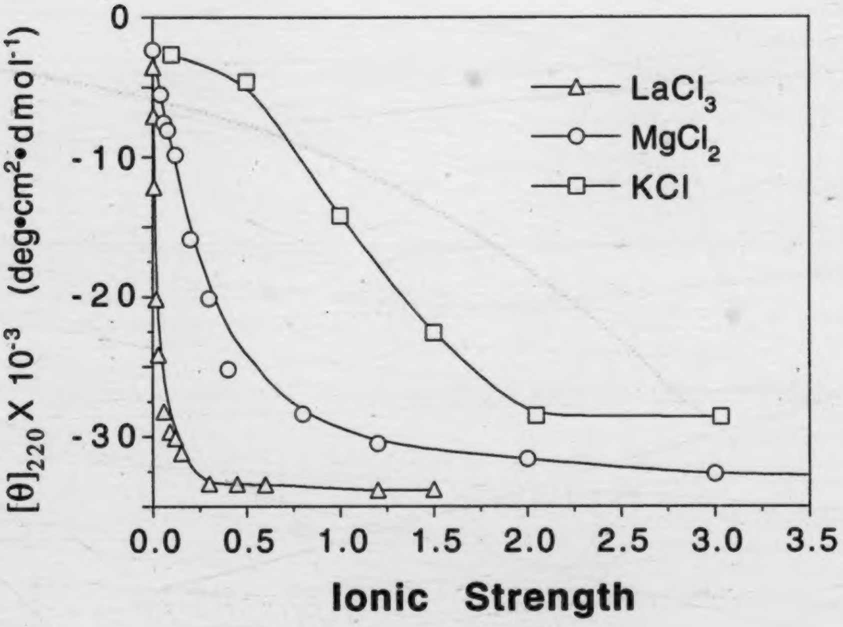

Figure IV.10 Effects of different chloride salts on the helicity of E10x at pH 7 and 20°C in a 20 mM imidazole buffer. Peptide concentration was in the range 60-80 μM. Salt concentration has been converted to ionic strength: $I = 1/2[c_iq_i^2 + c_{ii}q_{ii}^2]$ where c_i and c_{ii} are the concentrations of cation and anion, respectively, and q_i and q_{ii} are the charges of the cation and anion, respectively. For example, at equal concentrations the ionic strength of $LaCl_3$ is six-fold more than that of KCl.

ionized Glu substitution (Chapter III, Kohn *et al.*, 1995a), approximately 0.6 kcal/mol (4 X 0.15) of this 1.2 kcal/mol destabilization is due to differences in the intrinsic properties of ionized Glu versus Gln, and the other 0.6 kcal/mol may be due to two Glu-Glu repulsions for every four residues. This would suggest two i to i+5 repulsions of 0.3 kcal/mol each, which is somewhat less than the 0.45 kcal/mol we previously determined in low salt conditions (Chapter III, Kohn *et al.*, 1995a), suggesting that some screening of the repulsions by salt occurs.

In contrast to the results of the urea denaturation, the denaturation in GdnHCl at pH 7 shows that $\Delta\Delta G_u$ is essentially unaffected (Fig. IV.11), demonstrating the ability of GdnHCl to screen the effects of the electrostatic repulsions on coiled-coil stability. At pH 3 the stability increases (a positive $\Delta\Delta G_u$ indicating the coiled-coil is more stable than Nx) with the number of Glu residues per helix, as indicated in Figure IV.7C. In the middle part of the coiled-coil (going from 2 to 8 Glu residues per chain) there is a linear increase in stability of about 1.8 kcal/mol for each additional two Glu residues substituted per chain (four in the dimer). This corresponds to 0.45 kcal/mol increase in stability per Gln to protonated Glu substitution, which is consistent with the study of Zhou *et al.* (1994b), in which protonated Glu was substituted for Gln only at the **e** positions. The agreement between the results suggests the protonated Glu residues have similar effects on stability at the **e** and **g** positions of the heptad repeat.

g) Effects of N-terminal Gln to Glu substitutions

The substitution of glutamic acid residues actually has an additional effect on coiled-coil stability, which is apparent in the behavior of the E2 analog. It contains Glu residues at positions 1 and 6 of the peptide chain, and its stability as determined by urea denaturation at pH 7 in low salt (100 mM KCl) is actually greater than that of Nx both in the oxidized and reduced forms. E2x and Nx have $[\text{urea}]_{1/2}$ values of 6.8 M and 6.1 M, respectively ($\Delta\Delta G_u$ versus Nx of +0.6 kcal/mol), and E2r and Nr have $[\text{urea}]_{1/2}$ values of 3.2 M and 2.5 M,

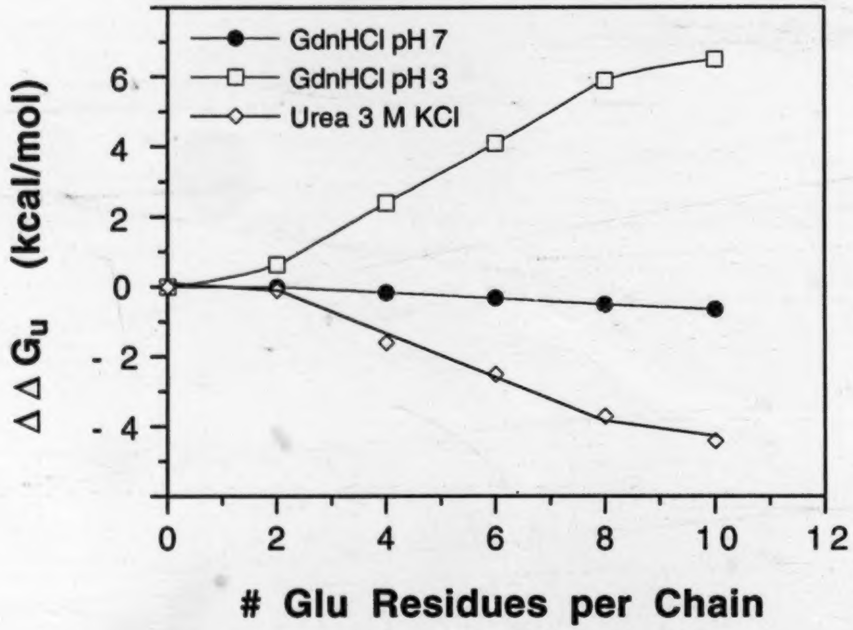

Figure IV.11 Summary of the effects of KCl and pH on the apparent stabilities of the disulfide-bridged coiled-coils in the presence of urea and GdnHCl. $\Delta\Delta G_u$ (the apparent difference in free energy between the specified analog and Nx) is plotted versus the number of Glu substitutions per peptide chain under different denaturation conditions. Results shown are for GdnHCl denaturation in 50 mM PO_4, 100 mM KCl buffer at pH 7 and pH 3, and for urea denaturation in 50 mM PO_4, 3 M KCl buffer at pH 7. All measurements were performed at 20°C, and $\Delta\Delta G_u$ was calculated as outlined in Table IV.2.

respectively ($\Delta\Delta G_u$ versus Nr of +0.8 kcal/mol). Therefore, the stabilization of the coiled-coil by Glu substitutions at the N terminus is independent of the presence of the interhelical disulfide bridge. This unexpected stability increase indicates that the negative charges are interacting favorably with the helix macrodipole of the helices that make up the coiled-coil. The helix macrodipole is due to alignment of the dipole moments of all the peptide bonds in a helix and is estimated to be equivalent to a charge of + 0.5 at the N terminus of the helix and - 0.5 at the C terminus of the helix (Hol *et al.*, 1981; Scholtz *et al.*, 1993). Previous studies have estimated the energetic effects of a favorable charge-helix dipole interaction in the range 0.5 to 2 kcal/mol (Sali *et al.*, 1988; Sancho *et al.*, 1992).

The addition of 3 M KCl to the solution brings the $[\text{urea}]_{1/2}$ value for E2x back below that of Nx (Fig. IV.9A), indicating that the proposed charge-helix dipole interaction is screened by high salt concentration. This result indicates that KCl is able to screen charge-dipole interactions even though it could not effectively screen the charge-charge interactions between Glu side chains (Figs. IV.9A and IV.11), suggesting that the charge-charge interaction is stronger. Similarily, the positioning of negatively charged residues at the C-terminal end of the coiled-coil is likely to have a destabilizing effect due to an unfavorable interaction with the negatively charged end of the helix macrodipole, and a high salt concentration should screen this interaction. This may expain why there is a large decrease in helicity between E8x and E10x under low salt conditions (Fig. IV.3A), but there is not a significant difference in the stability of E8X and E10x by urea denaturation in the presence of 3 M KCl (Fig. IV.9A) where charge-dipole effects are screened. The proposed charge-helix dipole interaction is further investigated in Chapter V (Kohn *et al.*, 1997b).

h) General discussion of the results

The model coiled-coils from our previous study (Chapter III, Kohn *et al.*, 1995a), serve as key controls for this paper since they unequivocally show that an interchain Glu-

Glu repulsion in the i to i'+5 orientation destabilizes a coiled-coil by 0.45 kcal/mol. It has been subsequently shown in the present study that a series of coiled-coils containing a systematic increase in the number of such Glu-Glu repulsions display a gradual loss of helical content and stability. The fact that the helical content and stability decrease gradually indicate that the repulsive effects introduced by Glu substitutions are roughly additive. While there is not a critical point at which an all helical coiled-coil is transformed to a random coil by the substitution of two additional Glu residues, the loss of helical content is significant in going from E6x to E8x in the oxidized coiled-coils and from E4r to E6r in the reduced coiled-coils, indicating the importance of subtle changes in interchain electrostatic interactions in determining coiled-coil formation, specificity, and stability.

The question still remains as to the mechanism of destabilization of the coiled-coil by the interchain repulsions. As mentioned in Chapter I and previously (Adamson *et al.*, 1993; Zhou *et al.*, 1994c), interhelical electrostatic repulsions can disrupt the formation and stability of coiled-coils in two ways. First, specific i to i'+5 (**g**-**e'**) repulsions between two like-charged side chains could destabilize the coiled-coil. The repulsion between two like-charged residues on opposing helices of the coiled-coil may not destabilize the folded state through the electrostatic repulsion forcing the chains apart, since to do so, it would have to overcome the much more significant hydrophobic effect , which is the major force driving coiled-coil formation. Normally the side chains that occur in the **e** and **g** positions lie across the dimer interface and interact with each other forming salt bridges when they are oppositely charged; however, when they are similarly charged, the repulsions between the side chains may force them apart and away from the dimer interface. This would leave the hydrophobic core **a** and **d** positions more exposed, resulting in reduced burial of nonpolar surface area and decreased stability through reduced solvent entropy in the folded state (the traditional view of the hydrophobic effect) and reduced van der Waals packing interactions. Secondly, the buildup of a large net charge on the dimer interface could also lead to general electrostatic effects in which like net charges on the faces of the two helices repel.

Determining the relative roles of these two effects is somewhat difficult from the current understanding of interhelical electrostatic effects on coiled-coil formation and stability. However, it was found that a heterodimeric coiled-coil held together with a disulfide bridge that contains 5 interhelical Glu-Glu and 5 interhelical Lys-Lys repulsions but zero net charge at the dimer interface forms a coiled-coil with substantially reduced stability (Monera *et al.*, 1993, 1994a). This is illustrated for the parallel heterodimer KE-EKx, which contains an N-terminal disulfide bridge, in Figure IV.12. The coiled-coil is highly folded despite the large number of interhelical **g-e'** repulsions (Fig. IV.12, middle), but the stability is substantially reduced by the repulsions, as shown by comparison of its urea denaturation profile to that of the homodimer KE-KEx, which contains interhelical ionic attractions (Fig. IV.12, bottom). In contrast, coiled-coils containing 10 interhelical Lys-Lys or 10 interhelical Glu-Glu repulsions with high net charges at the dimer interface are unfolded at pH 7 (Graddis *et al.*, 1993; O'Shea *et al.*, 1993; Zhou *et al.*, 1994c; this study). In addition, a synthetic triple-stranded coiled-coil with a net charge of -3 in the trimer interface forms despite seven pairs of specific interhelical ionic repulsions between residues at the **e** and **g** positions of the helices which lie antiparallel to each other (Lovejoy *et al.*, 1993). Therefore, a high net charge may prevent the chains from approaching each other through general electrostatic repulsions while specific repulsions between like-charged residues may destabilize the coiled-coil by disrupting side-chain packing around the dimer interface. However, the relative roles of these two forms of electrostatic destabilization will probably depend on the surrounding amino acids.

The effects of disulfide bridges on the stability of two-stranded coiled-coils have been described previously (Hodges *et al.*, 1990; Zhou *et al.*, 1993a). In the present study, we have illustrated the ability of disulfide bridges to overcome the effects of interhelical charge-charge repulsion on coiled-coil formation (Figs. IV.3 and IV.4). While the effect of the disulfide bridge on stability is difficult to interpret because it involves the comparison of a bimolecular, concentration-dependent unfolding process for the reduced coiled-coil and a

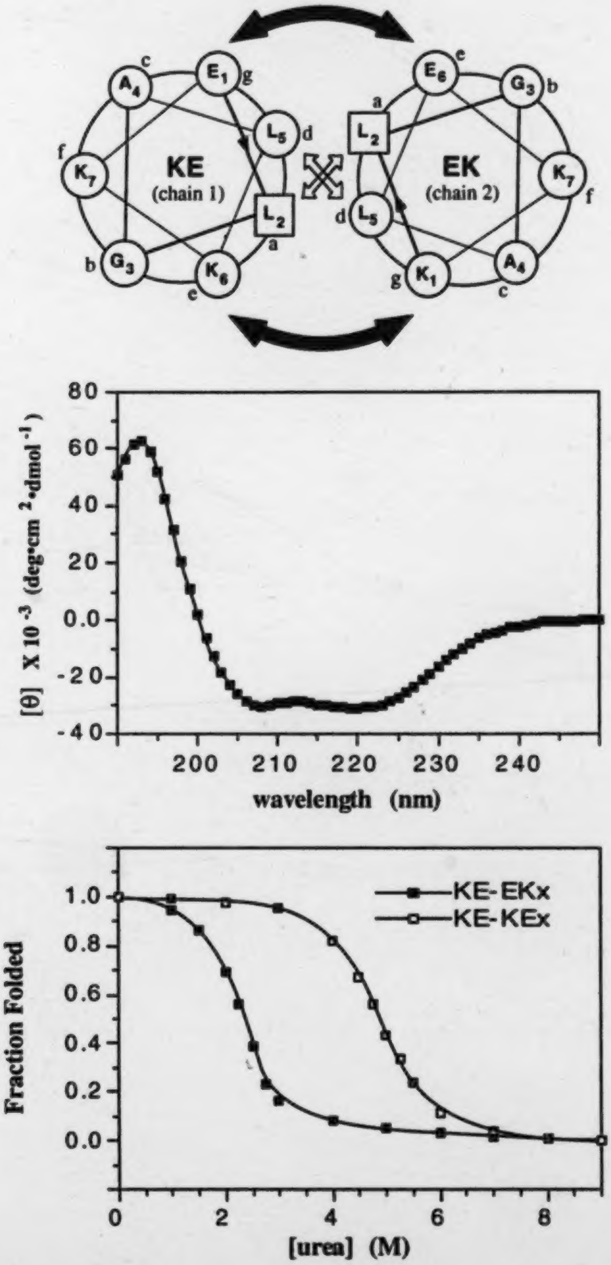

Figure IV.12 Net charge *versus* specific repulsions effects. **Top**, helical wheel diagram of the heterodimer KE-EKx, which contains zero charge at the dimer interface but five **g-e'** Glu-Glu and five **g-e'** Lys-Lys repulsions. **Middle**, helical CD spectrum of KE-EKx at 20°C in 25 mM phosphate, 50 mM KCl, pH 7 buffer. **Bottom**, urea denaturation profile of KE-EKx compared with that of the homodimer KE-KEx at 20°C in 50 mM phosphate, 100 mM KCl, pH 7 buffer.

unimolecular, concentration-independent unfolding process for the oxidized coiled-coil (Regan *et al.*, 1994), we have estimated the interchain disulfide bridge to offer about 3-4 kcal/mol additional stability to the coiled-coil (Hodges *et al.*, 1990; Kohn *et al.*, 1995a, Chapter III). This stabilizing effect would be expected to be capable of counteracting a large number of interchain electrostatic repulsions, which as stated above have been estimated to destabilize by 0.45 kcal/mol per Glu-Glu repulsion. In the case of the E8x peptide with a net charge of -16 and containing 8 interhelical Glu-Glu repulsions the disulfide bridge is able to promote nearly 50% coiled-coil structure. Therefore in this case the stabilizing factors including the disulfide bridge are being almost offset by the charge repulsion so that the peptide is equally populating the folded and unfolded states.

Although the disulfide bridge does not generally apply to native coiled-coils, there are some cases where redox control of transcription factor activity in eukaryotic cells has been suggested. Recently it has been found that the basic-helix-loop-helix transcription factor E2A binds DNA at physiological temperature as a homodimer only in the presence of an interhelical disulfide bond while under reducing conditions E2A binds DNA only as a heterodimer with MyoD or Id (Benezra, 1994). Nuclear translocation of the transcription factor NF-κB is activated by oxidative stress (Meyer *et al.*, 1993; Schreck *et al.*, 1991) while USF (a basic-helix-loop-helix-zipper protein) forms both intra- and intermolecular disulfide bonds, which appear to decrease its affinity for DNA (Pognonec *et al.*, 1992). Therefore, the fact that an intermolecular disulfide bond is required for high affinity DNA binding of certain transcription factors and that the presence or absence of this bond can profoundly direct dimerization specificity at physiological temperatures suggests that, as observed in this study, the ability of the disulfide bridge to overcome destabilizing effects on homodimerization such as intermolecular charge repulsion is the key to its role in transcription factor activity.

The dramatic effects of pH and salt on protein folding observed in this study and previously in model coiled-coils (Zhou *et al.*, 1994c) and other model helical proteins

(Ramalingam *et al.*, 1992) have suggested major implications for the potential of *de novo* design of environmentally sensitive proteins. One of the best examples of salt effects on protein folding in native proteins is the case of extreme halophilic bacteria, which are adapted to living in high salt concentration environments and whose cytoplasm is close to saturated in KCl. The proteins of these bacteria are often rich in acidic amino acids and have lower hydrophobicity than their counterparts in non-halophilic bacteria (Lanyi, 1974). These proteins, when isolated, require high salt concentrations to stabilize their folded structures. This stabilization may be due to the combined effects of the salt stabilizing the hydrophobic core as well as interactions of hydrated salt ions with the surface of the folded protein (Zaccai & Eisenberg, 1990). It has been suggested that clustering of negatively charged residues on the surface of halophilic proteins may cause structural instability, possibly due to charge repulsion, that is removed by the effects of salts (Ramalingam *et al.*, 1992). pH sensitive coiled-coil formation has recently been illustrated for the influenza virus hemagglutinin protein, which is required for fusion of the viral and cellular membranes. The protein undergoes a conformational shift to become active under the mildly acidic (pH 5) conditions of the mature endosome (Carr & Kim, 1994). The protein forms a three-stranded coiled-coil stem adjacent to a sequence of about 35 residues which forms an extended loop at pH 7 but at pH 5 becomes helical and extends the triple-stranded coiled-coil, thereby inducing the activating changes in the structure. It has been found that this pH-sensitive 35-residue sequence probably forms an extended loop at pH 7 due to interchain electrostatic repulsion, which prevents coiled-coil propagation through this region but which is alleviated by protonation of acidic side chains at lower pH (Carr & Kim, 1993).

In conclusion, this study illustrates that a systematic increase in interhelical charge repulsion leads to a progressive loss of helical content and stability of a model coiled-coil. These effects can be modulated by changes in pH and high salt concentrations.

CHAPTER V

POSITIONAL DEPENDENCE OF THE EFFECT OF A NEGATIVELY-CHARGED GLU SIDE CHAIN ON THE STABILITY OF AN α-HELICAL COILED-COIL[3]

A. Introduction

Statistical studies of α-helices in protein structures have shown that different types of amino acids preferentially occur in different regions of the helix. Charged and neutral polar residues occur more often at the ends of helices while nonpolar residues occur more frequently near the middle of helices (Blagdon & Goodman, 1975; Chou & Fasman, 1974; Dasgupta & Bell, 1993; Richardson & Richardson, 1988). In particular, potentially negatively charged side chains (Asp, Glu) strongly prefer positions near the N terminus of a helix while potentially positively charged side chains (His, Arg, Lys) have a less pronounced preference for the C terminus.

Explanations for the preferences of polar side chains for the ends of helices fall into two principal models. Firstly, because the first four backbone NH groups and final four backbone CO groups of a helix are not able to form the i to i+4 hydrogen bond to other backbone groups, polar side chains at the ends of the helix are often able to form hydrogen bonds to these unfulfilled backbone groups (Doig & Baldwin, 1995; Presta & Rose, 1988). This is termed helix capping and has been demonstrated most clearly with the N-cap residue, defined as the N-terminal residue of the helix with partly helical and partly nonhelical character (Lyu *et al.*, 1993; Serrano & Fersht, 1989; Zhou *et al.*, 1994a), although such capping may also occur with side chains at other positions near the ends of helices (Dasgupta & Bell, 1993). Secondly, electrostatic "charge-helix dipole" interactions between charged side chains and the net dipole moment of the α-helix formed by the alignment of individual peptide backbone dipoles may also stabilize or destabilize a protein. This net "helix dipole" was originally suggested to result from parallel alignment of the peptide bond dipoles along the entire helix (Wada, 1976) and was shown to be equivalent to the effect of + 0.5 unit charge at the N terminus and -0.5 unit charge at the C terminus of a helix (Hol *et al.*, 1978), but recent theoretical studies (Åqvist *et al.*, 1991; Pflugrath & Quiocho, 1985; Tidor, 1994) suggest it may arise principally from the four uncompensated NH groups with partial positive charge at the N terminus and four CO groups with partial negative charge at the C-terminus of the helix. We therefore refer to the "helix dipole" as arising from one of these proposed phenomena, but the resulting charge distribution of +0.5 and -0.5 remains the same in both cases.

---

[3] A version of this chapter has been published: Kohn, W. D., Kay, C. M., and Hodges, R. S. (1997) *J. Pept. Sci.* **3**, 209-223.

Both explanations for the preference of polar residues for the ends of helices have their merits; however, neither is able to explain all the experimental observations. Nor are these mechanisms mutually exclusive since charged side chains could participate both as hydrogen bond donors or acceptors to the helix backbone as well as in electrostatic interactions with the helix dipole, as recently suggested by Tidor (1994), with the resulting effect on stability being due to a combination of these interactions.

In recent years, the effects of charged residues at the termini of helices have been studied in both isolated helical peptides (Armstrong & Baldwin, 1993; Fairman *et al.*, 1989; Huyghues-Despointes *et al.*, 1993a; Kippen *et al.*, 1994; Lockhart & Kim, 1993; Shoemaker *et al.*, 1985, 1987; Takahashi *et al.*, 1989) and in helices of intact globular proteins (Eijsink *et al.*, 1992; Nicholson *et al.*, 1988, 1991; Sali *et al.*, 1988; Sancho *et al.*, 1992). In all of these studies, strong evidence is shown to support the charge-helix dipole interaction model. However, both of these approaches for the study of stabilizing or destabilizing substitutions in α-helices have inherent problems. Complex tertiary structural interactions in globular proteins can complicate the analysis of intrahelical interactions. Peptide models avoid this complication but can suffer from low inherent helicity, which is generally highly dependent on even single residue substitutions (Chakrabartty *et al.*, 1994;

Zhou *et al.*, 1994d), and significant fraying at the helix ends (Chakrabartty *et al.*, 1991; Waltho *et al.*, 1993). In contrast, a coiled-coil is a stable structure with very high helicity in benign medium, and single residue mutations can be carried out without a significant change in helical content (O'Neil & DeGrado, 1990). This makes the coiled-coil advantageous for studying point mutations in helices since quantitative comparison of the thermodynamic stability characteristics is most meaningful when there are not dramatic variations in structure between analogs.

Studies in Chapter IV (Kohn *et al.*, 1995b) of interhelical electrostatic repulsions between Glu residues at the **e** and **g** positions of coiled-coils suggested the potential contribution of charge-helix dipole interactions to the overall effect of a charged residue substitution on coiled-coil stability. In this followup study, single Glu to Gln substitutions at different **e** and **g** positions along the sequence were studied for their effects on stability, to establish further evidence for charge-helix dipole interactions. If such interactions are present, a Glu substitution, which is intrinsicly destabilizing at the middle of the helix, is expected to have opposite effects on stability at the N and C termini due to favorable and unfavorable charge-helix dipole interactions, respectively. Effects of salt and pH were also probed for their effects on the proposed charge-helix dipole interactions. Intrinsic differences between the **e** and **g** positions were also demonstrated.

B. Results and Discussion

a) Peptide design and nomenclature

Single 'point' substitutions of Glu for Gln residues at various positions along the length of the 35-residue native coiled-coil (described on p. 60) have been carried out as shown in the sequences in Figure V.1, and the effects of these substitutions on coiled-coil stability were determined. The analogs in this Chapter are designated by the position at

Peptide Name	Amino Acid Sequence
	1 5 10 15 20 25 30 35
	g a b c d e f g a b c d e f g a b c d e f g a b c d e f g a b c d e f
native	Ac-**Q**-C-G-A-L-**Q**-K-**Q**-V-G-A-L-**Q**-K-**Q**-V-G-A-L-**Q**-K-**Q**-V-G-A-L-**Q**-K-**Q**-V-G-A-L-**Q**-K-amide
E1	Ac-**E**-C-G-A-L-**Q**-K-**Q**-V-G-A-L-**Q**-K-**Q**-V-G-A-L-**Q**-K-**Q**-V-G-A-L-**Q**-K-**Q**-V-G-A-L-**Q**-K-amide
E6	Ac-**Q**-C-G-A-L-**E**-K-**Q**-V-G-A-L-**Q**-K-**Q**-V-G-A-L-**Q**-K-**Q**-V-G-A-L-**Q**-K-**Q**-V-G-A-L-**Q**-K-amide
E15	Ac-**Q**-C-G-A-L-**Q**-K-**Q**-V-G-A-L-**Q**-K-**E**-V-G-A-L-**Q**-K-**Q**-V-G-A-L-**Q**-K-**Q**-V-G-A-L-**Q**-K-amide
E20	Ac-**Q**-C-G-A-L-**Q**-K-**Q**-V-G-A-L-**Q**-K-**Q**-V-G-A-L-**E**-K-**Q**-V-G-A-L-**Q**-K-**Q**-V-G-A-L-**Q**-K-amide
E34	Ac-**Q**-C-G-A-L-**Q**-K-**Q**-V-G-A-L-**Q**-K-**Q**-V-G-A-L-**Q**-K-**Q**-V-G-A-L-**Q**-K-**Q**-V-G-A-L-**E**-K-amide

Figure V.1 Amino acid sequences of the peptides studied to determine the positional dependence of the effect of a Glu substitution at position **e** or **g** of the heptad repeat (in bold type) on the stability of a two-stranded coiled-coil. Substitutions of Glu (E) for Gln (Q) are highlighted by boxes. A cysteine at position 2 allows formation of an interchain disulfide bridge. Peptide nomenclature is based on the position of the single Glu substitution. For example, E1 contains a Glu substitution at position 1 of the 35 residue peptide chain.

which the Glu substitution is made. For example, E6 refers to a single Glu substitution at position 6.

b) Structural characterization of the model coiled-coils

We have previously demonstrated that the native sequence, N, used for this study forms a stable two-stranded α-helical coiled-coil both in the presence and absence of the N-terminal interhelical disulfide bridge (Chapters III and IV, Kohn *et al.*, 1995a, 1995b). The peptide appears highly helical by CD spectroscopy and is two-stranded, as determined by size-exclusion HPLC and sedimentation-equilibrium ultracentrifugation studies.

The various analogs in this study all display CD spectra similar to that of N, and mean residue molar ellipticities at 222 nm in a range from -30,000 to -33,000 deg•cm^2•dmol^{-1} in both the reduced and oxidized forms, indicative of very high helical content. These results are similar since CD ellipticity measurements and peptide concentration measurements combined are accurate to about ± 5%. In addition, all of the analogs, including N, are eluted at very similar times on size-exclusion HPLC: between 21.3 and 21.6 min for the reduced form and between 22.3 and 22.7 min for the oxidized form (data not shown). The longer retention times of the oxidized peptides indicate that they are more compact than their reduced counterparts, likely due to the disulfide bridge restricting chain mobility. However, based on these results, it is apparent that no large conformational changes (i.e. changes in oligomerization state) have occurred in the overall structure of the peptides containing the various substitutions.

c) Stability studies

i) Single Glu substitutions at the N terminus, C terminus and middle of the helix. The effects on stability of a single Glu for Gln substitution per chain at various positions along the length of the helices comprising the coiled-coil are shown in Figure V.2. The urea denaturation profiles of the disulfide-bridged coiled-coils show that Glu substitutions near the N terminus (at positions 1 and 6) lead to enhanced stability relative to

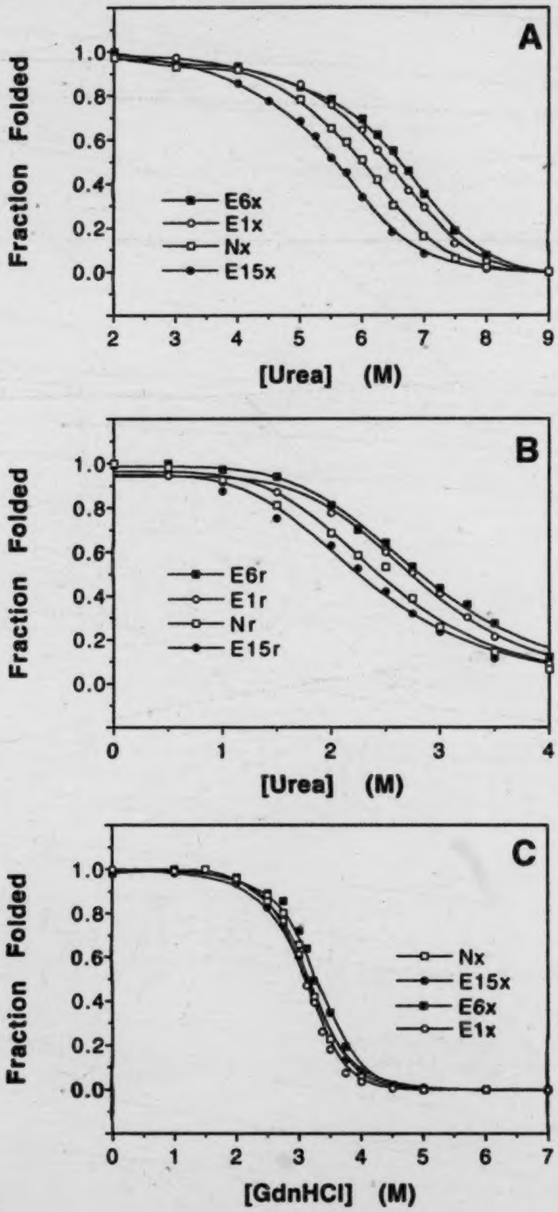

Figure V.2 Denaturation profiles at 20 °C in 100 mM KCl, 50 mM PO_4, pH 7 buffer for peptides N, E1, E6, and E15. **A,** Urea denaturation of disulfide-bridged peptides; **B,** Urea denaturation of reduced peptides; **C,** GdnHCl denaturation of disulfide-bridged peptides. The buffer contained 5 mM DTT for the reduced samples. The fraction of folded peptide was calculated from the mean residue molar ellipticity at 222 nm, as described in Chapter II (pp. 56-59).

the control peptide Nx (Fig. V.2A). In contrast, substitutions near the middle of the coiled-coil (positions 15 and 20) and the C terminus (position 34) lead to reduced stability relative to Nx (see also Table V.1). The differing effects of these substitutions on coiled-coil stability is consistent with the charge-helix dipole interaction model. In this model placement of a negatively charged residue near the N terminus of an α-helix is stabilizing due to favorable interaction with the positive pole of the helix macrodipole, while placement of a negatively charged residue near the C terminus should have the opposite effect due to unfavorable interaction with the negative pole of the helix macrodipole (Hol *et al.*, 1978; Wada, 1976).

Other factors may also contribute to the change in stability caused by a Gln to Glu substitution. These include intrinsic properties of the amino acid side chains such as helical propensity and hydrophobicity, which have been attributed to the decrease in stability for Gln to Glu substitutions at the **e** and **g** heptad positions of coiled-coils (Chapters III and IV, Kohn *et al.*, 1995a, 1995b). For example, the coiled-coil E20x, discussed in Chapter III where it was referred to as $E_1(20)x$, has a single Glu substitution for Gln per chain at position 20 (position **e**). This residue is near the middle of the coiled-coil and should have no significant interactions with the helix dipole, but the mutation destabilizes the coiled-coil by 0.2 kcal/mol (0.1 kcal/mol per Glu residue). Similarly, E15x in which Glu is substituted at position **g** of the heptad near the middle of the sequence is destabilized to an even greater degree (0.38 kcal/mol or 0.19 kcal/mol per Glu substitution, Table V.1). In both cases, this can be partly attributed to the lower helical propensity of an ionized Glu compared to Gln (Chakrabartty *et al.*, 1994; Wójcik *et al.*, 1990; Zhou *et al.*, 1994d). The helical propensity of an amino acid has been shown to affect coiled-coil stability from substitution studies at the outer (**c** and **f**) heptad positions where no interhelical packing contacts occur (Hodges *et al.*, 1981; O'Neil & DeGrado, 1990). In addition, the lower hydrophobicity of an ionized Glu compared to Gln (Fauchere & Pliska, 1983; Guo *et al.*, 1986; Sereda *et al.*, 1994) will be significant, particularly in the **e** and **g** positions, which can pack against the residues at

Table V.1: Stability data at pH 7 from urea denaturation [a]

Peptide [b]	Heptad Position	$[\text{urea}]_{1/2}$ [c] (M)	*m* [d]	Observed [e] $\Delta\Delta G_u$ (kcal/mol)	Calculated [f] $\Delta\Delta G_u^{\text{helix dipole}}$ (kcal/mol)
Nx	---	6.0	0.84	----	----
E1x	g	6.4	0.83	+0.33	+0.36
E6x	e	6.6	0.81	+0.50	+0.35
E15x	g	5.55	0.86	-0.38	----
E20x	e	5.8 [g]	1.0	-0.19	----
E34x	e	5.6	0.89	-0.35	-0.08
Nr	---	2.5	1.47	----	----
E1r	g	2.8	1.31	+0.42	+0.35
E6r	e	2.8	1.23	+0.41	+0.35
E15r	g	2.3	1.38	-0.29	----
E20r	e	2.3	1.30	-0.28	----
E34r	e	2.2	1.50	-0.45	-0.08

[a] Data was collected at 20°C in a 50 mM PO_4, 100 mM KCl buffer.

[b] The sequences are given in Figure V.1, and nomenclature is described under Peptide design and nomenclature.

[c] The $[\text{urea}]_{1/2}$ is the concentration of urea at which the peptide is 50% unfolded, as determined by the decrease in molar ellipticity at 222 nm with increasing denaturant concentration.

[d] *m* is the slope of the assumed linear relationship between ΔG_u and the denaturant concentration.

[e] $\Delta\Delta G_u$ is the observed difference in the free energy of unfolding between the analog and the native coiled-coil calculated from the $[\text{urea}]_{1/2}$ values as described under Materials and Methods (pp. 56-59). A positive $\Delta\Delta G_u$ value indicates that the analog is more stable than the native coiled-coil.

[f] The free energy change for the charge-helix dipole effect per single Gln to Glu substitution, $\Delta\Delta G_u^{\text{helix dipole}}$ is calculated as follows:

$$\text{Total } \Delta\Delta G_u^{\text{helix dipole}} = \Delta\Delta G_u^{\text{ observed}} - n(\Delta\Delta G_u^{\text{ helix prop., hydrophobicity}})_e - m(\Delta\Delta G_u^{\text{ helix prop., hydrophobicity}})_g$$

where n and m are the number of Gln to Glu substitutions at positions **e** and **g**, respectively, of the heptad; $\Delta\Delta G_u^{\text{helix prop., hydrophobicity}}$ represents the intrinsic effect on stability from a single Gln to Glu substitution and equals -0.1 kcal/mol at position **e** of the heptad and -0.20 kcal/mol at position **g** of the heptad based on the stabilities of E20x and E15x, respectively, versus Nx at pH 7.

Example: Total $\Delta\Delta G_u^{\text{helix dipole}}$ for E1x = +0.33 - 2(-0.20)= +0.73 kcal/mol

This gives a charge helix dipole effect of 0.73/2 = +0.36 kcal/mol per Glu.

g Data taken from Kohn *et al.* (1995a, Chapter III) the hydrophobic core (O'Shea *et al.*, 1991) and for which hydrophobicity can profoundly affect coiled-coil stability (Hodges *et al.*, 1994; Schmidt-Dörr *et al.*, 1991). However, these effects appear to be much less significant at the ends of the coiled-coil than in the middle (Chapter IV, Kohn *et al.*, 1995b). In general, intrinsic properties of the amino acid, such as helical propensity and hydrophobicity, have a lower effect on helicity and stability, as the residue becomes closer to either the N or C terminus, presumably due to increased flexibility at the ends (Zhou *et al.*, 1992a). This was shown experimentally in monomeric α-helical peptides with Gly and Ala, which are at opposite ends of the helical propensity scale (Chakrabartty *et al.*, 1991; Strehlow & Baldwin, 1989).

Where there is an N-terminal Glu substitution for Gln, as in E1x or E6x, the negative effect on stability of the intrinsic helical propensity and hydrophobicity contributions is opposite to the positive effect on stability of the proposed charge-helix dipole interaction. Therefore, the observed $\Delta\Delta G_u$ values of +0.33 and +0.50 kcal/mol for E1x and E6x, respectively (Table V.1), represent a lower limit for the magnitude of the charge-helix dipole interaction. The actual charge-helix dipole interaction could be estimated by accounting for the intrinsic differences mentioned above through comparisons of peptides E1x and E15x (where the substitution of Glu for Gln at the N terminus versus the middle of the helix is compared, in both cases, at the equivalent position g of the heptad repeat) and peptides E6x and E20x (where the substitution of Glu for Gln at the N terminus versus the middle of the helix is compared, in both cases, at the equivalent position e of the heptad repeat). However, because the intrinsic properties of the amino acids appear, as discussed above, to have less pronounced effects on stability at the ends of an α-helix than in the middle, this estimation represents an upper limit for the true value of the charge-helix dipole interaction. This calculated $\Delta\Delta G_u^{\text{helix dipole}}$ (see Table V.1, footnote *f* for details of calculation) is +0.36 kcal/mol and +0.35 kcal/mol per Glu residue (per chain) in peptides E1x and E6x, respectively (Table V.1). The similarity of these results indicates that a similar magnitude charge-helix dipole interaction occurs for Glu residues within the first two turns of the helices comprising the coiled-coil.

The substitution of a Glu residue in each chain of the coiled-coil may lead one to question whether these residues (for example at positions 1 and 1' in E1x) are in close enough proximity to each other to exert a repulsive destabilizing influence, which would result in an underestimation of the stabilizing interaction of these Glu residues with the helix dipole. However, as shown in the helical wheel diagram (Fig. I.3A, p. 23), the substituted residues at positions **g** and **g'** (or **e** and **e'**) lie on opposite sides of the dimer interface, and interactions between them should be minimal.

Upon a C-terminal Glu for Gln substitution, as in E34x, the stability decrease due to decreased intrinsic helical propensity and hydrophobicity should be in addition to the predicted unfavorable charge-helix dipole interaction introduced by a negatively charged residue at the C terminus; therefore, the overall stability decrease would be predicted to be greater for a C-terminal Glu substitution than one at a position near the middle of the helix. Indeed, the observed $\Delta\Delta G_u$ for E34x is -0.35 kcal/mol compared to -0.19 kcal/mol for E20x, in which Glu is substituted at the comparable position **e** of the heptad repeat (Table V.1); the value of the calculated $\Delta\Delta G_u^{\text{helix dipole}}$ is -0.08 kcal/mol per Glu (per chain). In the case of this C-terminal substitution, the observed $\Delta\Delta G_u$ of -0.18 kcal/mol per Glu (-0.35 kcal/mol total) represents the upper limit of the charge-helix dipole interaction since accounting for the intrinsic effects of the substitution on stability at the C terminus reduces the estimated dipole interaction, while at the N terminus it has the opposite effect of increasing the predicted helix dipole interaction.

The unfavorable interaction between the Glu carboxylate and the helix dipole estimated for E34x is significantly smaller than the favorable charge-helix dipole interactions calculated for E1x and E6x. This would suggest that charge-helix dipole interactions at the N terminus are more important for protein stability and is consistent with the statistical observation that charge distribution in α-helices is more commonly due to preferential distribution of negative charges at the N terminus than of positive charges at the C terminus. This is illustrated by the observation among a large sampling of proteins that the average charge of the side chains is +0.34 near the C terminus and is -0.64 near the N terminus (Dasgupta & Bell, 1993). One potential reason for less dramatic effects at the C terminus is that in an α-helix the C^{α}-C^{β} bonds of the side chains are oriented towards the N terminus, so that the side chains near the N terminus interact strongly with the positive pole of the helix dipole, while those at the C terminus point away from the C terminus and as a result may interact less strongly with the helix dipole (Nicholson *et al.*, 1991).

For the reduced coiled-coils (Figure V.2B), the relative stabilities remain generally the same as for the oxidized coiled-coils. Those containing N-terminal Glu substitutions, E1r and E6r, are more stable than the control, Nr, while those with Glu substitutions in positions 15, 20 and 34 are less stable than Nr (Table V.1). The $\Delta\Delta G_u^{\text{helix dipole}}$ values of +0.35, +0.35 and -0.08 kcal/mol for E1r, E6r and E34r, respectively, are essentially identical to those obtained for their oxidized counterparts (Table V.1). The results for the reduced peptides therefore show that the effect of charge-helix dipole interactions are independent of the presence of the N-terminal 2-2' disulfide bridge between the chains of the coiled-coil and merely add to the large effect of the disulfide bridge on coiled-coil stability (indicated by the large increase in $[\text{denaturant}]_{1/2}$ between oxidized and reduced forms and the estimated $\Delta\Delta G_u$ value of 3-4 kcal/mol (Hodges *et al.*, 1990)).

Interestingly, while the stabilities of the oxidized coiled coils E15x and E20x are substantially different, in the reduced form these analogs display equal stability (Table V.1). The only difference in these peptides is the substitution of Glu for Gln at heptad repeat position **g** in E15x and at position **e** in E20x. These positions are nonequivalent, with the **g** position packing primarily against the following **a'** position and the **e** position packing against the preceding **d'** position of the other helix (O'Shea *et al.*, 1991). The results for the oxidized peptides suggest that the inferior packing of Glu relative to that of Gln is more apparent at position **g**, where it packs against Val at position **a'** rather than at position **e** where it packs against Leu at position **d'**. In the reduced form, the coiled-coil is much more flexible (less compact, as indicated by lower retention times on size-exclusion HPLC) than in its oxidized form and may adjust its structure and interchain packing to accommodate the destabilizing effect of the Glu substitution, such that substitutions at positions **g** and **e** appear similar. The oxidized coiled-coil could be more restricted in structure and less capable of reorganizing its interface packing in response to substitutions, so that the differences in positions **g** and **e** are more apparent in the stability. Similar results were observed in the hydrophobic core **a** and **d** positions, where Ala substitutions for Leu were more destabilizing at position **a** than position **d** in coiled-coils containing an interchain disulfide bridge (at either the N or C terminus), but Ala mutations had the same effect on stability at adjacent positions **a** and **d** in reduced coiled-coils (Zhou *et al.*, 1992b).

ii) Salt effects on the stabilities of Glu substituted coiled-coils. One of the basic tests for determining whether a stabilizing (or destabilizing) substitution is due to electrostatic effects is its ionic strength dependence. Salt is generally believed to screen electrostatic interactions, so raising the ionic strength should reduce the contribution of stabilizing electrostatic effects (see Chapter I). However, the effects of ionic strength on electrostatic interactions in proteins can vary, and indeed electrostatic interactions are not always reduced by increased ionic strength, as indicated by computations (Hendsch & Tidor, 1994) and experimental results (Monera *et al.*, 1993; Perutz *et al.*, 1985). The coiled-coils in the present study offer a good model system in which to examine the screening effects of salts on charge-helix dipole interactions at protein surfaces.

The effect of ionic strength on the stabilities of the coiled-coils has been determined by varying the concentration of KCl from 0 to 3 M. As indicated in Figure V.3A, the $[\text{urea}]_{1/2}$ values of the coiled-coils Nx, E1x, and E15x are dramatically increased by increased ionic strength (increased KCl concentration). As suggested by Mo *et al.* (1990) for tropomyosin and by previous studies on model coiled-coils (Chapter IV, Kohn *et al.*,

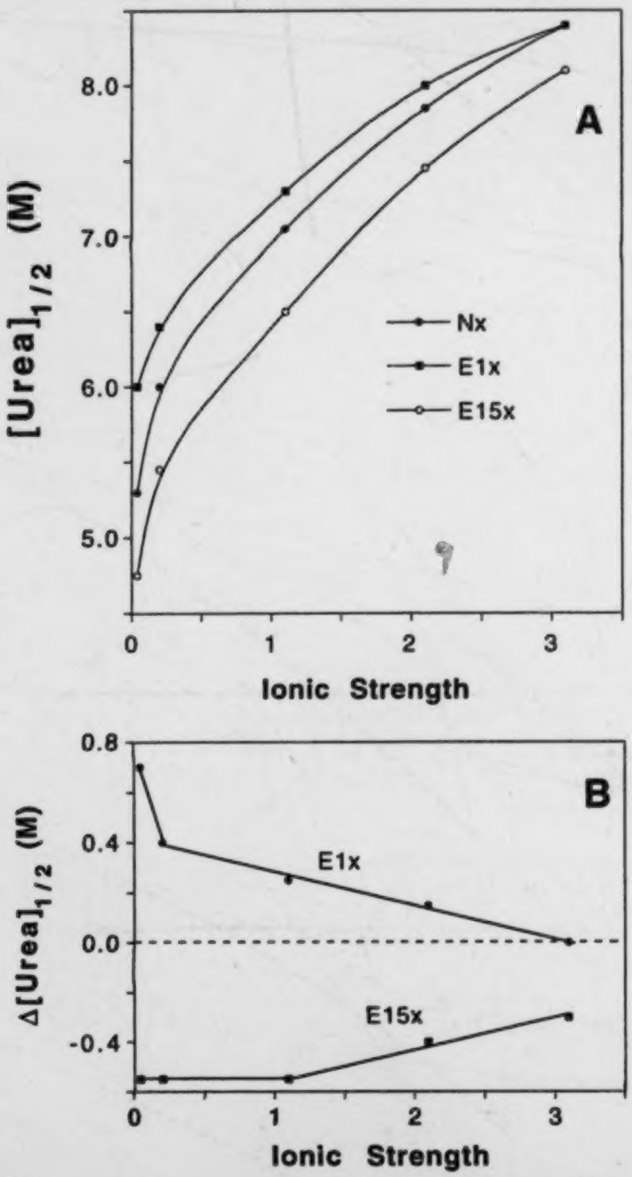

Figure V.3 Effect of salt concentration on coiled-coil stability. **A,** Effect of ionic strength on the stabilities (expressed as the [urea]$_{1/2}$ or concentration of urea at which the coiled-coil is 50% unfolded) of the disulfide-bridged coiled-coils Nx, E1x and E15x at 20 °C in sodium phosphate, pH 7 buffer. Ionic strength was varied by increasing the KCl concentration from 0 to 3 M. In addition, sodium phosphate concentration was 20 mM for the lowest ionic strength data and 50 mM for the remaining data points. **B,** Difference between the [urea]$_{1/2}$ values of E1x and Nx and the [urea]$_{1/2}$ values of E15x and Nx (denoted Δ[urea]$_{1/2}$) as a function of ionic strength.

1995b; Monera *et al.*, 1993), this stabilization is most likely due to an increase in the hydrophobic effect induced by the added KCl (as discussed in Chapter I) and possibly anion binding to the Lys residues along the solvent exposed face at position **f** of the helices (Chapter IV). It may also involve screening of unfavorable electrostatic interactions between helix dipoles caused by parallel packing of the helices, which has been estimated by computational studies (Gilson & Honig, 1989; Rogers & Sternberg, 1984) and experimental data (Robinson & Sligar, 1993) to account for anywhere between 0.5 and 3 kcal/mol difference in the stability of parallel and antiparallel four-helix bundles.

In addition, the $[\text{urea}]_{1/2}$ value of E1x, which at low ionic strength is higher than that of Nx presumably due to charge-helix dipole interactions, becomes equal to that of Nx at a high KCl concentration of 3 M (Fig. V.3A). The charge-helix dipole interactions thus appear to be screened at very high salt concentrations, consistent with the results of previous studies (Fairman *et al.*, 1989; Huyghues-Despointes *et al.*, 1993a, 1993b; Ihara *et al.*, 1982; Lockhart & Kim, 1993; Takahashi *et al.*, 1989) which observed a requirement for large concentrations of NaCl (3 to 5 M) to fully screen interactions between charged side chains and the N-terminal pole of the helix dipole. In contrast, E15x, in which the substituted Glu residue should not interact significantly with the helix dipole as a result of being in the middle of the helix, is much less affected by KCl concentration in terms of its stability relative to Nx. This is clearly demonstrated in Figure V.3B, where the $\Delta[\text{urea}]_{1/2}$ values of E15x and E1x relative to Nx are plotted versus ionic strength. For E1x, $\Delta[\text{urea}]_{1/2}$ decreases dramatically from 0.7 to 0.25 M upon changing the ionic strength from 0.04 to 1.1; whereas, for E15x the $\Delta[\text{urea}]_{1/2}$ value is unchanged below 1 M KCl (ionic strength 1.1) and is still -0.3 M even at 3 M KCl. The inability of KCl to fully remove the $[\text{urea}]_{1/2}$ difference between Nx and E15x supports the conclusion that the lower stability of E15x is due to an "intrinsic" destabilization from the substituted residue rather than a charge-charge or charge-dipole interaction.

The effect of GdnHCl on the charge-helix dipole interactions was also investigated. GdnHCl, as an ionic species, has been shown to behave like a salt in screening interchain electrostatic interactions involving Lys and Glu residues in coiled-coils (Chapters III and IV, Kohn *et al.*, 1995a, 1995b; Monera *et al.*, 1993, 1994a, 1994b). As such, GdnHCl would be expected to screen the charge-helix dipole interactions in a manner similar to KCl. The GdnHCl denaturation profiles for the coiled-coils containing Glu substitutions at the N terminus are essentially identical to Nx (Fig. V.2C), with $[\mathrm{GdnHCl}]_{1/2}$ values around 3.1-3.2 M, indicating that GdnHCl has masked the interactions between charged residues and the helix dipole. These results emphasize the importance of choosing the appropriate denaturant to measure the effect of ionic interactions on protein stability. For example, in the recent study of Zhukovsky *et al.* (1994), it was concluded that the charge-helix dipole stabilization provided by Glu74 at the N terminus of helix 2 in human growth hormone is negligible. However, the authors used GdnHCl denaturation to reach this conclusion which, as the present results show, would lead to an incorrect conclusion as to the importance of the charge-helix dipole interaction. In addition, the stability of E15x is equal to that of Nx from GdnHCl denaturation (Fig. V.2C), indicating that GdnHCl "screens" the intrinsic destabilization of E15x, which 3 M KCl present during urea denaturation was unable to do completely (Fig. V.3A and B).

iii) Effects of Glu substitutions on coiled-coil stability at low pH. Typically, evidence that a particular residue is involved in a stabilizing or destabilizing electrostatic interaction lies in the pH dependence of its effect on stability. In the absence of other effects, a substitution that introduces a favorable interaction of an acidic side chain group with the N-terminal end of the helix dipole is expected to have no effect on stability at low pH where the Glu side chain is protonated.

For peptides E1x and E6x, the net effect of the substitution at neutral pH is an increase in stability, apparently due to the charge-helix dipole interaction, despite the slightly destabilizing effects of the lower intrinsic helical propensity and hydrophobicity of ionized Glu versus Gln. At pH 3, the Glu side chain carboxylate should be mostly protonated, and the strength of the charge-helix dipole interaction should be correspondingly reduced. Thus, E1x displays a lower $\Delta\Delta G_u$ value (+0.09 kcal/mol, Table V.2) at pH 3 than at pH 7 (+0.33 kcal/mol, Table V.1). Protonation of Glu 1 therefore reduces the stabilizing influence of the Gln to Glu substitution, supporting the conclusion that the effect is electrostatic in nature. In contrast, E6x has the same $\Delta\Delta G_u$ value at pH 3 and pH 7 (Tables V.1 and V.2). In this case, the expected loss of stabilization from the proposed charge-helix dipole interaction upon protonation of Glu6 appears to be offset by increased intrinsic coiled-coil stabilizing properties of protonated Glu. As mentioned above, the substitution of a Glu residue for Gln at pH 7, as in E20x, reduces stability due to the reduced helical propensity and hydrophobicity of ionized Glu relative to Gln. In contrast, at low pH, Glu 20 is mostly protonated and E20x is more stable than Nx (Chapter III, Kohn *et al.*, 1995a). E20x has a $\Delta\Delta G_u$ of +0.71 kcal/mol at pH 3, suggesting each Gln to Glu substitution results in 0.36 kcal/mol stabilization. Both the helical propensity (Scholtz *et al.*, 1993; Wójcik *et al.*, 1990) and the hydrophobicity (Guo *et al.*, 1986; Sereda *et al.*, 1994) of protonated Glu are higher than for Gln, making protonated Glu a better intrinsically-stabilizing residue than Gln.

The stability results at pH 3 (Table V.2) show that the hydrophobic and helical propensity contribution that a protonated Glu makes to stability varies with the position in the peptide, with the largest effect in the center of the coiled-coil (E15x). The results for E15x and E20x show that protonated Glu has significant stabilizing effects at both heptad repeat positions **e** and **g**, but that the stabilization is slightly larger at position **g**. Similarly, the destabilizing effect of ionized Glu was found to be greater at position **g** (in E15x) than at position **e** (in E20x). Overall, the stability results with Glu substitutions at low pH indicate that the charge-dipole interactions are removed but replaced by other stabilizing effects of the protonated Glu residue.

Table V.2: Stability data at pH 3 from urea denaturation

Peptide [a]	$[\text{urea}]_{1/2}$ (M)	m	Observed $\Delta\Delta G_u$ (kcal/mol)
Nx	6.0	0.91	----
E1x	6.1	0.87	+0.09
E6x	6.6	0.79	+0.51
E15x	7.25	0.79	+1.06
E20x	6.8 [b]	0.87	+0.71
E34x	6.4	0.81	+0.34

[a] The sequences of the peptides are shown in Figure V.1.

[b] Data taken from Kohn *et al.* (1995a, Chapter III)

All symbols were described in Table V.1 and under Materials and Methods (pp. 56-59). Data was collected at 20 °C in a 50 mM PO_4, 100 mM KCl buffer.

iv) Charge-helix dipole interactions versus side chain to main chain hydrogen bonding. Because both Glu and Gln side chains could act as hydrogen-bond acceptors for the main chain NH group of the i+3 residue (the 4th residue), it is possible that a difference in hydrogen bond strength could account for the stability increase observed for E1x relative to Nx. Gln should serve as a good control for Glu because the hydrogen bonding groups of the two amino acids have similar geometry. The charged side chain of Glu could form a stronger hydrogen bond to the main chain because charged hydrogen bond acceptors usually form stronger hydrogen bonds (Taylor & Kennard, 1984); however, as pointed out by Tidor (1994), the ionized Glu must pay a greater desolvation penalty than Gln in order to hydrogen bond to the backbone due to its charged character, which should roughly offset its stronger hydrogen-bonding potential. A recent comprehensive report in which the N- and C-cap propensities of all 20 amino acids were determined (Doig & Baldwin, 1995) concluded that Gln is the worst N-capping residue while Asn is the best. Glu was also poorly stabilizing relative to other acidic residues, its pK_a value being raised at the N terminus, instead of the expected pK_a decrease. However, an observed increase in helical content with increased pH was ascribed to stabilization due to interaction of the negatively charged Glu side chain with the positive, N-terminal end of the helix macrodipole (Doig & Baldwin, 1995). In another study, Lumb and Kim (1995b) measured the pK_a of two Glu side chains involved in predicted interhelical Lys-Glu ion pairs in the GCN4 coiled-coil. No pK_a change was observed upon coiled-coil formation for one of the Glu residues while an increased pK_a was observed for the other. Based on these results, it was concluded that no stabilization due to the ion pair was apparent. The participation of an acidic side chain in favorable polar/electrostatic interactions need not necessarily be accompanied by a reduced pK_a (Lavigne *et al.*, 1996; see Chapter VII Discussion, pp. 208-211).

Because both Gln and Glu appear to be weak N-capping (hydrogen bonding) residues, the increased stability resulting from a Gln to Glu substitution is probably electrostatic in nature, particularly in light of the results with E6x, in which the substituted Glu residue is not at an N-capping position but stabilizes the coiled-coil to a similar extent as it does in E1x. Similarly, the C-terminal helix capping propensities were found to be essentially identical for Glu and Gln (Doig & Baldwin, 1995).

Further, crystallographic studies of mutant lysozymes with Asp substitutions at the N termini of α-helices suggested a stabilization due to electrostatic interaction rather than to precise hydrogen bonding between the substituted Asp side chain and the helix backbone (Nicholson *et al.*, 1988, 1991). In addition, Chakrabartty *et al.* (1993) reported that an N-terminal acetyl group is very effective in forming the helix capping hydrogen bond between its carbonyl oxygen and the i+3 NH group. In fact, this interaction is equivalent in strength to that of the best helix capping side chain, Asn (Doig & Baldwin, 1995), and cancels the effect on helicity of differences in N-cap propensity of the N-terminal amino acid. Accordingly, it could be expected that in the acetylated peptides employed in the present study, the acetyl group would negate any possible difference in hydrogen bonding effects of the residues substituted at position 1.

The above considerations suggest that precise hydrogen bonding from amino acid side chains to the helix backbone is an unlikely explanation for the stability changes observed in this study. The so called "charge-helix dipole" effect employed above to account for these observations could result from interaction of the substituted charged side chain with either the classical helix macrodipole that results from alignment of peptide bond dipoles or the unfulfilled main chain polar groups at either end of the helix. The results of the current study cannot distinguish between these possibilities.

C. Conclusions

This work has shown that the substitution of a Glu for a Gln residue in the e and g heptad repeat positions of a stable two-stranded α-helical coiled-coil can have a significant effect on the stability of the coiled-coil, the direction of which depends on the position of the substitution along the coiled-coil sequence. At the N terminus, Glu substitution increases stability, which can be explained by the charge-helix dipole interaction theory. This stability increase is modulated by ionic strength and pH changes, serving as evidence that the effect is electrostatic in origin. The apparent magnitude of these interactions is approximately 0.35 kcal/mol per Glu substitution. Various other studies of charge-helix dipole interactions listed in the introduction have estimated magnitudes for the charge-helix dipole interaction in either isolated helical peptides or globular proteins in the range of 0.3 -2.1 kcal/mol (see for example: Eijsink *et al.*, 1992; Kippen *et al.*, 1994; Lockhart & Kim, 1993; Nicholson *et al.*, 1991; Sali *et al.*, 1988; Sancho *et al.*, 1992; Serrano & Fersht, 1989). The wide range of experimentally-determined values suggests that the apparent charge-helix dipole interaction is highly dependent on the environment and the amino acid being studied. For example, while Lys appears to interact weakly with the helix dipole when present at the C terminus of an α-helix, His appears to interact much more strongly at the C terminus (Kippen *et al.*, 1994; Perutz *et al.*, 1985; Sali *et al.*, 1988). While the values obtained in the coiled-coil model are at the low end of this range , they are quite close to the results obtained by Eijsink *et al.* (1992), in which replacement of a Lys at the N terminus of a helix in *Bacillus subtilis* neutral protease by Ser increased stability by 0.3 kcal/mol and replacement of the Lys with Asp increased stability by 0.6 kcal/mol. The small effect of the substitution on the stability of the coiled-coil may be related to the inherent stability of the model. A less stable coiled-coil may exhibit a larger apparent charge-helix dipole interaction. In contrast to N-terminal substitution, Glu substitution in the middle of the helix leads to a loss of stability due to the lower helical propensity and hydrophobicity of the negatively-charged Glu relative to Gln, for which it is substituted. The intrinsic nature of this effect is confirmed by the inability of salt to screen it. At the C terminus, a larger destabilization occurs (compare E20 and E34, both **e** positions) due to both intrinsic destabilization and unfavorable charge-helix dipole interactions, the opposite of what occurs at the N terminus.

This initial positional dependence study has concentrated only on the effects of Glu for Gln substitutions for two major reasons: Glu has been the focus of studies in our previous work on interhelical repulsions in coiled-coils (Chapters III and IV, Kohn *et al.*, 1995a, 1995b) from which the current work originated, as well as the fact that Glu is the most commonly occurring residue at the **e** and **g** positions of coiled-coils (Hu & Sauer, 1992). For example, 29 of 80 residues in the **e** and **g** positions of rabbit skeletal α-tropomyosin are Glu, the next most plentiful being Lys with 16 occurrences. The generality of charge-helix dipole effects in coiled-coils should be further established through additional experiments incorporating other amino acids.

These results are important for coiled-coil (leucine zipper) design, which is potentially useful in regulation of transcription and other biotechnological applications (Adamson *et al.*, 1993; Hodges, 1996; Krylov *et al.*, 1994; Pack & Pluckthun, 1992; Wu *et al.*, 1995). In order to design coiled-coils successfully for various applications, the effects of substitutions at all positions of the coiled-coil on dimerization stability and specificity must be quantitated. For example, in the recent study of Krylov *et al.* (1994), in which a stability scale for the interhelical **g-e'** interactions between various residues was presented, it was suggested that the $\Delta\Delta G_u$ value per **g-e'** pair is nearly independent of the heptad in which it occurs. However, while this approximation may be the case for many amino acid combinations in the **g-e'** pair, the results from our studies with Glu substitutions illustrate that this will not always hold true. Specifically, while a Glu-Glu pair is destabilizing at pH 7 in the central heptad of the 35-residue model coiled-coil studied here (Chapter III, Kohn *et al.*, 1995a), it is actually stabilizing in the N-terminal heptad (Chapter IV, Kohn *et al.*, 1995b), illustrating that end effects due to charge-helix dipole interactions can in some cases significantly affect overall protein stability.

In addition, it is clear from this and other studies (Villegas *et al.*, 1996) that placement of charged residues near the ends of helices can be used advantageously to alter the stability of engineered proteins in general.

CHAPTER VI

SALT EFFECTS ON PROTEIN STABILITY: TWO-STRANDED α-HELICAL COILED-COILS CONTAINING INTER- OR INTRAHELICAL ION PAIRS[4]

A. Introduction

The effects of various salts on coiled-coil folding and stability observed in Chapter IV (Kohn *et al.*, 1995b) suggested that information regarding the role of the side chains at positions **e** and **g** might be obtained by such experiments. As outlined in Chapter I, salts can have various effects on the electrostatics in proteins due to charge screening, ion binding, and effects on the solution properties. However, salts are often assumed to act primarily by screening electrostatics through effects on the dielectric constant, and the effects of salt on protein stability and interactions between molecules are generally interpreted in this way. The results of Chapter IV (Kohn *et al.*, 1995b) and Monera *et al.* (1993) show that, even at very high concentration, salt does not always completely screen electrostatic interactions. Recently, the effect of salt concentration on coiled-coils containing ion pairs has been addressed (Thompson-Kenar *et al.*, 1995; Yu *et al.*, 1996), and it was concluded in these studies that salt does affect the stability of coiled-coils through modulation of electrostatic interactions.

Here, the ability of salts to perturb the stability of coiled-coils containing interhelical ion pairs, intrahelical ion pairs, or no ion pairs has been studied. The effect of KCl concentration on stability was measured at both pH 7 and pH 3 to get a better idea of the role of salt at a pH where interhelical ion pairs are possible and at a pH where the acidic (Glu) side chains are protonated (precluding ion pair formation). The phenomenon of increased stability upon acidification is examined in terms of the combined effects of both

---

[4] A version of this chapter has been published: Kohn, W. D., Kay, C. M., and Hodges, R. S. (1997) *J. Mol. Biol.* **267**, 1039-1052.

Glu protonation and interactions with salt ions. The prediction that the large differences in the effects of KCl, $MgCl_2$, and $LaCl_3$ on stability of the coiled-coils containing Glu-Glu repulsions (Chapter IV) would also be observed in their effects on coiled-coils containing ion pairs was investigated. In particular, the relative roles of charge screening, ion binding, and effects on solution structure/properties in the overall salt effects on stability were expected to be different. For example, ion binding should be greater with a higher charged ion (La^{3+}), and $LaCl_3$ could therefore have a more dramatic effect on stability. With progressively less charge on the cation, $MgCl_2$ and KCl would be expected to have lesser effects on stability since they would be less likely to bind to the protein. Comparison of the effects of salts on the stability of ion pair-containing coiled-coils to a control peptide containing no electrostatic interactions was used as a reference point in order to correct for effects of salt on the stability for reasons other than modulation of electrostatics within the coiled-coil. The goal of these experiments was to gain insight into the nature of ion-pair stabilization of coiled-coils from the proposed mechanism of action of the various salt ions.

B. Results

a) Peptide design and nomenclature

The sequences for the coiled-coils studied in this chapter are shown in Figure VI.1. These coiled-coils are similar to those studied in the other chapters of this thesis, but the hydrophobic core is different. Rather than the Val_aLeu_d core, a sequence containing mostly Leu residues at heptad positions **a** and **d** was used. An Ala substitution at position 16 (heptad position **a**) was required for reduction of the stability, so that chemical denaturation could be performed at room temperature over a reasonable denaturant concentration range. The Ala mutation also specifies two-stranded versus four-stranded coiled-coil formation (Monera *et al.*, 1996). This generation of coiled-coils was previously studied by Zhou *et al.* (1994b, 1994c).

Peptide Name	Amino Acid Sequence
	1 5 10 15 20 25 30 35
	g a b c d e f g a b c d e f g a b c d e f g a b c d e f g a b c d e f
QQ	Ac-**Q**-C-G-A-L-**Q**-K-**Q**-L-G-A-L-**Q**-K-**Q**-A-G-A-L-**Q**-K-**Q**-L-G-A-L-**Q**-K-**Q**-L-G-A-L-**Q**-K-Amide
KE	Ac-**E**-C-G-A-L-**K**-K-**E**-L-G-A-L-**K**-K-**E**-A-G-A-L-**K**-K-**E**-L-G-A-L-**K**-K-**E**-L-G-A-L-**K**-K-Amide
EQ	Ac-**Q**-C-G-A-L-**E**-K-**Q**-L-G-A-L-**E**-K-**Q**-A-G-A-L-**E**-K-**Q**-L-G-A-L-**E**-K-**Q**-L-G-A-L-**E**-K-Amide
KQE	Ac-**Q**-C-**E**-A-L-**K**-G-**Q**-L-**E**-A-L-**K**-G-**Q**-A-**E**-A-L-**K**-G-**Q**-L-**E**-A-L-**K**-G-**Q**-L-**E**-A-L-**K**-G-Amide

Figure VI.1 Amino acid sequences of the peptides studied to determine the effects of salts on coiled coils containing intra- or interhelical Lys-Glu ion pairs. A cysteine at position 2 allows formation of an interchain 2-2' disulfide bridge. Peptide nomenclature is based on the amino acids at positions **e** and **g** heptad positions (highlighted by bold type) and for KQE by the residues at positions **e**, **g**, and **b**.

The nomenclature used for the analogs in this study is based on the one letter code and for each peptide indicates the amino acid residues present in the **e** and **g** positions of the heptad repeat. In this case, the native sequence is designated 'QQ' (Figs. VI.1 and VI.2) and provides a stable reference coiled-coil containing no intra- or interhelical electrostatic interactions, to which the mutant peptides could be compared (as described in Chapter II, p. 60). Similarly, KE denotes Lys in position **e** and Glu in position **g**, and EQ contains Glu in position **e** and Gln in position **g** (Fig. VI.1). KE was designed to have interhelical i to i'+5 Glu-Lys ion pairs without any i to i+3 or i to i+4 intrahelical ionic interactions (Fig. VI.2). KQE (designated by the residues at the **e**, **g** and **b** positions, respectively) contains potential intrahelical i to i+3 (**b**-**e**) and i to i+4 (**e**-**b**) Lys-Glu interactions but no interhelical ionic interactions (Fig. VI.2). As in the preceding studies, all analogs contain a Cys residue at position 2 allowing formation of an interchain 2-2' disulfide bridge, designated with an "x".

b) Structural characterization

Peptides QQx and EQx were shown to form stable two-stranded coiled-coils in a previous study (Zhou *et al.*, 1994b) with high $[\theta]_{220}$ values of -30,340 and -30,220, respectively, in benign 50 mM PO_4, 100 mM KCl, pH 7 buffer. Similarly, the $[\theta]_{220}$ values for KEx and KQEx were found to be -31,700 and -31,400, respectively, indicating high helical content for all peptides in this study. In addition, the peptides were eluted from a size-exclusion HPLC column within a retention time range of 20.9 to 22.4 min (data not shown). This is within the expected retention time range for the two-stranded coiled-coil structure as predicted from a calibration curve derived from a set of helical peptide standards of varying length (see Materials and Methods, Fig. II.6). It was also found that the addition of 50 mM $LaCl_3$ or increasing concentrations of $MgCl_2$ or KCl to the run buffer had no effect on the retention times of the peptides. The absence of aggregation was also demonstrated by sedimentation-equilibrium ultracentrifugation for peptide KEx.

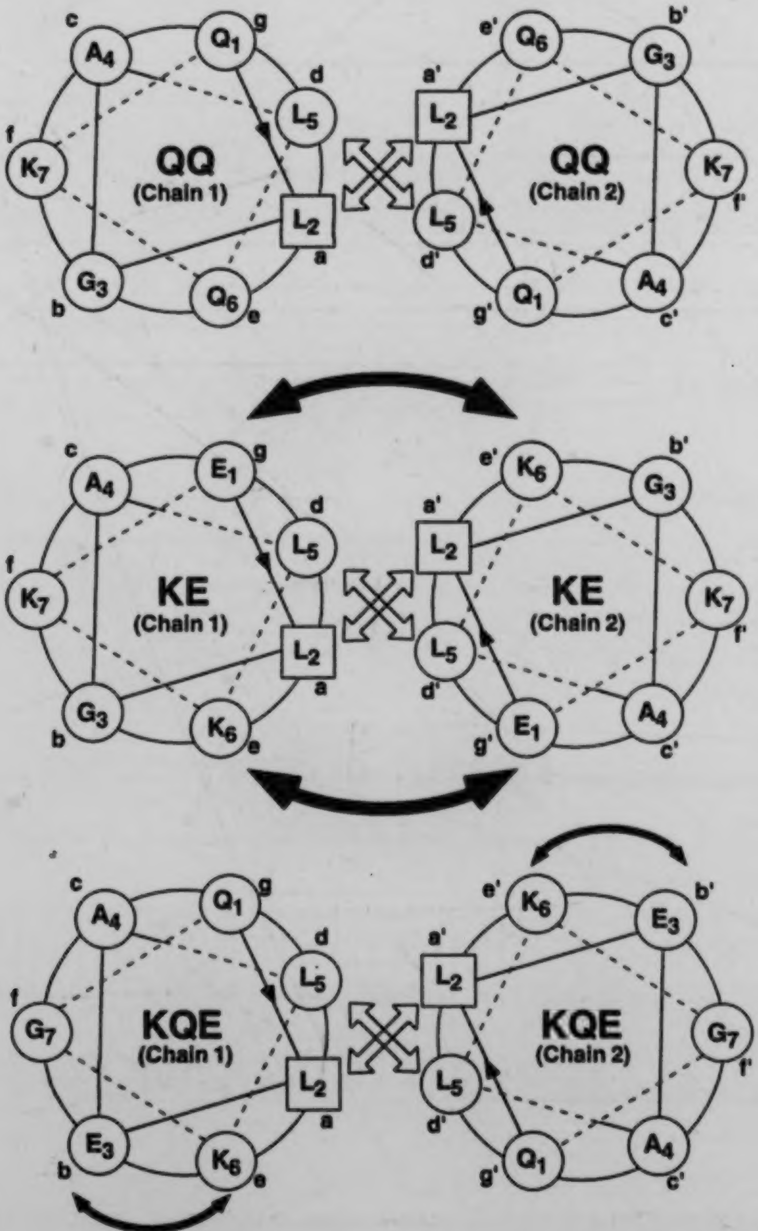
QQ
(Chain 1)
QQ
(Chain 2)
KE
(Chain 1)
KE
(Chain 2)
KQE
(Chain 1)
KQE
(Chain 2)
A4
Q1
L5
L2
K7
G3
Q6
E1
K6
G7
E3
a
b
c
d
e
f
g
a'
b'
c'
d'
e'
f'
g'

Figure VI.2 Cross-sectional helical wheel representation of one heptad in the model coiled-coils QQ (top), KE (middle) and KQE (bottom) viewed from the N-terminus. Open arrows indicate hydrophobic interactions between the **a-a'** and **d-d'** positions, while the solid arrows depict ionic interactions. These are interhelical i to i'+5 (**g-e'**) interactions in KE and intrachain i to i+3 (**b-e**) in KQE. In KQE, Lys at position **e** can also ion pair to Glu at position **b** of the following heptad in an i to i+4 (**e-b**) intrachain ionic attraction (see also Fig. VI.1).

Samples were run under the following buffer conditions with rotor speeds at which data was collected in brackets: (1) 50 mM tris, pH 7 buffer containing 100 mM KCl (32,000; 40,000); 1 M KCl (40,000; 48,000); 100 mM KCl and 50 mM $LaCl_3$ (32,000; 36,000); or 100 mM KCl and 400 mM $MgCl_2$ (36,000; 42,000) and (2) 50 mM PO_4, pH 3 buffer containing 100 mM (30,000; 36,000) or 1 M KCl (28,000; 34,000). Under all the buffer conditions tested, KEx was found to behave as a two-stranded monomer. As shown in Figure VI.3, the data fit a single species model with a predicted molecular weight of 8290 at 100 mM KCl and 7470 at 1 M KCl, very close to the actual MW of 7410. Similar good fits of the data to a single-species model were obtained for the other buffer conditions (data not shown). The sedimentation-equilibrium data for KEx and the correlation between the retention times of all the peptides on size-exclusion HPLC indicate that none of the disulfide-bridged peptides in this study form four-stranded dimers or higher order aggregates and that no significant conformational differences occur between them.

c) *Stability studies by chemical denaturation*

i) *Effects of increasing KCl concentration on coiled-coil stability.*

The control coiled-coil, QQx, was designed to have no intra- or interhelical ionic interactions but does contain 5 Lys residues at position **f** to maintain solubility of the peptide (Figs. VI.1 and VI.2). The effect of KCl concentration on stability, as determined by urea denaturation, for the coiled-coils QQx (containing no ion pairs) and KEx (containing 10 interhelical i to i'+5 Glu-Lys ion pairs) is shown in Figure VI.4. At pH 7, the stability of QQx increases gradually with increasing KCl concentration from a $[urea]_{1/2}$ value of 4.15 M at 0 M KCl to 5.45 M at 1 M KCl (Table VI.1 and Fig. VI.4). As expected, since there are no charged residues in this coiled-coil which change their ionization state over the pH range 3 to 7, the effect of increasing KCl concentration on QQx stability is the same at pH 3 as at pH 7 (Fig. VI.4 and Table VI.1).

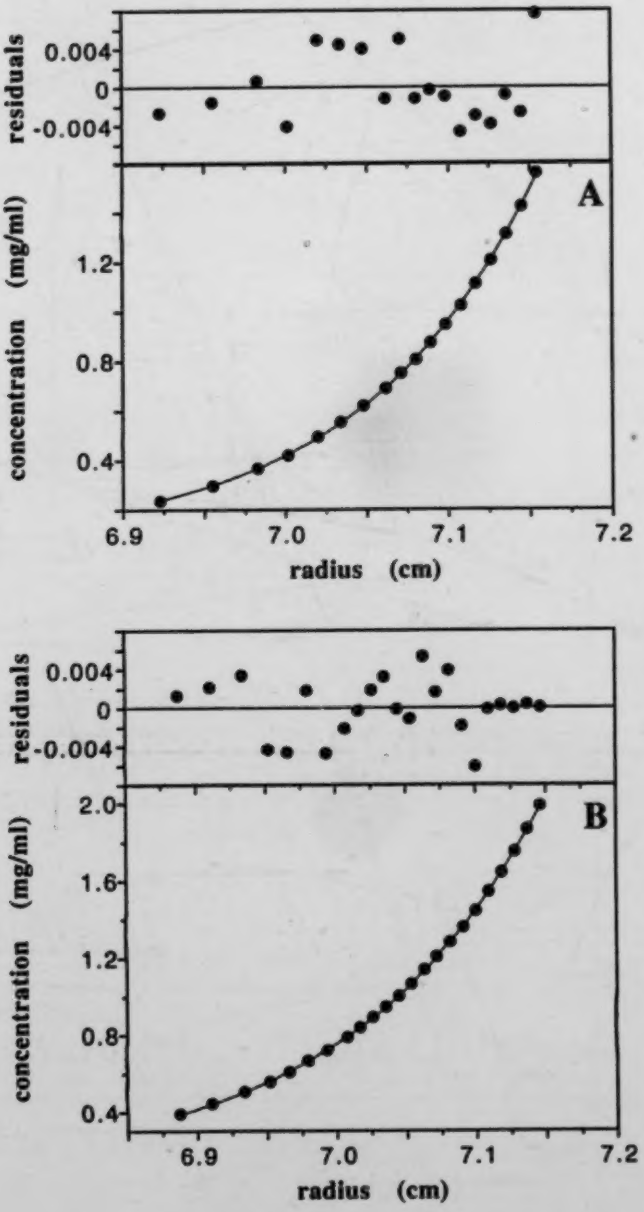

Figure VI.3 Sedimentation-equilibrium results for KEx at 20 °C in 50 mM tris, pH 7 buffer containing 100 mM KCl (**A**) and 1 M KCl (**B**). A single species (two-stranded monomer) curve fit is shown with residuals from the curve fits shown in the upper panels. The data shown was collected at a rotor speed of 40,000 rpm. Experiments at different rotor speeds for both conditions yielded similar results (data not shown).

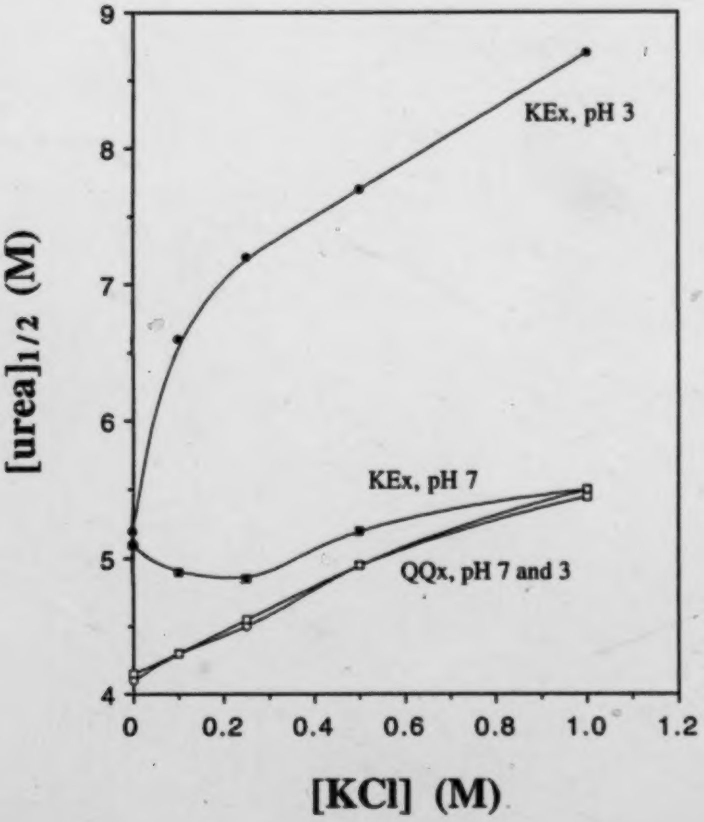

Figure VI.4 Dependence of KEx and QQx stability at 20 °C on KCl concentration at pH 7 and pH 3. The $[\text{urea}]_{1/2}$ is the transition midpoint, the concentration of urea at which a 50 % decrease in mean residue molar ellipticity at 220 nm is observed. Measurements were done in a 50 mM PO_4 buffer. Peptide concentrations were in the range 43 µM to 89 µM.

Table VI.1: Effects of varying KCl concentration on coiled-coil stability.

	Peptide [a]	[urea]$_{1/2}$ (M) [b]				
		0 M KCl	100 mM KCl	250 mM KCl	500 mM KCl	1 M KCl
a) pH 7	KEx	5.1	4.9	4.85	5.2	5.5
	QQx	4.15	4.3	4.55	4.95	5.45
	Δ[urea]$_{1/2}$ [c]	+0.95	+0.60	+0.30	+0.25	+0.05
b) pH 3	KEx	5.2	6.6	7.2	7.7	8.7
	QQx	4.1	4.3	4.5	4.95	5.5
	Δ[urea]$_{1/2}$ [c]	+1.1	+2.3	+2.7	+2.75	+3.2
a) pH 3	KEx	5.2	6.6	7.2	7.7	8.7
pH 7		5.1	4.9	4.85	5.2	5.5
	Δ[urea]$_{1/2}$ [c]	+0.1	+1.7	+2.35	+2.5	+3.2
b) pH 3	EQx	7.9	8.2	8.4		9.5
pH 7		2.2	2.3	2.5		4.0
	Δ[urea]$_{1/2}$ [c]	+5.7	+5.9	+5.9		+5.5

[a] Peptide sequences are shown in Figure VI.1.

[b] [urea]$_{1/2}$ is the transition midpoint , the concentration of urea (M) at which a 50 % decrease in ellipticity at 220 nm is observed.

[c] Δ[urea]$_{1/2}$ is the difference in [urea]$_{1/2}$ values for peptide KEx - QQx or for one peptide at two different pH values (pH 3 - pH 7).

All measurements were done at 20 °C in a 50 mM PO_4 buffer.
The final peptide concentrations were in the range 43 µM to 89 µM.

At pH 7, the effect of increasing KCl concentration on the stability of KEx is significantly different than for QQx (Fig. VI.4). The $[\text{urea}]_{1/2}$ value of KEx (5.1 M) is much higher than that of QQx (4.15 M) at low salt concentration, but as the KCl concentration is increased up to 250 mM KCl, its $[\text{urea}]_{1/2}$ value decreases slightly, in contrast to the stability increase observed for QQx (Table VI.1). Between 250 mM and 1 M KCl, the $[\text{urea}]_{1/2}$ of KEx increases to a value slightly above that observed at 0 M KCl (5.5 M compared to 5.1 M). The stability of QQx appears, however, to increase almost linearly with increasing KCl concentration over the entire range studied. The different effects of KCl addition on the stability of these coiled-coils, which only differ by the residues in the **e** and **g** heptad repeat positions, supports the assumption that the Glu and Lys residues at positions **g** and **e**, respectively, in KEx are involved in interhelical ionic interactions.

In contrast to the pH 7 results, the stability of KEx at pH 3 was dramatically higher than that of QQx at all KCl concentrations between 0 and 1 M (Fig. VI.4). The $[\text{urea}]_{1/2}$ values of both peptides are increased by the added KCl, but the $[\text{urea}]_{1/2}$ of KEx is much more sensitive to increasing KCl concentration than is that of QQx. This can be seen from Figure VI.5A, where the $\Delta[\text{urea}]_{1/2}$ between QQx and KEx increases dramatically between 0 and 0.1 M KCl and continues to increase up to 1 M KCl. In contrast, the $\Delta[\text{urea}]_{1/2}$ at pH 7 gets smaller as the KCl concentration is increased (Fig. VI.5A). At pH 3, the only charged residues at the **e** and **g** positions in KEx are the lysines at position **e** while no charged residues are present in QQx at these positions. Thus, the difference in the KCl dependence observed for the two peptides may be due to interactions of the added salt with these Lys side chains (see below).

ii) Effects of different salts on coiled-coil stability. The above results indicate that KCl may partially screen the ionic attractions proposed to occur in KEx. However, there is only a small decrease in stability (the $[\text{urea}]_{1/2}$ is decreased from 5.1 M at 0 M KCl to 4.85 M at 250 mM KCl (Table VI.1), corresponding to a $\Delta\Delta G_u$ of about 0.2 kcal/mol).

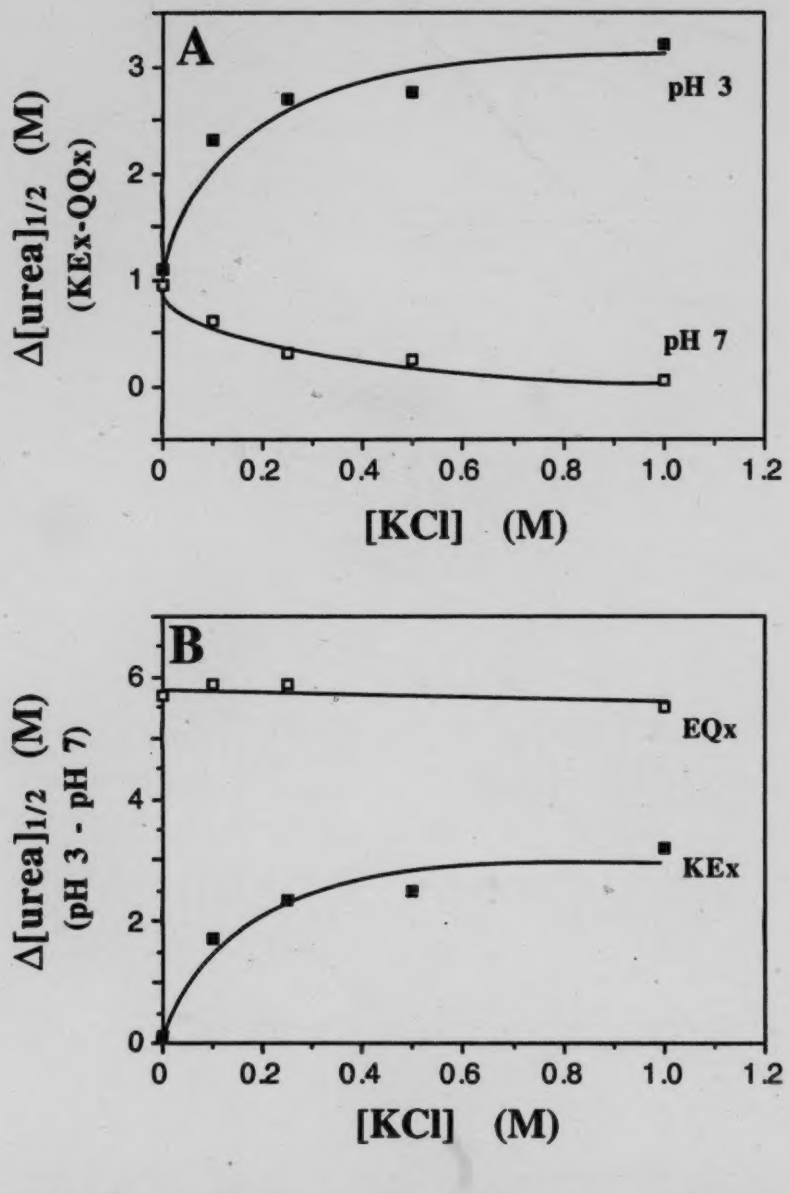

Figure VI.5 **A,** Difference in $[\text{urea}]_{1/2}$ values ($\Delta[\text{urea}]_{1/2}$) between KEx and QQx plotted as a function of the KCl concentration at pH 7 and pH 3. **B,** the $\Delta[\text{urea}]_{1/2}$ between pH 3 and pH 7 for the coiled coils EQx and EKx as a function of KCl concentration . The PO_4 concentration is kept constant at 0.05 M.

A salt containing a higher charged cation such as La^{3+} may be more effective in disrupting Lys-Glu ion pairs by specific interactions with the Glu residues involved in those ion pairs. To investigate this possibility, the effect of 50 mM $LaCl_3$ on the stabilities of coiled-coils KEx and QQx was determined. As shown in Figure VI.6A, the stability of QQx, as determined by urea denaturation studies, was increased by the addition of 50 mM $LaCl_3$. The $[urea]_{1/2}$ was increased from 3.95 M to 4.45 M, corresponding to a stability increase ($\Delta\Delta G_u^{obs}$) of 0.51 kcal/mol (Table VI.2). In contrast, KEx stability was decreased by the addition of 50 mM $LaCl_3$ at pH 7 (Fig. VI.6A) with an observed stability decrease of 1.63 kcal/mol (Table VI.2). This result can be explained by specific binding of the La^{3+} ion to the glutamate residues present in the protein and disruption of interhelical ion pairs. The 0.51 kcal/mol increase in stability of QQx resulting from the addition of 50 mM $LaCl_3$ is most likely due to changes in intrinsic properties of the solution (such as an increased hydrophobic effect resulting from the increased ionic strength), which should affect the stability of KEx to a similar extent. Correcting for this intrinsic salt effect leads to an estimation of the actual destabilizing effect of $LaCl_3$ on KEx through disruption of the ion pairs of 1.63 + 0.51 = 2.14 kcal/mol (denoted as $\Delta\Delta G_u^{cor}$ in Table VI.2).

At pH 3, QQx shows a similar change in stability upon the addition of 50 mM $LaCl_3$ as was observed at pH 7 (Fig. VI.6B). Therefore, the enhancement of QQx stability by the added $LaCl_3$ is relatively pH independent, as was the case with KCl (Fig. VI.4). However, at pH 3, $LaCl_3$ led to a stabilization of KEx rather than the destabilization observed at pH 7. Because the Glu residues will be mostly protonated at this low pH, they would not bind La^{3+} ions as avidly as when negatively charged, and the stabilizing effect of the added $LaCl_3$ is therefore likely to be due to the same factors as for QQx. Since $LaCl_3$ addition leads to destabilization of KEx only when Glu residues are ionized, this destabilization is likely due to specific interactions of the La^{3+} ion and the ionized Glu side chains.

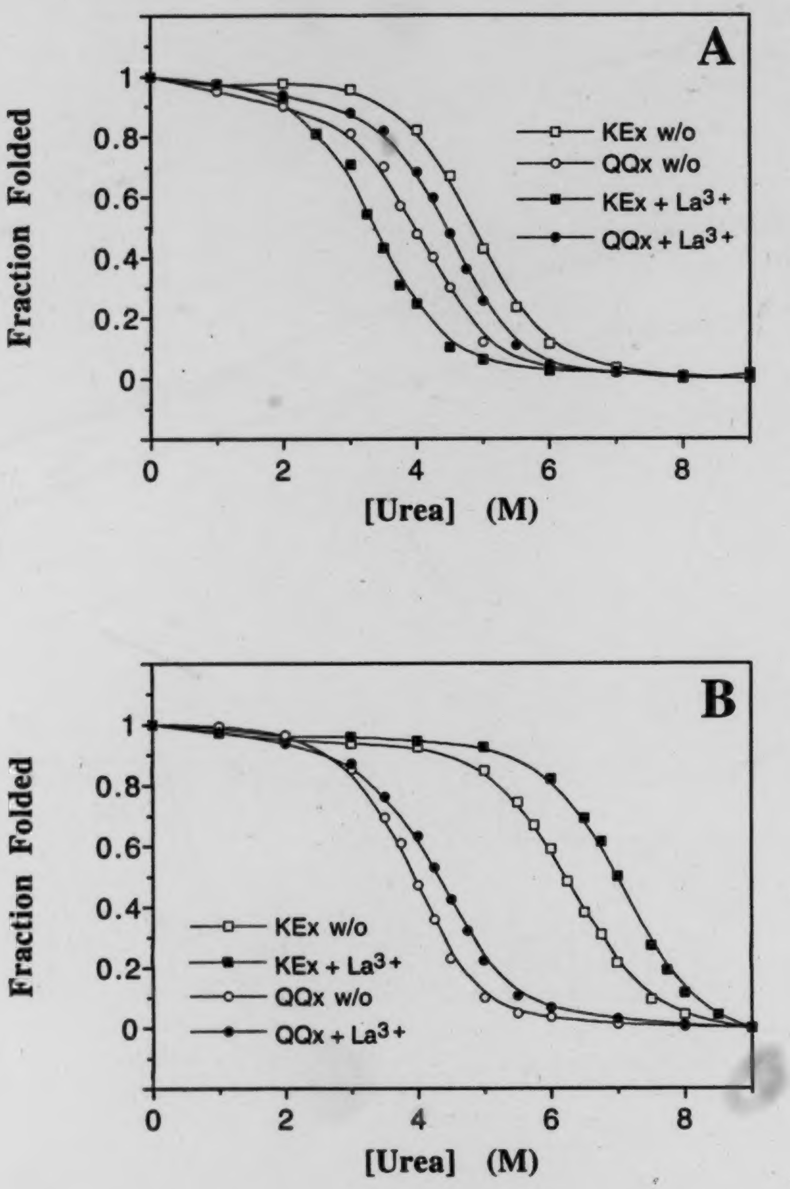

Figure VI.6 Urea denaturation profiles of QQx and KEx at 20 °C in the presence and absence of 50 mM $LaCl_3$ at pH 7 (A) and pH 3 (B). The buffers used were 50 mM tris, 100 mM KCl at pH 7 and 20 mM Glycine, 100 mM KCl at pH 3. Peptide concentration was in the range 56 µM to 79 µM. The fraction of folded peptide was calculated from the mean residue molar ellipticity at 222 nm, as described in Chapter II (pp. 56-59).

Table VI.2: Effects of 50 mM $LaCl_3$ on stability at pH 7 - urea denaturation

	w/o La^{3+}		50 mM La^{3+}			
Peptide [a]	$[urea]_{1/2}$ [b]	*m* [c]	$[urea]_{1/2}$ [b]	*m* [c]	$\Delta\Delta G_u^{obs}$ [d]	$\Delta\Delta G_u^{cor}$ [d]
QQx	3.95	0.96	4.45	1.08	+0.51	-----
KEx	4.9	0.96	3.3	1.08	-1.63	-2.14
KQEx	7.2	0.81	5.5	0.80	-1.36	-1.87
EQx	2.15	0.83	3.85	1.12	+1.66	+1.15

[a] Peptide sequences are shown in Figure VI.1.

[b] $[urea]_{1/2}$ is the transition midpoint , the concentration of urea (M) at which a 50 % decrease in ellipticity at 220 nm is observed.

[c] *m* is the slope of the equation $\Delta G_u = \Delta G_u^{H_2O} - m[urea]$ where $\Delta G_u^{H_2O}$ is the free energy of unfolding in the absence of denaturant estimated by linear extrapolation of a plot of ΔG_u versus [urea].

[d] $\Delta\Delta G_u$ represents the difference in the free energy of unfolding between two peptides or between two conditions for the same peptide. For example, using the equation from Serrano *et al.* (1990) (see Materials and Methods pp. 56-59):

$$\Delta\Delta G_u(KEx\text{-}QQx) = ([urea]_{1/2}KEx - [urea]_{1/2}QQx)(m_{KEx} + m_{QQx})/2$$
$$= (4.9 - 3.95)(0.96+0.96)/2$$
$$= +0.91 \text{ kcal/mol}$$

$\Delta\Delta G_u^{obs}$ is the difference in ΔG_u for the analog upon addition of 50 mM $LaCl_3$ to the buffers. A positive value of $\Delta\Delta G_u^{obs}$ indicates the stability is increased upon addition of $LaCl_3$. $\Delta\Delta G_u^{cor}$ is the difference in $\Delta\Delta G_u^{obs}$ between the given coiled-coil and QQx, which represents the change in stability of the analog upon $LaCl_3$ addition relative to the effect on QQx.

All measurements were done at 20 °C in 50 mM tris, 100mM KCl buffer.

The final peptide concentrations were in the range 56 µM to 76 µM.

In addition to interhelical ion pairs, coiled-coils, like α-helices in general, can contain intrahelical i to i+3 and i to i+4 ion pairs, as suggested by the X-ray structure of the GCN4 leucine zipper (O'Shea *et al.*, 1991). Intrahelical Glu-Lys ion pairs have been shown to contribute 0.4 to 0.5 kcal/mol to the stability of monomeric α-helical peptides (Lyu *et al.*, 1992; Scholtz *et al.*, 1993; Stellwagen *et al.*, 1992) and to affect the stability of coiled-coils (Zhou *et al.*, 1993c). The present study includes the peptide KQEx, in which there are no interhelical electrostatic interactions, but there are 10 E_b-K_e (i to i+3) and 8 K_e-E_b (i to i+4) potential intrachain ion pairs (Figs. VI.1 and VI.2). KQEx displays very high stability in the absence of $LaCl_3$ with a $[urea]_{1/2}$ value of 7.2 M, and its stability is decreased 1.36 kcal/mol by 50 mM $LaCl_3$, with a $\Delta\Delta G_u^{cor}$ of 1.87 kcal/mol (Table VI.2). Therefore, as observed for KEx, this coiled-coil appears to be destabilized by the binding of La^{3+} ions to the Glu residues, leading to potential disruption of intrachain ion pairs. The similar $\Delta\Delta G_u^{cor}$ values of KEx and KQEx correlate with the fact that the stabilization of coiled-coils by intrachain and interchain ion pairs are estimated to be similar (in the range 0.4 to 0.5 kcal/mol per ion pair (Zhou *et al.*, 1994b, 1993c).

The apparent effects on the stabilities of the coiled-coils resulting from the addition of 50 mM $LaCl_3$ were also determined by GdnHCl denaturation. The results show that the effect of $LaCl_3$ addition on the coiled-coils containing ion pairs compared to the control QQx (denoted by $\Delta\Delta G_u^{cor}$) were much smaller than those obtained by urea denaturation (compare Tables VI.2 and VI.3). This result would have been predicted on the basis of earlier studies (Chapters III, IV, and V, Kohn *et al.*, 1995a, 1995b, 1997b), which showed that the ionic nature of GdnHCl allows it to screen the effects of electrostatic interactions on coiled-coil stability (Monera *et al.*, 1993, 1994a, 1994b). The GdnHCl denaturation results support the idea that the destabilizing effects of $LaCl_3$ are due to the binding of La^{3+} ions, leading to a disruption of the electrostatic interactions in the coiled-coil; an effect which could be decreased by the presence of GdnHCl due to its charge

Table VI.3: Effects of 50 mM $LaCl_3$ on stability at pH 7 - GdnHCl denaturation

	w/o La^{3+}		50 mM La^{3+}			
Peptide [a]	$[GdnHCl]_{1/2}$ [b]	m [c]	$[GdnHCl]_{1/2}$ [b]	m [c]	$\Delta\Delta G_u^{obs}$ [d]	$\Delta\Delta G_u^{cor}$ [d]
QQx	2.35	1.93	2.25	1.65	-0.18	-----
KEx	2.69	1.83	2.05	2.00	-1.23	-1.05
KQEx	3.54	1.59	2.86	1.60	-1.08	-0.90
EQx	1.93	1.58	2.82	1.86	+1.53	+1.71

[a] Peptide sequences are shown in Figure VI.1.

[b] $[GdnHCl]_{1/2}$ is the transition midpoint , the concentration of GdnHCl (M) at which a 50 % decrease in ellipticity at 220 nm is observed.

[c] m is the slope of the equation $\Delta G_u = \Delta G_u^{H_2O} - m[GdnHCl]$ where $\Delta G_u^{H_2O}$ is the free energy of unfolding in the absence of denaturant estimated by linear extrapolation of a plot of ΔG_u versus [GdnHCl].

[d] $\Delta\Delta G_u$ represents the difference in the free energy of unfolding between two peptides or between two conditions for the same peptide. For example, using the equation from Serrano *et al.* (1990) (see Materials and Methods pp. 56-59) :

$$\Delta\Delta G_u(KEx\text{-}QQx) = ([GdnHCl]_{1/2}KEx - [GdnHCl]_{1/2}QQx)(m_{KEx} + m_{QQx})/2$$
$$= (2.69 - 2.35)(1.83+1.93)/2$$
$$= +0.64 \text{ kcal/mol}$$

$\Delta\Delta G_u^{obs}$ is the difference in ΔG_u for the peptide upon addition of 50 mM $LaCl_3$ to the buffers. A positive value of $\Delta\Delta G_u^{obs}$ indicates the stability is increased upon addition of $LaCl_3$. $\Delta\Delta G_u^{cor}$ is the difference in $\Delta\Delta G_u^{obs}$ between the given coiled-coil and QQx, which represents the change in stability of the analog upon $LaCl_3$ addition relative to the effect on QQx.

All measurements were done at 20 °C in 50 mM MOPS, 100mM KCl buffer.

The final peptide concentrations were in the range 52 µM to 72 µM.

screening nature. These data may also reflect a competition between the guanidinium ions and La^{3+} ions for binding sites on the coiled-coil.

Having investigated the destabilizing effects of $LaCl_3$ on coiled-coil stability, the effects of $LaCl_3$, $MgCl_2$, and KCl all present at equal ionic strength were compared. These studies were carried out to compare the effects of a singly, doubly or triply charged metal ion with the same anion present in each case. The effect of adding 0.2 M $LaCl_3$, 0.4 M $MgCl_2$ or 1.2 M KCl (all equivalent to an ionic strength increase of 1.2) to the buffer were compared. The addition of 1.2 M KCl to the normal buffer conditions of 50 mM tris, 100 mM KCl led to an increase in QQx stability ($\Delta\Delta G_u^{obs}$) of 1.95 kcal/mol and a stability increase of 0.52 kcal/mol for KEx (Table VI.4). The difference in the $\Delta\Delta G_u^{obs}$ values (again denoted $\Delta\Delta G_u^{cor}$) is an estimate of the effect of the added salt on the electrostatic interactions in KEx, assuming all other effects of the salt are the same for both coiled-coils. Upon addition of 1.2 M KCl, $\Delta\Delta G_u^{cor}$ is -1.38 kcal/mol, suggesting KCl destabilizes KEx relative to QQx by screening of the ion pairs. Addition of 0.4 M $MgCl_2$ resulted in a $\Delta\Delta G_u^{cor}$ of -1.34 kcal/mol, indicating that these salt conditions had about the same effect on the electrostatic interactions as 1.2 M KCl. Addition of 0.2 M $LaCl_3$ had a much more dramatic effect, destabilizing KEx by 3.03 kcal/mol and stabilizing QQx by 1.34 kcal/mol. The resulting $\Delta\Delta G_u^{cor}$ of -4.37 kcal/mol for these conditions indicates that the apparent effect of the $LaCl_3$ on ionic interactions in KEx is approximately three-fold higher than an equivalent ionic strength of $MgCl_2$ or KCl. Therefore, the destabilizing effects are not only related to the ionic strength of the solution, which determines general charge screening effects, but rather to the identity, and specifically the charge, of the metal ion. Thus, La^{3+} has a much more significant destabilizing effect, even at much smaller concentration compared to the amount of K^+ or Mg^{2+} added (the concentration of La^{3+} was one sixth the concentration of K^+).

Table VI.4: Effects of $LaCl_3$, KCl and $MgCl_2$ on coiled-coil stability at pH 7.

Additive [a]	Ionic strength [b]	$[urea]_{1/2}$		m		$\Delta\Delta G_u^{obs}$ [c]		$\Delta\Delta G_u^{cor}$ [d]
		QQx	KEx	QQx	KEx	QQx	KEx	
none	0	3.95	4.9	0.96	0.96	----	----	----
1.2 M KCl	1.2	5.9	5.5	1.04	0.93	+1.95	+0.52	-1.38
0.4 M $MgCl_2$	1.2	5.1	4.7	1.04	0.96	+1.15	-0.19	-1.34
0.2 M $LaCl_3$	1.2	5.3	1.9	1.03	1.06	+1.34	-3.03	-4.37

[a] Salt conditions in addition to the standard buffer of 50 mM tris, 100 mM KCl.

[b] Increase in ionic strength by the added salt.

[c] Apparent change in free energy of unfolding in kcal/mol for the coiled-coil caused by the added salt calculated as described under Materials and Methods (pp. 56-59).

[d] Difference in the $\Delta\Delta G_u^{obs}$ values for KEx and QQx.

The final peptide concentrations were in the range 57 µM to 82 µM.

C. Discussion

The increased stability of proteins with added salt (in the specific case of QQx in this study) may be due to several factors, which were outlined in Chapter I. Firstly, the increase in KCl concentration likely leads to an increase in the apparent hydrophobic effect (a Hofmeister effect leading to salting-out of the nonpolar core) due to changes in the solvent structure (Leberman & Soper, 1995). In particular, this effect is believed to stem from an increase in the surface tension at the water-protein interface and preferential hydration of the protein (i.e. exclusion of the salt from the protein-solvent interface) (Arakawa *et al.*, 1990a, 1990b; Baldwin, 1996; Lin & Timasheff, 1996). Long suggested as a stabilizing effect of salt on globular proteins, this phenomenon has previously been used to explain the apparent KCl-induced stabilization of model synthetic coiled-coils (Kohn *et al.*, 1995b, Chapter IV; Lau *et al.*, 1984b; Monera *et al.*, 1993) and the muscle coiled-coil tropomyosin (Mo *et al.*, 1990). Secondly, the screening of unfavorable electrostatic interactions between parallel helix macrodipoles, suggested by computational studies (Gilson & Honig, 1989) and by experimental results (Robinson & Sligar, 1993) to be destabilizing by 0.5-3 kcal/mol, would be expected to increase stability. A third potential effect of salt is anion binding to the Lys residues along the solvent exposed face at position **f** of the helices (Fig. VI.2), which has also been proposed previously as a stabilizing effect of salt on coiled-coils (Thompson-Kenar *et al.*, 1995; Yu *et al.*, 1996). Privalov and co-workers suggested that due to higher charge density in the folded form of the coiled-coil, anions preferentially bind to the folded form versus the unfolded form (Yu *et al.*, 1996). This phenomenon has been well documented in explaining the effects of cation binding on dsDNA stability (Manning, 1972, 1978; Privalov *et al.*, 1969).

The slight drop in stability of KEx between 0 and 250 mM KCl may be due to screening of the interchain ion pairs, which would be expected to destabilize the coiled-coil if the ion pairs were indeed important for stability. The recent study of Thompson-Kenar *et al.* (1995) showed that KCl destabilizes the GCN4 leucine zipper domain up to a KCl concentration of 0.5 M, after which further increase in KCl concentration stabilized the protein. However, even at 1 M KCl, the coiled-coil had not regained its initial stability observed at low ionic strength in the absence of KCl. The stability of a synthetic 30-residue heterodimeric coiled-coil containing 8 interhelical Lys-Glu ion pairs showed a dependence on NaCl concentration similar to GCN4 (O'Shea *et al.*, 1993). The initial destabilization observed for GCN4 was explained by general screening of the ion pairs by the increased ionic strength, while subsequent stabilization at higher salt concentrations was attributed to specific interactions between salt ions and charged side chains of the coiled-coil. One possible explanation for the contrasting stability dependence of our model coiled-coil, KEx, and the GCN4 leucine zipper on varying KCl concentration is that KEx has a more uniform hydrophobic core lacking any hydrophilic residues in the **a** and **d** heptad positions and may therefore be more susceptible to an increased hydrophobic effect by the added salt relative to GCN4. In addition, both the coiled-coils QQx and KEx may be influenced more than GCN4 by a salt binding effect because of the high charge density on the solvent exposed face due to Lys residues in the **f** positions of the helices. Therefore, in the model coiled-coils in this study, the stabilizing effects of added KCl outweigh the destabilizing effect of charge screening, particularly above 0.25 M KCl concentration.

The dramatic increase in the stability of KEx relative to QQx with increased KCl concentration at pH 3 is likely due to the binding of chloride ions to the Lys residues at position **e** of the heptad repeat in KEx (Yu *et al.*, 1996). At pH 7, the Lys residues participate in ion pairs with the Glu residues at position **g** in the other helix, and the interface region (residues **a**, **d**, **e**, and **g** of both helices) has zero net charge. At pH 3, where the Glu residues are protonated, the Lys residues at position **e** are unpaired and the net charge at the dimer interface is +10 (the overall net charge on the dimer is +20 due to 5 Lys at position **e** and 5 Lys at position **f** of each chain). The unpaired Lys residues at position **e** are likely destabilizing due to non-specific electrostatic repulsion between the helices, which is screened by KCl, and/or lack of interaction between the hydrophobic portion of the Lys side chain and the coiled-coil hydrophobic core resulting from increased side chain solvation (see below).

Only at pH 3, where there is a high net positive charge, would singly charged chloride anions be expected to be strongly attracted to the interface region of the coiled-coil. Thompson-Kenar *et al.* (1995) attributed the observed increase in GCN4 leucine zipper stability at higher salt concentrations to ion binding, the extent to which appeared to depend on the anion added (KF was much more stabilizing than KCl). However, the results of this study suggest that at neutral pH, where all the measurements of Thompson-Kenar and associates were taken, the anion binding effect to Lys residues involved in interhelical ion pairs is small compared to that at low pH. In addition, urea denaturation of KEx at pH 3 in 20 mM Glycine buffer containing 100 mM KCl or 100 mM NaF yielded $[\text{urea}]_{1/2}$ values of 6.25 and 6.6 M, respectively. Therefore, unlike in the previous study of the GCN4 leucine zipper (Thompson-Kenar *et al.*, 1995), no large difference in the effect of chloride and fluoride ions is observed.

It has commonly been observed that coiled-coils are more stable at low pH than at neutral pH, despite the loss of ion pairs resulting from protonation of acidic residues at low pH (Lowey, 1965; Noelken & Holtzer, 1964; O'Shea *et al.*, 1992; Zhou *et al.*, 1992c; Zhu *et al.*, 1993). Zhou *et al.* (1994b) attributed this phenomenon to the finding that a protonated Glu at position **e** was intrinsicly more stabilizing to a coiled-coil by 0.65 kcal/mol over an ionized Glu, which could outweigh the loss of an interhelical Lys-Glu ion pair for each Glu residue protonated (estimated at 0.4 kcal/mol in the same study), ultimately leading to an average net stabilization of 0.25 kcal/mol for each Glu residue protonated. The intrinsicly higher stabilization of the coiled-coil by protonated Glu is likely due to both its higher helical propensity (Chakrabartty *et al.*, 1994; Scholtz *et al.*, 1993; Stellwagen *et al.*, 1992) and more hydrophobic character (Guo *et al.*, 1986; Sereda *et al.*, 1994), which allows it to pack better at the dimer interface (Chapters III and IV, Kohn *et al.*, 1995a, 1995b). The effect of protonating Glu residues at the **g** position on the hydrophobicity of the coiled-coil interface and resulting change in stability was illustrated recently with reversed-phase HPLC (Hodges *et al.*, 1994). Yu *et al.* (1996) found that their model coiled-coil was more stable at pH 3 than at pH 6.5 in a 10 mM phosphate buffer in the presence of 150 mM NaCl but was less stable at pH 3 in the absence of NaCl. It was concluded that the increased stability occurring at low pH *versus* neutral pH was dependent on the presence of salt and that the anion-binding effect in the presence of salt would lead to the higher observed stability. This agrees with the fact that in all previous studies in which increased coiled-coil stability was observed at low pH, significant NaCl or KCl concentrations were present (typically 0.1 to 0.5 M). However, KEx is slightly more stable at pH 3 than pH 7 even in the absence of any KCl (Table VI.1, Fig. VI.4). The difference between these results and those of Yu *et al.* (1996) is likely due to the use of a higher buffer concentration of 50 mM phosphate in this study, indicating that the phosphate ions are also likely able to bind to the Lys residues and stabilize the protein.

Protonation of Glu residues in the absence of Lys residues at the dimer interface results in a large increase in stability, as is apparent from the large increase in stability of the coiled-coil EQx upon lowering of the pH from 7 to 3 (Table VI.1). Furthermore, this effect was relatively independent of the KCl concentration: the difference in $[\text{urea}]_{1/2}$ for EQx between pH 7 and 3 (denoted $\Delta[\text{urea}]_{1/2}(\text{pH7-pH3})$) was fairly consistent (5.5 to 5.9 M) over a KCl range of 0 to 1 M (Figure VI.5B). However, for KEx, where the Glu residues may form interhelical g-e' ion pairs with Lys near neutral pH, protonation of Glu residues by reducing the pH to 3 only changes the $[\text{urea}]_{1/2}$ by 0.1 M in the absence of KCl, and this value is significantly increased to 3.2 M at 1 M KCl (Figure VI.5B). A possible explanation for the differing behavior of KEx and EQx is that protonation of the Glu residues in KEx leaves Lys residues in the dimer interface, which no longer participate in ion pairs, thus destabilizing the coiled-coil. This destabilization offsets the stabilization resulting from Glu protonation. As salt is added, the Lys residues may be neutralized by anion binding, thus reducing the destabilization caused by having unpaired Lys residues at the interface. As a result, the stabilizing effect of Glu protonation becomes more apparent. Therefore, it is clear that both the intrinsic effects of Glu protonation and anion binding to the positively charged Lys residues significantly influence the stability of coiled-coils containing interhelical Lys-Glu ion pairs when the pH is reduced.

While the results (Table VI.4) clearly indicate that of the three salts KCl, $MgCl_2$ and $LaCl_3$, $LaCl_3$ has by far the greatest effect on the stability of KEx relative to the control QQx, the mechanism accounting for this greater destabilization is uncertain from these experiments. It appears that the major component of this destabilization is not simply general (Debye-Hückel) screening, which should only be dependent on the ionic strength. It therefore is most likely a result of specific metal ion binding. Part of the reason $LaCl_3$ destabilizes KEx at pH 7 may be because the dimer interface region is neutral in this coiled-coil, with 10 Lys and 10 Glu residues, and binding of La^{3+} ions would upset this charge balance by introducing a net positive charge. The hypothesis that binding of La^{3+} ions to ionized Glu residues would disrupt interhelical or intrahelical ion pairs, leading to a loss of stability of the folded state, appears to be supported by the experimental results, but we cannot from the present data rule out the possibility that La^{3+} preferentially binds to the unfolded state and stabilizes it with respect to the folded state. However, it was observed that $LaCl_3$ increases the stability of EQx, in which the **e** and **g** positions contain Glu and Gln, respectively (Tables VI.2 and VI.3). This result suggests that the effect of La^{3+} binding to KEx is not simply to drive the equilibrium toward the unfolded form; if it were, one would expect the same to occur with EQx. It is more likely that La^{3+} preferentially binds to the folded form of both EQx and KEx in which the negative charge density is higher (Manning, 1972, 1978; Privalov *et al.*, 1969; Yu *et al.*, 1996).

Assuming that the effect of La^{3+} binding is on the folded form of the coiled-coil, we propose the following model for the destabilization of KEx by La^{3+}, as shown in Figure VI.7: normally i to i'+5 (g-e') ion pairs between oppositely charged Lys and Glu residues across the dimer interface assist the side chains in packing against the Leu

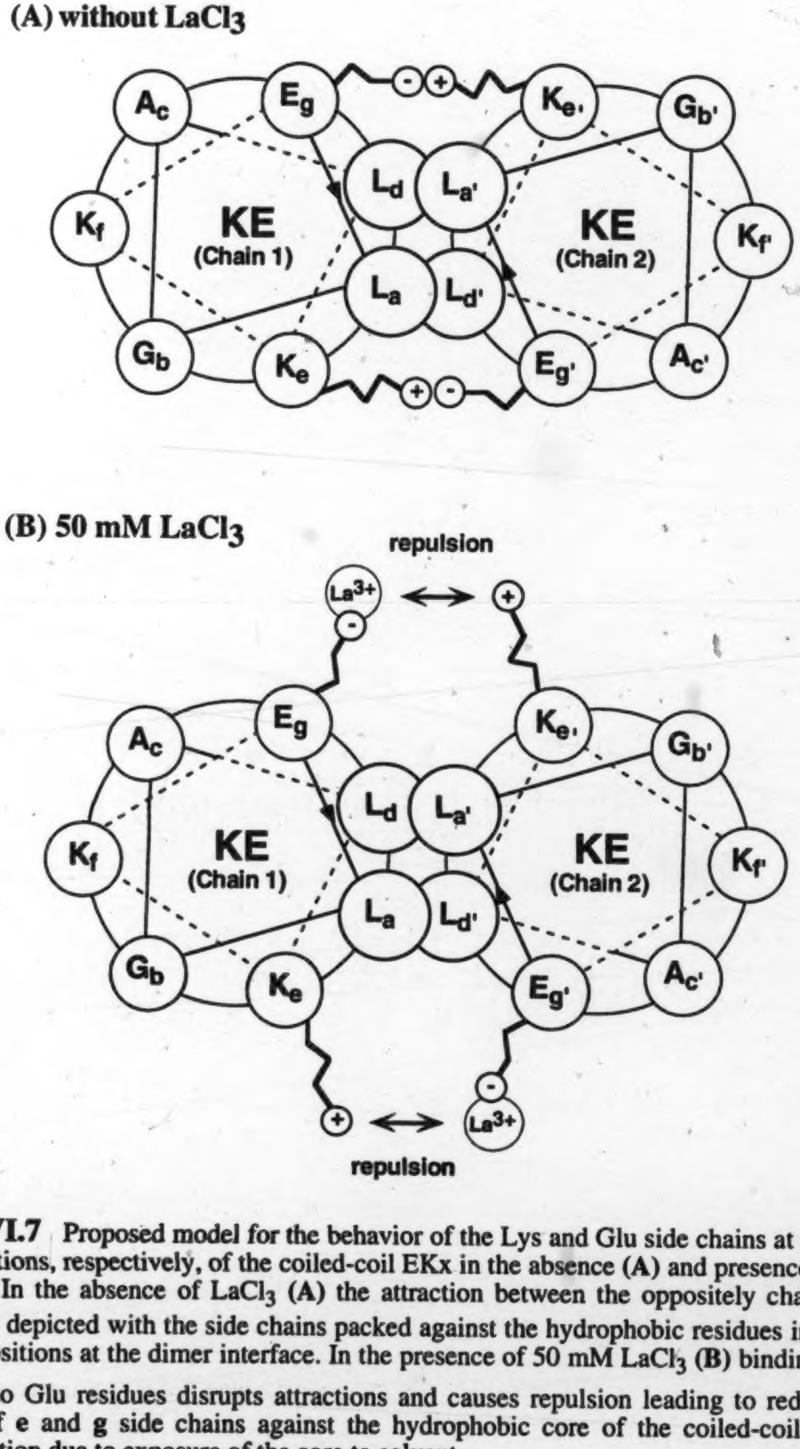
(A) without $LaCl_3$
A_c
E_g
$K_{e'}$
$G_{b'}$
L_d
$L_{a'}$
K_f
KE
(Chain 1)
KE
(Chain 2)
$K_{f'}$
L_a
$L_{d'}$
G_b
K_e
$E_{g'}$
$A_{c'}$
(B) 50 mM $LaCl_3$
repulsion
La^{3+}
A_c
E_g
$K_{e'}$
$G_{b'}$
L_d
$L_{a'}$
K_f
KE
(Chain 1)
KE
(Chain 2)
$K_{f'}$
L_a
$L_{d'}$
G_b
K_e
$E_{g'}$
$A_{c'}$
La^{3+}
repulsion

Figure VI.7 Proposed model for the behavior of the Lys and Glu side chains at the **e** and **g** positions, respectively, of the coiled-coil EKx in the absence **(A)** and presence **(B)** of $LaCl_3$. In the absence of $LaCl_3$ **(A)** the attraction between the oppositely charged residues is depicted with the side chains packed against the hydrophobic residues in the **a** and **d** positions at the dimer interface. In the presence of 50 mM $LaCl_3$ **(B)** binding of La^{3+} ion to Glu residues disrupts attractions and causes repulsion leading to reduced packing of **e** and **g** side chains against the hydrophobic core of the coiled-coil and destabilization due to exposure of the core to solvent.

hydrophobes at the **a** and **d** positions in the dimer core. Addition of a highly charged metal ion like La^{3+} can lead to ion pairing with the Glu side-chain carboxylate group. This reduces the Glu-Lys interaction and replaces it with a repulsion between Lys^+ and the Glu^- •La^{3+} complex (net charge +2). Such interchain repulsions have been shown to have effects on coiled-coil stability similar in magnitude to interchain ion pairs (Krylov *et al.*, 1994; Kohn *et al.*, 1995a, 1995b, Chapters III and IV). The loss of the Lys-Glu attraction should lead to a reduction in packing of the charged side chains across the hydrophobic interface because their charges are no longer complemented by an opposite charge, increasing the desolvation energy required for removal of the charged side chain from bulk solvent into the partially hydrophobic microenvironment of the coiled-coil interface. The proposed repulsion would likely cause the side chains to move further apart and thus further expose the hydrophobic core. This effect does not seem to occur to a large extent with addition of K^+ and Mg^{2+} ions, probably because the attraction of the metal ion for the Glu side chain carboxylate must be high to be able to compete with the Lys side chain. Being covalently attached to the peptide, the effective concentration of the Lys side chains is much higher than that of the metal ions diffusing freely in solution. The K_a for binding of a K^+ or Mg^{2+} ion to a single Glu might be too low to allow interaction with a Glu side chain, which is participating in an ion pair. However, due to its higher charge, La^{3+} should have a much higher binding affinity for the Glu carboxylate, allowing it to compete more effectively with the Lys residue for interactions with the Glu side chain. The unpaired Lys residues at position **e** resulting from binding of La^{3+} to Glu residues might be expected to bind chloride ions to some extent (as discussed above for the pH 3 results), but the magnitude of the chloride binding effect cannot be easily determined in this case.

In general, it has been concluded that surface-exposed pairs of oppositely-charged residues are conformationally flexible and do not come together to form structurally fixed salt bridges. Instead, the residues remain mobile and interact only weakly, therefore contributing little to protein stability (Dao-pin *et al.*, 1991). The entropic cost of fixing a pair of solvent-exposed oppositely-charged residues would be expected largely to offset the energy of interaction between them in a defined salt bridge. However, in the case of coiled-coils, the interhelical ion pairs are important likely because they assist the residues at positions **e** and **g** in folding across the dimer interface and making interactions with the hydrophobic core side chains through the methylene groups of their side chains (O'Shea *et al.*, 1991; Talbot & Hodges, 1982). The resulting increased burial of hydrophobic surface area (which should increase solvent entropy) and enhanced van der Waals interactions would offset the loss of side-chain conformational energy resulting from ion pair formation. Thus, in coiled-coils there appears to be a synergy of electrostatic attraction between Lys and Glu side chains with hydrophobic packing of those side chains in the **e** and **g** positions across the **a** and **d** residues of the hydrophobic core (Hendsch & Tidor, 1994). The apparent effect of interhelical attractions or repulsions is therefore closely linked to their effect on side chain packing at the positions involved in the interaction and those they pack against rather than simply to an electrostatic effect. Thus, the observation of a relatively unchanged pK_a value for a Glu side chain participating in a **g-e'** ion pair does not, in this context, mean that the ion pair is irrelevant to coiled-coil stability. The inability of KCl to reduce significantly the apparent stabilization due to ion pairs may be because the synergy of the electrostatic interaction with the packing across the hydrophobic core is able to resist partially the effects of general charge screening (the hydrophobic interaction between the **e** and **g** side chains and the dimer interface core might actually be increased by the high KCl concentration). However, the addition of a more highly charged La^{3+} ion significantly perturbs coiled-coil stability because it can bind directly to the Glu residues and disrupt the fine balance of electrostatics within the protein.

The results of this study illustrate the complexity of effects that salt concentration can have in either stabilization or destabilization of proteins. In addition to the ionic strength effect of general charge screening, specific counterion binding to charged residues on the protein as well as effects of the salt on the solvent structure/properties can all work individually or in combination to perturb protein stability (Goto *et al.*, 1990). In particular, although it is clear that coiled-coil formation is mainly a result of the interactions in the hydrophobic core, there are both general and specific electrostatic interactions in these molecules, which can affect the stability in either direction, and these are sensitive to the buffer conditions. In conclusion, these model protein studies underline the importance of environment in determining protein stability as well as the potential modulation of folding and stability of both *de novo* designed and native proteins by changes in buffer and pH conditions.

CHAPTER VII

ORIENTATION, POSITIONAL, ADDITIVITY, AND OLIGOMERIZATION-STATE EFFECTS OF INTERHELICAL ION PAIRS IN α-HELICAL COILED-COILS[5]

A. Introduction

In Chapter VI (Kohn *et al.*, 1997c), the goal was to determine some insights into the importance of interhelical ion pairs to coiled-coil stability from the observed effects of various salt ions on stability. The results appeared to be consistent with the idea that the electrostatic ion-pairing interaction itself is synergistic with the packing of side chains at the interface, as was suggested by Hendsch and Tidor (1994). If this is indeed the case, it might be expected that the packing of the **e** and **g** side chains at the coiled-coil interface, promoted by the ion pair, would occur preferentially in one orientation versus the other (Lys-Glu versus Glu-Lys). In the knobs into holes packing scheme, the residues at positions **e** and **g** pack against the hydrophobes at positions **a** and **d** of the opposing helix (see Fig. I.3B, p. 23), and it could be expected that the charged residues at positions **e** and **g** may therefore pack better in one of the possible orientations .

In this study, the effect of orientation on Lys-Glu interhelical ion pairs was probed with double mutant cycle analyses (Serrano *et al.*, 1990) in order to gain further understanding of the mechanism of stabilization and destabilization of coiled-coils by **g-e'** ionic interactions. A greater ion pair coupling energy in one orientation over the other was observed only in the presence of an interhelical disulfide bridge, possibly suggesting that the nondisulfide-bridged coiled-coil exists in a dynamic state. Additionally, information regarding the dependence of ion-pair coupling energy on position along the coiled-coil was obtained by the comparison of coiled-coils containing ion pairs only in the middle heptad to coiled-coils containing ion pairs in all five heptads of a 35-residue sequence. In the same way, an indication of the degree of additivity involved in ion-pair stabilization of the coiled-coil was obtained. This study also demonstrates the effect of **g-e'** ion pairs (and the **g** and **e** positions in general) on coiled-coil oligomerization states.

---

[5] A version of this chapter has been submitted for publication: Kohn, W. D., Kay, C. M., and Hodges, R. S. (1998). *J. Mol. Biol.*

B. Results

a) Peptide design and nomenclature

Figure VII.1 shows the amino acid sequences of the synthetic peptides that were used in this study. All the analogs are once again based on a native sequence, designated 'N', which provides a stable reference coiled-coil containing no interhelical electrostatic interactions to which the mutant peptides could be compared (as described in Chapter II, p. 60).

Substitutions of Glu and/or Lys for Gln at the **e** and **g** positions were made as shown in Figure VII.1. For the first six analogs listed, substitutions were made only in the middle heptad (positions 15 and 20). Each of these analogs is named for the type and position(s) of substitution(s). For example, E15K20 contains a Glu substitution at position 15 and a Lys substitution at position 20. The last six analogs contain the same substitutions in all five heptad repeats (Fig. VII.1). The nomenclature used for these peptides is based on the amino acid residues present at the **e** and **g** positions. For example, peptide KE(VL) contains Lys at position **e** and Glu at position **g** of each heptad. The '(VL)' signifies the presence of Val and Leu at the hydrophobic positions and distinguishes these peptides from similar peptides that were studied in Chapter VI (Kohn *et al.*, 1997c) and previously (Zhou *et al.*, 1994b, 1994c). All the peptides contain a single Cys residue at position 2, allowing formation of two-stranded disulfide-bridged (2-2') peptides. Therefore, each peptide is further designated with 'x' if it is present in the disulfide-bridged (oxidized) form or 'r' if present in the reduced noncovalently-linked form.

Peptide Name	Amino Acid Sequence
	1 5 10 15 20 25 30 35
	g a b c d e f g a b c d e f g a b c d e f g a b c d e f g a b c d e f
native	Ac-**Q**-C-G-A-L-**Q**-K-**Q**-V-G-A-L-**Q**-K-**Q**-V-G-A-L-**Q**-K-**Q**-V-G-A-L-**Q**-K-**Q**-V-G-A-L-**Q**-K-amide
E15	Ac----------------------------**E**-V-G-A-L-**Q**-K-----------------------------amide
E20	Ac----------------------------**Q**-V-G-A-L-**E**-K-----------------------------amide
K15	Ac----------------------------**K**-V-G-A-L-**Q**-K-----------------------------amide
K20	Ac----------------------------**Q**-V-G-A-L-**K**-K-----------------------------amide
E15K20	Ac----------------------------**E**-V-G-A-L-**K**-K-----------------------------amide
K15E20	Ac----------------------------**K**-V-G-A-L-**E**-K-----------------------------amide
EQ(VL)	Ac-**Q**-C-G-A-L-**E**-K-**Q**-V-G-A-L-**E**-K-**Q**-V-G-A-L-**E**-K-**Q**-V-G-A-L-**E**-K-**Q**-V-G-A-L-**E**-K-amide
QE(VL)	Ac-**E**-C-G-A-L-**Q**-K-**E**-V-G-A-L-**Q**-K-**E**-V-G-A-L-**Q**-K-**E**-V-G-A-L-**Q**-K-**E**-V-G-A-L-**Q**-K-amide
KQ(VL)	Ac-**Q**-C-G-A-L-**K**-K-**Q**-V-G-A-L-**K**-K-**Q**-V-G-A-L-**K**-K-**Q**-V-G-A-L-**K**-K-**Q**-V-G-A-L-**K**-K-amide
QK(VL)	Ac-**K**-C-G-A-L-**Q**-K-**K**-V-G-A-L-**Q**-K-**K**-V-G-A-L-**Q**-K-**K**-V-G-A-L-**Q**-K-**K**-V-G-A-L-**Q**-K-amide
EK(VL)	Ac-**K**-C-G-A-L-**E**-K-**K**-V-G-A-L-**E**-K-**K**-V-G-A-L-**E**-K-**K**-V-G-A-L-**E**-K-**K**-V-G-A-L-**E**-K-amide
KE(VL)	Ac-**E**-C-G-A-L-**K**-K-**E**-V-G-A-L-**K**-K-**E**-V-G-A-L-**K**-K-**E**-V-G-A-L-**K**-K-**E**-V-G-A-L-**K**-K-amide

Figure VII.1 Sequences of the peptides studied for determination of double mutant analyses on interhelical **g-e'** Lys-Glu ion pairs. These peptides are described in the text under Peptide design and nomenclature.

b) Structural characterization

The native peptide has been shown to form a stable two-stranded coiled-coil in both the oxidized and reduced forms based on circular dichroism spectroscopy, size-exclusion chromatography and sedimentation-equilibrium ultracentrifugation (Chapters III and IV, Kohn *et al.*, 1995a, 1995b). The disulfide-bridged analogs presented in the current study were also found to form two-stranded monomers at low peptide concentration, as judged by size-exclusion chromatography and sedimentation-equilibrium ultracentrifugation (data not shown). At higher concentration (above 1 mg/ml) some aggregation was observed for some of the analogs, but all stability measurements were performed below the aggregation threshold (at about 0.5 mg/ml or less). No significant difference in the denaturation results were observed over the peptide concentration range 0.05 to 0.5 mg/ml (data not shown). The reduced analogs showed a variety of behavior in their oligomerization state as illustrated below (see page 196).

c) Stability studies

i) Substitution of Lys or Glu at position **e** *or* **g** *- pH 7*

The effects on stability of a substitution at heptad position **e** or **g** of a coiled-coil have been investigated previously (Hu *et al.*, 1993; Kohn *et al.*, 1995b, 1997b, Chapters IV and V; Krylov *et al.*, 1994; Schmidt-Dörr *et al.*, 1991; Zeng *et al.*, 1997; Zhou *et al.*, 1994b). In this paper, the focus is on comparing the effect on stability of a substitution at position **e** *versus* that at position **g**.

The results of urea denaturation studies of disulfide-bridged coiled-coils at pH 7 are summarized in Table VII.1. In peptide EQ(VL)x all five Gln residues at position **e** have been substituted with Glu (Fig. VII.1). A stability decrease of 0.97 kcal/mol was observed relative to the control Nx (Table VII.1). In QE(VL)x, the five Glu substitutions are at position **g** instead, and a destabilization relative to Nx of 1.57 kcal/mol was observed. Therefore, the results suggest that charged residues are more destabilizing at position **g**.

Table VII.1: Urea denaturation results at pH 7 - Lys or Glu substitution [a]

Peptide [b]	Heptad Position	$[\text{urea}]_{1/2}$ [c]	m [d]	$\Delta\Delta G_u^{obs}$ [e]	$\Delta\Delta G_u^{res}$ [f]
Nx	-	6.0	0.87	--	--
E15x	g	5.55	0.86	-0.39	-0.20
QE(VL)x	g	4.1	0.78	-1.57	-0.16
E20x	e	5.8	1.0	-0.19	-0.10
EQ(VL)x	e	4.8	0.74	-0.97	-0.10
K15x	g	4.95	0.98	-0.97	-0.48
QK(VL)x	g	2.1	1.19	-4.02	-0.40
K20x	e	5.5	0.94	-0.45	-0.22
KQ(VL)x	e	3.6	1.16	-2.44	-0.24

[a] Data were collected at 20°C in a 50 mM tris, 100 mM KCl buffer, pH 7.0.

[b] The sequences are given in Figure VII.1, and nomenclature is described under Peptide design and nomenclature.

[c] $[\text{urea}]_{1/2}$ is the concentration of urea at which the peptide is 50% unfolded, as determined by the decrease in molar ellipticity at 222 nm with increasing denaturant concentration.

[d] m is the slope of the assumed linear relationship between ΔG_u and denaturant concentration.

[e] $\Delta\Delta G_u^{obs}$ is the observed change in free energy of unfolding in kcal/mol upon the specified substitution(s) and is calculated by multiplication of the change in $[\text{urea}]_{1/2}$ by the average of the m terms (see Materials and Methods, pp. 56-59). A negative value indicates that the analog is less stable than the native coiled-coil, Nx.

[f] $\Delta\Delta G_u^{res}$ is the change in free energy of unfolding in kcal/mol per substitution.

The analogs KQ(VL)x and QK(VL)x were 2.44 kcal/mol and 4.02 kcal/mol less stable than Nx, respectively. Once again substitution of the neutral Gln side chain with a charged residue has a much larger effect at position **g** than position **e**. For both Glu and Lys, the destabilization observed at position **g** is about 1.6-fold more than that at position **e**.

For peptides with a single Lys or Glu substitution for Gln per chain, the results are similar (Table VII.1). E15x, in which there is a single substitution of Glu for Gln at position **g** of the middle heptad (Fig. VII.1), is destabilized by 0.39 kcal/mol while E20x, which contains a single Glu substitution at position **e**, is destabilized by 0.19 kcal/mol. Similarly, K15x is destabilized by 0.97 kcal/mol, and K20x is destabilized by 0.45 kcal/mol. In both cases, the destabilization is about two-fold higher at position **g** than position **e**, similar to the value of 1.6-fold observed with charged residue substitutions at all five heptads. The results clearly show that a charged residue (Lys or Glu at pH 7) substituted for Gln is significantly more destabilizing at position **g** than at position **e**.

The amount of intrinsic destabilization per Glu or Lys substitution, denoted $\Delta\Delta G_u^{res}$, is listed in Table VII.1 for the peptides studied. The data shows that the estimation of this value is almost the same whether calculated from a peptide containing substitutions in all five heptads or only in the middle heptad. However, the estimate from the middle heptad is slightly larger than that averaged over all five heptads, particularly at position **g**. Roughly, Lys is destabilizing relative to Gln by 0.2 kcal/mol at position **e** and 0.4 kcal/mol at position **g** while Glu is destabilizing relative to Gln by 0.1 kcal/mol at position **e** and 0.2 kcal/mol at position **g**. Therefore, the destabilization is about two-fold higher for Lys *versus* Glu (when at the same heptad position) and also about two-fold higher at position **g** *versus* position **e** (for the same amino acid substitution). A Lys substitution at position **g** is therefore about four-fold more destabilizing than a Glu substitution at position **e**.

ii) Substitution of Lys or Glu at position ***e*** *or* ***g*** *- pH 3.2*

The results of urea denaturation studies at pH 3.2 are summarized in Table VII.2. The peptides with Gln to Lys substitutions show very similar stability losses to what was observed at pH 7 (the effect of a single Lys substitution is approximately 0.20 to 0.25 kcal/mol at position **e** and 0.40 to 0.45 kcal/mol at position **g**). This is the expected result since the Lys side chain has a pK_a of about 10.5 (in the unfolded peptide) and would be expected to be fully protonated (charged) over the pH range 3 to 7. It was previously observed that the effect on stability of a Gln to Lys substitution at position **g** of a coiled-coil was approximately the same over the pH range 3 to 7 (Zhou *et al.*, 1994b).

In contrast to what occurred with Lys, the substitution of Glu for Gln had a very different effect on stability at pH 3.2 than at pH 7. While it was destabilizing at pH 7 (Table VII.1), Glu substitution was significantly stabilizing at pH 3.2 (Tables VII.2 and VII.3). With a pK_a of about 4 to 4.5 in an unfolded peptide, the Glu side chain carboxylate is generally expected to be mostly ionized at pH 7 and mostly protonated (neutralized) at pH 3.2. Thus, substitution of Glu at position **e** or **g** of the coiled-coil is stabilizing at low pH where the Glu is mostly in the protonated form, as observed in Chapters III-V of this thesis (Kohn *et al.*, 1995a, 1995b, 1997b) and previously (Lumb & Kim, 1995b; Zhou *et al.*, 1994b). The peptides EQ(VL)x and QE(VL)x are too stable to allow significant denaturation at 20°C by urea (Table VII.2). These peptides could be denatured with GdnHCl, which is a stronger denaturant (Table VII.3). GdnHCl appears to give an accurate measure of the stability change resulting from a Gln to protonated Glu substitution since the observed $\Delta\Delta G_u$ values for E15x and E20x obtained from urea denaturation (Table VII.2) and GdnHCl denaturation (Table VII.3) are very similar. Interestingly, the amount of stabilization per protonated Glu substitution is not quite as dependent on whether the residue is at position **e** or **g** of the heptad repeat, as was observed for the destabilizing effects of Lys and ionized Glu at pH 7 (Table VII.1). Lys and ionized Glu were both found to be 1.6- to 2-fold more destabilizing at position **g** than position **e**, while the pH 3.2 data

Table VII.2: Urea denaturation results at pH 3.2 - Lys or Glu substitution [a]

Peptide [b]	Heptad Position	$[\text{urea}]_{1/2}$	*m*	$\Delta\Delta G_u^{obs}$	$\Delta\Delta G_u^{res}$
Nx	-	5.7	0.86	--	--
E15x	g	7.25	0.79	+1.28	+0.64
QE(VL)x	g	>10	-	-	-
E20x	e	6.8	0.87	+0.96	+0.48
EQ(VL)x	e	>10	-	-	-
K15x	g	4.7	0.94	-0.90	-0.45
QK(VL)x	g	1.8	1.24	-4.10	-0.41
K20x	e	5.1	0.89	-0.53	-0.26
KQ(VL)x	e	3.3	1.15	-2.41	-0.24

[a] Data were collected at 20°C in a 20 mM Glycine, 100 mM KCl buffer.

[b] The sequences are given in Figure VII.1, and nomenclature is described under Peptide design and nomenclature.

Symbols were described in Table VII.1 and under Materials and Methods (pp. 56-59).

Table VII.3: GdnHCl denaturation results at pH 3.2 [a]

Peptide [b]	Heptad Position	$[\mathrm{GdnHCl}]_{1/2}$	*m*	$\Delta\Delta G_u^{obs}$	$\Delta\Delta G_u^{res}$
Nx	-	3.1	1.8	--	--
E15x	g	3.8	1.91	+1.29	+0.64
QE(VL)x	g	5.6	1.98	+4.83	+0.48
E20x	e	3.6	1.92	+0.92	+0.46
EQ(VL)x	e	5.3	1.99	+4.16	+0.42

[a] Data were collected at 20°C in a 20 mM Glycine, 100 mM KCl buffer.

[b] The sequences are given in Figure VII.1, and nomenclature is described under Peptide design and nomenclature.

Symbols were described in Table VII.1 and under Materials and Methods (pp. 56-59).

indicate that a protonated Glu is only about 1.1- to 1.4-fold more stabilizing at position **g** than at position **e**. In all cases, position **g** has a greater effect on stability than position **e** (an ionized Glu is more destabilizing at position **g** and a protonated Glu is more stabilizing at position **g**). Unlike at pH 7, the average stabilizing effect per protonated Glu substitution obtained from the middle heptad only is greater than that obtained from averaging over all five heptads. This is particularly true at position **g** where the $\Delta\Delta G_u^{res}$ values at pH 3.2 are +0.64 kcal/mol and +0.48 kcal/mol for E15x and QE(VL)x, respectively (Table VII.3), *versus* -0.20 kcal/mol and -0.16 kcal/mol, respectively, at pH 7 (Table VII.1). Previously, it was found that protonated Glu substitutions at the middle of the coiled-coil are more stabilizing than those near the ends of the coiled-coil (Chapter V, Kohn *et al.*, 1997b), which would reduce the average $\Delta\Delta G_u^{res}$ value in QE(VL)x *versus* that in E15x.

*iii) Substitution of Lys and Glu at positions **e** and **g** - interhelical ionic attractions at pH 7*

The major goal of this study was to measure the **g-e'** ion-pair interactions between Lys and Glu residues in both orientations (with Lys at position **g** and Glu at position **e**, or *vice versa*). The urea denaturation profiles of peptides EK(VL)x and KE(VL)x in comparison to the control Nx in benign buffer at pH 7 (Fig. VII.2A) indicate that relative to Nx, in which no ion pairs are present, the Lys-Glu ion pair is slightly stabilizing in one orientation [peptide EK(VL)x] and more destabilizing in the other orientation [peptide KE(VL)x]. The results of GdnHCl denaturation at pH 7 (Fig. VII.2B) are very different than those with urea since all three peptides appear to have identical stabilities in this case. The ability of GdnHCl to 'screen' the apparent effects of ionic interactions on coiled-coil stability have been extensively demonstrated in this thesis and previously (Monera *et al.*, 1993, 1994a, 1994b). The fact that EK(VL)x and KE(VL)x have different apparent stabilities by urea denaturation but the same stability by GdnHCl denaturation therefore suggests that the stability difference observed with urea denaturation is at least partly due to ionic effects.

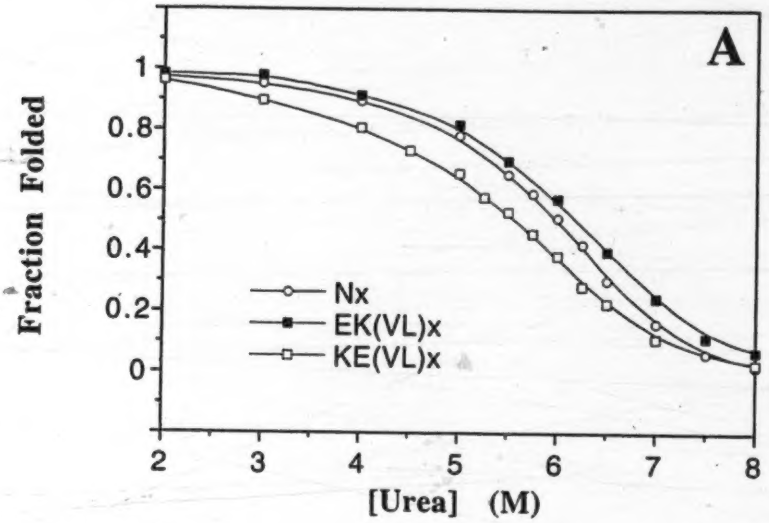

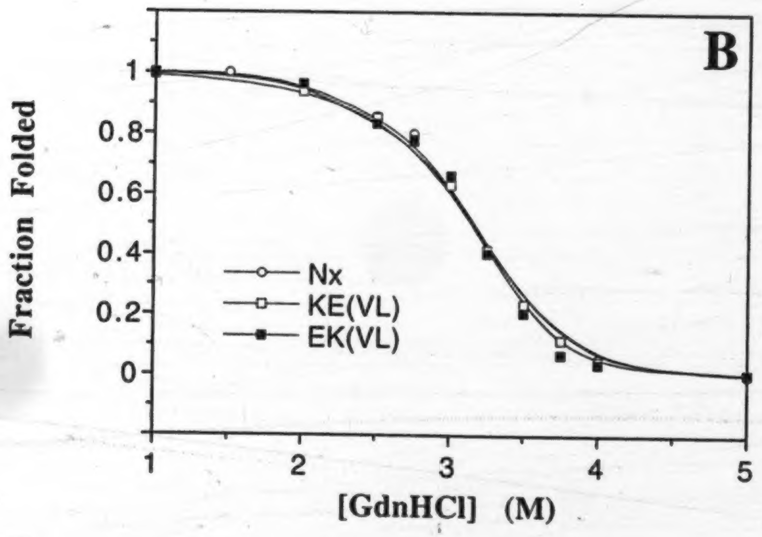

Figure VII.2 Chemical denaturation profiles at 20°C in 100 mM KCl, 50 mM tris, pH 7 buffer for Nx, EK(VL)x and KE(VL)x with: **(A)** urea and **(B)** GdnHCl as denaturant. The fraction of folded peptide was calculated from the mean residue molar ellipticity at 222 nm, as described under Materials and Methods (Chapter II, pp. 56-59). Peptide concentration was in the range 60 μM to 80 μM.

The stability difference between EK(VL)x and KE(VL)x by urea denaturation is 0.5 kcal/mol (Table VII.4), suggesting simplistically that each ion pair is 0.05 kcal/mol more stabilizing in EK(VL)x (in the orientation K_g-E_e). However, to get a true measure of the stabilization occurring due to ionic interactions between the Lys and Glu side chains, the stability changes of the single substitutions (Lys or Glu only) have to be taken into account. The single substitutions give a measure of the intrinsic effects of the substituted residue in the absence of the ion pair. Subtracting the stability changes resulting from the single substitutions from the overall stability change resulting from introduction of the ion pair can then be used to give the apparent energetic effect of the ion pair interaction. For example, Glu substitution for Gln at position **e** [EQ(VL)x] destabilizes by 0.97 kcal/mol while Lys substitution at position **g** [QK(VL)x] destabilizes by 4.02 kcal/mol for a total destabilization of 4.99 kcal/mol (Table VII.1); yet introducing both substitutions simultaneously (peptide EK(VL)x) results in an overall stabilization of 0.17 kcal/mol (Table VII.4). Thus, it appears that 10 ion pairs can overcome the 4.99 kcal/mol intrinsic destabilization plus give a net stabilization of 0.17 kcal/mol, suggesting that the 10 ion pairs stabilize the coiled-coil by a total of 0.17 + 4.99 = 5.16 kcal/mol (0.52 kcal/mol each).

Such a thermodynamic analysis is termed a double mutant cycle (Serrano *et al.*, 1990). The cycle is shown in Figure VII.3A for EK(VL)x, and another way of analyzing a double mutant cycle is outlined in Figure VII.3B. In the latter case, the effect of a charged residue substitution is compared when the other substitution position contains a charged residue and when it does not (in the presence and absence of an ionic interaction). For example, the stability change between EQ(VL)x and Nx is a result of the intrinsic effect of a Glu to Gln substitution. The stability change between EK(VL)x and QK(VL)x involves the loss of the Lys-Glu ion pair contribution to stability, as well as the other intrinsic effects of a Glu to Gln substitution, which are not involved in ionic interactions. The difference between these two stability changes is then a measure of the apparent effect of the Lys-Glu interaction on coiled-coil stability. A similar calculation can be done for a Lys to Gln

Table VII.4: Urea denaturation results at pH 7 - ion pair peptides [a]

Peptide [b]	Ion Pair Orientation	$[\text{urea}]_{1/2}$	*m*	$\Delta\Delta G_u^{obs}$	$\Delta\Delta G_u^{int}$ [c]
Nx	-	6.0	0.87	--	--
E15K20x	E_g-K_e	6.0	0.83	0	+0.41
KE(VL)x	E_g-K_e	5.6	0.72	-0.32	+0.36
K15E20x	K_g-E_e	6.0	0.83	0	+0.58
EK(VL)x	K_g-E_e	6.2	0.81	+0.17	+0.51

[a] Data were collected at 20°C in a 50 mM tris, 100 mM KCl buffer.

[b] The sequences are given in Figure VII.1, and nomenclature is described under Peptide design and nomenclature.

[c] $\Delta\Delta G_u^{int}$ is the free energy of interaction per Lys-Glu **g-e'** ion pair. The value reported is the average from three independent calculations using double mutant analysis as described in Figure VII.3.

All other symbols were described in Table VII.1 and under Materials and Methods (pp. 56-59).

Figure VII.3 A double mutant cycle analysis for the estimation of the energetic contribution of an interchain **g-e'** interaction between Lys and Glu residues to stability of a two-stranded coiled-coil (denoted $\Delta\Delta G_u^{int}$). Three independent calculations of $\Delta\Delta G_u^{int}$ are illustrated, one in **(A)** and two in **(B)**. In panel A the stability difference between a Gln-Gln and a Lys-Glu interaction is corrected for the intrinsic stability changes due to Lys and Glu substitutions, while in panel B the substitution of a charged residue leading to ion pair formation ($E^-Q \rightarrow E^-K^+$ and $QK^+ \rightarrow E^-K^+$) is compared with the substitution of the same charged residue when the other position is neutral ($QQ \rightarrow QK^+$ and $QQ \rightarrow E^-Q$, respectively). The change in free energy of unfolding ($\Delta\Delta G_u$) resulting from a substitution was calculated by multiplying the the change in $[\text{urea}]_{1/2}$ by the average slope term *m* , as outlined in Materials and Methods (Chapter II, pp. 55-58). A positive $\Delta\Delta G_u$ indicates that the substitution results in increased stability. A positive $\Delta\Delta G_u^{int}$ is therefore indicative of a stabilizing Lys-Glu interaction.

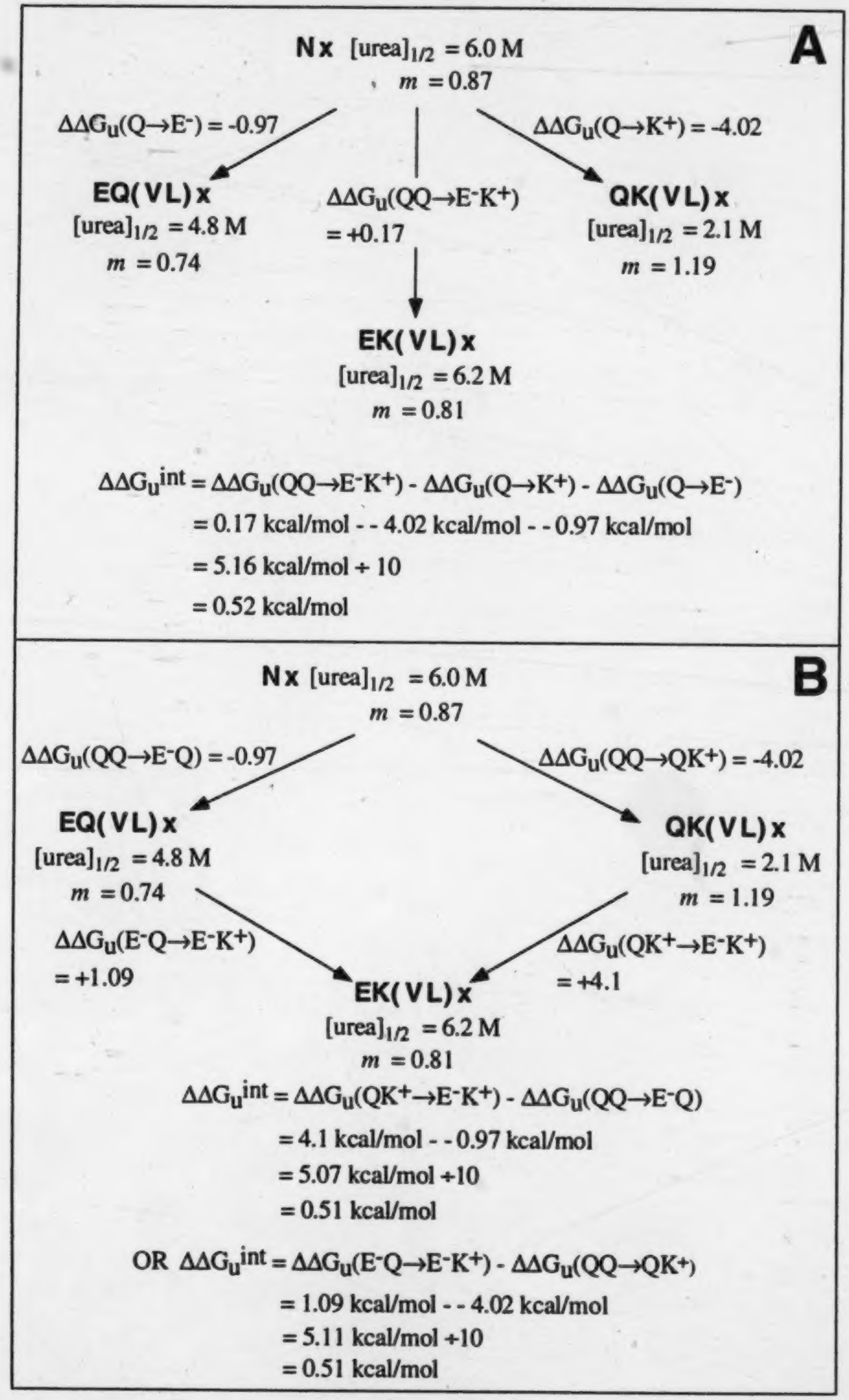
A
Nx [urea]1/2 = 6.0 M
m = 0.87
ΔΔGu(Q→E-) = -0.97
ΔΔGu(Q→K+) = -4.02
EQ(VL)x
[urea]1/2 = 4.8 M
m = 0.74
ΔΔGu(QQ→E-K+)
= +0.17
QK(VL)x
[urea]1/2 = 2.1 M
m = 1.19
EK(VL)x
[urea]1/2 = 6.2 M
m = 0.81
B
Nx [urea]1/2 = 6.0 M
m = 0.87
ΔΔGu(QQ→E-Q) = -0.97
ΔΔGu(QQ→QK+) = -4.02
EQ(VL)x
[urea]1/2 = 4.8 M
m = 0.74
QK(VL)x
[urea]1/2 = 2.1 M
m = 1.19
ΔΔGu(E-Q→E-K+)
= +1.09
ΔΔGu(QK+→E-K+)
= +4.1
EK(VL)x
[urea]1/2 = 6.2 M
m = 0.81

$$\begin{aligned}\Delta\Delta G_u^{int} &= \Delta\Delta G_u(QQ\rightarrow E^-K^+) - \Delta\Delta G_u(Q\rightarrow K^+) - \Delta\Delta G_u(Q\rightarrow E^-)\\ &= 0.17\ \text{kcal/mol} - -4.02\ \text{kcal/mol} - -0.97\ \text{kcal/mol}\\ &= 5.16\ \text{kcal/mol} \div 10\\ &= 0.52\ \text{kcal/mol}\end{aligned}$$

$$\begin{aligned}\Delta\Delta G_u^{int} &= \Delta\Delta G_u(QK^+\rightarrow E^-K^+) - \Delta\Delta G_u(QQ\rightarrow E^-Q)\\ &= 4.1\ \text{kcal/mol} - -0.97\ \text{kcal/mol}\\ &= 5.07\ \text{kcal/mol} \div 10\\ &= 0.51\ \text{kcal/mol}\end{aligned}$$

$$\begin{aligned}\text{OR }\ \Delta\Delta G_u^{int} &= \Delta\Delta G_u(E^-Q\rightarrow E^-K^+) - \Delta\Delta G_u(QQ\rightarrow QK^+)\\ &= 1.09\ \text{kcal/mol} - -4.02\ \text{kcal/mol}\\ &= 5.11\ \text{kcal/mol} \div 10\\ &= 0.51\ \text{kcal/mol}\end{aligned}$$

substitution in the presence of Gln or Glu at the other substitution site. Thus, three independent values can be calculated for the ion-pair energetic effect. The average net energetic contribution of an interchain ionic attraction to stability, $\Delta\Delta G_u^{int}$, is summarized in Table VII.4 for the four peptides studied. EK(VL)x yields an average ion-pair interaction of about 0.51 kcal/mol compared to 0.36 kcal/mol for KE(VL)x (about 1.4-fold higher). K15E20x yields an average ion-pair interaction of 0.58 kcal/mol compared to 0.41 kcal/mol for E15K20x (also about 1.4-fold higher). Thus, the apparent ion-pair effect is 1.4-fold greater with Glu at position **e** and Lys at position **g** both when the ion pair is present in all five heptads and when it is present in only the middle heptad. In addition, in both orientations the average energetic effect per ion pair is slightly lower when averaged over all five heptads *versus* that obtained from the middle heptad only (about 12% in both cases), perhaps indicating that the ion pairs contribute slightly less to stability at the ends of the coiled-coil.

iv) Substitution of Lys and Glu at positions **e** *and* **g** *- at pH 3.2*

The effects of ion pairs on coiled-coil stability should be dependent on the ionization state of the participating charged groups. Thus, protonating Glu residues by reducing the pH is expected to remove the electrostatic component of the Lys-Glu interaction. The $\Delta\Delta G_u^{obs}$ values of the four peptides containing Lys-Glu interactions are higher at pH 3.2 (Table VII.5) than at pH 7 (Table VII.4). The difference is most dramatic for KE(VL)x, where the $\Delta\Delta G_u^{obs}$ is increased from -0.32 kcal/mol to +3.06 kcal/mol. These results are consistent with previous observations of increased coiled-coil stability at low pH (Chapter VI, Kohn *et al.*, 1997c and references therein). Comparing the two peptides E15K20x and K15E20x, in which Lys-Glu interactions are present in the middle heptad only, the more stable analog at pH 3.2 is the one containing Glu at position **g**. The same is true in comparing the two peptides with Lys-Glu interactions in all five heptads. In both cases, the E_g-K_e orientation has a $\Delta\Delta G_u^{obs}$ value about 3.5-fold higher than the K_g-

Table VII.5: Urea denaturation results at pH 3.2 - ion pair peptides [a]

Peptide [b]	Ion Pair Orientation	$[\text{urea}]_{1/2}$	*m*	$\Delta\Delta G_u^{obs}$	$\Delta\Delta G_u^{int}$ [c]
Nx	-	5.7	0.86	--	--
E15K20x	E_g-K_e	6.75	0.94	+0.95	+0.09
KE(VL)x	E_g-K_e	9.1	0.93	+3.06	+0.06
K15E20x	K_g-E_e	6.0	0.92	+0.27	+0.10
EK(VL)x	K_g-E_e	6.6	1.07	+0.86	+0.08

[a] Data were collected at 20°C in a 20 mM Glycine, 100 mM KCl buffer.

[b] The sequences are given in Figure VII.1, and nomenclature is described under Peptide design and nomenclature.

[c] $\Delta\Delta G_u^{int}$ is the free energy of interaction per Lys-Glu **g-e'** ion pair. The value reported is the average from three independent calculations using double mutant analysis as described in Figure VII.3.

All other symbols were described in Table VII.1 and under Materials and Methods (pp. 56-59).

E_e orientation. This observation correlates with the findings from Gln to Glu and Gln to Lys substitutions that showed protonated Glu is more stabilizing at position **g** than at position **e** (Tables VII.2 and VII.3) and Lys is less destabilizing at position **e** than at position **g** (Table VII.1) both of which favor K_g-E_e as the more stable orientation at low pH. Calculation of the net free energy per Lys-Glu interaction, $\Delta\Delta G_u^{int}$, resulted in much smaller numbers than were obtained at pH 7 (compare Tables VII.4 and VII.5), consistent with the loss of favorable ionic interactions. However, there still remains a small favorable interaction between the Lys and Glu side chains at pH 3.2, which is over and above any interaction that may occur between Lys and Gln. The most likely explanation for this remaining $\Delta\Delta G_u^{int}$ at pH 3.2 is that the Glu residues are still partially ionized under these conditions. For example, the Henderson-Hasselbach equation predicts that an acidic group with a pK_a of 4.0 would be about 15% ionized at pH 3.2. Indeed, the $\Delta\Delta G_u^{int}$ values obtained for all four peptides at pH 3.2 (Table VII.5) are about 15% of the values observed at pH 7 (Table VII.4).

v) Role of ionic strength in the stability of the coiled-coil

As shown in the previous chapter (Kohn *et al.*, 1997c), salt has effects on the stability of a coiled-coil containing interhelical Lys-Glu **g-e'** ion pairs (Mo *et al.*, 1990; Thompson-Kenar *et al.*, 1995; Yu *et al.*, 1996). An increase in salt concentration from very little to near physiological levels has been shown to slightly decrease the stability of the GCN4 coiled-coil (Thompson-Kenar *et al.*, 1995) and a synthetic coiled-coil (Chapter VI, Kohn *et al.*, 1997c), suggesting screening of stabilizing ion pairs by the salt occurred while another synthetic coiled-coil was slightly stabilized by an increase from 0 to 100 mM KCl (Yu *et al.*, 1996). The urea denaturation experiments were repeated for EK(VL)x in a low ionic strength buffer at pH 7 (20 mM phosphate, 0 M KCl). EK(VL)x underwent a slight increase in $[\text{urea}]_{1/2}$ from 6.2 to 6.3 M upon decreasing the salt concentration (Fig. VII.4) while Nx underwent a slight decrease in the $[\text{urea}]_{1/2}$ from 6.0 to 5.7 M (data not shown).

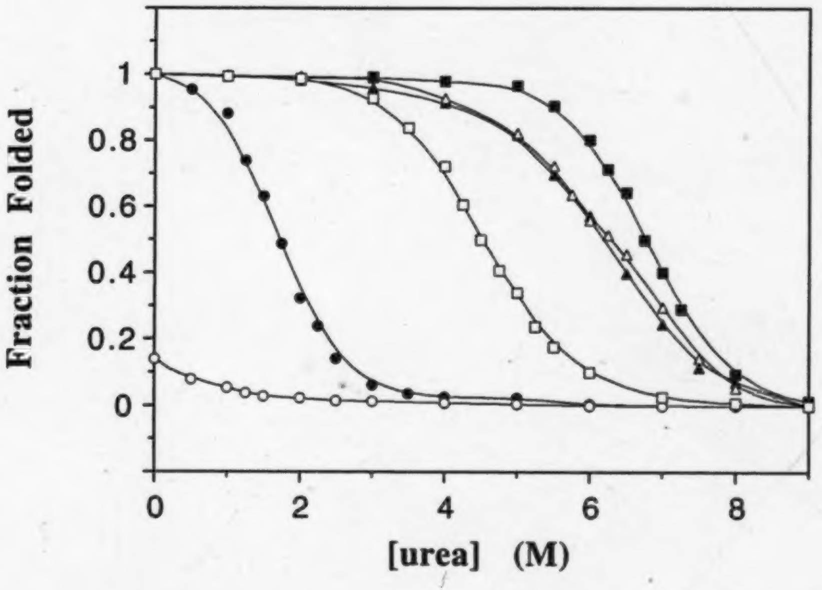

Figure VII.4 Urea denaturation profiles of EK(VL)x (squares) and QK(VL)x (circles) in 20 mM Glycine, pH 3.2 buffer containing no KCl (open symbols) and 100 mM KCl (closed symbols). Also shown are urea denaturation profiles of EK(VL)x at pH 7 in 20 mM sodium phosphate buffer (open triangles) and 50 mM tris, 100 mM KCl buffer (closed triangles). The fraction of folded peptide was calculated from the mean residue molar ellipticity at 222 nm, as described under Materials and Methods (Chapter II, pp. 56-59). Peptide concentrations were in the range 60 to 80 μM.

A $\Delta\Delta G_u^{int}$ value of 0.54 kcal/mol was obtained for EK(VL)x from the double mutant cycle under the low salt conditions, essentially equal to the value of 0.51 kcal/mol obtained in 50 mM tris, 100 mM KCl buffer. Thus, KCl has very little effect on the energy of the ion-pair interaction, as was suggested in Chapter VI (Kohn *et al.*, 1997c). In contrast, KCl has a large effect on the stability of coiled-coils containing Lys residues at the **e** or **g** positions that are not involved in ion pairs. Both QK(VL)x and EK(VL)x undergo large losses of stability in 20 mM Glycine buffer (pH 3.2) when the KCl concentration is reduced from 0.1 to 0 M (Fig. VII.4). In addition, while EK(VL)x is more stable at pH 3.2 than at pH 7 with 100 mM KCl present, it becomes significantly less stable at pH 3.2 in low salt conditions (Fig. VII.4).

*vi) Effects of substitutions at positions **e** and **g** on the stability and oligomerization of reduced coiled-coils*

The oligomerization state of coiled-coils is controlled by the **a** and **d** heptad positions (Harbury *et al.*, 1993, 1994; Lumb & Kim, 1995a) but can also be affected by substitutions at positions **e** and **g** (Alberti *et al.*, 1991; Beck *et al.*, 1997; Krylov *et al.*, 1994; Zeng *et al.*, 1997). A GCN4 leucine zipper mutant with Val at all **a** positions and Leu at all **d** positions formed a mixture of dimer and trimer (Harbury *et al.*, 1993), suggesting that the peptides in the current study have the potential to form two- or three-stranded coiled-coils or a mixture of oligomeric states. The reduced native peptide Nr forms a two-stranded coiled-coil, as indicated by sedimentation-equilibrium ultracentrifugation (Fig. VII.5A). In contrast, EK(VL)r and KE(VL)r were both observed to favor trimer formation. For both peptides the sedimentation-equilibrium data collected at pH 7 primarily fit to the trimeric species (Fig. VII.5B and VII.5C). E15K20r and K15E20r, which contain Lys-Glu ion pairs only in the middle heptad form a mixture of dimer and trimer by sedimentation-equilibrium with the dimer being preferred at lower concentrations (concentrations at which EK(VL)r and KE(VL)r are both still trimeric) (Fig. VII.5D and VII.5E). The results

Figure VII.5 Sedimentation-equilibrium results for **A)**, Nr; **B)**, EK(VL)r; **C)**, KE(VL)r; **D)**, E15K20r; and **E)**, K15E20r. All data were collected at 20°C in a 50 mM tris, 100 mM KCl, 5 mM DTT, pH 7 buffer. The rotor speed for all samples was in the range 32,000 to 36,000 rpm, and the initial peptide concentration for all runs was 0.9 to 1.4 mg/ml. For an ideal, single-species system, the sedimentation-equilibrium data represented as a graph of ln Y versus r^2 yields a linear plot, in which the slope is proportional to the molecular weight of the molecule or complex. An upward curved plot is indicative of a multi-species system, in which a mixture of oligomeric states is present. In such a multi-species system, the increase in total peptide concentration toward the bottom of the centrifuge cell (at larger r) results in an increase in the apparent oligomeric state. The expected slopes for the monomer, dimer, and trimer are indicated on each plot and labelled 1, 2, and 3, respectively. The data show that Nr is primarily dimeric, EK(VL)r and KE(VL)r are primarily trimeric, and E15K20r and K15E20r are present as a mixture of dimer and trimer.

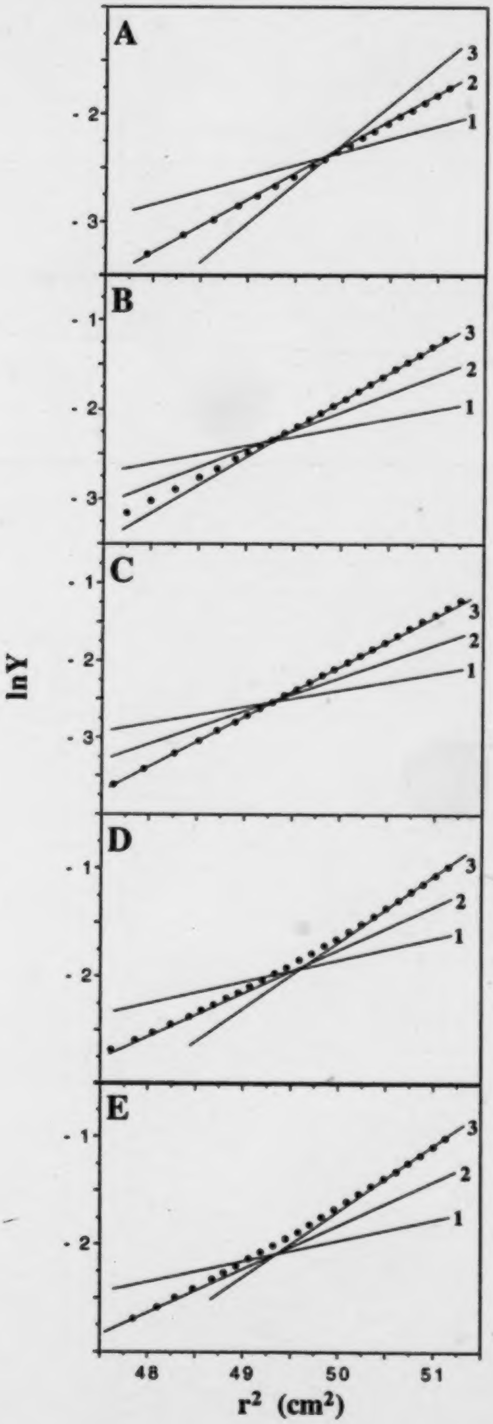
A
B
C
D
E
3
2
1
- 1
- 2
- 3
lnY
48
49
50
51
r^2 (cm^2)

suggest that Lys-Glu **g-e'** ion pairs favor trimer formation while Gln-Gln **g-e'** interactions favor dimer formation in the model coiled-coil. Modelling of a 29-residue peptide Coil-V_aL_d, which is almost identical in sequence to EK(VL)r, indicated that efficient packing of the hydrophobic residues occurs in both the dimer and the trimer, but calculations suggested that hydration forces favor the trimeric form (Boice *et al.*, 1996). The peptide was confirmed to form a trimer by sedimentation-equilibrium ultracentrifugation and X-ray crystallography (Ogihara *et al.*, 1997).

Urea denaturation of EK(VL)r and KE(VL)r at pH 7 indicates that they have dramatically different stabilities with $[\text{urea}]_{1/2}$ values of 7.4 and 2.25 M, respectively (Fig. VII.6A). The respective extrapolated $\Delta G_u^{H_2O}$ values were 24.4 and 14.5 kcal/mol, assuming a cooperative trimer-monomer unfolding process in which the dimer is not present in significant amounts (Boice *et al.*, 1996). However, GdnHCl denaturation yielded more similar $[\text{GdnHCl}]_{1/2}$ values of 1.9 M and 1.3 M (Fig. VII.6B) and very similar $\Delta G_u^{H_2O}$ values of 17.3 and 15.5 kcal/mol for EK(VL)r and KE(VL)r, respectively. A $\Delta G_u^{H_2O}$ of 18.4 kcal/mol was obtained for Coil-V_aL_d from GdnHCl denaturation (Boice *et al.*, 1996), in agreement with the value of 17.3 kcal/mol obtained here for EK(VL)r. The results show that the E_e-K_g orientation is highly favored in the trimeric form, to an even greater extent than was observed in the two-stranded disulfide-bridged peptides. Because the control peptide Nr has a different oligomerization state from EK(VL)r and KE(VL)r, a double mutant cycle could not be employed to determine the apparent $\Delta\Delta G_u^{int}$ for the Lys-Glu ion pairs.

E15K20r and K15E20r and the peptides containing the relevant single mutations were all dimeric at the concentration range used for stability measurements, allowing a double mutant cycle analysis to be performed. Previously, it was reported that E15r and E20r have the same stability, in contrast to the disulfide-bridged counterparts, which have different stabilities (Chapter V, Kohn *et al.*, 1997b) (compare Tables VII.1 and VII.6). Similarly, K15r and K20r have the same stability while K15x and K20x do not. The effect

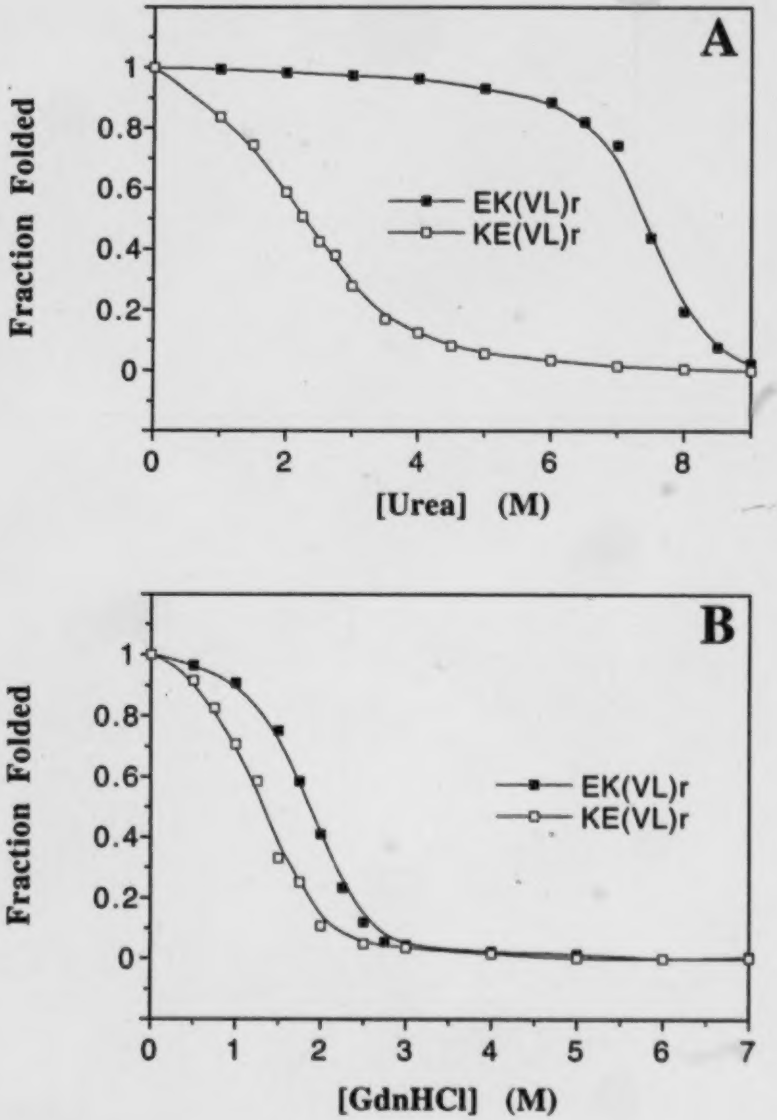

Figure VII.6 Chemical denaturation profiles for EK(VL)r and KE(VL)r at 20°C in 100 mM KCl, 50 mM tris, pH 7 buffer containing 5 mM DTT with: **A)** urea and **B)** GdnHCl as denaturant. The fraction of folded peptide was calculated from the mean residue molar ellipticity at 222 nm, as described under Materials and Methods (Chapter II, pp. 56-59). Peptide concentrations were in the range 100 to 120 μM.

Table VII.6: Urea denaturation results at pH 7 - reduced coiled-coils *a*

Peptide *b*	$[\text{urea}]_{1/2}$	*m*	$\Delta\Delta G_u^{obs}$	$\Delta\Delta G_u^{res}$	$\Delta\Delta G_u^{int}$
Nr	2.5	1.47	--	--	--
E15r	2.3	1.38	-0.29	-0.15	--
E20r	2.3	1.30	-0.28	-0.14	--
K15r	1.7	1.52	-1.20	-0.60	--
K20r	1.7	1.50	-1.19	-0.60	--
E15K20r	2.5	1.45	0.0	--	0.75
K15E20r	2.5	1.33	0.0	--	0.74

a Data were collected at 20°C in a 50 mM tris, 100 mM KCl buffer.

b The sequences are given in Figure VII.1, and nomenclature is described under Peptide design and nomenclature.

c $\Delta\Delta G_u^{int}$ is the free energy of interaction per Lys-Glu **g-e'** ion pair. The value reported is the average from three independent calculations using double mutant analysis as described in Figure VII.3.

All other symbols were described in Table VII.1 and under Materials and Methods (pp. 56-59).

of a single substitution is therefore not dependent on whether it occurs at position **e** or **g** when the peptide chains are not covalently linked. However, as was observed in the disulfide-bridged coiled-coils, Lys is more destabilizing than Glu (Table VII.6). Indeed, in the reduced coiled-coils Lys is about four-fold more destabilizing than Glu, while in the disulfide-bridged coiled-coils it is only twice as destabilizing. The resultant $\Delta\Delta G_u^{int}$ for both E15K20r and K15E20r is approximately 0.75 kcal/mol (Table VII.6), somewhat higher than was observed for the disulfide-bridged coiled-coils.

C. Discussion

Origins of the destabilizing effects of charged residue substitutions at positions e and g

In this study, substitutions of charged residues at the **e** and **g** positions were compared for their effects on the stability of two-stranded α-helical coiled-coils. The neutral Gln side chains in the 'native' coiled-coil, Nx, are likely able to stabilize the coiled-coil by lying across the hydrophobic dimer interface. In so doing, hydrophobic surface area of both the side chain and the hydrophobic core **a** and **d** residues are buried from solvent. In fact, it was found that positioning of Gln residues opposing one another in the **g-e'** orientation in a two-stranded coiled-coil was about 1.2 kcal/mol more stabilizing than with Ala at the respective positions (Krylov *et al.*, 1994). As mentioned in Chapter II (under peptide design, pp. 60-62), interhelical hydrogen bonding can potentially occur between the Gln carboxamide groups, but the folding of the **e** and **g** side chains at the interface is opposed by the loss of side chain entropy involved in fixing their conformation (Doig & Sternberg, 1995), and the partial desolvation involved in bringing the polar side chain carboxamide groups into the partially hydrophobic protein-water interface.

As discussed in previous chapters (Chapters III and IV, Kohn *et al.*, 1995a, 1995b), the stability change resulting from Gln to Glu or Gln to Lys substitutions has been attributed to α-helical propensity and apparent hydrophobicity differences (see also Zhou *et* *al.*, 1994b). α-helical propensity scales derived from amino acid substitutions into helices in globular proteins or model helical peptides generally score ionized Glu lower for intrinsic α-helical propensity than Gln (Blaber *et al.*, 1993; Chakrabartty *et al.*, 1994; Horovitz *et al.*, 1992; Myers *et al.*, 1997; O'Neil & DeGrado, 1990; Rohl *et al.*, 1996; Zhou *et al.*, 1994d), while one study showed the opposite (Yang *et al.*, 1997). Thus, the destabilization resulting from substitution of ionized Glu for Gln, could be at least partially a result of the lower helical propensity of an ionized Glu residue. In contrast, Lys has higher intrinsic α-helical propensity than Gln by most reports (Chakrabartty *et al.*, 1994; Horovitz *et al.*, 1992; O'Neil & DeGrado, 1990; Rohl *et al.*, 1996; Yang *et al.*, 1997; Zhou *et al.*, 1994d) with only two studies showing a lower helical propensity for Lys relative to Gln (Blaber *et al.*, 1993; Myers *et al.*, 1997). The destabilization occurring as a result of Lys substitution for Gln at position **e** or **g** of the coiled-coil is therefore unlikely to be due to helical propensity changes, and the most important factor is likely to be the apparent hydrophobicities of the side chains involved. A charged side chain is clearly more hydrophilic than a neutral polar side chain. The aqueous solvation free energy of a charged group was calculated to be approximately 60 kcal/mol more than that of a neutral polar group (Warshel & Russell, 1984). Therefore, the destabilization resulting from substitution of Gln with a charged side chain is most likely a result of the side chain extending into solvent to maximize solvation of the charged moiety, resulting in decreased packing of the side chain at the dimer interface and more exposure of the hydrophobic core surface area to water. If the charged side chain remains closely packed at the interface, a much greater desolvation penalty will occur and a hydrogen bond interaction between the charged group and the Gln side chain opposing it would not be sufficiently able to compensate for this effect.

Protonation of a Glu side chain causes it to be stabilizing rather than destabilizing relative to Gln (Tables VII.2 and VII.3). Protonated Glu has been shown to display a slightly higher intrinsic helical propensity (Chakrabartty *et al.*, 1994; Scholtz *et al.*, 1993) and higher apparent hydrophobicity (Hodges *et al.*, 1994; Sereda *et al.*, 1994) than Gln, both of which will contribute to the higher stability. The true hydrophobicity of the Gln and Glu side chains is essentially the same since they have the same amount of nonpolar (aliphatic) surface area, so the higher apparent hydrophobicity of protonated Glu versus Gln may be a result of different hydrogen bonding characteristics of the carboxylic acid and carboxamide groups (Karplus, 1997) and different partial charge distributions.

*Context may play a role in the effects of positions **e** and **g** on stability*

The results of the current study suggest that a Lys substitution for Gln is about twice as destabilizing as a Glu substitution (when at the same heptad position) (Table VII.1). In addition, substitution of both Lys and Glu is found to be about twice as destabilizing at position **g** as at position **e**. In previous studies (Krylov *et al.*, 1994; Zhou *et al.*, 1994b), these substitutions had different relative effects on stability than those observed here. The lack of a clear consensus among these experiments strongly suggests that context may play a significant role in determining the effects of substitutions at the **e** and **g** heptad positions on coiled-coil stability. Similar disparities in the observed energetic effect of substitutions in the hydrophobic core of coiled-coils point to context dependence as an important issue (Moitra *et al.*, 1997). Positions **e** and **g** pack against the hydrophobic core **a** and **d** positions, which may play a role in the observed stability effects of substitutions at **e** and **g**. Thus, the differences in the hydrophobic core between peptides in this study (a uniform $V_{\mathbf{a}}L_{\mathbf{d}}$ core) and those of Krylov *et al.* (1994) (nonuniform core in a native coiled-coil sequence) and Zhou *et al.* (1994b) ($L_{\mathbf{a}}L_{\mathbf{d}}$ core except for Ala at position 16**a**) is one potential reason for the observed discrepancies. Intrahelical interactions between side chains at positions **e** and **g** with those at positions **b** and **c**, respectively, could also contribute to the apparent context dependence. A uniform context, as in the present study, is likely to give the most reliable quantitative data.

Another important context effect on the role of substitutions at positions **e** and **g** in coiled-coil stability appears to be the presence of an interhelical disulfide bridge. Substitution of both Lys and Glu for Gln was observed to be more destabilizing at position **g** than at position **e** when an N-terminal disulfide bridge was present (Table VII.1). In contrast, the destabilizing effect of Lys is the same at positions **e** and **g** of the middle heptad in non-crosslinked peptides (Table VII.6), as previously noted for Glu substitutions (Tables V.1 and VII.6). It has been suggested that an interhelical disulfide bridge can lock a coiled-coil into a more rigid structure, such that substitutions at the nonequivalent **a** and **d** positions in the hydrophobic core (Zhou *et al.*, 1992b) and **e** and **g** positions (Chapter V, Kohn *et al.*, 1997b) have differing effects on stability; whereas in the absence of the disulfide bridge, the chains may be more flexible and able to reorganize interface packing in response to a substitution, resulting in a loss of the distinctiveness between positions **a** and **d** (Zhou *et al.*, 1992b) or positions **e** and **g** (Chapter V, Kohn *et al.*, 1997b). The reduced coiled-coils therefore display properties of the molten-globule state, in which secondary structure is fully formed, but tertiary interactions are absent or transiently formed (Ptitsyn, 1995).

A Lys-Glu ion pair is more stabilizing in the E_e-K_g orientation than the K_e-E_g orientation

The experiments at pH 7 with disulfide-bridged coiled-coils have shown that a preference occurs for the E_e-K_g orientation over the K_e-E_g orientation (Table VII.4). Whether the interaction energy, $\Delta\Delta G_u^{int}$, was measured in only the middle heptad or was averaged over all five heptads, it was about 1.4-fold higher in the E_e-K_g orientation. Krylov *et al.* (1994) reported a large difference in the $\Delta\Delta G_u^{int}$ between the K_e-E_g orientation (0.14 kcal/mol) and the E_e-K_g orientation (0.91 kcal/mol) relative to Ala as the control residue (a 6.5-fold preference for the E_e-K_g orientation). If $\Delta\Delta G_u^{int}$ is recalculated from their existing data using Gln as the control residue, the values for the E_e-K_g and K_e-E_g orientations are 1.42 kcal/mol and 0.59 kcal/mol, respectively. This represents a 2.3-

fold preference for the E_e-K_g orientation, which is significantly larger than in the present study (1.4-fold). Krylov and co-workers suggested that context is not important for the **g-e'** interactions in two-stranded coiled-coils, based on the observation of similar $\Delta\Delta G_u^{int}$ values measured at various positions along a nonuniform coiled-coil sequence (Krylov *et al.*, 1994). However, this conclusion seems inconsistent with the large orientation dependence that they report for the Lys-Glu interaction, which is likely to be due at least partly to different packing interactions against the hydrophobic **a** and **d** heptad positions (see below).

The origin of the apparent preference for the E_e-K_g orientation observed in this study for disulfide-bridged synthetic coiled-coils and by Krylov *et al.* (1994) in a native leucine zipper is difficult to confirm from the present data. The electrostatic interaction between the Lys and Glu side chains should not be affected by orientation since inspection of Lys-Glu ion pairs in the crystal structures of the GCN4 (O'Shea *et al.*, 1991) and Fos/Jun (Glover & Harrison, 1995) leucine zippers indicate that in both orientations the distance between the proton and oxygen atoms involved in the ion pair is approximately 3 Å. The most likely origins of an energetic preference for the E_e-K_g orientation are packing effects and side chain conformational angles. Because the residue at position **g** packs against Val at position **a'** of the other helix and a residue at position **e** packs against Leu at position **d'** of the other helix, the preference for E_e-K_g may be a result of better packing of Lys against Val and of Glu against Leu. This hypothesis is consistent with the intrinsicly lower destabilization resulting from a Gln to Glu substitution at position **e** versus position **g** but not the intrinsicly higher destabilization of a Gln to Lys substitution at position **g** versus position **e** (Table VII.1). In other words, Lys is more destabilizing at position **g** than at position **e** when the opposing residue is Gln but the opposite is true when the opposing residue is ionized Glu. Similarly, when the opposing Glu residue is protonated, the more stable coiled-coil is that in which Lys is at position **e** (Table VII.5). Therefore, only when ion-pair formation is possible, is the Lys residue preferred at position **g**.

In the reduced form, there is no apparent orientation preference for the ion pair in the middle heptad (Table VII.6), which may be due to the proposed looser packing at the coiled-coil interface in the reduced versus the disulfide-bridged coiled-coil that negates the differences between the **e** and **g** positions. The native VBP leucine zipper used by Krylov *et al.* (1994) showed a distinct orientation dependence in the absence of an interchain disulfide bridge, but it differs from the synthetic coiled-coils in the current study because it has a nonuniform hydrophobic core which may make the structure more highly specific and retain the clear differences between positions **e** and **g** that were observed in our model coiled-coils only when a disulfide bridge was present. For example, a specific interhelical hydrogen bond interaction is expected to occur between Asn residues present at the normally hydrophobic **a** position in the VBP leucine zipper, and such an interaction has been shown to regulate the native-like properties of coiled-coils (Gonzalez *et al.*, 1996b; Harbury *et al.*, 1993; Lumb & Kim, 1995a).

Preferred side chain conformational angles may be a factor in the observed preference of the E_e-K_g orientation over the K_e-E_g orientation because of the different χ_1 angles adopted by residues at the **g** and **e** positions when engaged in a **g-e'** interhelical interaction. For extended side chains (chi angles near 180°) the required χ_1 angle is approximately -60 to -80° at position **e** and 180° at position **g**. χ_1 values in this range are observed for several **g-e'** Lys-Glu ion pairs in the crystal structures of GCN4 (O'Shea *et al.*, 1991) and Fos/Jun (Glover & Harrison, 1995), in which both the Lys and Glu side chains are primarily extended. In the GCN4 structure for example, a **g-e'** ion pair between Glu22 (position **g**) and Lys27 (position **e**) occurs with a χ_1 angle of -174° and χ_2 angle of 179° for Glu22' (chain B), as would be expected. However, Glu22 (chain A) displays χ_1 and χ_2 angles of -75° and -70°, respectively. Thus, instead of being in the extended conformation properly positioned for **g-e'** ion pair formation, the side chain begins to point away and then must fold back on itself in order to make the **g-e'** interaction. A similar situation occurs in the Fos/Jun crystal structure, in which each unit cell contains two independent Fos-Jun-DNA complexes (Glover & Harrison, 1995). Glu189 (position **g**) in Fos ion pairs with Lys318 (position **e**) in Jun. In one of the complexes, Glu189 has a χ_1 angle of -79.8° while in the other it has a χ_1 angle of -168°, suggesting some degree of fluctuation may occur in this side chain. It is known from NMR experiments that the **e** and **g** side chains in a two-stranded coiled-coil are flexible in solution (Saudek *et al.*, 1991); indicating that the interactions between them are weak and insufficient to fix their positions fully. Perhaps on a time average in solution, the side-chain carboxylate of a Glu at position **g** spends less time in close proximity to its ion pairing partner Lys than when it is at position **e**, resulting in lower stability for the K_e-E_g orientation.

Double mutant cycles versus pK_a shifts for measurement of ionic interactions

The double mutant cycle method is intended to separate out the electrostatic interaction between two residues from the interactions between these residues and the rest of the protein (Sali *et al.*, 1991; Serrano *et al.*, 1990). However, there are two important factors that must be considered in interpreting double mutant cycle results. The first is the choice of reference mutant state (Faiman & Horovitz, 1996). For example, previous results show that the $\Delta\Delta G_u^{int}$ between Glu and Lys involved in a **g-e'** interaction is higher with Ala as the reference (control) residue than with Gln (Krylov *et al.*, 1994). This suggests some stabilization may occur due to interaction between Gln and either Lys or Glu in the single mutants. Indeed, Ala is generally used to mutate out other amino acids, particularly in solvent-exposed positions, due to its abbreviated side chain, which should minimize noncovalent interactions. However, it was pointed out that Ala is not necessarily an ideal reference state due to its unusually high α-helical propensity and lack of side chain size (Hendsch & Tidor, 1994). Gln is isosteric with Glu and somewhat isosteric with Lys and has no charge, making it a reasonable reference for studying **g-e'** ionic interactions.

The other critical issue in the use of double mutant cycles, which is particularly pertinent to the current study, is what the double mutant cycle actually measures. Ideally, the mutations in the double mutant cycle would lead to the loss of the interaction of interest while other interactions between the unmutated charged residue and the rest of the protein remain the same (Serrano *et al.*, 1990). However, significant structural relaxation can occur, resulting in a different conformation for the remaining charged side chain in the single mutant than when the ion pair is in place. This is exactly what would be expected for the interhelical **g-e'** interactions of α-helical coiled-coils because substitution of one charged residue with Gln will likely cause the opposing charged residue to be more extended in solution (as discussed above). It follows, as pointed out previously (Lumb & Kim, 1996), that the $\Delta\Delta G_u^{int}$ measured in a double mutant cycle for a **g-e'** interaction is not simply electrostatic, because any reorganization of the side chains upon ion-pair formation will increase packing at the hydrophobic interface, enhancing stability. As discussed in Chapter VI (Kohn *et al.*, 1997c), there is likely to be a synergy between electrostatic **g-e'** attractions and packing interactions of the side chains at positions **e** and **g** with the hydrophobic core **a** and **d** positions, such that the role of interhelical ionic attractions and repulsions on coiled-coil stability is manifested at least partly in their effects on side-chain packing. An orientation preference for the Glu-Lys interaction (E_e-K_g preferred over K_e-E_g) can be explained by better packing interactions in E_e-K_g, consistent with the hypothesis that ion pairs assist packing interactions.

The use of pK_a shifts to study ionic interactions in proteins is another established technique (Anderson *et al.*, 1990; Fersht, 1972; Yang & Honig, 1993). Several factors can affect the pK_a value of an ionizable group in a folded protein relative to that in the unfolded state. These include desolvation, interactions with neighboring charged residues, and interactions with neighboring neutral polar residues and other dipolar portions of a protein (such as the backbone). When considering the interaction of two charged residues, all other effects on the pK_a of one of the participating residues can be grouped as intrinsic effects of the protein structure. Importantly, the difference in pK_a between the folded and unfolded states provides a direct measure of the contribution of an ionizable residue to the free energy of folding (Yang & Honig, 1993). Thus, if the pK_a of an acidic (Asp or Glu) side chain is reduced in the folded state, the residue is more stabilizing to the protein when ionized, as observed for a buried His-Asp interaction in T4 lysozyme which led to a reduction of the pK_a of Asp70 by 3 pH units (Anderson *et al.*, 1990). However, the observed pK_a is not simply a direct measurement of the strength of the Asp-His ion pair since it has an intrinsic component as well as a component due to interaction with the His side chain (Yang & Honig, 1993).

The discovery that two Glu residues which were predicted from the X-ray structure to be involved in **g-e'** ion pairs in the GCN4 leucine zipper (O'Shea *et al.*, 1991) did not display reduced pK_a values in the folded peptide led to the conclusion that either the ion pairs do not form in solution, or that they contribute negligibly to stability (Lumb & Kim, 1995b). The results challenged the long held assumption that interhelical ion pairs specified the folding and enhanced the stability of coiled-coils. However, the key issue in pK_a shifts is whether ionization of the residue contributes favorably to stability, and coiled-coils have long been paradoxically observed to increase in stability at low pH despite the loss of ion pairs as acidic side chains are protonated (Lowey, 1965; O'Shea *et al.*, 1992; Zhou *et al.*, 1992c). Results in Chapters III to VI (Kohn *et al.*, 1995a, 1995b, 1997b, 1997c) demonstrated that protonated Glu at position **e** or **g** of a coiled-coil is intrinsicly very stabilizing. This result partly explains the higher stability observed for some coiled-coils at low pH because the greater intrinsic stabilization by protonated *versus* ionized Glu is apparently more than enough to overcome the loss of the Lys-Glu ionic attraction (Zhou *et al.*, 1994b). However, as discussed in Chapter VI (Kohn *et al.*, 1997c), the higher stability observed for some coiled-coils at low pH is very ionic strength dependent. For example, at very low ionic strength EK(VL)x is more stable at pH 7 than at pH 3.2, but at higher ionic strength (near physiological levels) the peptide stability is greatly increased at pH 3.2 and surpasses that at pH 7 (Fig. VII.4). The pK_a measurements on the GCN4 leucine zipper were carried out in a 150 mM KCl buffer , in which the coiled-coil displayed higher thermal stability at low pH than at neutral pH (Lumb & Kim, 1995b). It is therefore possible that the observed absence of a pK_a decrease is not because the ion pair is absent or contributes nothing to stability but because the protonated form is actually more stabilizing under the conditions used. Apparently, any decrease in the pK_a due to ionic attraction with the opposing Lys residue is offset by an intrinsic increase in the pK_a favoring the protonated form (Lavigne *et al.*, 1996).

Measurement of the pK_a of five Glu residues in a model coiled-coil, which could participate in a network of inter- and intrahelical ionic attractions with Lys residues, was performed using potentiometry, and an average pK_a of about 3.5 was obtained under very low ionic strength conditions (Yu, 1996). This is well below the unfolded pK_a of 4.1 to 4.2 obtained for the two Glu residues in the unfolded GCN4 peptide (Lumb & Kim, 1995b) and is suggestive of a significant stabilization at low ionic strength upon Glu ionization.

In a recent report, ^{13}C NMR spectra of a coiled-coil selectively labelled with [$^{13}C^{\delta}$] glutamate contained four upfield-shifted resonances, which were suggested to originate from four Glu residues that participate in interhelical **g-e'** ion pairs with Arg residues (Krylov *et al.*, 1998). These results were obtained near neutral pH in buffer containing 150 mM KCl.

Further experiments are currently underway to characterize the pK_a of a Glu residue involved in a **g-e'** interaction in a coiled-coil and its possible salt dependence.

*Effects of the **e** and **g** positions on coiled-coil oligomerization state*

A major outstanding issue in understanding the structure of both native and *de novo* designed coiled-coils is control of the oligomerization state. Studies of the GCN4 leucine zipper have suggested that preferred packing geometries of side chains at the **a** and **d** positions in the hydrophobic core play a major role in the oligomerization state (Harbury *et al.*, 1993, 1994), as do specific **a-a'** interactions between polar residues (Gonzalez *et al.*, 1996b; Harbury *et al.*, 1993; Lumb & Kim, 1995a). However, it appears that the **e** and **g** positions can also significantly influence the oligomerization state. For example, replacement of the charged residues at the **e** and **g** positions of the dimeric GCN4 leucine zipper with Ala led to tetramer formation (Alberti *et al.*, 1993). Similar results were observed upon substitution of Ala at all four **e** positions of the VBP leucine zipper (Krylov *et al.*, 1994) and most of the **e** positions of a coiled-coil based on the C-terminal oligomerization domain of the Lac repressor (Fairman *et al.*, 1995). Random mutagenesis of the **e** and **g** positions of GCN4 had dramatic effects on oligomerization state with only 30% of the mutants that form stable coiled-coils present in the dimeric form and the rest in various higher-order states (Zeng *et al.*, 1997). In other cases, a single amino acid change at an **e** or **g** position was able to cause a change from a three- to a four-stranded coiled-coil (Beck *et al.*, 1997; Kammerer *et al.*, 1998).

The current study provides additional evidence that the **e** and **g** positions play a role in determining the oligomerization states of coiled-coils. Specifically, the results indicate that Gln-Gln **g-e'** interactions are most compatible with dimer formation (Fig. VII.5A) and that Lys-Glu **g-e'** ion pairs in both orientations prefer trimer formation instead (Figs. VII.5B and VII.5C). A mixture of Gln-Gln and Lys-Glu interactions led to a dimer-trimer mixture (Figs. VII.5D and VII.5E), possibly due to competition between the oligomerization preferences of Gln-Gln and Lys-Glu interactions. The basis for the observed behavior is not clear, but may be related to the fact that the **e** and **g** positions are less exposed to solvent in a three-stranded coiled-coil than in the two-stranded form (Harbury *et al.*, 1993, 1994). It is clear from the existing data that the positions **a**, **d**, **e**, and **g**, which make up the interface, all play a role in oligomerization, and there is probably a complex interplay between the side chains at these positions as they pack together. Thus, it is important not to overemphasize the effect of any of these interfacial positions on the oligomerization state.

Additivity of ***g-e'*** *ionic interactions in coiled-coils*

The issue of additivity is crucial to efforts to study, and in particular to quantify, the noncovalent interactions that control protein folding and stability (Dill, 1997). Additivity can be broken down into two categories. The first is group additivity, which refers to interactions of a similar type within a molecule (van der Waals, hydrogen bonding, electrostatic, entropy, etc.). The second is energy component additivity, which is the sum of all the different types of energetic effects. This study has demonstrated that the interhelical **g-e'** ion pairs in α-helical coiled-coils show a high degree of group additivity. The estimation for the free energy of interaction, $\Delta\Delta G_u^{int}$, obtained from the middle heptad is only slightly higher than that obtained from the average of all five heptads in the 35 residue disulfide-bridged coiled-coils studied (Table VII.4). The results suggest perhaps a slightly lower contribution of the ion pairs to stability in the first and fifth heptads. The ends of a coiled-coil are predicted to be somewhat frayed and have been observed to contribute less to stability both at the hydrophobic core **a** and **d** positions (Zhou *et al.*, 1992a) and the **e** and **g** positions (Chapters IV and V, Kohn *et al.*, 1995b, 1997b). If it is assumed that the second, third, and fourth heptads all have the same $\Delta\Delta G_u^{int}$ that was measured in the third (middle) heptad (a good assumption based on Fig. IV.11, p. 120), the N- and C-terminal heptads appear to contribute about 75% as much to the overall ion-pair stabilization energy observed in both EK(VL)x and KE(VL)x.

The success of group additivity in any type of molecule is likely to be dependent primarily on the degree of uniformity of the surrounding environment (Dill, 1997), which is generally not very high in proteins. However, the α-helical coiled-coil has a very repetitive structure in which each **g-e'** ion pair is in a very similar environment, and some level of additivity would be expected, particularly in synthetic coiled-coils with repetitive sequences. A Glu-Glu **g-e'** repulsion has been shown to destabilize a coiled-coil by about 0.5 kcal/mol (Chapter III, Kohn *et al.*, 1995a), and the additivity observed in the current study for interhelical Lys-Glu attractions also occurs for Glu-Glu repulsions (Chapter IV, Kohn *et al.*, 1995b). The $\Delta\Delta G_u^{int}$ of a **g-e'** repulsion approximately offsets the stabilization due to a Lys-Glu ion pair in either orientation (about 0.4-0.6 kcal/mol). In reality, however, **g-e'** repulsions play a larger role in the stability of a coiled-coil. For example, EK(VL)x and KE(VL)x have stabilities close to that of Nx (Fig. VII.2A). A Lys-Glu ion pair is therefore not significantly stabilizing or destabilizing relative to a Gln-Gln interaction because the intrinsic destabilization resulting from Gln to Lys and Gln to Glu substitutions is largely offset by the ion-pair interaction. In contrast, a Glu-Glu repulsion is very destabilizing relative to a Gln-Gln interaction due to both the intrinsic destabilization of a Gln to Glu substitution and the unfavorable Glu-Glu **g-e'** repulsion (Chapter III, Kohn *et al.*, 1995a).

Concluding remarks

In nature, it seems likely that the assortment and assembly of a large number of coiled-coil sequences will be governed by positions **e** and **g** primarily through minimizing the number of interhelical repulsions but also by maximizing the number of interhelical attractions, which promote ideal side chain packing at the dimer interface (including positions **a**, **d**, **e**, and **g**). Therefore, ion pairs do not stabilize coiled-coils per se, but they offset the destabilization that results from placing charged side chains into the partially nonpolar environment of the coiled-coil interface (the results of the present study show charged residues at positions **e** and **g** are destabilizing when not involved in ion pairs). Charged residues at positions **e** and **g** could have other important roles in coiled-coil function, including aiding in solubility and participation in interactions with other proteins.

CHAPTER VIII

EFFECTS OF LANTHANIDE BINDING TO GLUTAMIC ACID RESIDUES ON THE STABILITY OF α-HELICAL COILED-COILS: THE La^{3+}-BRIDGING MODEL[6]

A. Introduction

As mentioned in the introduction to this thesis (Chapter I), incorporation or alteration of metal-binding sites has been a significant focus in protein engineering in recent years (Hellinga, 1996; Lu & Valentine, 1997; Matthews, 1995b; Regan, 1993, 1995). For example, novel metal-binding sites have been successfully incorporated into naturally-occurring proteins with stabilizing effects (Arnold & Haymore, 1991; Arnold, 1993; Kellis *et al.*, 1991; Klemba *et al.*, 1995). Engineered metal-binding sites have also been designed to act as chemical switches for controlling activity of enzymes (Browner *et al.*, 1994; Corey & Schultz, 1989; Halfon & Craik, 1996; Higaki *et al.*, 1990; McGrath *et al.*, 1993), activity of transmembrane-channel proteins (Russo *et al.*, 1997; Yellen *et al.*, 1994), and affinity of hormone-receptor interactions (Matthews, 1995b). The high specificity and affinity of metal binding observed in native proteins suggests a strong potential for control of *de novo* designed protein folding, stability, and activity by incorporation of metal-binding sites. In particular, metal-binding sites have already been shown to promote a unique native-like fold in synthetic proteins by replacing relatively nonspecific hydrophobic interactions with highly specific metal-ligand interactions (Bryson *et al.*, 1995; Handel *et al.*, 1993). More importantly, the reactive properties of bound metal ions, particularly for catalyzing hydrolytic or redox reactions, may be incorporated into synthetic metalloenzymes with useful activities (Iverson *et al.*, 1990; Wade *et al.* 1993).

---

[6] A version of this chapter has been published: Kohn, W. D., Kay, C. M., and Hodges, R. S. (1998). *J. Pept. Res.* **51**, 9-18.

In Chapter IV (Kohn *et al.*, 1995b), it was observed that $LaCl_3$ could effectively remove the effects of interhelical Glu-Glu repulsions on coiled-coil stability but that $MgCl_2$ and KCl at even higher concentrations could not. The results suggested that the La^{3+} ion may bind to the negatively-charged Glu side-chain carboxylate groups; more specifically, complexing (or bridging) between Glu side chains that normally repel one another across the dimer interface. This "La^{3+}-bridging model" therefore predicts that Glu side chains involved in specific i to i'+5 repulsions in the apo-state would cooperate to bind a metal ion between them and this would stabilize the folded structure. To test the validity of the La^{3+}-bridging model, the peptides originally studied in Chapter III (Kohn *et al.*, 1995a) to demonstrate the specificity of interhelical i to i'+5 **g-e'** interactions were again employed. If the bridging hypothesis is correct, E_2(15,20), which was shown in Chapter III to be destabilized by i to i'+5 Glu-Glu repulsions, should be stabilized by bridging of a metal ion between the Glu side chains. The stabilities of E_2(13,22) and E_2(20,22), which contain noninteracting Glu residues, were expected to be influenced little by the addition of the metal ion. Whether a La^{3+} binding site containing a cluster of three Glu side chains on the coiled-coil surface could be designed to give an even larger effect on stability, was also investigated. The specific binding effects of La^{3+} were contrasted with the response of coiled-coil stability to Ca^{2+} and Mg^{2+}.

B. Results and Discussion

a) Peptide design and nomenclature

The analogs studied are based on the native 35-residue coiled-coil (described in Chapter II, p. 60) which once again acts as the control (reference) peptide against which effects of changes in buffer conditions on stability can be compared.

The analogs in this study contain substitutions of two or three Glu residues for Gln at heptad positions **e** and **g** (Fig. VIII.1). Peptide nomenclature is based on the number and positions of Glu substitutions. For example, E_3(13,15,20) contains 3 Glu residues at

Figure VIII.1 Helical rod diagrams depicting a side view of the metal-binding coiled-coils studied. An identical view exists on the opposite side (facing into the page) of each coiled-coil. N and C refer to the amino and carboxy termini, respectively. Hydrophobic Val and Leu residues at the **a** and **d** heptad positions, respectively, pack together in the dimer interface. Residues in position **g** of one helix lie opposite residues at position **e'** of the following heptad in the other helix. These can form interhelical **g-e'** (i to i'+5) interactions (Chapter III, Kohn *et al.*, 1995a) while interhelical **e-g'** (i to i'+2) interactions (between "nearest neighbors") do not occur due to the interference of large Leu side chains at position **d**. All peptides are identical to the native sequence (N) shown in Figure II.7, except for two or three Glu substitutions for Gln at heptad positions **e** and **g** (highlighted as shaded circles). Peptide nomenclature is based on the number and positions of Glu substitutions, as described under Peptide design and nomenclature.

$E_2(13,22)$

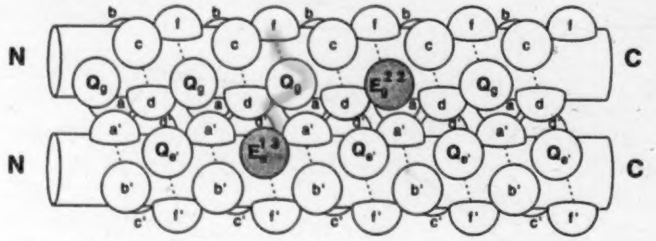
N
C
N
C
b
f
c
Q_g
E_g^{22}
d
a
a'
$Q_{e'}$
$E_{e'}^{13}$
b'
f'
c'

$E_2(20,22)$

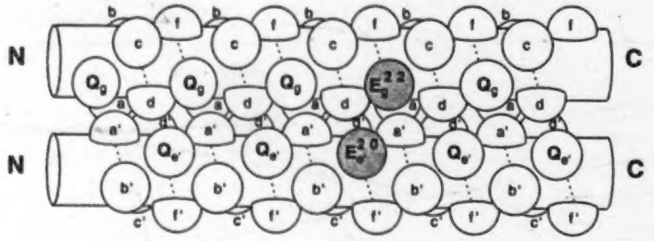
N
C
N
C
b
f
c
Q_g
E_g^{22}
d
a
a'
$Q_{e'}$
$E_{e'}^{20}$
b'
f'
c'

$E_2(15,20)$

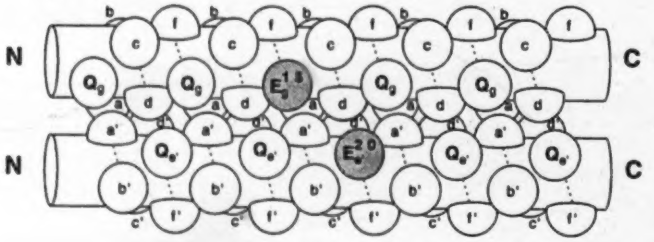
N
C
N
C
b
f
c
Q_g
E_g^{15}
d
a
a'
$Q_{e'}$
$E_{e'}^{20}$
b'
f'
c'

$E_3(13,15,20)$

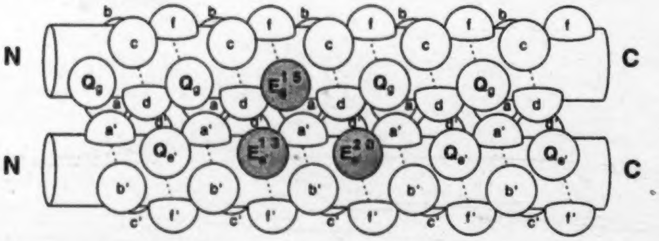
N
C
N
C
b
f
c
Q_g
E_g^{15}
d
a
a'
$Q_{e'}$
$E_{e'}^{13}$
$E_{e'}^{20}$
b'
f'
c'

$E_3(15,20,22)$

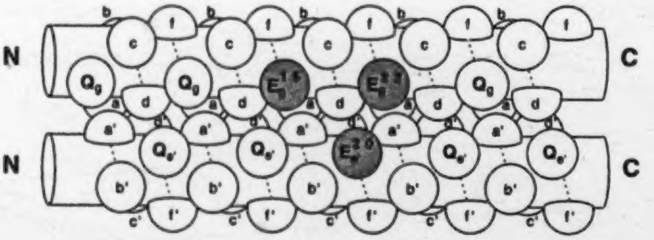
N
C
N
C
b
f
c
Q_g
E_g^{15}
E_g^{22}
d
a
a'
$Q_{e'}$
$E_{e'}^{20}$
b'
f'
c'

positions 13, 15, and 20. The native sequence is designated "N". Each peptide is further designated with "x" if it is present in the disulfide-bridged (oxidized) form or "r" if present in the reduced, noncovalently-linked form.

As discussed in the introduction to this chapter, $E_2(15,20)$ was compared to $E_2(13,22)$ and $E_2(20,22)$ to test the La^{3+}-bridging model that was proposed based on the observed stabilization of coiled-coils by $LaCl_3$ in Chapter IV (Kohn *et al.*, 1995b). $E_3(13,15,20)$ and $E_3(15,20,22)$ were designed with the intention of creating a three residue metal ion-binding cluster on the side of the coiled-coil, involving two residues from one helix and one residue from the other helix. For example, in $E_3(13,15,20)$ residues 13 and 20 of one helix may potentially bind a metal ion cooperatively with residue 15 of the other helix (Fig. VIII.1).

b)Structural characterization

The native sequence, N, has previously been demonstrated to form a stable, two-stranded α-helical coiled-coil in either the presence or absence of an interchain disulfide bridge. The peptide appears highly helical by CD spectroscopy and is two-stranded, as determined by size-exclusion HPLC and sedimentation-equilibrium ultracentrifugation (Chapters III and IV, Kohn *et al.*, 1995a, 1995b).

The analogs in this study all have high helicity in the oxidized form, as judged by CD spectroscopy. The mean residue molar ellipticity at 222 nm, θ_{222}, which is a diagnostic measure of helical content, ranges from -31,200 to -33,800 $deg \cdot cm^2 \cdot dmol^{-1}$; this is close to the expected θ_{222} value for a 100% helical 35-residue peptide (-33,600 $deg \cdot cm^2 \cdot dmol^{-1}$) based on the equation of Chen *et al.* (1974). The reduced peptides Nr, $E_2(13,22)$r and $E_2(20,22)$r have ellipticities approximately equal to that of the oxidized peptides (Chapter III, Kohn *et al.*, 1995a). However, the θ_{222} value for $E_2(15,20)$ is reduced from -33,800 to -26,000 upon reduction of the disulfide bridge, as a result of destabilizing interhelical Glu-Glu repulsions (Chapter III, Kohn *et al.*, 1995a). $E_3(13,15,20)$ and $E_3(15,20,22)$

experience a similar reduction in helicity in the reduced form (data not shown). For all three of these peptides, addition of 50 mM $LaCl_3$ to the buffer increases the θ_{222} value to over -34,000 deg•cm^2•dmol^{-1}. Thus, La^{3+} binding appears to enhance the coiled-coil structure.

All of the oxidized analogs are eluted from a size-exclusion HPLC column over a narrow time range of 22.2 to 22.8 min, which corresponds to the retention time of a two-stranded coiled-coil based on a coiled-coil standard curve (Fig. II.6, p. 50). Addition of 50 mM $LaCl_3$ to the buffer has no effect on the size-exclusion chromatographic behavior of the oxidized peptides. The reduced peptides, Nr, E_2(13,22)r, and E_2(20,22)r are all eluted over the narrow range 21.3 to 21.8 min. Addition of 50 mM $LaCl_3$ to the buffer also has no effect on the retention times of these reduced peptides. The chromatograms of E_2(15,20)r, E_3(13,15,20)r and E_3(15,20,22)r all contain two peaks near 22 and 24 min due to dimer and monomer, respectively. Addition of 50 mM $LaCl_3$ to the buffer results in disappearance of the monomer peak at 24 min, indicating that La^{3+} binding enhances dimerization (data not shown).

The combined results of CD spectroscopy and size-exclusion HPLC show that the analogs studied are in the two-stranded coiled-coil form and that binding of La^{3+} ions increases the amount of coiled-coil dimer for the reduced analogs that contain Glu-Glu repulsions.

c)Stability studies

i) Urea denaturation, oxidized peptides

Controls: Nx, E_2(13,22)x, and E_2(20,22)x

The native sequence, Nx, has a $[\text{urea}]_{1/2}$ value of 6.0 M and $\Delta G_u^{H_2O}$ of 5.0 kcal/mol at 20°C. The addition of 50 mM $LaCl_3$ to the buffer had no effect on the denaturation of Nx by urea (Table VIII.1; Fig. VIII.2). Thus, the presence of a small concentration of $LaCl_3$ does not change the apparent stability of the coiled-coil model in the absence of electrostatic interactions within the coiled-coil and in the absence of negatively charged residues, which could bind to La^{3+} ions.

Table VIII.1: Effects of $LaCl_3$ on the stability of oxidized peptides: urea denaturation at pH 7 [a].

Peptide [b]	- $LaCl_3$			+ 50 mM $LaCl_3$			$\Delta\Delta G_u$ [f]
	$[urea]_{1/2}$ [c]	*m* [d]	$\Delta\Delta G_u$ [e]	$[urea]_{1/2}$	*m*	$\Delta\Delta G_u$	
Nx	6.0	0.83	---	6.0	0.85	---	---
$E_2(13,22)x$	5.15	0.83	-0.71	4.4	0.83	-1.34	-0.62
$E_2(20,22)x$	5.1	0.82	-0.74	4.7	0.87	-1.12	-0.34
$E_2(15,20)x$	4.25	0.95	-1.57	5.55	0.71	-0.35	+1.08
$E_3(13,15,20)x$	3.5	0.88	-2.14	5.75	0.76	-0.20	+1.85
$E_3(15,20,22)x$	3.4	0.88	-2.22	5.0	0.73	-0.79	+1.29

[a] Data was collected at 20ºC in a 50 mM tris, 100 mM KCl, pH 7 buffer.

[b] Peptide nomenclature is detailed under Peptide design and nomenclature (see also Figure VIII.1).

[c] $[urea]_{1/2}$ is the concentration of urea, in M, at which the peptide is 50% unfolded, as determined from the decrease in molar ellipticity at 222 nm with increasing denaturant concentration.

[d] *m* is the slope of the assumed linear relationship between ΔG_u and urea concentration.

[e] $\Delta\Delta G_u$ is the change in free energy of unfolding in kcal/mol from the native peptide Nx. A negative $\Delta\Delta G_u$ is indicative of an apparent decrease in stability.

[f] $\Delta\Delta G_u$ is the change in free energy of unfolding in kcal/mol upon $LaCl_3$ addition to the buffer. $\Delta\Delta G_u$ is calculated by the method of Serrano and Fersht (1989) (see Methods, Chapter II, pp. 56-59).

Peptide concentrations were in the range 70 µM to 90 µM.

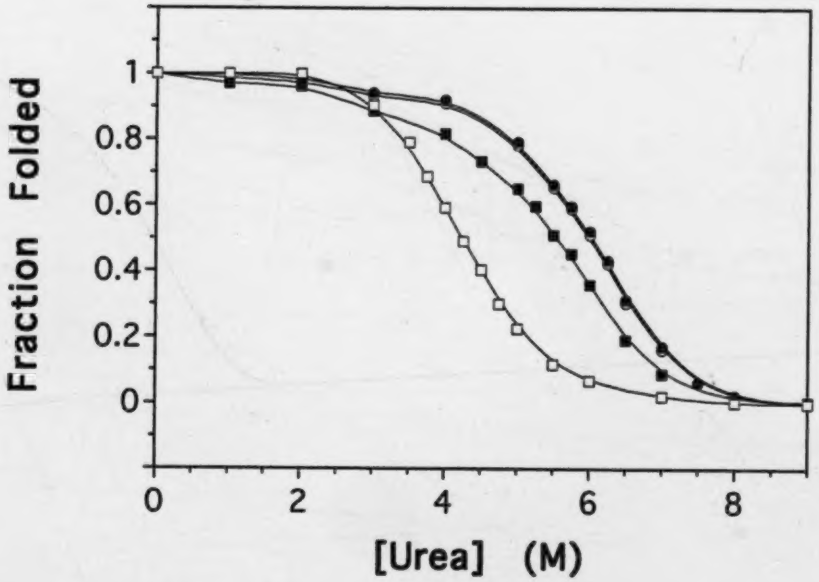

Figure VIII.2 Urea denaturation profiles of disulfide-bridged coiled-coils Nx (circles) and E_2(15,20)x (squares) at 20°C in 50 mM tris, 100 mM KCl, pH 7 buffer in absence (open symbols) and presence (closed symbols) of 50 mM $LaCl_3$. The fraction of folded peptide was calculated from the observed mean residue molar ellipticity at 222 nm, as described under Materials and Methods (Chapter II, pp. 56-59). The peptide concentration in the final solutions for CD measurements ranged from 70 to 90 μM.

$E_2(13,22)x$ contains Glu substitutions at positions such that Glu13 of one chain and Glu22 of the other are spaced far enough apart that they do not interact directly across the dimer interface (Fig. VIII.1). This analog is destabilized relative to Nx by about 0.7 kcal/mol under standard buffer conditions (Table VIII.1), which has been attributed to the lower α-helical propensity and hydrophobicity of ionized Glu relative to Gln (Chapters III and VII, Kohn *et al.*, 1995a, 1998c). In the presence of 50 mM $LaCl_3$, the $[urea]_{1/2}$ value of $E_2(13,22)x$ is reduced, corresponding to a stability decrease of about 0.6 kcal/mol (Table VIII.1). This contrasts with Nx, for which the stability is independent of 50 mM $LaCl_3$, and suggests that $LaCl_3$ may destabilize the coiled-coil structure of $E_2(13,22)x$ relative to the unfolded state by preferential binding of La^{3+} ions to the unfolded state. This conclusion is consistent with the fact that Glu residues in the folded form are spaced far apart and thus unable to bind a La^{3+} ion cooperatively but could be closer together and able to do so in the unfolded state.

Similarly to $E_2(13,22)x$, $E_2(20,22)x$ is destabilized about 0.7 kcal/mol relative to Nx in standard buffer by reduced α-helical propensity and hydrophobicity contributions, and there appears to be no significant i to i'+2 Glu-Glu repulsive interaction (Chapter III, Kohn *et al.*, 1995a). Addition of $LaCl_3$ also decreases the apparent stability of this analog with a decrease in $[urea]_{1/2}$ from 5.1 M to 4.7 M and a resulting $\Delta\Delta G_u$ value of -0.3 kcal/mol (Table VIII.1). This reduction in stability upon 50 mM $LaCl_3$ addition is about half that observed for $E_2(13,22)x$. Because Glu20 and Glu22' are close together in the folded form of $E_2(20,22)x$ (Fig. VIII.1), they may be able to cooperatively bind La^{3+} ions to the folded state, which would partially counteract the effect on ΔG_u of metal binding to the unfolded state. However, the observation of an overall net stability loss again suggests preferential binding of La^{3+} ions to the unfolded peptide.

A metal-binding cluster formed from two Glu residues - $E_2(15,20)x$

$E_2(15,20)x$ is destabilized relative to $E_2(13,22)x$ and $E_2(20,22)x$ by about 0.9 kcal/mol (Table VIII.1), due to two i to i'+5 Glu-Glu repulsions destabilizing the coiled-coil by about 0.45 kcal/mol each (Chapter III, Kohn *et al.*, 1995a). The addition of 50 mM $LaCl_3$ increased the $[urea]_{1/2}$ of this analog significantly from 4.25 to 5.55 M (Fig. VIII.2), in contrast to what was obtained for Nx, $E_2(13,22)x$ and $E_2(20,22)x$ (Table VIII.1). However, the slope of the unfolding transition (Fig. VIII.2) and the resulting slope of the ΔG_u versus [urea] dependence, *m* (Table VIII.1) are decreased in the presence of $LaCl_3$ while the *m* values of Nx, $E_2(13,22)x$ and $E_2(20,22)x$ were not affected by $LaCl_3$. When calculated at the midpoint of the $[urea]_{1/2}$ values (see Methods, pp. 58-59) the change in free energy of unfolding upon 50 mM $LaCl_3$ addition is +1.08 kcal/mol (a positive $\Delta\Delta G_u$ indicates a stabilization).

$E_2(15,20)x$ was also subjected to temperature denaturation in the presence and absence of 50 mM $LaCl_3$ (Fig. VIII.3), and the T_m increased from about 60 to 80°C upon $LaCl_3$ addition. A gradual loss of helicity preceding the major transition is indicative of a temperature dependence of the folded state, as discussed by Qian (1994). This temperature dependence appears similar in the absence and presence of $LaCl_3$, suggesting the overall structure is not significantly changed upon La^{3+} binding.

The results indicate that $E_2(15,20)x$ binds La^{3+} ions in the folded state, likely by cooperative binding (bridging) of Glu residues normally involved in interhelical i to i'+5 repulsions to a single La^{3+} ion, resulting in an increased resistance to temperature or urea denaturation. Two La^{3+} ions are predicted to bind per coiled-coil; one on each side of the dimer interface. Such metal ion binding should increase coiled-coil stability primarily by promoting better side chain packing at the dimer interface. The i to i'+5 repulsions most likely affect stability by causing exposure of the hydrophobic core **a** and **d** positions (Chapter IV, Kohn *et al.*, 1995b); whereas if they are not involved in repulsive interactions and particularly if they are engaged in ion pairs (or are complexed to a metal ion), the residues at the **e** and **g** positions are able to fold across the dimer interface and shield it from solvent (O'Shea *et al.*, 1991) (see also Chapters VI and VII, Kohn *et al.*, 1997c, 1998c).

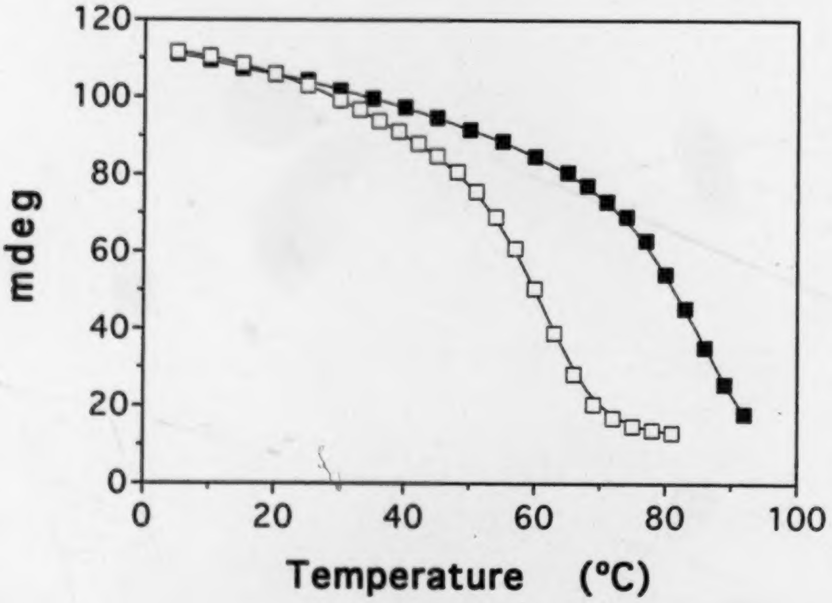

Figure VIII.3 Temperature denaturation profiles of $E_2(15,20)x$ in absence (open squares) and presence (closed squares) of 50 mM $LaCl_3$ at 20°C in 50 mM MOPS, 50 mM KCl, pH 7 buffer. Ellipticity in mdeg was measured at 222 nm. Peptide concentration in the final solutions for CD measurements was 90 μM under both buffer conditions.

Because the *m* value is thought to be a measure of the amount of surface area exposed upon unfolding (Makhatadze & Privalov, 1993; Myers *et al.*, 1995), which is related to the number of denaturant binding sites (Mayo & Baldwin, 1993), the results for E_2(15,20)x suggest that the unfolded state may be less unfolded in presence of 50 mM $LaCl_3$. In contrast, $LaCl_3$ had no effect on the *m* value of E_2(13,22)x and E_2(20,22)x. It is unclear as to why the extent of unfolding should be affected differently by $LaCl_3$ for E_2(15,20)x. Another possibility is that the reduced *m* value is due to reduced cooperativity (two-state behavior) of the unfolding process. It has been shown that stabilization of folding intermediates results in reduced *m* values (Carra & Privalov, 1995; Shortle, 1995). Thus, it is possible that the Glu-Glu repulsions in E_2(15,20)x promote unfolding and enhance cooperativity of the unfolding process, leading to an increased *m* value versus that observed for Nx (Table VIII.1). In contrast, binding of La^{3+} ions by Glu residues in the folded form of E_2(15,20)x may decrease cooperativity (stabilize intermediates) and decrease *m* . A similar argument was previously used to explain the effects of interchain and intrachain ionic attractions and repulsions on the *m* values for a series of coiled-coils (Monera *et al.*, 1994b). The energetic effect of La^{3+} binding to E_2(15,20)x is unclear, and it is possible that La^{3+} binds to and affects the free energy of both the folded and unfolded states.

A metal-binding cluster containing three Glu residues - E_3(13,15,20)x and E_3(15,20,22)x

The analogs E_3(13,15,20)x and E_3(15,20,22)x are further destabilized compared to E_2(15,20)x (Table VIII.1). Both of these peptides, like E_2(15,20)x, show a large increase in the $[\text{urea}]_{1/2}$ value and a decrease in the *m* value in the presence of 50 mM $LaCl_3$ (Table VIII.1). For both analogs, there is a larger $LaCl_3$-induced $\Delta\Delta G_u$ compared with that obtained for E_2(15,20)x, which may be attributed to cooperation of the additional Glu substitution per chain in the La^{3+}-binding site. The addition of a third Glu residue to each proposed metal-binding site should make metal binding more favorable since it will lead to electrostatic neutrality at the interface of the coiled-coil upon binding of La^{3+} (there are six

Glu residues total and presumably two La^{3+} ions). Therefore, even if it makes no direct interaction with the bound La^{3+} ion, the third Glu side chain could promote tighter binding due to general electrostatic considerations.

A comparison of the stabilities of E$_2$(15,20)x and E$_3$(13,15,20)x at various LaCl$_3$ concentrations is illustrated in Figure VIII.4A. While E$_3$(13,15,20)x is significantly less stable in the absence of LaCl$_3$, it is much more sensitive to LaCl$_3$ addition. The observed dependence of the [urea]$_{1/2}$ value on LaCl$_3$ concentration resembles a binding curve and may be indicative of the binding affinity (the transition midpoints of 3 mM for E$_3$(13,15,20)x and 14 mM for E$_2$(15,20)x would approximate the respective dissociation constant, K$_d$, values). Thus, the larger stability increase observed for E$_3$(13,15,20)x upon LaCl$_3$ addition is a result of roughly five-fold higher affinity La^{3+} binding. The binding constants approximated from Figure VIII.4 predict a difference between the metal-induced increase in stability of the two peptides - 0.9 kcal/mol - close to that measured by urea denaturation - 0.75 kcal/mol Table VIII.1. The *m* values of the two analogs have a similar dependence on LaCl$_3$ concentration as do the [urea]$_{1/2}$ values (Fig. VIII.4B), indicating that as more LaCl$_3$ is present and La^{3+} ions are bound to a greater extent, the *m* value decreases accordingly. As discussed above, this result may be due to a decrease in the cooperativity of unfolding for the metal bound peptide.

It is apparent that E$_3$(13,15,20)x is stabilized about 0.55 kcal/mol more than E$_3$(15,20,22)x by 50 mM LaCl$_3$ (Table VIII.1). This may be a result of differences in how the Glu residues in the **e** and **g** positions of these peptides pack against the Val and Leu residues of the hydrophobic core. Specifically, Leu at position **d** protrudes from the dimer interface of a two-stranded coiled-coil (Fig. VIII.5) and blocks i to i'+2 interhelical interactions between nearest neighbor **e** and **g'** residues, as seen in GCN4 (Nilges & Brunger, 1993; O'Shea *et al.*, 1991). In E$_3$(15,20,22)x, Leu residues at position 19(**d**) protrude from the interface in the middle of the Glu triad, which is proposed to form a La^{3+} binding site (Fig. VIII.1) and may therefore interfere with participation of Glu22 in binding

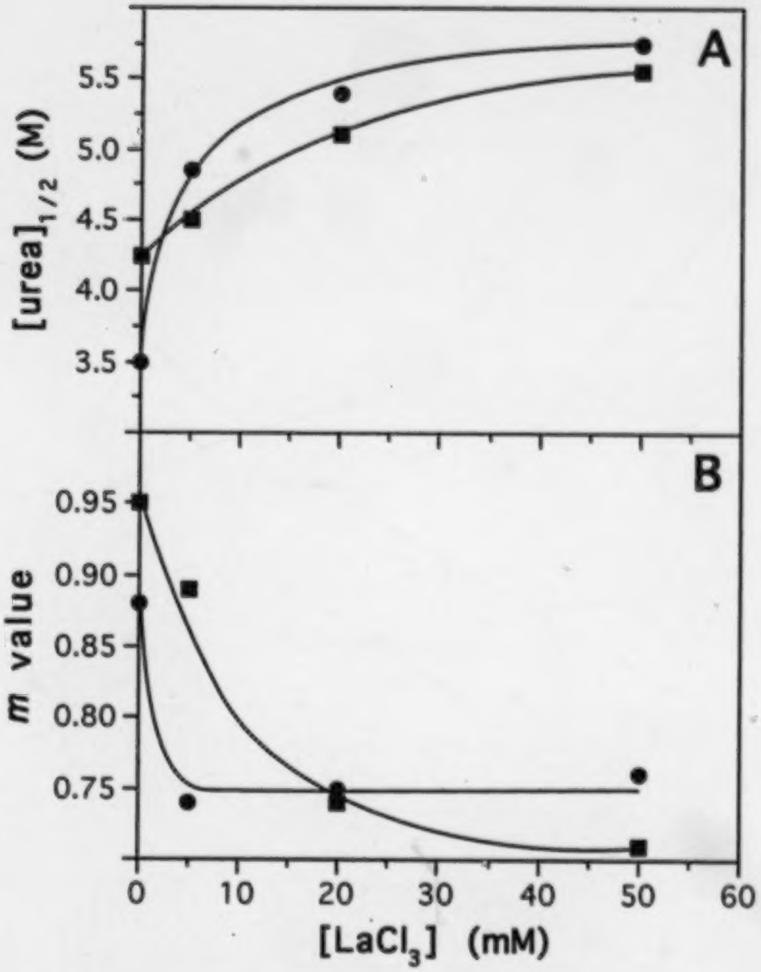

Figure VIII.4 Dependence of the urea denaturation behavior on LaCl$_3$ concentration for the disulfide-bridged coiled-coils E$_2$(15,20)x (squares) and E$_3$(13,15,20)x (circles). Data were collected at 20°C in 50 mM tris, 100 mM KCl, pH 7 buffer containing 0, 5, 20, or 50 mM LaCl$_3$. **A)** effect of LaCl$_3$ on [urea]$_{1/2}$ value (urea concentration at which the peptide is 50% unfolded). **B)** Effect of LaCl$_3$ on the *m* value (slope of the linear dependence of ΔG_u on urea concentration).

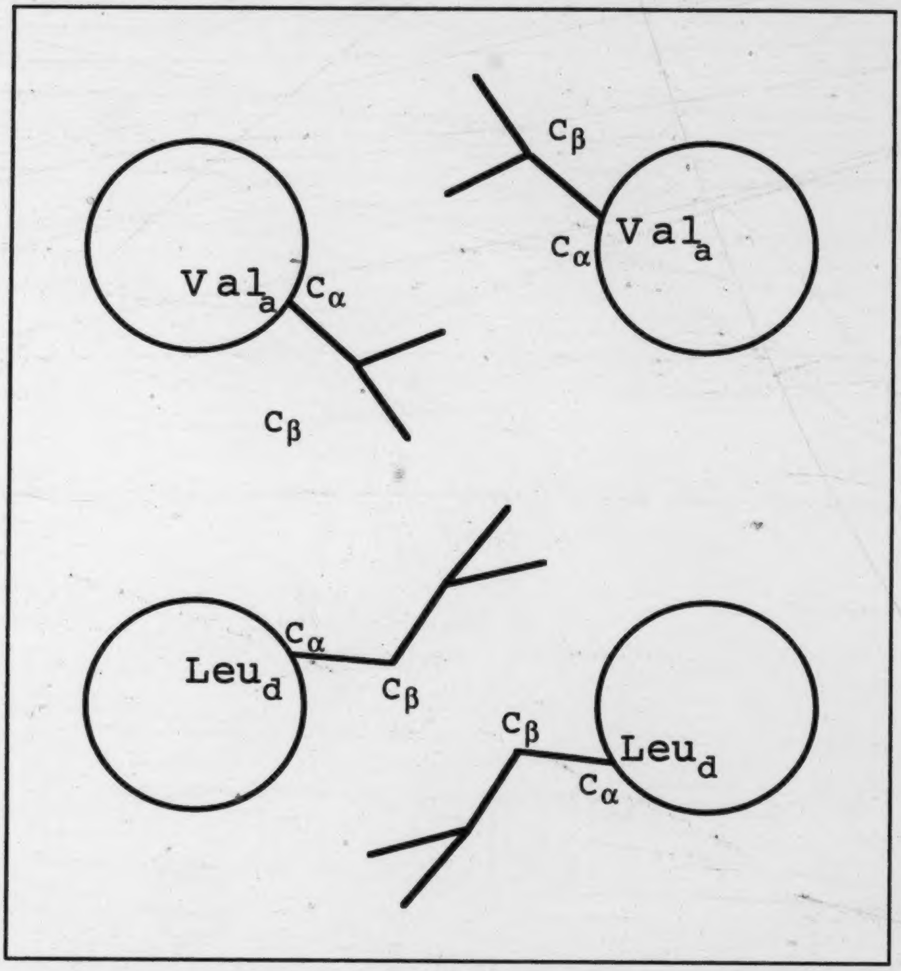
C_β
C_α
Val_a
Val_a
C_α
C_β
C_α
Leu_d
C_β
C_β
Leu_d
C_α

Figure VIII.5 Schematic representation of the GCN4 coiled-coil X-ray structure, showing the orientations of Val and Leu side chains at the **a** and **d** heptad positions, respectively. The C_α-C_β vector points into the dimer interface at position **d** but out of the interface at position **a** (O'Shea *et al.*, 1991). The C_β-C_γ vector of Leu side chains at position **d** points out of the interface (O'Shea *et al.*, 1991). Circles represent the helices in cross section.

to a La^{3+} ion. In contrast, Val at position **a** of a two-stranded coiled-coil does not protrude as significantly from the interface (Fig. VIII.5). Therefore, a Val residue in the middle of the Glu triad in E_3(13,15,20)x (Fig. VIII.1) may allow greater participation of all three Glu residues in La^{3+} ion-binding.

Modelling of the metal binding site on the GCN4 backbone coordinates (O'Shea *et al.*, 1991) also suggested that E_3(13,15,20)x may bind the metal ion better than E_3(15,20,22)x because of more favorable side chain conformational angles. For example, with Glu15 and Glu20 in the standard conformations (χ_1 = -170° and -80°, respectively, and χ_2 = +165° for both) a binding site can be formed with Glu13 (χ_1 = -180° and χ_2 = +49°) in which the metal ion is about 3.2 to 3.5 Å from the oxygen ligands of each Glu side chain. In contrast, with Glu15 and Glu20 at the above listed conformational angles and Glu22 positioned with χ_1 = -60° and χ_2 = 180°, the metal ion placed in between the three Glu side chains makes weaker contacts with the oxygens of the carboxylate groups (distances 4.2 to 4.9 Å). Improvement of the oxygen-metal distance can be achieved by changing the χ_2 angles of Glu15 and Glu20 to +60° and -60°, respectively. However, extended side chains with χ_2 near 180° are usually preferred (Janin & Wodak, 1978).

ii) Urea denaturation, reduced peptides

The urea denaturation results listed in Table VIII.2 for several reduced peptides are qualitatively similar to those of the oxidized peptides in Table VIII.1. As for their oxidized counterparts, Nr shows no dependence on $LaCl_3$ and E_2(13,22)r is destabilized by $LaCl_3$. E_2(15,20)r and E_3(13,15,20)r are only 70% and 50%, respectively, as helical in the absence of $LaCl_3$ as in the presence of 50 mM $LaCl_3$: the fraction of folded peptide is therefore calculated from comparison with the ellipticity in 50 mM $LaCl_3$, which is taken as a fraction folded of 1.0 (Fig. VIII.6). E_2(15,20)r and E_3(13,15,20)r display the same apparent $\Delta\Delta G_u$ of +2.9 kcal/mol (Table VIII.2), indicating that Glu13 in E_3(13,15,20) plays a lesser role in binding of La^{3+} ion to the reduced coiled-coil. As shown in Chapter VII (Kohn *et al.*, 1998c), the effects of the **e** and **g** positions on stability in the oxidized

Table VIII.2: Effects of $LaCl_3$ on coiled-coil stability: urea denaturation of reduced peptides at pH 7 [a].

Peptide [b]	- $LaCl_3$		+ 50 mM $LaCl_3$		$\Delta\Delta G_u$ [e]
	$[\text{urea}]_{1/2}$ [c]	*m* [d]	$[\text{urea}]_{1/2}$	*m*	
Nr	2.5	1.42	2.5	1.48	0.00
E_2(13,22)r	1.9	1.50	1.25	1.89	-1.10
E_2(15,20)r	0.5	1.42	2.6	1.39	+2.95
E_3(13,15,20)r	0.0	1.37	2.25	1.20	+2.9

[a] Data was collected at 20°C in a 50 mM tris, 100 mM KCl, pH 7 buffer.

[b] Peptide nomenclature is detailed under Peptide design and nomenclature (see also Figure VIII.1).

[c] $[\text{urea}]_{1/2}$ is the concentration of urea, in M, at which the peptide is 50% unfolded, as determined from the decrease in molar ellipticity at 222 nm with increasing denaturant concentration.

[d] *m* is the slope of the assumed linear relationship between ΔG_u and urea concentration.

[e] $\Delta\Delta G_u$ is the change in free energy of unfolding in kcal/mol upon $LaCl_3$ addition to the buffer. A positive $\Delta\Delta G_u$ is indicative of an apparent increase in stability. $\Delta\Delta G_u$ is calculated by the method of Serrano and Fersht (1989) (see Materials and Methods, pp. 56-59).

Peptide monomer concentrations were in the range 100 µM to 140 µM.

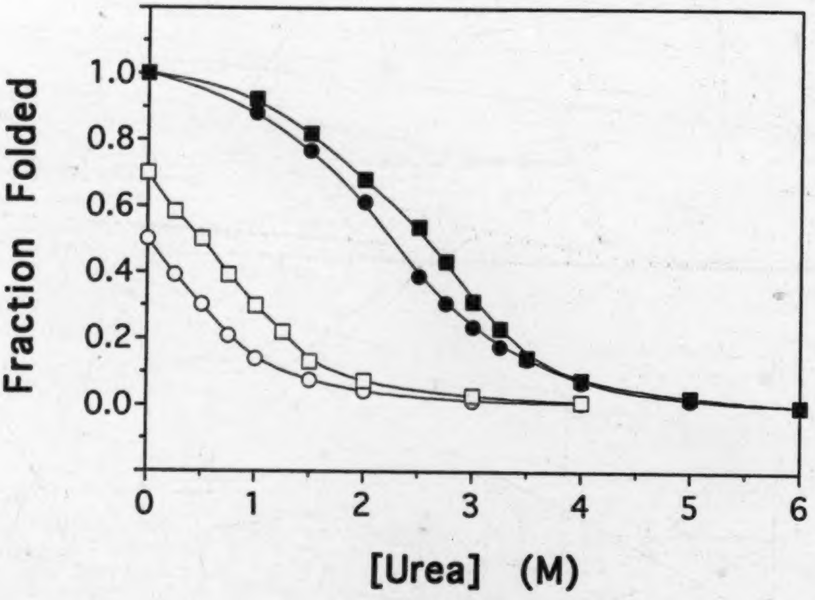

Figure VIII.6 Urea denaturation profiles of the reduced coiled-coils $E_3(13,15,20)x$ (circles) and $E_2(15,20)x$ (squares) at 20°C in 50 mM tris, 100 mM KCl, 5 mM DTT, pH 7 buffer in absence (open symbols) and presence (closed symbols) of 50 mM $LaCl_3$. The fraction of folded peptide was calculated from the observed mean residue molar ellipticity at 222 nm, as described under Materials and Methods (Chapter II, pp. 56-59). A fraction folded of 1.0 is assigned from the ellipticity in 50 mM $LaCl_3$ as described in the Results section (p. 230). The peptide concentration in the final solutions for CD measurements were 115 μM for $E_2(15,20)r$ and 108 μM for $E_3(13,15,20)r$.

and reduced forms of these model coiled-coils is often different, possibly as a result of greater dynamics in the reduced form. The much larger apparent $\Delta\Delta G_u$ for the reduced versus the oxidized form of both $E_2(15,20)$ and $E_3(13,15,20)$ may be a result of the energy of La^{3+} binding between helices helping to offset the loss of entropy resulting from dimerization. Such an effect is less of a factor for folding of the oxidized coiled-coils since they are covalently linked.

iii) Effects of 1 M $MgCl_2$ and $CaCl_2$ on urea denaturation behavior

Results for urea denaturation of Nx, $E_2(13,22)$x, and $E_2(15,20)$x, performed in the presence of 1 M $MgCl_2$ or in the presence of 1 M $MgCl_2$ and 50 mM $LaCl_3$, are summarized in Table VIII.3. The control, Nx, undergoes a large increase in $[\text{urea}]_{1/2}$ from 6.0 to 8.0 M and a $\Delta\Delta G_u$ of +1.5 kcal/mol upon addition of 1 M $MgCl_2$. We have previously observed that a high concentration of $MgCl_2$ or KCl increases the apparent stability of the native coiled-coil (Chapters IV, V, and VI, Kohn *et al.*, 1995b, 1997b, 1997c) and have suggested that this is due primarily to effects of the added salt on the solvent properties and modulation of nonlocal electrostatics within the peptide by salt ions (anion binding to Lys residues at heptad position f). Addition of 1 M $MgCl_2$ and 50 mM $LaCl_3$ results in a $\Delta\Delta G_u$ of +1.6 kcal/mol for Nx, about the same as for addition of 1 M $MgCl_2$ alone. $E_2(13,22)$x is also stabilized by 1 M $MgCl_2$ with a $\Delta\Delta G_u$ of +0.9 kcal/mol. Interestingly, the difference of 0.6 kcal/mol in the 1 M $MgCl_2$-induced $\Delta\Delta G_u$ values for Nx and $E_2(13,22)$x (Table VIII.3) is equal to the $\Delta\Delta G_u$ observed for $E_2(13,22)$x upon 50 mM $LaCl_3$ addition (Table VIII.1). This correlation suggests that $MgCl_2$ increases the apparent ΔG_u of both Nx and $E_2(13,22)$x by 1.5 kcal/mol due to general salt effects, but decreases the ΔG_u of $E_2(13,22)$x by about 0.6 kcal/mol due to preferential Mg^{2+} ion binding to the unfolded state, in a fashion similar to La^{3+}. With both 1 M $MgCl_2$ and 50 mM $LaCl_3$ present, the observed $\Delta\Delta G_u$ for $E_2(13,22)$x is only slightly lower (0.77 kcal/mol) and indicates that there is little additional destabilization resulting from the 50 mM La^{3+} with

Table VIII.3: Combined effects of $LaCl_3$ and $MgCl_2$ on stability of oxidized peptides: urea denaturation at pH 7 [a].

Peptide [b]	standard buffer		+ 1 M $MgCl_2$			+ 50 mM $LaCl_3$ & 1 M $MgCl_2$		
	$[urea]_{1/2}$ [c]	*m* [d]	$[urea]_{1/2}$	*m*	$\Delta\Delta G_u$ [e]	$[urea]_{1/2}$	*m*	$\Delta\Delta G_u$
Nx	6.0	0.83	8.0	0.71	+1.54	7.9	0.89	+1.63
E_2(13,22)x	5.15	0.83	6.35	0.66	+0.89	6.2	0.65	+0.77
E_2(15,20)x	4.25	0.95	5.5	0.99	+1.21	7.4	0.62	+2.47

[a] Data was collected at 20°C in a 50 mM tris, 100 mM KCl, pH 7 buffer (the 'standard' buffer conditions).

[b] Peptide nomenclature is detailed under Peptide design and nomenclature (see also Figure VIII.1).

[c] $[urea]_{1/2}$ is the concentration of urea, in M, at which the peptide is 50% unfolded, as determined from the decrease in molar ellipticity at 222 nm with increasing denaturant concentration.

[d] *m* is the slope of the assumed linear relationship between ΔG_u and urea concentration.

[e] $\Delta\Delta G_u$ is the change in free energy of unfolding in kcal/mol upon addition of the specified salts to the standard buffer. A positive $\Delta\Delta G_u$ is indicative of an apparent increase in stability. $\Delta\Delta G_u$ is calculated by the method of Serrano and Fersht (1989) (see Materials and Methods, pp. 56-59).

Peptide concentrations were in the range 70 µM to 90 µM.

20-fold more Mg^{2+} present. Thus, the excess of Mg^{2+} ions must effectively compete with La^{3+} ions for binding sites on the unfolded peptide.

Surprisingly, 1 M $MgCl_2$ results in a slightly smaller $\Delta\Delta G_u$ value for $E_2(15,20)x$ than for Nx (Table VIII.3). One would have expected that $E_2(15,20)x$ would undergo a larger stability increase than Nx resulting from binding of Mg^{2+} ions to Glu residues in the folded form of $E_2(15,20)x$, as appears to occur with La^{3+}. However, the presence of both 1 M $MgCl_2$ and 50 mM $LaCl_3$ leads to a much larger $\Delta\Delta G_u$ for $E_2(15,20)x$ than does 1M $MgCl_2$ itself. This contrasts with Nx and $E_2(13,22)x$, for which 1 M $MgCl_2$ affected the stability to about the same extent, regardless of whether 50 mM $LaCl_3$ was present. The $\Delta\Delta G_u$ for $E_2(15,20)x$ is 1.2 kcal/mol higher when 50 mM $LaCl_3$ and 1 M $MgCl_2$ are added to the buffer than for the addition of 1 M $MgCl_2$ alone, which compares closely to the $\Delta\Delta G_u$ of 1.08 kcal/mol obtained for 50 mM $LaCl_3$ in the absence of 1 M $MgCl_2$ (Table VIII.1). Thus, while Mg^{2+} appears to substitute for the destabilizing effect of La^{3+} on $E_2(13,22)x$ (presumably through binding to the unfolded state) it does not affect or substitute for the stabilizing effect of La^{3+} on $E_2(15,20)x$ (which presumably occurs through preferential binding to the folded state). Mg^{2+} could potentially have a much lower affinity than La^{3+} for the folded form of $E_2(15,20)x$ due to its smaller ionic radius (approximately 0.7 Å *versus* 1.0 Å) and its lower charge (leading to a lower attraction for ionized Glu residues). Urea denaturation of $E_2(15,20)x$ was repeated in the presence of 1 M $CaCl_2$ (Ca^{2+} has about the same ionic radius as La^{3+}). The result was similar to that obtained with 1 M $MgCl_2$ (data not shown); there was no apparent stabilizing effect due to metal ion binding. Thus, for $E_2(15,20)x$ the metal-binding effect is more specific for trivalent cations.

C. Conclusions

In nature, proteins require metal ions for binding of substrates, maintenance of structure and stability, catalysis, and allosteric control and regulation. While all of these functions for metal ions eventually could be incorporated into *de novo* designed proteins, designs to this point have focused primarily on metal ion-enhancement of protein conformation and stability. Several studies have demonstrated enhancement of secondary structure in peptides through metal ion-binding, either α-helical (Ghadiri & Choi, 1990; Ghadiri & Fernholtz, 1990; Ruan *et al.*, 1990) or β-turn (Cheng *et al.*, 1996; Schneider & Kelly, 1995; Tian & Bartlett, 1996). Metal-binding sites incorporated into designed helical bundles have resulted in metal-dependent stability and structural specificity. Two approaches have been used: incorporation of a metal-binding site into the hydrophobic core of the helical bundle, replacing nonspecific hydrophobic interactions with more geometrically specific metal-ligand interactions (Handel & DeGrado, 1990; Handel *et al.*, 1993; Regan & Clarke, 1990), or incorporation of a metal-binding moiety at one end (or both ends) of the helices allowing bound metal ion to tether the helices together (Ghadiri & Case, 1993; Ghadiri *et al.*, 1992a, 1992b; Lieberman & Sasaki, 1991).

In this study, it was demonstrated that metal ion-binding sites can be incorporated into a two-stranded α-helical coiled-coil. Residues involved in metal binding include those at the **e** and **g** heptad positions, which commonly contain hydrophilic side chains involved in interhelical interactions; however, the hydrophobic core is not altered. Binding of metal ions at these sites can have profound effects on coiled-coil stability, but the results also indicate that the metal ion bound form may have a less cooperative unfolding mechanism. This could be due to increased rigidity of the structure around the metal-binding site, resulting in greater resistance to unfolding in the middle of the coiled-coil. Thus, partially unfolded intermediates may be stabilized by the bound metal ion and present at higher concentration at equilibrium than in the absence of metal ion. The apparent enhancement of stability by metal binding was specific for a trivalent cation (La^{3+}), as the divalent cations Mg^{2+} and Ca^{2+} had no apparent metal-binding effect. The binding of La^{3+} to E$_2$(15,20)x appears to be weak (mM range), and one would predict Mg^{2+} and Ca^{2+} to bind even weaker due to the lower charge.

This study has shown that stabilizing metal ion-binding sites can be incorporated into coiled-coil proteins and suggests a potential for metal-dependent regulation of coiled-coil folding. To exploit this technology further, new design strategies will be investigated to increase metal-binding affinity, which in turn will increase the extent to which folding/stability can be modulated by metal binding.

CHAPTER IX

METAL ION INDUCED FOLDING OF A *DE NOVO* DESIGNED COILED-COIL PEPTIDE[7]

A. Introduction

In nature, proteins that perform important functions in catalysis, signalling, gene transcription, *etc.* are commonly under the control of external signals, such as metal ion or hormone ligands and phosphorylation, which exert allosteric control over protein function (conformational change from an inactive to an active state triggered by the external stimulus). One long-term goal of the *de novo* protein design process is to mimic the specific regulation of protein structure and function found in nature. As a first step toward the design of synthetic proteins that can be regulated, synthetic peptides or proteins that undergo large changes in conformation upon changes in environment or due to external stimuli such as ligand binding or covalent modification have been a design target. For example, peptides that switch from an α-helical to a β-sheet conformation upon a change in pH (Mutter *et al.*, 1991) or redox conditions (Dado & Gellman, 1993) have been successfully designed. Gonzalez *et al.* (1996a) recently designed an α-helical coiled-coil which switches from a dimer to a trimer upon binding of benzene within a cavity in its hydrophobic core. Vinson and co-workers have designed coiled-coils which are stabilized (Szilak *et al.*, 1997b) or destabilized (Szilak *et al.*, 1997a) by phosphorylation of a serine residue. Results in preceding chapters of the current work and other experiments (Fairman *et al.*, 1996; Graddis *et al.*, 1993; O'Shea *et al.*, 1993; Zhou *et al.*, 1994c) have illustrated that charged residues at the **e** and **g** positions can confer environmental sensitivity on coiled-coil stability due to the effects of pH and salt conditions on interhelical ionic interactions. For example, a coiled-coil that is unfolded at neutral pH, due to a large number of interhelical repulsions, can be induced to fold through a change in pH (resulting from neutralization of repelling side chains) or salt conditions (resulting from induction of hydrophobic interactions, charge screening, and/or ion binding) (Chapter IV, Kohn *et al.*, 1995b; Zhou *et al.*, 1994c). Similar effects of salts and pH have been observed for other helix-forming peptides (Goto & Aimoto, 1991; Goto & Hagihara, 1992; Ramalingam *et al.*, 1992).

---

[7] A version of this chapter has been published: Kohn, W. D., Kay, C. M., Sykes, B. D., and Hodges, R. S. (1998). *J. Am. Chem. Soc.* **120**, 1124-1132.

High affinity metal-binding sites can occur in proteins when the stereochemical requirements of the metal ion are accommodated by ligands on the protein, which are preorganized in conformationally-constrained environments in the folded structure. In Chapter VIII (Kohn *et al.*, 1998a), the stabilization of coiled-coil structure by bridging of metal ions between negatively-charged residues that normally repel one another across the dimer interface was illustrated. However, the binding energy was observed to be weak, with K_d values of around 15 mM for E_2(15,20)x (containing two Glu residues per metal-binding site) and 3 mM for E_3(13,15,20)x (containing three Glu residues per metal-binding site). The low binding affinity is a likely result of cooperation of only two or three carboxylate groups, which are conformationally unrestricted in the apo-state, in binding.

The next desired step in the design process was to use metal binding at a finite number of specific sites comprising residues in the **e** and **g** heptad positions to control coiled-coil folding. The ideal metal-dependent peptide would be designed in such a way that in the absence of bound metal ion, ionic repulsions would highly destabilize the coiled-coil and favor the unfolded state. In contrast, in the presence of metal ions negatively charged side chains, which would otherwise repel one another, are involved in preferential metal ion binding to the folded structure. It had already been shown in Chapter IV (Kohn *et al.*, 1995b) that E10x could be induced to fold by La^{3+} binding, but the nature of the peptide-metal complex was difficult to assess because of the large number of Glu residues present on the peptide that could act as metal ligands. The more defined metal binding sites in E_2(15,20)x and E_3(13,15,20)x in Chapter VIII (Kohn *et al.*, 1998a) were not highly successful for the purpose of inducing folding, partly because the peptides contained significant structure in the absence of metal ion. In addition, destabilization of the hydrophobic core to inhibit folding of the apo-peptide resulted in analogs in which metal binding was not of high enough affinity to induce folding. Success in overcoming the low-affinity problem was achieved by using metal-binding side-chain groups with multi-dentate binding ability, thereby increasing the strength of the metal-chelating effect. The design process, structural properties, and metal-binding behavior of the disulfide-bridged two-stranded coiled-coil, Gla$_2$Nx, are reported in this chapter.

B. Results

a) Peptide design

The metal binding peptides discussed in this paper are based on the 35-residue peptide Native-x (described in Chapter II, p. 60), which has been used as a control throughout the studies of electrostatic effects on coiled-coil stability contained within this thesis. Native-x consists of 35-residue peptide chains containing the heptad repeat $Q_gV_aG_bA_cL_dQ_eK_f$ (Fig. IX.1A). Val and Leu residues at positions **a** and **d**, respectively, form the hydrophobic face, which packs against the other helix in the dimer interface (Fig. IX.1B). Native-x contains Gln residues at all of the **e** and **g** positions, and there are no inter- or intrahelical electrostatic interactions in the peptide, making it a good control for studying electrostatics. A Cys residue substituted for Val at position 2 (heptad position **a**) allows formation of an interchain disulfide bridge. The disulfide bridge enhances formation of a parallel, in-register coiled-coil and simplifies the folding process from a bimolecular to a unimolecular process. The peptides can also be studied in the absence of a disulfide bridge by treating them with a reducing agent. An "x" after the peptide name indicates the peptide is present in the disulfide-bridged form. Native-x forms a stable coiled-coil at 20°C in pH 7 buffer with a ΔG_u of about 5.1 kcal/mol (Chapter III, Kohn *et al.*, 1995a).

Figure IX.1 (A) Sequences of the "Native" 35-residue model coiled-coil used as a starting point for design of a metal binding peptide (top) and the metal binding analog Gla_2Nx (bottom). A Cys residue at position 2 (heptad position **a**) allows formation of an interchain disulfide bridge. Substitutions at positions 15, 20, and 23 (shown boxed) are involved in design of Gla_2Nx as described under Peptide Design. In the sequence of Gla_2Nx, the Gla residues are represented by "X". **(B)** Cross-sectional helical wheel representation of the middle heptad (residues 15-21) of Gla_2Nx in the absence (left) and presence (right) of bound metal ions. The peptide is projected into the page from N- to C-terminus. Interchain **a-a'** and **d-d'** van der Waals packing interactions occur in the hydrophobic core between Val and Leu residues, respectively, and are indicated with arrows. The Gla side chains at positions **g** and **e** flank the hydrophobic interface and can thus lie across the interface and help shield it from water. However, interhelical **g-e'** ionic repulsions occur between these negatively charged side chains, greatly destabilizing the coiled-coil structure. Metal ions are proposed to stabilize the folded peptide via chelation of Gla15 on one chain and Gla20' on the other chain (four carboxylate groups total) to one metal ion. Two such binding sites are present on the coiled coil, which contains a two-fold symmetry axis.

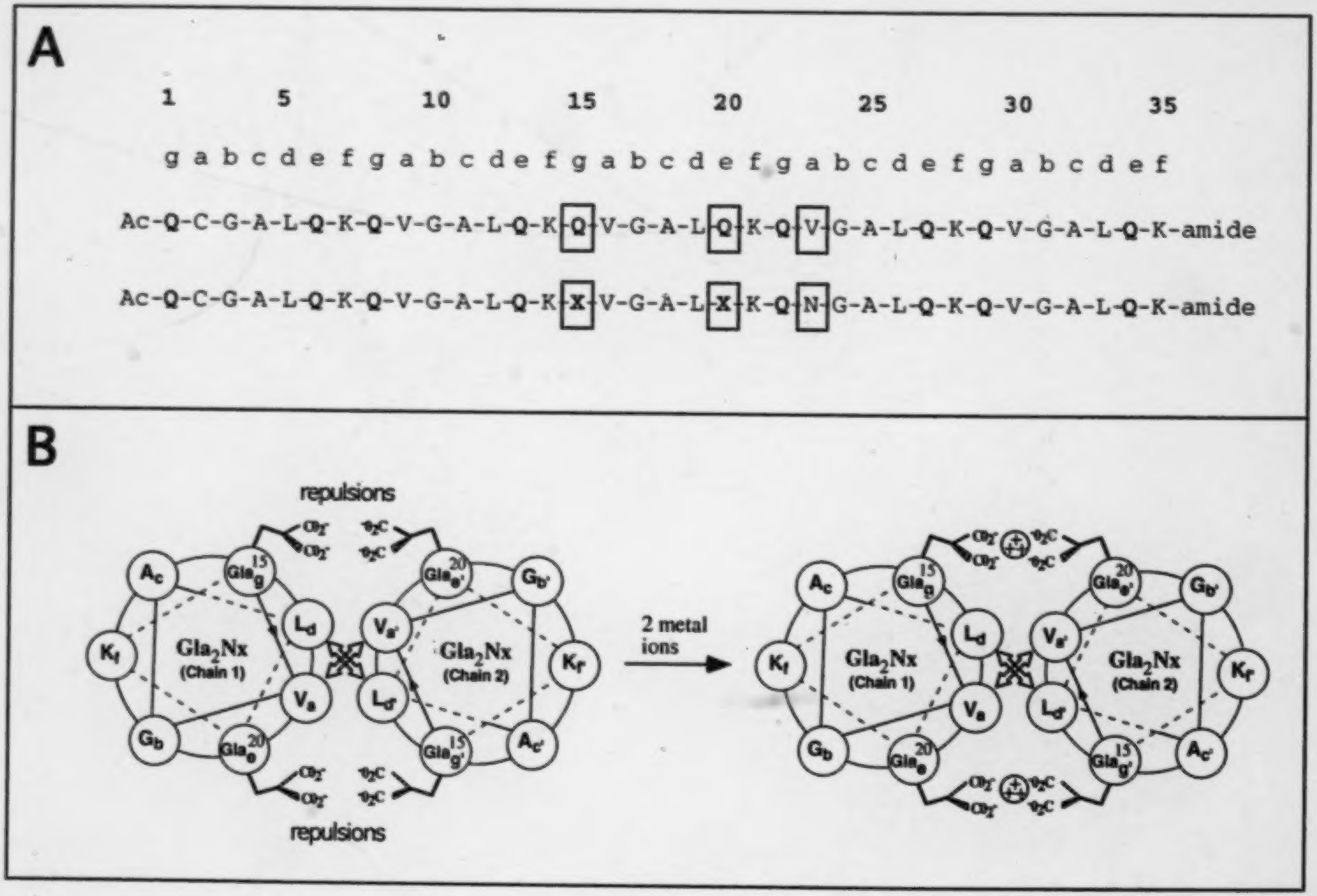
A
1 5 10 15 20 25 30 35
g a b c d e f g a b c d e f g a b c d e f g a b c d e f g a b c d e f
Ac-Q-C-G-A-L-Q-K-Q-V-G-A-L-Q-K-Q-V-G-A-L-Q-K-Q-V-G-A-L-Q-K-Q-V-G-A-L-Q-K-amide
Ac-Q-C-G-A-L-Q-K-Q-V-G-A-L-Q-K-X-V-G-A-L-X-K-Q-N-G-A-L-Q-K-Q-V-G-A-L-Q-K-amide
B
repulsions
repulsions
Gla2Nx (Chain 1)
Gla2Nx (Chain 2)
2 metal ions
Gla2Nx (Chain 1)
Gla2Nx (Chain 2)

A successfully designed analog, which undergoes a metal-induced folding transition, should be unstable enough that it is completely or nearly completely unfolded in the absence of the metal ion. The metal ion must bind to the folded state with a high enough affinity that the free energy of metal binding is enough to overcome the inherent instability of the peptide. Previously, it was shown that E_2(15,20)x, which is the same as Native-x but with substitutions of Glu for Gln at positions 15 and 20 (positions **g** and **e**, respectively, of the middle heptad), is destabilized relative to Native-x by about 1.5 kcal/mol at pH 7; this destabilization is due both to the introduction of interhelical Glu-Glu repulsions and to the lower inherent helical propensity and hydrophobicity characteristics of ionized Glu compared with Gln (Chapter III, Kohn *et al.*, 1995a). Addition of $LaCl_3$ to the buffer increases the stability of E_2(15,20)x, likely due to preferential binding of La^{3+} ions to the folded peptide (Chapter VIII, Kohn *et al.*, 1998a). Overall, the experiments in Chapter VIII supported the suggestion that a metal ion could bridge the Glu residues at positions 15 and 20', which are otherwise involved in repulsions. However, the binding affinity appears to be weak both with the metal binding site containing two Glu side chains and in the subsequent peptide E_3(13,15,20)x, in which the binding site contains three Glu side chains (on the order of 10^2 M^{-1}).

A further design evolution of E_3(13,15,20)x was performed in which the Val residue at position 16 was replaced with Glu. As can be deduced from Figure VIII.1 (p. 217), position 16 is the **a** position lying at the center of the three Glu residues in positions 13', 15, and 20'. This substitution was predicted to have a significant destabilizing effect due to introduction of the charged residue in the hydrophobic core, and the additional Glu residue was predicted to be able to increase the metal-binding affinity of the site (with four Glu side chains now potentially able to cooperatively bind a metal ion). Indeed, while E_3(13,15,20)x had a θ_{222} value of over -32,000 deg•cm^2•dmol^{-1} in benign buffer at 20°C, the new analog E_4(13,15,16,20)x was destabilized to a θ_{222} value of about -2,200 (almost completely unfolded). Addition of $LaCl_3$ led to a maximum θ_{222} value of -27,000 for

E_4(13,15,16,20)x, with the midpoint in the helicity increase obtained at about 0.5 mM $LaCl_3$, suggesting that the K_d was increased about ten-fold over that in E_3(13,15,20)x (estimated in Chapter VIII to be about 3 mM). In the reduced form, the peptide E_4(13,15,16,20) could not be induced to fold at all, apparently because the electrostatic destabilization of the coiled-coil was not overcome by the energy of metal binding alone but required the additional stabilization of the interhelical disulfide bridge. The oxidized peptide E_4(13,15,16,20)x, which was induced to fold by $LaCl_3$ was found to form large aggregates in the presence of $LaCl_3$ by sedimentation-equilibrium ultracentrifugation but did not aggregate in normal buffer (data not shown). Metal ions likely bind between the coiled-coil molecules to enhance this aggregation, and the metal-binding properties of the peptide cannot be easily characterized.

To amplify the effects of interhelical repulsions and metal binding on coiled-coil structure and at the same time achieve a metal binding peptide with more defined metal-binding properties (and which in particular does not aggregate), we have employed the unusual amino acid γ-carboxyglutamic acid (abbreviated Gla), which contains two carboxylate substituents on the γ-carbon (the side chain is a malonate type group). This amino acid occurs as a post-translational modification in human blood clotting factors and other proteins, in which it promotes conformational changes by binding Ca^{2+} (Furie & Furie, 1988; Hauschka & Carr, 1982; Prorok *et al.*, 1996; Soriano-Garcia *et al.*, 1992; Sunnerhagen *et al.*, 1995; Zell *et al.*, 1985). It has previously been shown that lanthanides preferentially bind free Gla at a 1:2 ratio (Sperling *et al.*, 1978). In such a complex, each Gla side chain can donate two carboxylate ligands so that the metal ion is coordinated by a total of four carboxylate groups. Sperling *et al.* (1978) had suggested that each carboxylate group may interact with the metal ion through both of its oxygen atoms (a bidentate carboxylate-metal interaction). This would fit with the known preference of lanthanides for a higher coordination number by providing a total of eight oxygens from four carboxylates to fill the primary coordination sphere. However, X-ray crystallographic results suggested that interaction of only one oxygen from each carboxylate of a malonate group is the preferred mode of interaction for a variety of metals including lanthanides (Zell *et al.*, 1985). Based on the previous experiments in Chapter VIII (Kohn *et al.*, 1998a), it was predicted that Gla residues substituted at positions 15 and 20 of each chain of the coiled-coil should result in formation of two lanthanide binding sites (with each site comprising Gla15 of one chain and Gla20' of the other chain) with much higher affinity than was observed with Glu at those positions (Fig. IX.1B). Destabilization due to Gla-Gla repulsion should also be much higher than for Glu-Glu repulsion due to the extra carboxylate (extra charge) on each side chain. This latter effect was important to achieve an unfolded apo-state.

NMR measurements of the metal-Gla complex gave an approximate distance of 3.7 Å between the γ-carbon of each Gla group and the metal ion (Sperling *et al.*, 1978). Computer modelling of Gla_2Nx using the high resolution X-ray structure of the GCN4 leucine zipper (O'Shea *et al.*, 1991) as a template for the backbone coordinates indicated that a metal ion could fit nicely between the Gla15 and Gla20' side chains. The distance between the γ-carbons of the Gla side chains and the metal in this model is about 3.5 Å, in close agreement with the results of Sperling *et al.* (1978). The computer model also predicts that the two bound metal ions are about 11 Å apart and are separated by the hydrophobic core residues (Fig. IX.1B).

The first analog containing Gla substitutions studied was Gla_2x, which contains Gln to Gla substitutions at positions 15 and 20. It was found to be about 45% as helical as Native-x by CD spectroscopy at 20°C in pH 7 buffer (data not shown). The reduced peptide, Gla_2r, was mostly unfolded in the apo state ($\theta_{222} = -2{,}000$ deg•cm^2•dmol^{-1}), and could be induced to a maximal θ_{222} value of only about -22,000 (about 65% helical). This peptide was observed by sedimentation-equilibrium ultracentrifugation to form a mixture of dimer and trimer in the presence of $LaCl_3$. The coiled-coil sequence was further destabilized by substitution of Asn for Val at position 23 (heptad position **a**) to obtain the peptide Gla_2Nx (Fig, IX.1A). Asn occurs frequently at position a in native dimeric coiled-coils, particularly leucine zippers (Hu & Sauer, 1992), and is destabilizing relative to Val but appears to play a role in specifying formation of dimers rather than higher order species due to formation of specific interhelical Asn-Asn hydrogen bonds (Harbury *et al.*, 1993; Lumb & Kim, 1995a). The latest design iteration was therefore intended to result in a disulfide-bridged peptide that was mostly unfolded and would be induced to a highly folded nonaggregated (two-stranded) state upon metal binding.

b) Structural Characteristics of Gla_2Nx

The CD spectra of Gla_2Nx and Native-x in benign, pH 7 buffer are shown in Figure IX.2. The spectrum of Native-x is characteristic of α-helical structure with minima at 208 and 222 nm and a maximum at 195 nm (Chen *et al.*, 1974). The ratio of the molar ellipticities at 222 and 208 nm, $\theta_{222}/\theta_{208}$, is greater than 1, which is indicative of coiled-coil structure (Cooper & Woody, 1990). The θ_{222} value is a measure of the amount of helical content. The θ_{222} value for Native-x is about -35,000 $deg \cdot cm^2 \cdot dmol^{-1}$, which is approximately the value expected for a fully helical 35-residue peptide (Chen *et al.*, 1974). In contrast, Gla_2Nx has a θ_{222} value of only -2,500 and the shape of the CD spectrum is characteristic of a random coil with a minimum at about 200 nm (Chen *et al.*, 1974). The helix-enhancing solvent TFE substantially increases the θ_{222} value of Gla_2Nx (Fig. IX.2) to -21,000 (about 60% helical) but has no effect on the helical content of Native-x (Chapter III, Kohn *et al.*, 1995a). Under aqueous conditions and assuming a two-state folding transition (see Chapter II), helix formation in Gla_2Nx requires burial of the hydrophobic face through coiled-coil formation. The folding process appears to be inhibited by interhelical Gla-Gla repulsion, as was observed in Chapter IV (Kohn *et al.*, 1995b) for Glu-Glu repulsions. In contrast, a 50:50 mixture of TFE and water is able to stabilize an isolated amphipathic helix because of the lower polarity of this solvent mixture and the helix-enhancing properties of TFE (Hirota *et al.*, 1998; Lau *et al.*, 1984a; Sonnichsen *et*

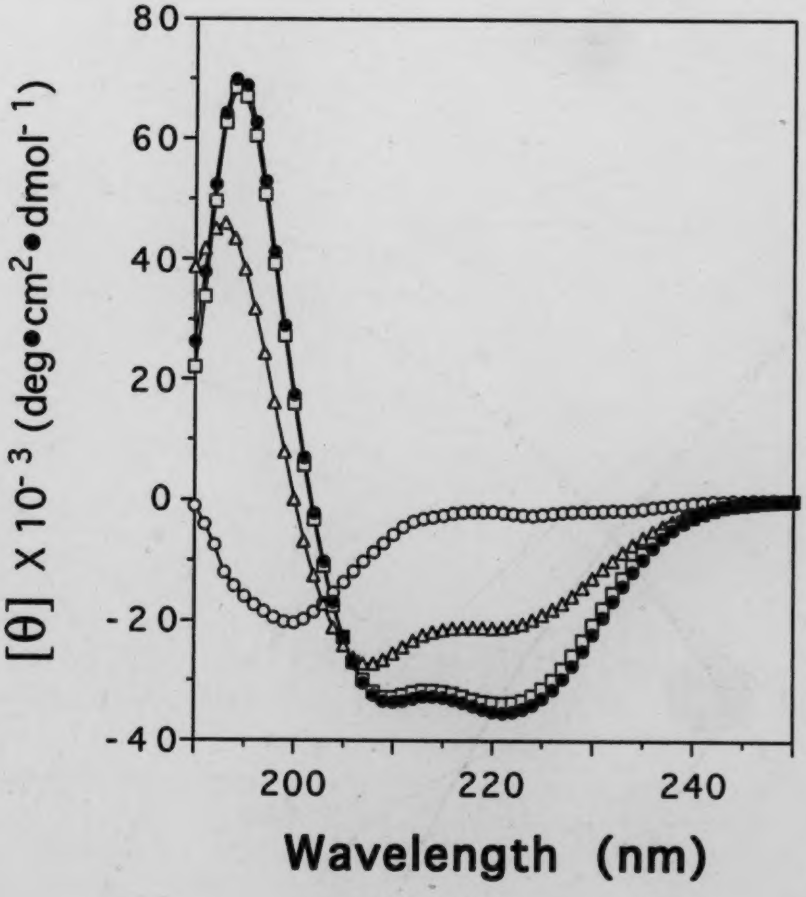

Figure IX.2 Circular dichroism spectra of Gla$_2$Nx (open symbols) and Native-x (closed symbols). Spectra were collected in a 25 mM MOPs, 25 mM KCl buffer at pH 7 and 20°C (circles) and also for Gla$_2$Nx in the same buffer containing 50% TFE (v:v) (triangles) or 5 mM LaCl$_3$ (squares).

al., 1992). The low θ_{222} of Gla$_2$Nx in 50% TFE suggests that Gla residues are helix destabilizing, as was observed for Glu residues in E10x in 50% TFE (Chapter IV, Kohn *et al.*, 1995b). The θ_{222} value of Gla$_2$Nx at 80°C is about -1600 deg•cm^2•dmol^{-1}. Taking this as the θ_{222} value of the fully unfolded peptide and the θ_{222} value of Native-x (-35,000) as the fully folded form, indicates that Gla$_2$Nx is about 3% folded under benign conditions at 20°C. Addition of 5 mM LaCl$_3$ to the buffer greatly increases the θ_{222} value of Gla$_2$Nx to -34,000 (Fig. IX.2), which is essentially equal to that of Native-x within experimental error. Thus, as predicted, LaCl$_3$ substantially increases the amount of coiled-coil formation by Gla$_2$Nx at 20°C from approximately 3 to 100%, presumably due to binding of La^{3+} ions to the Gla side chain carboxylate groups in the folded structure.

Sedimentation-equilibrium ultracentrifugation experiments were performed on Gla$_2$Nx at a peptide concentration of ~1 mg/ml (0.13 mM) both in the presence and absence of 5 mM LaCl$_3$ (about a 40:1 ratio of metal to peptide). The data fit a single-species model for the two-stranded form under both conditions (Fig. IX.3), indicating that no aggregation of this disulfide-bridged two-stranded coiled-coil peptide occurs upon La^{3+} binding. Further evidence against peptide aggregation in the presence of 5 mM LaCl$_3$ comes from the observation that the θ_{222} value is independent of peptide concentration over the range 10-400 μM (0.1-3 mg/ml) (data not shown). Additional sedimentation-equilibrium experiments were carried out at a peptide concentration of ~2 mg/ml (0.26 mM) in the presence of either 2.5 mM or 0.25 mM LaCl$_3$ (a 10:1 or 1:1 metal:peptide ratio, respectively). The results were fit to a single-species model equally as well as those shown in Figure IX.3. Thus, no evidence of aggregation was apparent under any of the conditions tested.

The ^{1}H NMR spectrum of Gla$_2$Nx in the absence of LaCl$_3$ is characteristic of a random coil peptide with little chemical shift dispersion (Fig. IX.4). Saturation of the peptide with La^{3+} ion causes significant changes in the spectrum. The amount of dispersion is increased, consistent with a more ordered structure. For example, the Leu methyl region

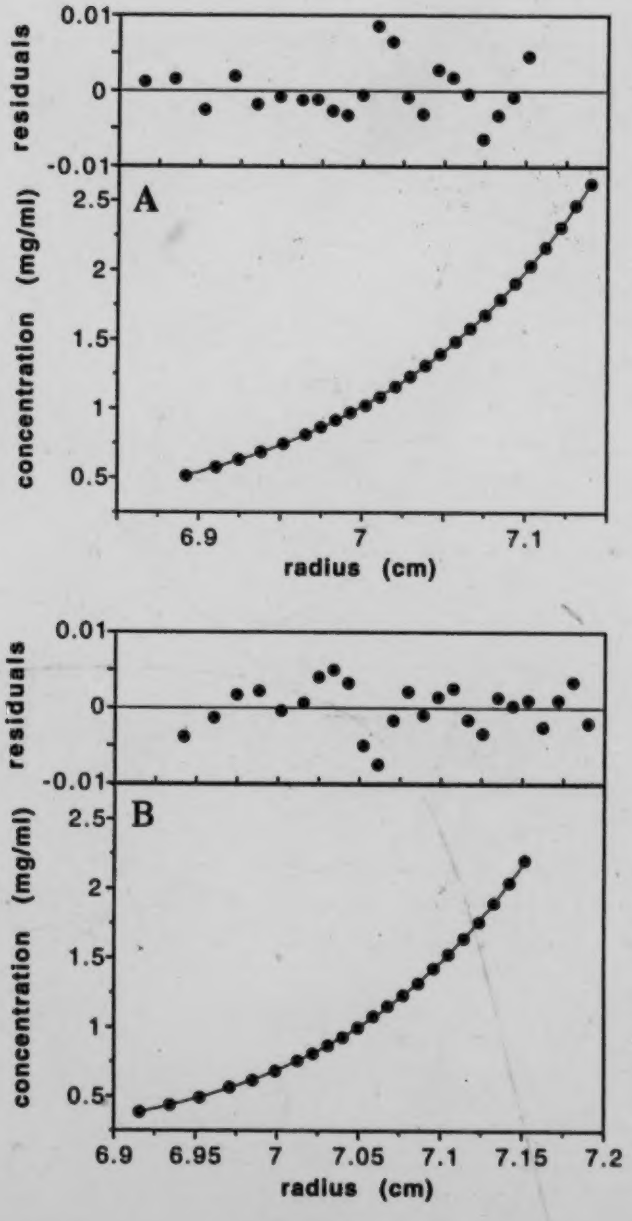

Figure IX.3 Sedimentation-equilibrium results for Gla$_2$Nx at 20°C and pH 7 in 50 mM tris, 100 mM KCl buffer in the absence (A) and presence (B) of 5 mM LaCl$_3$. Peptide concentration was approximately 1.2 mg/ml (0.16 mM) and 1.0 mg/ml (0.13 mM) in (A) and (B), respectively. A single species (two-stranded monomer) curve fit to the raw data is shown (lower panels) with the residuals from the curve fits (upper panels). The data were collected at a rotor speed of 34,000 rpm.

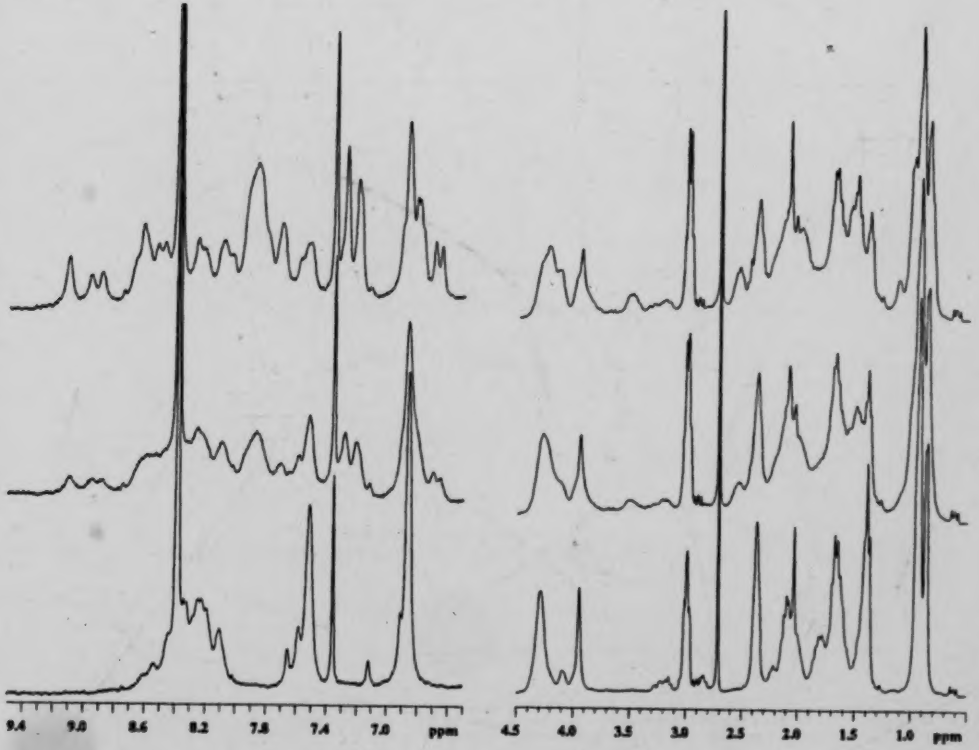

Figure IX.4 One-dimensional 300 MHz ^{1}H-NMR spectra of Gla$_2$Nx in the absence of LaCl$_3$ (bottom), presence of 0.5 mM LaCl$_3$ (middle), and presence of 1.0 mM LaCl$_3$ (top) in 50 mM deuterated imidazole, 50 mM KCl, 0.1 mM DSS buffer at pH 6.9 and 25°C. Peptide concentration was 0.5 mM.

near 1 ppm shows an increased chemical shift spread. The upfield shift of α-proton resonances is consistent with α-helix formation (Wishart *et al.*, 1991). In particular, the appearance of a peak at about 3.5 ppm is diagnostic for the α-proton of valine in a helical conformation (Wishart *et al.*, 1991). A large increase in the number of peaks in the backbone amide region around 7-9 ppm may arise both from greater dispersion and from increased protection from hydrogen exchange (Englander & Mayne, 1992) as the peptide adopts a helical conformation.

Binding of paramagnetic lanthanide ions leads to perturbations in both the line width (relaxation) and chemical shift of the NMR resonances of a peptide ligand (Geraldes, 1993). Both effects are dependent on the distance, r, from the nucleus to the metal ion ($1/r^6$ and $1/r^3$ dependence, respectively) while the chemical shift perturbation is also dependent on the orientation of the nucleus with respect to the metal ion (Geraldes, 1993). Typically, some of these shifted resonances appear well outside the envelope of the diamagnetic spectrum. Similarly, a number of highly shifted peaks appear in the ^{1}H-NMR spectrum of Gla_2Nx in the presence of the paramagnetic lanthanide ytterbium (III), Yb^{3+} (Fig. IX.5). The shifting of selected resonances in the NMR spectrum of Gla_2Nx in the presence of Yb^{3+} is evidence for the binding of the metal ion to specific sites on the peptide. Lanthanide-induced chemical shift and relaxation perturbations can be used to give fairly high definition structural information by fitting of the observed spectrum to a proposed structure (Geraldes, 1993; Lee & Sykes, 1980). Such investigations are currently underway on the $Yb^{3+}{\bullet}Gla_2Nx$ complex.

c) pH dependence

The helicity of Gla_2Nx, as indicated by CD spectroscopy, is highly dependent on pH. As the pH is decreased, side chain protonation reduces interhelical Gla-Gla repulsions and allows increased coiled-coil formation (Fig. IX.6). A similar effect has been observed previously for coiled-coil peptides prevented from folding at neutral pH by interhelical Glu-Glu repulsions (Graddis *et al.*, 1993; Kohn *et al.*, 1995b, Chapter IV; O'Shea *et al.*, 1993;

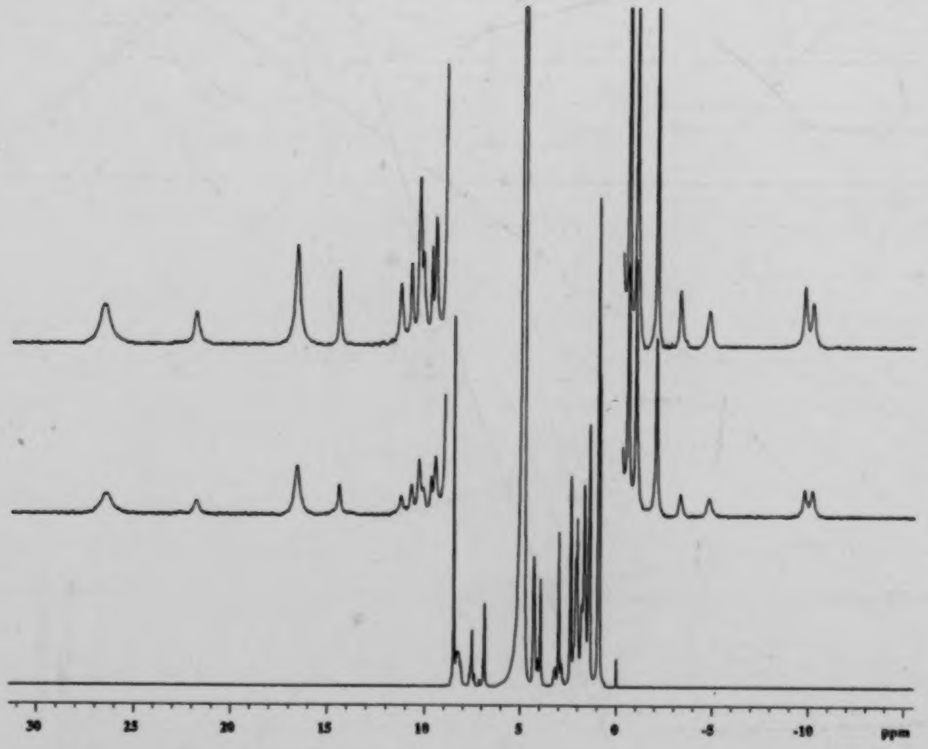

Figure IX.5 One-dimensional 300 MHz ^{1}H-NMR spectra of Gla$_2$Nx in the absence of YbCl$_3$ (bottom), presence of 0.6 mM YbCl$_3$ (middle), and presence of 1.2 mM LaCl$_3$ (top) in 50 mM deuterated imidazole, 50 mM KCl, 0.1 mM DSS buffer at pH 6.9 and 25°C. Peptide concentration = 0.6 mM. The vertical scale in the top and middle spectra is expanded approximately 1000-fold relative to the bottom spectrum.

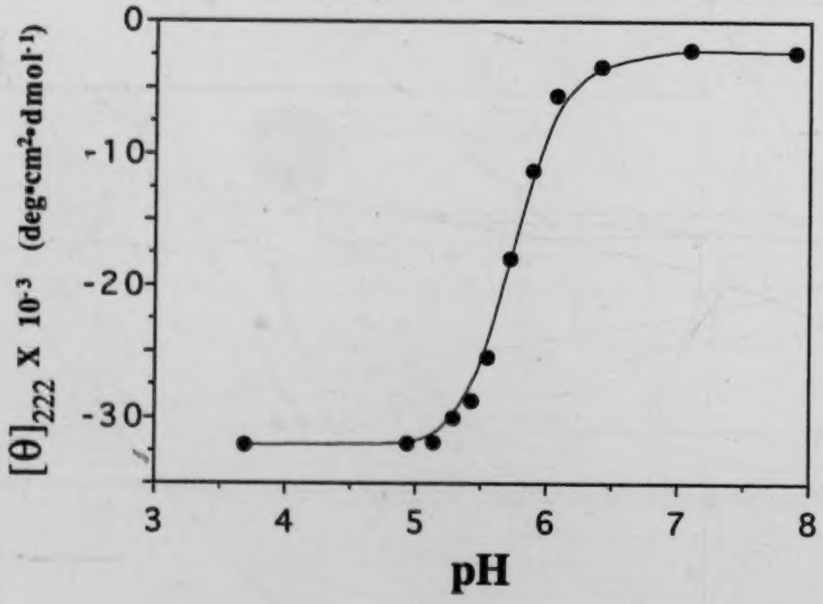

Figure IX.6 Effect of pH on the mean residue molar ellipticity at 222 nm (θ_{222}) of Gla$_2$Nx. Data were collected at 20°C in a 50 mM PO_4, 100 mM KCl, 1 mM EDTA buffer. Peptide concentration was 59 µM.

Zhou *et al.*, 1994c). The folding transition takes place over approximately one pH unit from pH 6.2 to 5.2 with the transition midpoint at about pH 5.7. The two γ-carboxylate groups of free Gla have pK_a values of approximately 5 and 3 (Marki *et al.*, 1977a, 1977b; Sperling *et al.*, 1978), so at pH 7 both should be fully ionized. The observed pH-dependent folding transition of Gla_2Nx may correlate with protonation of one carboxylate per Gla residue. This would leave one negative charge per Gla residue and might be expected to allow complete coiled-coil formation since the analog E_2(15,20)x is fully folded at pH 7 despite two interhelical Glu-Glu repulsions (Chapter III, Kohn *et al.*, 1995a). It was pointed out in Chapter IV (Kohn *et al.*, 1995b) that the midpoint of the pH-induced folding transition does not equal the pK_a of the carboxylate groups being titrated because this pK_a must be different in the folded and unfolded states in order for the side chain to have an effect on stability (Yang & Honig, 1993). Instead, the pK_a of the carboxylate groups changes from one value, which corresponds to the beginning of the transition, to another value, which corresponds to the end of the transition (Yang & Honig, 1993). Thus, if the transition observed in Figure IX.6 is indeed due to the protonation of one carboxylate on each Gla side chain, the pK_a would be about 5.2 in the unfolded peptide (comparable to the pK_a in free Gla) and 6.2 in the folded peptide.

d) Stability

As mentioned above, the control Native-x has a ΔG_u at 20°C of about 5.1 kcal/mol. Native-x has a $[urea]_{1/2}$ value of 6.0 M at 20°C and pH 7 and is unaffected by the addition of a small concentration of $LaCl_3$ (≤ 50 mM) to the buffer (Fig. IX.7). Gla_2Nx is only about 3% folded at pH 7 and 20°C (Fig. IX.2), which corresponds to a ΔG_u of about -2.0 kcal/mol. In the presence of 5 mM $LaCl_3$, it is fully folded (Fig. IX.2), and urea denaturation yields a $[urea]_{1/2}$ value of 3.7 M (Fig. IX.7) and a ΔG_u^{H2O} of approximately 3.1 kcal/mol. At 0.5 mM $LaCl_3$, a $[urea]_{1/2}$ of 3.5 M and ΔG_u of 2.9 kcal/mol were obtained. The small effect of a ten-fold increase in total $LaCl_3$ concentration on stability is an indication that metal binding is tight. Thus, Gla_2Nx can be stabilized by as much as 5.1

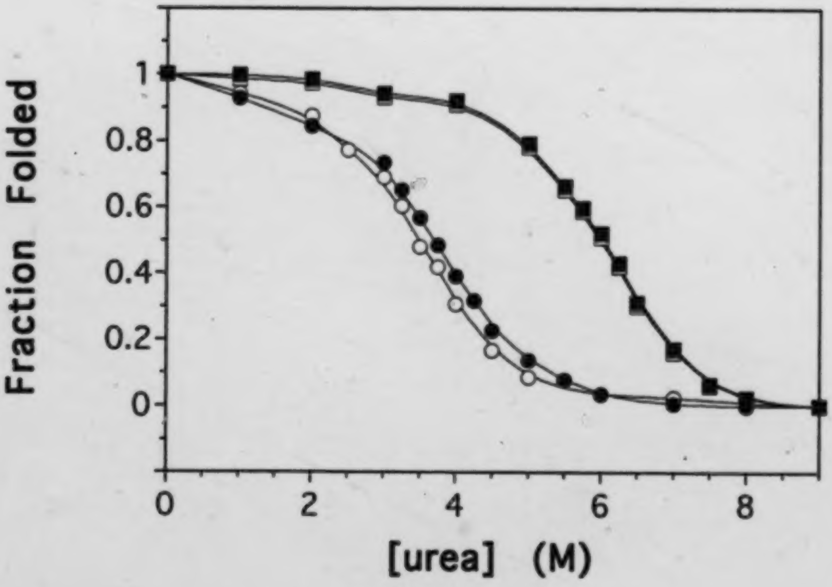

Figure IX.7 Urea denaturation curves for Gla_2Nx (circles) and Native-x (squares) at 20°C in 50 mM tris, 100 mM KCl, pH 6.9 buffer containing 0.5 mM $LaCl_3$ (open symbols) or 5 mM $LaCl_3$ (closed symbols). The fraction of folded peptide was calculated from the observed mean residue ellipticity at 222 nm as described under Materials and Methods (Chapter II, pp. 56-59). Peptide concentrations were in the range 60-70 μM.

kcal/mol by La^{3+} ion binding. In contrast, $E_2(15,20)x$, in which Glu rather than Gla side chains are involved in La^{3+} complexation, was stabilized only 1.1 kcal/mol by 50 mM $LaCl_3$ and 0.2 kcal/mol by 5 mM $LaCl_3$ (Chapter VIII, Kohn *et al.*, 1998a). Therefore, the effect of metal binding on stability is significantly higher in Gla_2Nx because of the chelate effect of the Gla side chain and resulting higher binding affinity.

e) Metal ion titration monitored by CD spectroscopy

CD spectroscopy can be used to indirectly monitor the binding of a ligand to a protein by measuring the induction of secondary structure upon ligand binding. For Gla_2Nx, the induction of helicity can be observed as a function of $LaCl_3$ concentration. Titration of Gla_2Nx with $LaCl_3$ leads to a somewhat linear increase in θ_{222} with increased La^{3+} concentration (Fig. IX.8A). The slope of the titration indicates that, as predicted, the stoichiometry of binding is two La^{3+} ions per peptide (where the 'peptide' is the disulfide-bridged two-stranded molecule). Thus, at the titration midpoint the metal/peptide ratio is about 1:1, and if the straight line is extended to the maximal θ_{222} value, the metal/peptide ratio is about 2:1. However, the actual amount of La^{3+} required to reach the maximum θ_{222} value is about 2.5 equivalents because the binding is not extremely tight. The data is similar in shape to what is generally obtained for a single binding site and suggests that there is no cooperativity between the sites. However, the actual binding mechanism is not totally clear from this data because it could also be fit to a model with complete positive cooperativity (see Discussion). Fitting of the titration curve to a model of two independent binding sites (see Chapter II, p. 55) gives an apparent average dissociation constant, K_d, of 0.6 ± 0.3 μM. Titration with $YbCl_3$ yielded a virtually identical result with an apparent K_d of 0.4 ± 0.2 μM (Fig. IX.8B). Therefore, the smaller radius of Yb^{3+} (0.86Å) versus that of La^{3+} (1.06 Å) has no effect on the binding affinity for Gla_2Nx.

Titration with $CaCl_2$ also was found to increase the θ_{222} value of Gla_2Nx (Fig. IX.8C). However, the maximum θ_{222} value induced by Ca^{2+} addition is only -21,000

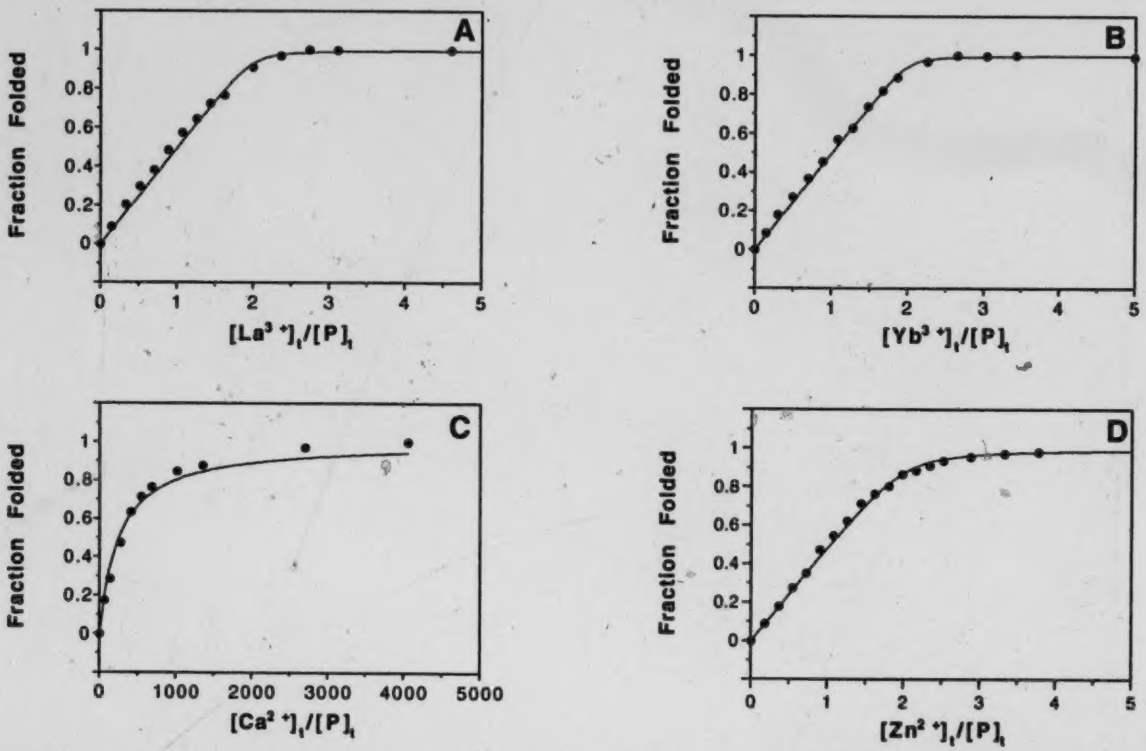

Figure IX.8 Metal titration profiles of Gla_2Nx as monitored by circular dichroism spectroscopy at 20°C and pH 6.9 in a 10 mM imidazole, 50 mM KCl buffer. The observed mean residue ellipticity at 222 nm was monitored and plotted as the fraction folded (described in Chapter II, pp. 56-59). Titrations were performed with **(A)** $LaCl_3$, **(B)** $YbCl_3$, **(C)** $CaCl_2$, and **(D)** $ZnCl_2$. Peptide concentration was 64, 64, 69, and 54 μM in panels A-D, respectively. The x coordinate is the ratio of total metal ion concentration to total peptide concentration. The data were fit using a least squares curve fitting procedure as detailed under Materials and Methods (Chapter II, p. 55).

deg•cm^2•dmol^{-1} (about 60% helix). In addition, the apparent K_d for binding of Ca^{2+} to Gla_2Nx is about 18 ± 2 mM, which is 30,000 fold weaker than the estimated affinity for La^{3+}. Ca^{2+} typically has a 100 to 1000 fold lower binding affinity than lanthanides for native proteins such as Gla-containing proteins (Furie & Furie, 1975; Furie *et al.*, 1976) and EF hand Ca^{2+}-binding proteins (Gariepy *et al.*, 1983; Wang *et al.*, 1981; Williams *et al.*, 1984) depending on the lanthanide used and the nature of the binding site. Thus, the metal binding sites of Gla_2Nx are more discriminatory for lanthanides over Ca^{2+} than those of many native Ca^{2+} binding proteins.

In contrast to the results obtained with Ca^{2+}, titration of Gla_2Nx with $ZnCl_2$ illustrated a reasonably high affinity for Zn^{2+} (Fig. IX.8D). In addition, the maximum θ_{222} obtained from binding of Zn^{2+} was -32,900 deg•cm^2•dmol^{-1}, close to that observed with the two lanthanides. The apparent K_d obtained from the $ZnCl_2$ titration curve is approximately 1.7 ± 0.3 μM. Thus, Zn^{2+} binds to Gla_2Nx slightly less tightly than either La^{3+} or Yb^{3+}, for which the apparent K_d values were about 0.5 μM. The large difference between the observed K_d values for Ca^{2+} and Zn^{2+} shows that binding affinity is not affected simply by the charge of the metal ion. The smaller radius of Zn^{2+} (about 0.74 Å) versus that of Ca^{2+} (about 1.0 Å) results in a charge density approximately 2.5 times higher, which likely plays a role in the tighter binding of Zn^{2+}. However, the differences in the electronic configurations (specifically the presence of 10 electrons in the 3d orbitals of Zn and no electrons in the 3d orbitals of Ca) and preferred coordination numbers, between Zn^{2+} and Ca^{2+} probably also play a role in their vastly different affinities for binding sites on Gla_2Nx.

f) Metal ion titration monitored by NMR spectroscopy

Binding of lanthanide ions to Gla_2Nx results in new peaks in the ^1H NMR spectrum arising from the metal-bound, folded form of the peptide (Figs. IX.4 and IX.5). These peaks gradually grow in intensity at their final chemical shift (the chemical shift observed in the metal-saturated spectrum). Thus, lanthanide binding is in the slow exchange limit on the NMR timescale since no averaging of proton resonances in the bound and unbound states occurs. The slow exchange behavior suggests an upper limit for the K_d of approximately 1 μM, similar to what was estimated by monitoring the titration with CD spectroscopy. The NMR data was not quantitatively analyzed. However, it did provide evidence to support the existence of two binding sites on Gla_2Nx because approximately two equivalents of lanthanide ion led to a maximum in the peak intensity of lanthanide shifted peaks (data not shown). In addition, lanthanide titration leads to the appearance of a single set of lanthanide-shifted NMR resonances (presumably due to the final species), which supports the conclusion that metal binding is highly cooperative (see Discussion).

C. Discussion

This paper describes the design and characterization of the disulfide-bridged two-stranded coiled-coil peptide Gla_2Nx, which undergoes a folding transition upon binding of lanthanide ions to two specific binding sites engineered into the molecule. While this peptide is almost completely unfolded under benign, pH 7 conditions at 20°C, it becomes highly helical upon addition of a small concentration of lanthanide ion. Indirect measurement of the titration of Gla_2Nx with either $LaCl_3$ or $YbCl_3$ using CD spectroscopy indicates tight binding of two metal ions per coiled-coil with a dissociation constant of around 0.5 μM. In contrast, Gla_2Nx shows a very weak affinity for Ca^{2+} ($K_d \approx 18$ mM), suggesting a dramatic preference for binding trivalent lanthanides over divalent alkali metal ions. Zn^{2+} was found to bind Gla_2Nx with an apparent affinity ($K_d \approx 1.7$ μM) close to that of the lanthanides. Thus, the charge of the metal ion is not the only important factor in controlling the strength of interaction.

The electronic configuration greatly affects the interaction of metal ions with ligands. Ca^{2+}, Yb^{3+}, and La^{3+} are comparable since all three have no electrons in the (n-1) d orbitals and are termed as class (a) or "hard" Lewis acids (Pearson, 1963). Zn^{2+} has completely filled 3d orbitals and is considered borderline between classes (a) and (b) (Pearson, 1963). The greater the "softness" of the metal ion, the greater the degree to which interactions with ligands can be covalent versus ionic in nature (Pearson, 1963). Accordingly, Zn^{2+} is able to interact with ligands through a higher degree of covalent bond character while the lanthanides and Ca^{2+} tend more toward ionic bonds. Therefore, the higher affinity of Gla_2Nx for the trivalent lanthanides over Ca^{2+} is at least partially due to the higher cation charge allowing for stronger ionic interactions. On the other hand, Zn^{2+} may be able to compensate for a weaker electrostatic interaction with the carboxylate ligands versus that of the trivalent lanthanides due to an increased covalent bond contribution.

The strength of the different metal complexes with Gla_2Nx may also be affected by the coordination number and geometry. Ca^{2+} typically is 6-coordinate with an octahedral geometry, Zn^{2+} is generally tetrahedral or octahedral and sometimes forms 5-coordinate complexes, and the lanthanides tend to have coordination numbers between 6 and 9 (Huheey, 1983). In Gla_2Nx the binding site is likely to contain four oxygen ligands (one from each of four carboxylate groups). This site could be well suited for tetrahedral Zn^{2+} coordination. Modelling of the metal binding site in Gla_2Nx using the backbone coordinates of the GCN4 leucine zipper (O'Shea *et al.*, 1991) as a starting structure suggests it is possible for the Gla15 and Gla20' side chains to be oriented such that a distorted tetrahedral geometry about a metal ion could be achieved. On the other hand, the four carboxylate oxygens proposed to bind the metal ion could also be coplanar and thus interact with the metal in a square planar type arrangement. These carboxylates could fill four positions of an octahedral complex with water filling the other sites. Such an arrangement might be expected to occur for binding of lanthanide ions or Ca^{2+}. However, from the present data it is not possible to make conclusions about these details of the metal-peptide interaction.

Several previous *de novo* design efforts have focused on enhancement of either α-helical (Ghadiri & Choi, 1990; Ghadiri & Fernholtz, 1990; Ruan *et al.*, 1990) or β-turn (Cheng *et al.*, 1996; Schneider & Kelly, 1995; Tian & Bartlett, 1996) structure in small peptides through complexation of metal ions. Metal binding sites have also been incorporated into designed four-helix bundles, resulting in metal ion-induced increases in stability but not folding (Handel & DeGrado, 1990; Handel *et al.*, 1993; Regan & Clarke, 1990). Metal binding sites engineered into the core of helical bundles were found to increase the specificity of the fold by replacing nonspecific hydrophobic interactions with defined metal-side chain interactions (Handel *et al.*, 1993). This approach has recently been applied in controlling coiled-coil oligomerization states (Dieckmann *et al.*, 1997). Another approach involves incorporation of a metal-binding group at one or both ends of short helix-forming sequences, which allows metal-induced helical bundle assembly (Ghadiri & Case, 1993; Ghadiri *et al.*, 1992a, 1992b; Lieberman & Sasaki, 1991). The latter studies illustrate metal-induced increases in folding, but the peptides are 30% or more helical in the absence of metal ion at room temperature. Thus, to our knowledge Gla_2Nx undergoes the largest metal-induced folding transition of a *de novo* designed peptide. However, while Gla_2Nx was estimated to be stabilized by about 5 kcal/mol from the binding of two La^{3+} ions, the binding of two Zn^{2+} ions to the four-helix bundle $H6\alpha_4$ induced a larger stabilization of 7.8 kcal/mol (Handel *et al.*, 1993).

The lanthanide binding affinity of Gla_2Nx is comparable with previous results from Gla-containing peptides and proteins. For example, fragment 12-44 of prothrombin was found to have a single high affinity ($K_d = 0.55\ \mu M$) Gd^{3+} binding site, which was postulated to involve two or three Gla residues situated at the ends of a disulfide loop and bridged by a metal ion (Furie *et al.*, 1979). Such an interaction is similar to the proposed bridging of Gla15 and Gla20' of Gla_2Nx by a metal ion. The Gla domains of the blood clotting enzymes Factor X and prothrombin were found to contain two high affinity sites and a number of lower affinity sites, which bind Gd^{3+} with K_d values of 0.1 to 1 μM and

10 to 20 mM, respectively (Furie & Furie, 1975; Furie *et al.*, 1976). Thus, the affinity of Gla_2Nx for lanthanide ions is similar to the high affinity sites of intact native Gla domains.

Elucidation of the mechanism for metal binding and resulting induced folding of Gla_2Nx is an interesting problem. A scheme for the process, which assumes two metal binding sites are present in the peptide and that peptide folding is a two-state process, is shown in Figure IX.9A. In the absence of added metal ion, there is only a small amount of folded peptide (species 2, Fig. IX.9A) present at 20°C. Added metal ion will preferentially bind to the folded state and remove folded peptide from the unfolded/folded equilibrium, thus shifting that equilibrium toward the folded state. Subsequently, a second metal ion can bind. In curve fitting the CD titration data, it was initially assumed that the two proposed binding sites are identical and independent ($K_1=K_2$). Such a situation can occur when the protein is a symmetrical oligomer and each subunit has the same binding site. Gla_2Nx is symmetrical with two identical binding sites and therefore meets these criteria. Alternatively, if binding of the first ligand changes the structure and enhances binding of subsequent ligands, cooperative binding results. In Gla_2Nx, cooperativity could occur as a result of the first bound metal decreasing the flexibility (dynamics) of the folded peptide. Such an effect was suggested to explain the cooperativity observed for Ca^{2+} binding to calbindin despite the absence of a conformational change upon binding of the first Ca^{2+} ion (Akke *et al.*, 1991).

In the lanthanide titration of Gla_2Nx, monitoring by CD spectroscopy results in a linear increase in helicity with added metal ion. The slope corresponds to a stoichiometry of two metal ions per two-stranded coiled-coil peptide. The data suggest that all the folded peptide being detected by CD is bound to two metal ions. If a significant amount of folded peptide with only one metal bound were present at equilibrium, the CD titration curve should be steeper and its midpoint should occur at less than a 1:1 ratio of metal ion to two-stranded coiled-coil peptide. Instead, this titration curve suggests that binding of one metal ion stabilizes the "folded" peptide and enhances binding of the second metal ion, such that

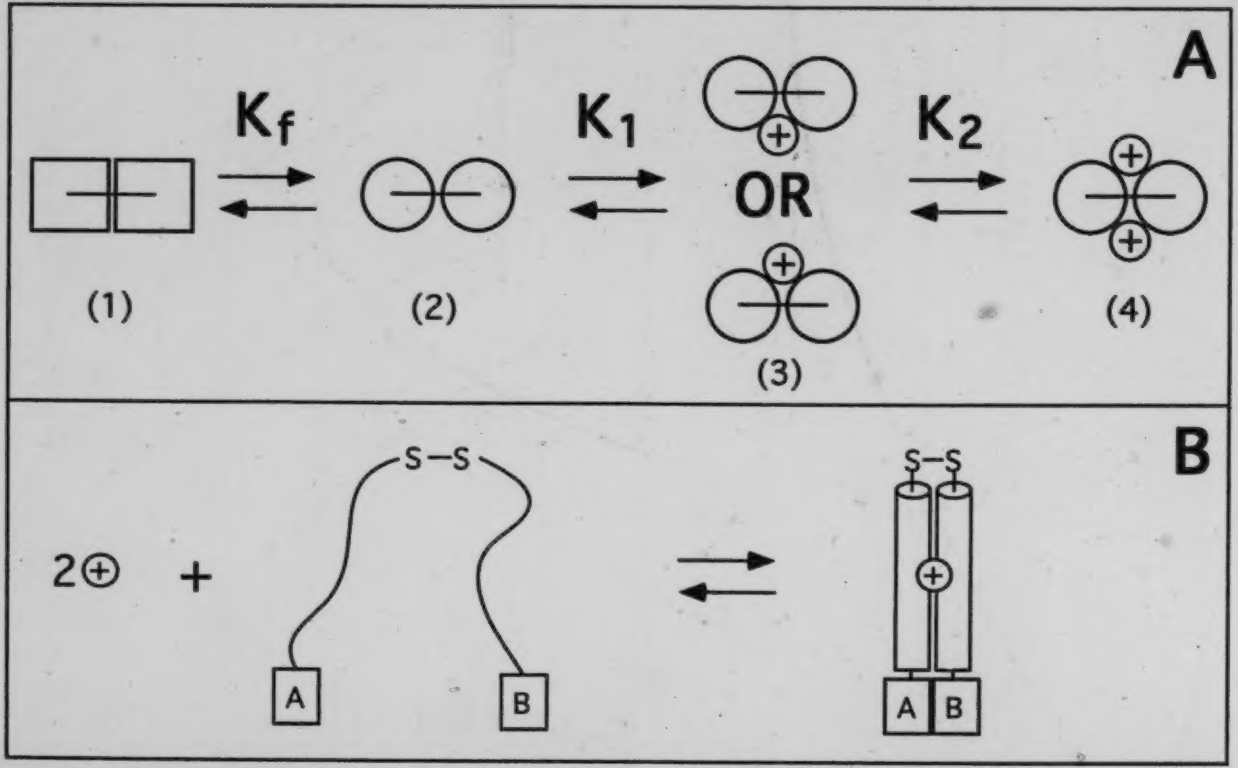

Figure IX.9 (A) Schematic representation of possible species and equilibria involved in lanthanide-induced folding of Gla_2Nx, assuming that peptide folding is a two-state process and that the metal ion binds to the folded peptide. Squares stand for unfolded peptide chains and circles represent α-helices. Four predicted species include the unfolded peptide (1), folded peptide (2), folded peptide bound to one metal ion (3), and folded peptide bound to two metal ions (4). (B) Potential application of metal-induced coiled-coil formation for reversible association of two molecules or domains A and B attached to the C-termini of the disulfide-bridged coiled-coil strands. Cylinders represent α-helices. In both panels, metal ions are represented by a circle with a plus sign.

peptide folding is coincident with binding of two metal ions. Therefore, the data can be interpreted in terms of complete positive cooperativity in which the second binding constant is many orders of magnitude larger than the first. The apparent binding affinity, which was obtained assuming independent binding sites, would in this case be indicative of the first binding constant only.

The lanthanide titration of Gla_2Nx monitored by NMR also supports the conclusion that metal binding is highly cooperative. Only a single set of lanthanide shifted peaks appear in the NMR spectrum, which it seems must arise from the final structure bound to two metal ions (species 4, Fig. IX.9A). However, if a significant amount of singly bound intermediate (species 3, Fig. IX.9A) were present during the titration, peaks characteristic of that structure would be expected to initially rise and then disappear in the NMR spectrum. Such peaks would originate from protons which are close to and thus perturbed by both metal ions, as observed for the binding of Yb^{3+} to the two Ca^{2+} binding sites of parvalbumin (Lee & Sykes, 1980).

There are several potential applications of metal binding peptides. For example, two groups recently designed zinc finger peptides with fluorescent tags, which undergo zinc dependent fluorescence changes and therefore can act as metal ion sensors (Godwin & Berg, 1996; Walkup & Imperiali, 1996). Similarly, Gla_2Nx could act as a sensor for lanthanide ions with relatively high specificity over Ca^{2+} and other alkali ions. More generally, a peptide such as Gla_2Nx could be used for reversible assembly of any two molecules (A and B) covalently attached to the C-termini of the two coiled-coil chains (Fig. IX.9B). In the absence of the metal ion, the coiled-coil would be unfolded and molecules A and B would not be closely associated. Metal-induced folding of the coiled-coil would bring domains A and B together in a well-defined, close proximity and could be used as a switch for some activity that is dependent on A-B association. This could include applications such as reversible receptor subunit assembly or assembly of a functional catalytic domain from two fragments. In addition, because metal ions have catalytic properties (Volbeda *et al.*, 1996; Williams, 1995), a metal-binding peptide could conceivably be developed into a synthetic enzyme at the metal-binding site itself. For example, lanthanides are known to promote phosphate ester hydrolysis and transesterification of RNA (Morrow *et al.*, 1992), suggesting that a lanthanide-binding peptide could be designed which binds to and cleaves a particular RNA sequence. Metal-binding peptides could be developed as carriers for radioimaging metals, specifically technetium-99m or other metals with diagnostic or therapeutic applications (Abrams & Murrer, 1993). It appears promising that metal-binding peptides will be developed for such uses in coming years.

Chapter X

GENERAL DISCUSSION

The studies contained herein were intended to further the understanding of the role of interhelical electrostatic interactions involving the **e** and **g** heptad positions in the specificity and stability of coiled-coil formation. Many insights have been obtained in this body of work which help explain the effects of both ionic attractions and repulsions on coiled-coil stability and, importantly, the modulation of these effects by buffer conditions. Understanding the effect of these interhelical electrostatic interactions on stability has, in addition to giving a better understanding of interhelical interactions in protein folding in general, led to the ability to design metal binding sites through manipulation of the electrostatics within the molecule. This has implications for further design of molecules that can be regulated by buffer conditions (such as salt and pH). Some of the important aspects of this work are discussed below.

1) Specificity of g-e' interactions

The effect of interhelical electrostatic repulsions on coiled-coil stability has been shown previously to be significant, as discussed in Chapter I. The specificity of these interactions was clearly shown in the studies presented in Chapter III (Kohn *et al.*, 1995a). As predicted by the previous modelling and X-ray crystallographic results, the interactions occur preferentially in the **g-e'** (i to i'+5) orientation rather than the **e-g'** (i to i'+2) orientation. The magnitude of the Glu-Glu repulsion was estimated to be about 0.45-0.5 kcal/mol, very similar to the previous measurements of electrostatic interactions in coiled-coils (Krylov *et al.*, 1994; Zhou *et al.*, 1994b) and other surface-exposed electrostatic interactions (Dao-pin *et al.*, 1991; Lyu *et al.*, 1992; Sali *et al.*, 1991; Scholtz *et al.*, 1993; Serrano *et al.*, 1990). As discussed in Chapter IV (Kohn *et al.*, 1995b), the effect of these repulsions on stability can be manifested both directly in their repulsive electrostatic energy and indirectly through their disruptive effect on folding of the **e** and **g** side chains at the dimer interface, resulting in reduced hydrophobic surface burial. For example, it was found that the distance between carboxylate oxygens of Glu15 and Glu20' could be increased from a minimum of about 3 Å to a maximum of almost 9 Å by orienting both side chains away from the dimer interface.

2) General versus specific ionic repulsions/attractions and effects of salts on interhelical electrostatics

One question that we have wished to address is the role of general electrostatics (net charge at the coiled-coil interface) *versus* specific charge-charge interactions on stability. In Chapter IV (Kohn *et al.*, 1995b), it was clearly shown that increasing the number of Gln to Glu substitutions (systematically increasing both the number of **g-e'** Glu-Glu repulsions and the net interface charge) led to a systematic loss of stability. A summary of the effect of these substitutions in the presence of low salt (0.1 M KCl) and high salt (3 M KCl) is shown in Figure X.1. The plot at high salt shows a linear loss of stability in the middle three heptads (going from 2 to 8 Glu substitutions per chain) of approximately 1.2 kcal/mol for every two Glu substitutions per chain. In Chapter IV, it was concluded that this destabilization is likely due to 0.6 kcal/mol destabilization from the intrinsic stability effects of Gln to Glu substitution and 0.6 kcal/mol due to two Glu-Glu repulsions (0.3 kcal/mol each rather than the 0.45 kcal/mol observed in Chapter III, suggesting some charge screening). However, in Chapter V (Kohn *et al.*, 1997b) it was observed that the intrinsic destabilization of a Gln to Glu substitution at position **g** was only 60% as large at 3 M KCl as at 100 mM KCl. In light of this result, the 1.2 kcal/mol destabilization observed at 3 M KCl could instead be 0.6 X 0.6 kcal/mol = 0.36 kcal/mol due to intrinsic effects and 0.84 kcal/mol due to repulsions (0.42 kcal/mol each). Therefore, the repulsions may be screened very little by the high KCl concentration. In Chapter VIII (Kohn *et al.*, 1998a) the $\Delta\Delta G_u$

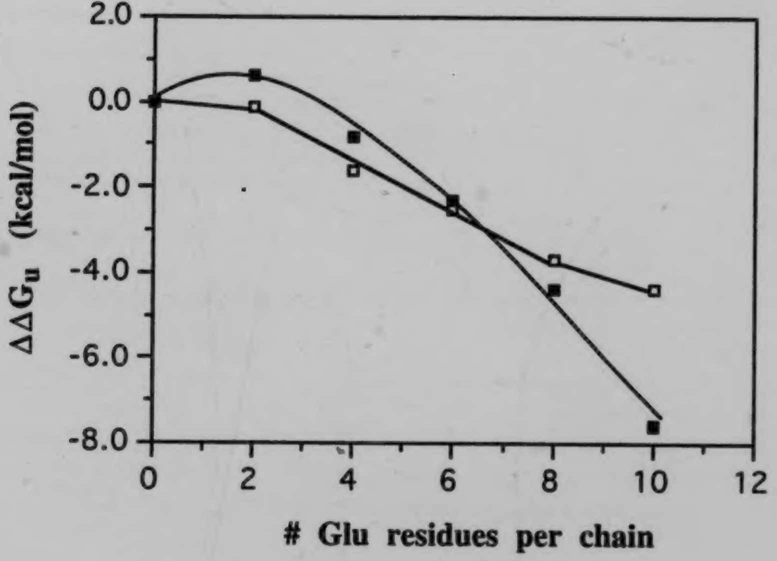

Figure X.1 Effects of increasing numbers of Glu substitutions for Gln at heptad positions e and g on coiled-coil stability at pH 7. Data were collected at 20°C in 50 mM PO_4 buffer containing 0.1 M (closed squares) or 3 M (open squares) KCl. The $\Delta\Delta G_u$ values are given in Table IV.2. For E10x at 0.1 M KCl, a denaturation curve could not be obtained. It was estimated to be 1% folded based on the difference in θ_{220} between E10r and E10x (see Table IV.1) and assuming E10r represents the fully unfolded state. $\Delta\Delta G_u$ for E10x was then calculated from $\Delta G_u = -RT\ln(f_u/f_f)$ and the ΔG_u for Nx of about 4.9 kcal/mol.

values for $E_2(13,22)x$ and $E_2(15,20)x$ relative to Nx in buffer containing 1 M $MgCl_2$ were -1.2 kcal/mol and -2.1 kcal/mol, respectively, suggesting a **g-e'** Glu-Glu repulsive effect of 0.45 kcal/mol under these conditions and again indicative of limited 'screening' of the Glu-Glu repulsions by the high salt concentration. Similarly, in Chapters VI and VII (Kohn *et al.*, 1997c and 1998c) KCl appeared to have little effect on the interhelical **g-e'** Lys-Glu ion pairs. As suggested in Chapter VI (Kohn *et al.*, 1997c), perhaps the synergy between **g-e'** electrostatic interactions and hydrophobic packing makes these interactions more difficult to screen than other surface-exposed electrostatics. The presence of a high salt concentration appears to stabilize the coiled-coils by promoting hydrophobic interactions, as seen in the increased stability of Nx at high salt concentration. Likewise, salt could promote the hydrophobic interactions of charged side chains at the **e** and **g** positions with the hydrophobic core and therefore keep the charged termini close together making it difficult to screen the electrostatics.

In contrast, general (or long-range) electrostatic effects will be more easily screened by salt due to the fact that D_{eff} increases with the separation distance between charges (see Chapter I, p. 12). Comparison of the effect on stability of ionized Glu substitutions at low *versus* high KCl concentration (Fig. X.1) shows that the increase in $\Delta\Delta G_u$ is steeper at low salt than at high salt, which may be due to the buildup of net interface charge that is effectively screened at 3 M KCl. The results suggest that net interface charge can play a significant role, particularly as it gets larger, but that this role is somewhat smaller in magnitude than the effect of specific repulsions on stability. The effect of salt on enhancing the folding of coiled-coils held apart by interhelical Lys-Lys or Glu-Glu repulsions seems to be to screen the general charge component of the repulsions and to enhance folding by promoting stronger hydrophobic interactions, emphasizing the importance of hydrophobic interactions in coiled-coil folding. It was also concluded in a recent study of a 30-residue coiled-coil containing Glu at all the **e** and **g** positions that the promotion of hydrophobic interactions by salts, particularly those containing kosmotropic anions like sulfate and fluoride, played a much more significant role in salt-induced folding than screening of electrostatic repulsions (Jelesarov *et al.*, 1998). The enhancement of folding by a high salt concentration (3.7 M KF) was characterized by a rapid folding rate ($k_{on} = 2 \times 10^7$ $M^{-1} \cdot s^{-1}$) and a large change in heat capacity upon unfolding ($\Delta C_p = 0.95$ kcal•mol^{-1}•K)

The results of Monera *et al.* (1993, 1994) and those shown in Figure IV.12 (p. 124) for the heterodimer KE-EKx also support a role for general electrostatics in coiled-coil folding. In these cases, it was observed that five Glu-Glu and five Lys-Lys **g-e'** repulsions did not prevent coiled-coil folding, presumably because the net charge on the interacting helix faces was zero. The stability was however decreased by about 2.5 to 3.0 kcal/mol relative to the case where all Glu-Lys attractions were present. This result is consistent with a smaller role for the specific **g-e'** interactions than for the general electrostatics on stability, in contrast to the results of the systematic Gln to Glu substitution study. Therefore, the results to date support a role for both general and specific electrostatics in coiled-coil stability, but the relative roles of each are not exactly clear and may indeed vary depending on the particular sequence context.

Recent stopped-flow kinetic experiments on coiled-coil folding also support a role for general electrostatics. The rate of formation (k_{on}) of a heterodimer consisting of one chain containing Lys at all **e** and **g** positions and the other chain containing Glu at all **e** and **g** positions was found to be decreased by increased ionic strength, suggesting the folding occurs via an electrostatically-stabilized transition state (Wendt *et al.*, 1997). Other recent kinetic experiments suggest helix formation is not rate-limiting for coiled-coil folding and that the transition state may not be very helical but instead a hydrophobic / electrostatic collapse intermediate (Sosnick *et al.*, 1996). The dissociation rate (k_{off}) was found to increase only slightly at higher ionic strength (Wendt *et al.*, 1997), suggesting a smaller role for ionic attractions in stabilizing the coiled-coil thermodynamically (see below).

3) Additivity of g-e' interactions

As discussed in Chapter VII (Kohn *et al.*, 1998c), the issue of additivity is central to attempts at quantifying the energetic effects of various noncovalent interactions on coiled-coil folding and extrapolation of these findings to protein design and the general understanding of protein folding. In Chapter VII, it was suggested that group additivity occurs for the **g-e'** Lys-Glu ion pairs since a similar average $\Delta\Delta G_u^{int}$ was obtained whether the effect was studied in all five heptads or only the middle (third) heptad of the coiled-coil. Similar results were obtained for Glu-Glu repulsions (Figs. IV.11 and X.1). For example, in going from E4x to E6x, the destabilization is 1.5 kcal/mol (Table IV.2), which equals the destabilization in going from Nx to E_2(15,20)x (Table III.2); these are the same substitutions (at positions 15 and 20) in different contexts: Gln at all the other **e** and **g** positions in E_2(15,20)x but Glu residues at some of the other **e** and **g** positions (1, 6, 8, and 13) in E6x. The effects of general electrostatics do appear to decrease the additivity of Glu-Glu repulsions at higher net interface charges under conditions of low ionic strength (Fig. X.1).

Another more difficult issue is the degree of energy component additivity, which is a measure of the degree of independence between various types of noncovalent interactions; for example, ionic and hydrophobic/packing interactions. If such additivity does not occur, then attempts to sum the different components to predict protein stability are rather futile, but there is very little sound evidence for general additivity in biochemistry (Dill, 1997). The assumptions of additivity, such as in molecular mechanics energy potentials (Harvey, 1989), therefore lie on somewhat shaky foundations. One significant difficulty is the importance of entropy in protein folding, for which additivity is often poor (Dill, 1997).

Site-directed mutagenesis in proteins has shown that multiple point mutations that are far apart in the tertiary structure generally act independently on protein stability and protein-protein interactions because the perturbations of structure and energetics resulting from a mutation are generally local (Wells, 1990). However, once the energetic effects of residues that are in close proximity are considered, proving additivity becomes more difficult, requiring the testing of thermodynamic cycles (Horovitz & Fersht, 1990). Currently, there is limited evidence from model protein studies in favor of energy component additivity. Comparison of the results in Chapter VII (Kohn *et al.*, 1998c) with previous mutational studies indicated that the context plays a role in stability effects of mutations in coiled-coils. Because the **e** and **g** positions pack against the hydrophobes at positions **a** and **d** and also can interact with residues at positions **b** and **c**, the apparent energy of a **g-e'** interaction determined from double mutant cycle analysis may be significantly affected by interactions of the residues at positions **g** and **e'** with their surrounding environment. Our results are consistent with the hypothesis of a synergy between **g-e'** electrostatics and the packing at the coiled-coil interface, supporting context as a major stability determinant. Other model peptide studies have demonstrated the role of context in determining effects of mutations on stability parameters (for example Merutka *et al.*, 1990; Moitra *et al.*, 1997; Sereda *et al.*, 1994). In general, determination of an exact quantitative value for a particular type of interaction that will apply in all contexts is not possible, but relative stability parameters are a more attainable goal. For example, a number of α-helical propensity scales that are experimentally derived from substitutions in different model systems give similar relative propensity rankings even though the absolute values vary (Myers *et al.*, 1997; Zhou *et al.*, 1994d). Similarly, our results in Chapter VII (Kohn *et al.*, 1998c) and those of Krylov *et al.* (1994) both suggest that interhelical Lys-Glu interactions occur preferentially in the E_e-K_g orientation, but the absolute values vary most likely as a result of context effects. Our studies have been carried out in a model system, in which the effects of context have been minimized as much as possible, but the results are still expected to be somewhat model dependent. Clearly, more work is needed to understand the effect of the surrounding environment on the additivity of noncovalent interactions in proteins. For example, the issue of context dependence could be addressed in our model coiled-coil by replacing the noninteracting Gly or Ala residues in the **b** and **c** positions, respectively, with residues that would be able to interact with the side chains at position **e** or **g** and repeating the double mutant cycle analysis

4) Dynamics of coiled-coil structure and mutational effects on stability

Dynamics is an important yet often overlooked aspect of protein structure. Short coiled-coils, such as the 35mers studied here, would be expected to be quite dynamic molecules. The available experimental evidence is mixed on the degree of dynamics / flexibility in short coiled-coils. Several recent kinetic experiments have shown a relatively rapid rate of strand exchange (exchange between the folded and unfolded states) in solution on the order of 1 s^{-1} (Patel *et al.*, 1994; Wendt *et al.*, 1995, 1997), although other experiments give much slower estimates for the rate of strand exchange in the range 10^{-3} to 10^{-4} s^{-1} (Chao *et al.*, 1996; Zitzewitz *et al.*, 1995). It was suggested that rapid strand exchange may be important for efficient sorting of some coiled-coils in the biological milieu (Wendt *et al.*, 1995). Backbone dynamics measurements of the Jun homodimer by two-dimensional ^{1}H-^{15}N NMR gave an order parameter ,S^2, of 0.7 to 0.9 over most of the sequence, which is in the range for the backbone of the 'rigid' core of most proteins (Wagner, 1995). Another NMR study of deuterium exchange rates in the GCN4 leucine zipper showed large variations over the length of the molecule, suggesting the presence of local dynamics that lead to conformational substates (Goodman & Kim, 1991). Holtzer and colleagues have further shown using ^{13}C NMR the presence of conformational flexibility along the GCN4 leucine zipper, leading to slowly interconverting folded substates (Holtzer *et al.*, 1997; Lovett *et al.*, 1996). These NMR experiments have shown, in particular, the tendency for greater conformational flexibility at the ends of the helices as would be predicted due to helix fraying (Goodman & Kim, 1991; Holtzer *et al.*, 1997; Mackay *et al.*, 1996) and fit with the observations by Zhou *et al.* (1992a, 1992b) that destabilizing hydrophobic core substitutions have a less pronounced effect at the ends of a coiled-coil than in the middle. Similarly, the current work, particularly in Chapters IV, V, and VII

(Kohn *et al.*, 1995b, 1997b, 1998c), showed that stability contributions of the **e** and **g** positions are also less significant at the N- and C-terminal heptads than in the middle of the coiled-coil. In addition, the effects of charged residues in positions **e** and **g** at the ends of the helices are complicated by the presence of interactions with the dipolar groups of the helix backbone, as demonstrated in Chapter V (Kohn *et al.*, 1997b).

An interchain disulfide bridge is expected to play a major role in altering the dynamics of short coiled-coils. For example, the dynamics study of the Jun homodimer was performed on a variant containing an N-terminal disulfide linker, and the S^2 values at the N terminus were the same as in the middle while those at the non-disulfide-linked C terminus were reduced due to fraying (Mackay *et al.*, 1996). In contrast, deuterium exchange studies of an N-terminally disulfide-bridged GCN4 leucine zipper showed similarly high rates of exchange at both the N and C termini (Goodman & Kim, 1991). The rate of exchange between the folded and unfolded states would be expected to be substantially decreased by the presence of a covalent linkage between the helices although there are no studies that have addressed this issue specifically.

One of the interesting results in our studies were the observation that both ionized Glu and Lys substitutions had significantly different effects on stability at positions 15(g) and 20(e) only when the N-terminal disulfide bridge was present (compare Tables VII.1 and VII.6). However, these effects are subtle. For example, at low pH there is a distinct stability difference between E15 and E20 both in the presence and absence of a disulfide bridge. Zhou *et al.* (1992b) observed a distinct difference between the effects on stability of Ala mutations at positions **a** and **d** only in the presence of a disulfide bridge (independent of disulfide bridge location). The authors suggested that the disulfide bridge restricts the ability of the coiled-coil to adjust interchain packing in response to the mutation, in essence locking the coiled-coil in a defined structure where the difference between the nonequivalent heptad positions is maintained. The reduced coiled-coil was assumed to be flexible and contain less distinctive packing interactions. It may be that the disulfide bridge restricts the inherent dynamic nature of the model coiled-coil, which may be in a somewhat molten-globule like structure with transient tertiary interactions in the reduced form. Dynamics experiments comparing the oxidized and reduced coiled-coils could potentially answer some of these questions.

5) Manipulation of protein stability and folding with buffer conditions - pH, salt, and metal binding

Proteins are generally evolved to operate under a relatively narrow range of conditions of temperature, pH, and ionic strength and, other than exceptions like transmembrane proteins, exclusively under aqueous conditions. This marginal stability profile is useful for controlling protein activity *in vivo* but is not so advantageous for *in vitro* purification, storage, and use. The application of enzymes as catalysts in industrial and commercial processes often creates demands for proteins that can withstand more extreme conditions. Bacteria that have evolved to live under various extreme conditions prove that there are few barriers to proteins in principle (Jaenicke, 1991), and some important industrial enzymes have been obtained from such extremophilic bacteria; a well known example being the use of a DNA polymerase from a thermophilic bacterium in the polymerase chain reaction (PCR) technique (Saiki *et al.*, 1988). In other cases, enzymes have been successfully engineered by rational or random mutagenesis for improved stability and/or activity under nonnatural conditions (Arnold, 1993).

Likewise, *de novo* designed proteins may also conceivably be designed to work under nonbiological conditions, and the activity of such proteins may be advantageously regulated by control of the buffer conditions. The results of our coiled-coil studies on pH and salt effects are very relevant toward this design goal. For example, while interhelical repulsion between negatively-charged Glu side chains was observed to prevent or destabilize folding at neutral pH, the protonation (neutralization) of Glu residues promoted folding. In addition, the least stable analog at neutral pH was the most stable at acidic pH. Such a pH-dependent transition, which was observed to occur over a narrow pH range, is an obvious switch for controlling protein folding and activity that has already been employed by nature in viral membrane fusion proteins (Carr & Kim, 1993, 1994) and by protein designers in controlling coiled-coil-template-assisted peptide ligation (Yao *et al.*, 1997). The concept of relieving interhelical charge repulsion by acidification should be generally applicable to the design of α-helical proteins that will function only under acidic conditions. In contrast, most native proteins, evolved to operate under physiological conditions near neutrality, are destabilized and generally denatured by low pH.

Salt conditions could also potentially be used to regulate the structure and function of *de novo* designed proteins. Coiled-coils prevented from folding at neutral pH by negative charge repulsions were induced to fold by salts (Chapter IV, Kohn *et al.*, 1995b) while salts also had effects on the stability of coiled-coils containing ion pairs, particularly due to metal binding effects of the La^{3+} ion (Chapter VI, Kohn *et al.*, 1997c). These studies illustrated the complex effects of salts on protein stability: the ionic strength effect of general charge screening, specific counter-ion binding to charged residues on the protein, and the effects of salt on the structure/properties of aqueous solution were all demonstrated in this work to contribute to the perturbation of protein stability by salt. Interestingly, general charge screening due to ionic strength seemed to have a particularly limited effect on the specific **g-e'** interactions in coiled-coils, possibly due to the synergy of these interactions with hydrophobic packing.

The most encouraging results from our studies of environmental control of protein folding and stability involved the design of coiled-coils that were controlled by metal binding specifically at designed sites (Chapters VIII and IX, Kohn *et al.*, 1998a, 1998b). The La^{3+}-bridging model in which a La^{3+} ion was predicted to bridge between Glu residues that normally repel one another across the coiled-coil interface, was proposed to explain the efficiency of $LaCl_3$ in inducing the structure of E10x (Chapter IV, Kohn *et al.*, 1995b). The results of Chapter VIII (Kohn *et al.*, 1998a) supported this model and led to further design of a molecule that underwent high affinity metal binding in Chapter IX (Kohn *et al.*, 1998b). There has been much work in recent years toward engineering of metal-binding sites into both naturally-occurring and *de novo* designed proteins (Hellinga, 1996; Lu & Valentine, 1997; Matthews, 1995b). The use of metal ions to template peptides into defined conformations (Ghadiri & Choi, 1990; Ruan *et al.*, 1990; Tian & Bartlett, 1996) or to promote α-helical bundle assembly (Ghadiri & Case, 1993; Ghadiri *et al.*, 1992a, 1992b; Lieberman & Sasaki, 1991) have demonstrated the potential for design of proteins that undergo metal-dependent folding. The design of the coiled-coil Gla_2Nx, which undergoes essentially a complete random coil to folded state transition upon binding of metal ions to two well-defined sites on the molecule (Chapter IX), is a dramatic example of the potential for metal binding as a method of controlling the structure and function of *de novo* designed proteins.

6) Roles of charged residues in coiled-coils - an overview

Clearly, the charged residues at positions **e** and **g** can play a significant role in coiled-coil folding. Repulsions and attractions between residues in the **g-e'** orientation affect side chain packing and ultimately protein stability. Maximizing the attractions and minimizing the repulsions will thus enhance the contributions of the **e** and **g** positions to the thermodynamic stability of a coiled-coil. Even though ion pairs 'stabilize' coiled-coils, higher or equivalent stability can be attained with certain neutral residues in these positions (Chapter VII, Kohn *et al.*, 1998c; Hendsch & Tidor, 1994; Hu & Sauer, 1992; Pu & Struhl, 1993; Schmidt-Dörr *et al.*, 1991). However, unpaired charged residues at positions **e** and **g** are destabilizing, suggesting that the **g-e'** ion pair is really a mechanism of offsetting the desolvation of the charged residues as they pack against the hydrophobic core of the coiled-coil interface. The ionic interactions clearly offer a way of attaining specificity of coiled-coil dimerization in nature while also modulating stability. However, in native sequences the electrostatic/polar interactions go beyond just the **e** and **g** positions because charged/polar residues at the **a** and **d** positions can also contribute to the specificity of coiled-coil dimerization through ionic and hydrogen-bond interactions (Glover & Harrison, 1995; Lavigne *et al.*, 1995). Specificity will ultimately be determined by the overall complementarity of the dimerization interface, not just by maximizing the electrostatic complementarity.

One interesting question is whether the role of electrostatics in coiled-coil folding is more relevant kinetically or thermodynamically. For example, the short coiled-coils of the bZIP transcription factors must associate and dissociate as part of their regulatory role. In a cell, the total number of these molecules is small and the specificity of interaction in a kinetic sense may be important. For example, the Fos/Jun heterodimer was shown to exchange (with the unfolded state) fairly rapidly (approximately 1 s^{-1}) in solution but to exchange very little when bound specifically to DNA (Patel *et al.*, 1994). A rapid association of Fos/Jun coupled to rapid DNA binding could be a kinetically-controlled process. As the study of Wendt *et al.* (1997) showed, electrostatic interactions can greatly affect the rate of association (at low ionic strength, the rate of association between negatively and positively charged peptides was near the diffusion-controlled limit of 10^9 $M^{-1}s^{-1}$). In contrast, interactions between like charges on the dimerization faces should decrease the on rate and increase the off rate of dimerization, and charge-neutral interacting faces would be expected to have less effect on the kinetics of folding. Rapid sampling of dimerization partners could be aided by electrostatics (attractions increasing the on rate and repulsions increasing the off rate) with the final proper dimerization partner being the one with higher thermodynamic stability. In effect, electrostatic attractions may influence the overall free energy of coiled-coil formation even without the formation of specific ion pairs.

Another aspect of the residues at the solvent-exposed positions of a coiled-coil is the potential for interaction with other molecules. This is relevant to both native coiled-coils and *de novo* designs, which could be developed to contain binding affinities with useful applications (Houston *et al.*, 1996; Miceli *et al.*, 1996). In tropomyosin, the **b**, **c**, **e**, **f**, and **g** positions have been analyzed for binding sites that would interact with actin. A 14-fold periodicity was proposed, which would give seven actin binding sites in the relaxed state and seven binding sites in the contracted state (McLachlan & Stewart, 1976). Each proposed binding site or 'band' contains a number of charged residues which are split into mostly positive and mostly negative zones. Interactions between tropomyosin and actin are Mg^{2+}-dependent, and it was suggested that the negative zones on the tropomyosin binding bands interact with negative charges on actin through Mg^{2+} bridges (McLachlan & Stewart, 1976), similarly to the proposed bridging of negative charges in our model coiled-coil by metal ions. More recently, the cooperative binding of the Fos/Jun bZIP heterodimer and the NFAT (nuclear factor of activated T cells) at the interleukin-2 gene promoter was observed through a crystallographic analysis of a complex between the DNA binding regions of the three proteins and site-specific DNA (Chen *et al.*, 1998). The interface between Fos/Jun and NFAT was found to contain extended networks of hydrogen bonds and salt bridges. In particular, Lys292 of Jun and Glu173 of Fos, which participate in an interhelical **g-e'** ion pair in the Fos/Jun structure (Glover & Harrison, 1995) are involved in direct contacts with NFAT residues. Seryl-tRNA synthetase contains an antiparallel coiled-coil domain, which acts through exposed side chains, including those at positions **e** and **g**, as the primary binding site for tRNA and directs the acceptor stem of the tRNA into the active site (Biou *et al.*, 1994). Thus, these residues play dual roles in the molecular recognition within the coiled-coil and between the coiled-coil and other molecules.

7) Future research directions

The research described in this thesis touches on a number of areas, including studies of coiled-coils, protein *de novo* design, and metal binding site design. Much could be said about the future of these research areas and how the current work relates. Only a few points are mentioned here. Several areas for potential future research have already been mentioned in the preceding portions of this chapter.

i) Up to this point, most of the research in *de novo* design has been focussed on the design of sequences that will fold into a particular structure, and there have been relatively few attempts at designing a molecule to carry out a specific function (see Kohn & Hodges, 1998, Appendix I). However, an increasing number of applications are being developed for both coiled-coils and other *de novo* designed peptides and proteins. Basic research into the fundamentals of the noncovalent interactions involved in folding must be continued in order to aid in the design of proteins for specific applications. For example, the metal-induced coiled-coil folding described in this thesis stemmed from purely basic research and may now potentially be applied in future work (see below). Our laboratory has identified the importance of balancing the applied and basic aspects of molecular design research. The ongoing basic research involves studies of both *de novo* (model) and native coiled-coil sequences. For example, the relative roles of different effects such as hydrophobicity at the interface and intrinsic α-helical propensities on coiled-coil stability are being addressed, and the subtle effects of amino acid substitutions and interchain disulfide bridges on coiled-coil oligomerization state is another area under study. As mentioned above, more studies need to be carried out to address the effect of context on the role of various noncovalent interactions in coiled-coil stability.

ii) The design of peptide/protein catalysts that function in organic solvents could be very useful in industrial processes. Studies have been carried out to engineer enzymes, which normally function in aqueous solution, to operate in polar organic solvents (Wong, 1989). A better approach could ultimately be to design *de novo* proteins to function specifically in a nonaqueous environment. A first step toward such an end might be the design of an α-helical coiled-coil that is folded in an organic solvent. For example, a coiled-coil might be designed with a polar dimer interface and a nonpolar exposed surface. Such a molecule would be expected to fold in a nonpolar solvent due to burial of the polar interface residues (a reverse hydrophobic effect), similar to designed α-helical ion channel peptides (Lear *et al.*, 1988). The design of active sites for catalysis on the exposed surface is a subsequent step (Broo *et al.*, 1997). However, catalysis by *de novo* designed peptides is a goal that has been difficult to achieve (Kohn & Hodges, 1998, Appendix I).

iii) A major area for further investigation stemming from this project is application of the metal-induced coiled-coil folding process (Fig. IX.9). For example, integration of the lanthanide binding site containing Gla residues with the heterodimerization concept (Hodges, 1996; Zhou *et al.*, 1994c) could allow for metal binding to control heterodimerization. A potential difficulty might be homodimerization of the peptide containing all negative charged residues at the **e** and **g** heptad positions upon addition of the metal ion (as for E10x in Chapter IV) rather than heterodimerization.

The concept of reversible dimerization could conceivably be used to control enzyme activity if one could break the enzyme into two separate fragments that might be able to reassociate into a functional form. It has long been known that some single polypeptide chain proteins could be cleaved into two fragments with the ability to recombine through noncovalent forces into a complex with properties and activity similar to the native protein (Anfinsen, 1973). The key would be to make the reassociation dependent on the metal-induced coiled-coil folding. One fragment would be attached covalently to each of the chains of the coiled-coil, and the spatial arrangement between the coiled-coil and the attached protein fragments would also be important to the success of such a design. A number of enzymes are known to function as dimers, and in some cases are not active in the monomeric form. Mutations in the subunit interface to weaken dimerization can make such a dimeric enzyme inactive (Mainfroid *et al.*, 1996), and the mutant could be controlled by attaching it to the ends of the metal-dependent coiled-coil dimerization domain to allow the coiled-coil to add back the dimerization energy required for activity in a metal-dependent manner. Already, metal-binding sites have been incorporated which can control the allosteric interactions involved in activation of the dimeric enzyme glycogen phosphorylase (Browner *et al.*, 1994).

A number of cell surface receptors function as homo- or heterodimers, and the coiled-coil has been demonstrated to direct assembly of the extracellular domains in solution (Wu *et al.*, 1995). Metal-dependent coiled-coil folding could therefore conceivably control receptor dimerization in a metal-dependent manner.

Use of peptides that undergo conformational changes upon metal binding as metal ion sensors is a concept that has recently been proposed (Godwin & Berg, 1996; Walkup & Imperiali, 1996). The peptide Gla_2Nx, developed in Chapter IX (Kohn *et al.*, 1998b), binds to lanthanides with μM affinity but very weakly to Ca^{2+} (K_d approximately 18 mM). Alternatively, it would be an interesting challenge to design an analog that binds to Ca^{2+} with μM or greater affinity. Such a molecule might be applied to detection of changes in cellular Ca^{2+} concentration, which is believed to control signal transduction processes. A previous metal ion sensor used fluorescence donor and acceptor groups that were covalently attached to the peptide (a zinc finger) and came into close contact with one another upon metal-induced folding (Godwin & Berg, 1996). This same visualization technique can be used with the dimeric coiled-coil motif where one of the peptide chains has the fluorescence acceptor attached and the other has the fluorescence donor attached, and the groups are brought into close proximity upon coiled-coil folding (Wendt *et al.*, 1995). The design of a Ca^{2+}-binding coiled-coil might include the derivation of a new side chain with three carboxylate ligands (rather than the two present in Gla). Two of these side chains at positions **g** and **e'** (i and i'+5) of the coiled-coil could, if properly designed, coordinate Ca^{2+} with an octahedral geometry and potentially lead to high affinity Ca^{2+} binding. An alternative approach to design of a Ca^{2+} induced dimer is the "hybritein", in which a coiled-coil and a helix-loop-helix Ca^{2+}-binding domain are fused together (Tripet *et al.*, 1995).

iv) Binding of a metal ion at the interface of a protein-protein complex can be important for mediating the interaction (Matthews, 1995b), as seen for dimers of human growth hormone (hGH) and the interaction of hGH with the prolactin receptor (Cunningham *et al.*, 1990, 1991). Engineering to enhance the interaction of two proteins by binding of a metal ion in the interface has been successfully carried out. For example, a mutant hGH receptor was designed that bound to hGH 20-fold tighter in the presence of Zn^{2+} than in the presence of EDTA (Matthews & Wells, 1994). An interfacial zinc binding site was engineered into trypsin, which induced histidine substrate specificity at the P2' position (the second residue C-terminal to the sissile bond) that could overrule the high specificity of trypsin for Arg or Lys at the P1 position (immediately N-terminal to the sissile bond) (Willett *et al.*, 1995). Attempts to engineer metal-binding sites into the variable domains of catalytic antibodies to change their binding and catalytic properties have also been made (Roberts & Getzoff, 1995; Stewart *et al.*, 1994; Wade *et al.*, 1993). In light of these experiments, a metal binding coiled-coil may provide a good model system for studies of intermolecular interactions where a metal ion plays an important role in the binding interface. A potential project would be to design a peptide that binds with high affinity to the metal binding site on the exposed surface of the coiled-coil in the presence of a bound metal ion. Such interactions could be monitored with techniques such as affinity chromatography or surface plasmon resonance (Chao *et al.*, 1996).

v) It is hoped that, ultimately, all the activities of native proteins can be recreated and even improved through *de novo* protein design. Of all the functions of proteins, probably the most desireable to mimic is enzymatic catalysis. Environmentally-benign, robust, synthetic peptide catalysts possessing the large reaction-rate enhancement and specificity of native enzymes could have enormous industrial applicability. Metal ions often play active roles in enzyme catalysis (Volbeda *et al.*, 1996; Williams, 1995), particularly redox and hydrolytic reactions. Synthetic metallopeptides may have a great potential for development of catalytic activity. For example, the copper-containing catalytic center of the enzyme galactose oxidase, which converts carbon 6 of galactose from an alcohol to an aldehyde moiety, was mimicked in a small molecule template that could catalytically oxidize benzylic and allylic alcohols to aldehydes under mild conditions (Wang *et al.*, 1998). In contrast, aldehydes and ketones are usually synthesized industrially by stoichiometric addition of hazardous, toxic oxidizing agents (Marko *et al.*, 1996). A key to the 'minimization' of enzyme activity into a simpler molecule is to be able to prevent side reactions, which the enzyme often does by isolating the active site in the protein matrix. Thus, *de novo* designed proteins of reduced size (relative to the native enzyme) and increased stability (ability to function under harsh conditions) may prove to be more successful catalysts than smaller organometallic complexes in some cases.

BIBLIOGRAPHY[8]

Abrams, M. J. & Murrer, B. A. (1993) Metal compounds in therapy and diagnosis. *Science* **261,** 725-730.

Adamson, J. G., Zhou, N. E., and Hodges, R. S. (1993) Structure, function and application of the coiled-coil protein folding motif. *Curr. Opin. Biotechnol.* **4,** 428-437.

Akke, M., Forsen, S., and Chazin, W. J. (1991) Molecular basis for co-operativity in Ca^{2+} binding to calbindin D_{9K}. ^{1}H nuclear magnetic resonance studies of $(Cd^{2+})_1$-bovine calbindin D_{9k}. *J. Mol. Biol.* **220,** 173-189.

Alber, T. (1989) Mutational effects on protein stability. *Annu. Rev. Biochem.* **58,** 765-798.

Albericio, F. & Carpino, L. A. (1997) Coupling reagents and activation. *Methods Enzymol.* **289,** 104-126

Alberti, S., Oehler, S., von Wilcken-Bergmann, B., and Müller-Hill, B. (1993) Genetic analysis of the leucine heptad repeats of Lac repressor: evidence for a 4-helical bundle. *EMBO J* **12,** 3227-3236.

Alberti, S., Oehler, S., Wilcken-Bergmann, B. V., Kramer, H., and Muller-Hill, B. (1991) Dimer-to tetramer assembly of lac repressor involves a leucine heptad repeat. *The New Biologist* **3,** 57-62.

Anderson, D. E., Becktel, W. J., and Dahlquist, F. W. (1990) pH-Induced denaturation of proteins: a single salt bridge contributes 3-5 kcal/mol to the free energy of folding of T4 lysozyme. *Biochemistry* **29,** 2403-2408.

Andrews, R. K., Blakeley, R. L., and Zerner, B. (1984) Urea and urease. *Adv. Inorg. Biochem.* **6,** 245-283.

Anfinsen, C. B. (1973) Principles that govern the folding of protein chains. *Science* **181,** 223-230.

Antosiewicz, J., Wlodek, S. T., and McCammon, J. A. (1996) Acetylcholinesterase: role of the enzyme's charge distribution in steering charged ligands toward the active site. *Biopolymers* **39,** 85-94.

Åqvist, J., Luecke, H., Quiocho, F. A., and Warshel, A. (1991) Dipoles localized at helix termini of proteins stabilize charges. *Proc. Natl. Acad. Sci. USA* **88,** 2026-2030.

Arakawa, T., Bhat, R., and Timasheff, S. N. (1990a) Preferential interactions determine protein solubility in three-component solutions: the $MgCl_2$ system. *Biochemistry* **29,** 1914-1923.

Arakawa, T., Bhat, R., and Timasheff, S. N. (1990b) Why preferential hydration does not always stabilize the native structure of globular proteins. *Biochemistry* **29,** 1924-1931.

---

[8] Publications arising from this thesis are printed in bold type

Arakawa, T., Langley, K. E., Kameyama, K., and Takagi, T. (1992) Molecular weights of glycosylated and non-glycosylated forms of recombinant human stem cell factor determined by low angle laser light scattering. *Anal. Biochem.* **203,** 53-57.

Armstrong, K. M. & Baldwin, R. L. (1993) Charged histidine affects α-helix stability at all positions in the helix by interacting with backbone charges. *Proc. Natl Acad. Sci. USA* **90,** 11337-11340.

Arnold, F. H. (1993) Engineering proteins for nonnatural environments. *FASEB J.* **7,** 744-749.

Arnold, F. H. & Haymore, B. L. (1991) Engineered metal-binding proteins: purification to protein folding. *Science* **252,** 1796-1797.

Babul, J. & Stellwagen, E. (1969) Measurement of protein concentration with interference optics. *Anal. Biochem.* **28,** 216-221.

Baldwin, R. L. (1986) Temperature dependence of the hydrophobic interaction in protein folding. *Proc. Natl. Acad. Sci. USA* **83,** 8069-8072.

Baldwin, R. L. (1996) How Hofmeister ion interactions affect protein stability. *Biophys. J.* **71,** 2056-2063.

Barlow, D. J. & Thornton, J. M. (1983) Ion-pairs in proteins. *J. Mol. Biol.* **168,** 867-885.

Baxevanis, A. D. & Vinson, C. R. (1993) Interaction of coiled-coils in transcription factors: where is the specificity? *Curr. Opin. Genet. Dev.* **3,** 278-285.

Beavil, A. J., Edmeades, R. L., Gould, H. J., and Sutton, B. J. (1992) α-helical coiled-coil stalks in the low-affinity receptor for IgE (FcεRII/CD23) and related C-type lectins. *Proc. Natl. Acad. Sci. USA* **89,** 753-757.

Beck, K., Gambee, J. E., Kamawal, A., and Bächinger, H. P. (1997) A single amino acid can switch the oligomerization state of the α-helical coiled-coil domain of cartilage matrix protein. *EMBO J.* **16,** 3767-3777.

Benezra, R. (1994) An intermolecular disulfide bond stabilizes E2A homodimers and is required for DNA binding at physiological temperatures. *Cell* **79,** 1057-1067.

Betz, S. F., Bryson, J. W., and DeGrado, W. F. (1995) Native-like and structurally characterized designed α-helical bundles. *Curr. Opin. Struct. Biol.* **5,** 457-463.

Betz, S. F. & DeGrado, W. F. (1996) Controlling topology and native-like behavior of *de novo* designed peptides: design and characterization of antiparallel four-stranded coiled-coils. *Biochemistry* **35,** 6955-6962.

Biou, V., Yaremchuk, A., Tukalo, M., and Cusack, S. (1994) The 2.9 Å crystal structure of *T. thermophilus* Seryl-tRNA synthetase complexed with tRNA^{Ser}. *Science* **263,** 1404-1410

Blaber, M., Zhang, X.-J., Lindstrom, J. D., Pepiot, S. D., Baase, W. A., and Matthews, B. W. (1994) Determination of α -helix propensity within the context of a folded protein. *J. Mol. Biol.* **235,** 600-624.

Blaber, M., Zhang, X.-J., and Matthews, B. W. (1993) Structural basis of amino acid α-helix propensity. *Science* **260,** 1637-1640.

Blagdon, D. E. & Goodman, M. (1975) Mechanisms of protein and polypeptide helix initiation. *Biopolymers* **14,** 241-245.

Bodanszky, M. (1988) *Peptide Chemistry: A Practical Textbook.*, Springer-Verlag, New York.

Boice, J. A., Dieckmann, G. R., DeGrado, W. F., and Fairman, R. (1996) Thermodynamic analysis of a designed three-stranded coiled-coil. *Biochemistry* **35,** 14480-14485.

Breslow, R. & Guo, T. (1990) Surface tension measurements show that chaotropic salting-in denaturants are not just water-structure breakers. *Proc. Natl. Acad. Sci. USA* **87,** 167-169.

Broo, K. S., Brive, L., Ahlberg, P., and Baltzer, L. (1997) Catalysis of hydrolysis and transesterification reactions of p-nitrophenyl esters by a designed helix-loop-helix dimer. *J. Am. Chem. Soc.* **119,** 11362-11372.

Browner, M. F., Hackos, D., and Fletterick, R. (1994) Identification of the molecular trigger for allosteric activation in glycogen phosphorylase. *Nature Struct. Biol.* **1,** 327-333.

Bryson, J. W., Betz, S. F., Lu, H. S., Suich, D. J., Zhou, H. X., O'Neil, K. T., and DeGrado, W. F. (1995) Protein design: a hierarchic approach. *Science* **270,** 935-941.

Burke, T. W. L., Black, J. A., Mant, C. T., and Hodges, R. S. (1991) Preparative reversed-phase shallow gradient approach to the purification of closely-related peptide analogs on analytical instrumentation. In *High-Performance Liquid Chromatography of Peptides and Proteins: Separation, Analysis, and Conformation* (Mant, C. T. & Hodges, R. S., eds), pp. 783-791, CRC Press, Baca Raton, Florida.

Busch, S. J. & Sassone-Corsi, P. (1990) Dimers, leucine zippers and DNA-binding domains. *Trends Genet.* **6,** 36-40.

Cantor, C. R. & Schimmel, P. R. (1980) *Biophysical Chemistry, Part 1, The Conformation of Biological Macromolecules*, p. 290, W. H. Freeman and Co., San Francisco.

Carr, C. M. & Kim, P. S. (1993) A spring-loaded mechanism for the conformational change of influenza hemagglutinin. *Cell* **73,** 823-832.

Carr, C. M. & Kim, P. S. (1994) Flu virus invasion: halfway there. *Science* **266,** 234-236.

Carra, J. H. & Privalov, P. L. (1995) Energetics of denaturation and *m* values of staphylococcal nuclease mutants. *Biochemistry* **34,** 2034-2041.

Chakrabartty, A., Doig, A. J., and Baldwin, R. L. (1993) Helix capping propensities in peptides parallel those found in proteins. *Proc. Natl. Acad. Sci. USA* **90,** 11332-11336.

Chakrabartty, A., Kortemme, T., and Baldwin, R. L. (1994) Helix propensities of the amino acids measured in alanine-based peptides without helix-stabilizing side-chain interactions. *Protein Sci.* **3,** 843-852.

Chakrabartty, A., Schellman, J. A., and Baldwin, R. L. (1991) Large differences in the helix propensities of alanine and glycine. *Nature* **351,** 586-588.

Chan, D. C., Fass, D., Berger, J. M., and Kim, P. S. (1997) Core structure of gp41 from the HIV envelope glycoprotein. *Cell* **89,** 263-273.

Chao, H., Houston, M. E., Jr., Grothe, S., Kay, C. M., O'Connor-McCourt, M., Irvin, R. T., and Hodges, R. S. (1996) Kinetic study on the formation of a *de novo* designed heterodimeric coiled-coil: use of surface plasmon resonance to monitor the association and dissociation of polypeptide chains. *Biochemistry* **35,** 12175-12185.

Chen, L., Glover, J. N. M., Hogan, P. G., Rao, A., and Harrison, S. C. (1998) Structure of the DNA-binding domains from NFAT, Fos and Jun bound specifically to DNA. *Nature* **392,** 42-48.

Chen, Y.-H., Yang, J. T., and Chau, K. H. (1974) Determination of the helix and beta form of proteins in aqueous solution by circular dichroism. *Biochemistry* **13,** 3350-3359.

Cheng, R. P., Fisher, S. L., and Imperiali, B. (1996) Metallopeptide design: tuning the metal cation affinites with unnatural amino acids and peptide secondary structure. *J. Am. Chem. Soc.* **118,** 11349-11356.

Chong, L. T., Dempster, S. E., Hendsch, Z. S., Lee, L. P., and Tidor, B. (1998) Computation of electrostatic complements to proteins: a case of charge stabilized binding. *Protein Sci.* **7,** 206-210.

Chou, P. Y. & Fasman, G. D. (1974) Conformational parameters for amino acids in helical, beta-sheet, and random coil regions calculated from proteins. *Biochemistry* **13,** 211-222.

Chou, P. Y. & Fasman, G. D. (1978) Empirical predictions of protein conformation. *Ann. Rev. Biochem.* **47,** 251-276.

Cohen, C. & Parry, D. A. D. (1990) α-Helical coiled-coils and bundles: how to design an α-helical protein. *Proteins: Struct. Funct. Genet.* **7,** 1-15.

Cohen, C. & Parry, D. A. D. (1994) α-helical coiled-coils: more facts and better predictions. *Science* **263,** 488-489.

Cohn, E. J. & Edsall, J. T. (1943) In *Proteins, Amino Acids, and Peptides as Ions and Dipolar Ions,* pp. 370-381. Reinhold Publishing Corp., New York.

Conway, J. F. & Parry, D. A. D. (1991) Three-stranded α-fibrous proteins: the heptad repeat and its implications for structure. *Int. J. Biol. Macromol.* **13,** 14-16.

Cooper, T. M. & Woody, R. W. (1990) The effect of conformation on the CD of interacting helices: a theoretical study of tropomyosin. *Biopolymers* **30,** 657-676.

Cordes, M. H. J., Davidson, A. R., and Sauer, R. T. (1996) Sequence space, folding and protein design. *Curr. Opin. Struct. Biol.* **6,** 3-10.

Corey, D. R. & Schultz, P. G. (1989) Introduction of a metal-dependent regulatory switch into an enzyme. *J. Biol. Chem.* **264,** 3666-3669.

Coulombe, P. A. (1993) The cellular and molecular biology of keratins: beginning a new era. *Curr. Opin. Cell Biol.* **5,** 17-29.

Cregut, D., Liautard, J. P., Heitz, F., and Chiche, L. (1993) Molecular modeling of coiled-coil α-tropomyosin: analysis of staggered and in register helix-helix interactions. *Protein Eng.* **6,** 51-58.

Creighton, T. (1993) *Proteins: Structures and Molecular Properties, 2nd edit.,* W. H. Freeman and Co, New York.

Creighton, T. E. (1990) Protein Folding. *Biochem. J.* **270,** 1-16.

Crick, F. H. C. (1953) The packing of α-helices: simple coiled-coils. *Acta Crystallogr.* **6,** 689-697.

Cunningham, B. C., Bass, S. H., Fuh, G., and Wells, J. A. (1990) Zinc mediation of the binding of human growth hormone to the human prolactin receptor. *Science* **250,** 1709-1712.

Cunningham, B. C., Mulkerrin, M. G., and Wells, J. A. (1991) Dimerization of human growth hormone by zinc. *Science* **253,** 545-548.

Dado, G. P. & Gellman, S. H. (1993) Redox control of secondary structure in a designed peptide. *J. Am. Chem. Soc.* **115,** 12609-12610.

Dao-pin, S., Sauer, U., Nicholson, H., and Matthews, B. M. (1991) Contributions of engineered surface salt bridges to the stability of T4 lysozyme determined by direct mutagenesis. *Biochemistry* **30,** 7142-7153.

Dasgupta, S. & Bell, J. A. (1993) Design of helix ends. Amino acid preferences, hydrogen bonding and electrostatic interactions. *Int. J. Peptide Protein Res.* **41,** 499-511.

Defay, T. & Cohen, F. E. (1995) Evaluation of current techniques for *ab initio* protein structure prediction. *Proteins: Struct. Funct. Genet.* **23,** 431-445.

DeGrado, W. F., Wasserman, Z. R., and Lear, J. D. (1989) Protein design, a minimalist approach. *Science* **243,** 622-628.

Dieckmann, G. R., McRorie, D. K., Tierney, D. L., Utschig, L. M., Singer, C. P., O'Halloran, T. V., Penner-Hahn, J. E., DeGrado, W. F., and Pecoraro, V. L. (1997) *De novo* design of mercury-binding two- and three-helical bundles. *J. Am. Chem. Soc.* **119,** 6195-6196.

Dill, K. (1990) Dominant forces in protein folding. *Biochemistry* **29,** 7133-7135.

Dill, K. A. (1997) Additivity principles in biochemistry. *J. Biol. Chem.* **272,** 701-704.

Doig, A. J. & Baldwin, R. L. (1995) N- and C-capping preferences for all 20 amino acids in α-helical peptides. *Protein Sci.* **4,** 1325-1336.

Doig, A. J. & Sternberg, M. J. E. (1995) Side-chain conformational entropy in protein folding. *Protein Sci.* **4,** 2247-2251.

Dyson, H. J., Rance, M., Hoghten, R. A., Wright, P. E., and Lerner, R. A. (1988) Folding of immunogenic peptide fragments of proteins in water solution. II. The nascent helix. *J. Mol. Biol.* **201,** 201-217.

Eijsink, V. G. H., Vriend, G., van den Burg, B., van der Zee, J. R., and Venema, G. (1992) Increasing the thermostability of a neutral protease by replacing positively charged amino acids in the N-terminal turn of α-helices. *Protein Eng.* **5,** 165-170.

Ellenberger, T. E., Brandl, C. J., Struhl, K., and Harrison, S. C. (1992) The GCN4 basic region leucine zipper binds DNA as a dimer of uninterrupted α-helices: crystal structure of the protein-DNA complex. *Cell* **71,** 1223-1237.

Engel, M., Williams, R. W., and Erickson, B. W. (1991) Designed coiled-coil proteins: synthesis and spectroscopy of two 78-residue α-helical dimers. *Biochemistry* **30,** 3161-3169.

Englander, S. W. & Mayne, L. (1992) Protein folding studied using hydrogen-exchange labeling and two-dimensional NMR. *Annu. Rev. Biophys. Biomol. Struct.* **21,** 243-265.

Erickson, B. W. & Merrifield, R. B. (1976) Solid-phase peptide synthesis. In *The Proteins, vol. 2* (Neurath, H. and Hill, R. L., eds), pp. 255-527, Academic Press, New York.

Eriksson, A. E., Baase, W. A., Zhang, X.-J., Heinz, D. W., Blaber, M., Baldwin, E. P., and Matthews, B. W. (1992) Response of a protein structure to cavity-creating mutations and its relation to the hydrophobic effect. *Science* **255,** 178-183.

Faiman, G. A. & Horovitz, A. (1996) On the choice of reference mutant states in the application of the double-mutant cycle method. *Protein Eng.* **9,** 315-316.

Fairman, R., Chao, H.-G., Lavoie, T. B., Villafranca, J. J., Matsueda, G. R., and Novotny, J. (1996) Design of heterotetrameric coiled-coils: evidence for increased stabilization by Glu^--Lys^+ ion pair interactions. *Biochemistry* **35,** 2824-2829.

Fairman, R., Chao, H.-G., Mueller, L., Lavoie, T. B., Shen, L., Novotny, J., and Matsueda, G. R. (1995) Characterization of a new four-chain coiled-coil: influence of chain length on stability. *Protein Sci.* **4,** 1457-1469.

Fairman, R., Shoemaker, K. R., York, E. J., Stewart, J. M., and Baldwin, R. L. (1989) Further studies of the helix dipole model: effects of a free alpha-NH_3^+ or alpha-COO^- group on helix stability. *Proteins: Struct. Funct. Genet.* **5,** 1-7.

Farrow, N. A., Muhandiram, R., Singer, A. U., Pascal, S. M., Kay, C. M., Gish, G., Shoelson, S. E., Pawson, T., Forman-Kay, J. D., and Kay, L. E. (1994) Backbone dynamics of a free and a phosphopeptide-complexed Src homology 2 domain studied by ^{15}N NMR relaxation. *Biochemistry* **33,** 5984-6003.

Fauchere, J. L. & Pliska, V. (1983) Hydrophobic parameters π of amino acid side chains from the partitioning of N-acetyl-amino-acid amides. *Eur. J. Med. Chem.* **18,** 369-375.

Fersht, A. R. (1972) Conformational equilibria in α- and δ-chymotrypsin. The energetics and importance of the salt bridge. *J. Mol. Biol.* **64,** 497-509.

Fields, G. B. (1997) Editor of *Solid-Phase Peptide Synthesis: Methods in Enzymology vol. 289,* Academic Press, New York.

Findlay, W. A., Shaw, G. S., and Sykes, B. D. (1992) Metal ion binding by proteins. *Curr. Opin. Struct. Biol.* **2,** 57-90.

Freifelder, D. (1982) *Physical Biochemistry: Applications to Biochemistry and Molecular Biology, 2nd edit.,* (Chapter 11), W. H. Freeman and Co, New York.

Friend, S. H. & Gurd, F. R. N. (1979) Electrostatic stabilization in myoglobin. pH dependence of summed electrostatic contributions. *Biochemistry* **18,** 4612-4619.

Froloff, N., Windemuth, A., and Honig, B. (1997) On the calculation of binding free energies using continuum methods: application to MHC class I protein-peptide interactions. *Protein Sci.* **6,** 1293-1301.

Furie, B. & Furie, B. C. (1988) The molecular basis of blood coagulation. *Cell* **53,** 505-518.

Furie, B. C., Blumenstein, M., and Furie, B. (1979) Metal binding sites of a γ-carboxyglutamic acid-rich fragment of bovine prothrombin. *J. Biol. Chem.* **254,** 12521-12530.

Furie, B. C. & Furie, B. (1975) Interaction of lanthanide ions with bovine Factor X and their use in the affinity chromatography of the venom coagulant protein of *Viperia ruselli. J. Biol. Chem.* **250,** 601-608.

Furie, B. C., Mann, K. G., and Furie, B. (1976) Substitution of lanthanide ions for calcium ions in the activation of bovine prothrombin by activated factor X. High affinity metal-binding sites of prothrombin and the derivatives of prothrombin activation. *J. Biol. Chem.* **251,** 3235-3241.

Gariepy, J., Sykes, B. D., and Hodges, R. S. (1983) Lanthanide-induced peptide folding: variations in lanthanide affinity and induced peptide conformation. *Biochemistry* **22,** 1765-1772.

Geraldes, C. F. G. C. (1993) Lanthanide shift reagents. *Methods Enzymol.* **227,** 43-78.

Ghadiri, M. R. & Case, M. A. (1993) *De novo* design of a novel heterodinuclear three-helix bundle metalloprotein. *Angew. Chem. Int. Ed. Engl.* **32,** 1594-1597.

Ghadiri, M. R. & Choi, C. (1990) Secondary structure nucleation in peptides. Transition metal ion stabilized α-helices. *J. Am. Chem. Soc.* **112,** 1630-1632.

Ghadiri, M. R. & Fernholtz, K. (1990) Peptide architecture. Design of stable α-helical metallopeptides via a novel exchange-inert Ru(III) complex. *J. Am. Chem. Soc.* **112,** 9633-9635.

Ghadiri, M. R., Soares, C., and Choi, C. (1992a) A convergent approach to protein design. Metal ion-assisted spontaneous self-assembly of a polypeptide into a triple-helix bundle protein. *J. Am. Chem. Soc.* **114,** 825-831.

Ghadiri, M. R., Soares, C., and Choi, C. (1992b) Design of an artificial four-helix bundle metalloprotein via a novel ruthenium(II)-assisted self-assembly process. *J. Am. Chem. Soc.* **114,** 4000-4002.

Gilson, M. K. & Honig, B. (1989) Destabilization of an α-helix-bundle protein by helix dipoles. *Proc. Natl. Acad. Sci. USA* **86,** 1524-1528.

Glover, J. N. M. & Harrison, S. C. (1995) Crystal structure of the heterodimeric bZIP transcription factor c-Fos-c-Jun bound to DNA. *Nature* **373,** 257-261.

Godwin, H. A. & Berg, J. M. (1996) A fluorescent zinc probe based on metal-induced peptide folding. *J. Am. Chem. Soc.* **118,** 6514-6515.

Gonzalez, L., Jr , Plecs, J. J., and Alber, T. (1996a) An engineered allosteric switch in leucine-zipper oligomerization. *Nature Struct. Biol.* **3,** 510-515.

Gonzalez, L., Jr, Woolfson, D. N., and Alber, T. (1996b) Buried polar residues and structural specificity in the GCN4 leucine zipper. *Nature Struct. Biol.* **3,** 1011-1018.

Goodman, E. M. & Kim, P. S. (1991) Periodicity of amide proton exchange rates in a coiled-coil leucine zipper peptide. *Biochemistry* **30,** 11615-11620.

Goto, Y. & Aimoto, S. (1991) Anion and pH-dependent conformational transition of an amphiphilic polypeptide. *J. Mol. Biol.* **218,** 387-396.

Goto, Y. & Hagihara, Y. (1992) Mechanism of the conformational transition of melittin. *Biochemistry* **31,** 732-738.

Goto, Y. & Nishikiori, S. (1991) Role of electrostatic repulsion in the acidic molten globule of cytochrome c. *J. Mol. Biol.* **222,** 11908-11914.

Goto, Y., Takahashi, N., and Fink, A. L. (1990) Mechanism of acid-induced folding of proteins. *Biochemistry* **29,** 3480-3488.

Graddis, T. J., Myszka, D. G., and Chaiken, I. M. (1993) Controlled formation of model homo- and heterodimer coiled-coil polypeptides. *Biochemistry* **32,** 12664-12671.

Green, S. M., Meeker, A. K., and Shortle, D. (1992) Contributions of the polar, uncharged amino acids to the stability of staphylococcal nuclease: evidence for mutational effects on the free energy of the denatured state. *Biochemistry* **31,** 5717-5728.

Greene, R. F. & Pace, C. N. (1974) Urea and guanidine hydrochloride denaturation of ribonuclease, lysozyme, α-chymotrypsin, and β-lactoglobulin. *J. Biol. Chem.* **249,** 5388-5393.

Greenfield, N. J. & Hitchcock-DeGregori, S. E. (1993) Conformational intermediates in the folding of a coiled-coil model peptide of the N-terminus of tropomyosin and αα-tropomyosin. *Protein Sci.* **2,** 1263-1273.

Guo, D., Mant, C. T., Taneja, A. K., Parker, J. M. R., and Hodges, R. S. (1986) Prediction of peptide retention times in reversed-phase high-performance liquid chromatography. Determination of retention coefficients of amino acid residues of model synthetic peptides. *J. Chromatogr.* **359,** 499-517.

Hagihara, Y., Aimoto, S., Fink, A. L., and Goto, Y. (1993) Guanidine hydrochloride-induced folding of proteins. *J. Mol. Biol.* **231,** 180-184.

Hagihara, Y., Kataoka, M., Aimoto, S., and Goto, Y. (1992) Charge repulsion in the conformational stability of melittin. *Biochemistry* **31,** 11908-11914.

Hagihara, Y., Tan, Y., and Goto, Y. (1994) Comparison of the conformational stability of the molten globule and native states of horse cytochrome c. *J. Mol. Biol.* **237,** 336-348.

Halfon, S. & Craik, C. S. (1996) Regulation of proteolytic activity by engineered tridentate metal binding loops. *J. Am. Chem. Soc.* **118,** 1227-1228.

Handel, T. & DeGrado, W. F. (1990) *De novo* design of a Zn^{2+}-binding protein. *J. Am. Chem. Soc.* **112,** 6710-6711.

Handel, T. M., Williams, S. A., and DeGrado, W. F. (1993) Metal ion-dependent modulation of the dynamics of a designed protein. *Science* **261,** 879-885.

Harbury, P. B., Kim, P. S., and Alber, T. (1994) Crystal structure of an isoleucine-zipper trimer. *Nature* **371,** 80-83.

Harbury, P. B., Zhang, T., Kim, P. S., and Alber, T. (1993) A switch between two-, three-, and four-stranded coiled-coils in GCN4 leucine zipper mutants. *Science* **262,** 1401-1407.

Harvey, S. C. (1989) Treatment of electrostatic effects in macromolecular modeling. *Proteins: Struct. Funct. Genet.* **5,** 78-92.

Hauschka, P. V. & Carr, S. A. (1982) Calcium-dependent α-helical structure in osteocalcin. *Biochemistry* **21,** 2538-2547.

Hellinga, H. W. (1996) Metalloprotein design. *Curr. Opin. Biotech.* **7,** 437-441.

Hendsch, Z. S. & Tidor, B. (1994) Do salt bridges stabilize proteins? A continuum electrostatic analysis. *Protein Sci.* **3,** 211-226.

Higaki, J. N., Haymore, B. L., Chen, S., Fletterick, R. J., and Craik, C. S. (1990) Regulation of serine protease activity by an engineered metal switch. *Biochemistry* **29,** 8582-8586.

Hirota, N., Mizuno, K., and Goto, Y. (1998) Group additive contributions to the alcohol-induced alpha-helix formation of melittin: implication for the mechanism of the alcohol effects on proteins. *J. Mol. Biol.* **275,** 365-378.

Hodges, R. S. (1992) Unzipping the secrets of coiled-coils. *Curr. Biol.* **2,** 122-124.

Hodges, R. S. (1996) *De novo* design of α-helical proteins: basic research to medical applications. *Biochem. Cell Biol.* **74,** 133-154.

Hodges, R. S., Saund, A. K., Chong, P. C. S., St.-Pierre, S. A., and Reid, R. E. (1981) Synthetic model for two-stranded α-helical coiled-coils. Design, synthesis, and characterization of an 86-residue analog of tropomyosin. *J. Biol. Chem.* **256,** 1214-1224.

Hodges, R. S., Semchuk, P. D., Taneja, A. K., Kay, C. M., Parker, J. M. R., and Mant, C. T. (1988) Protein design using model synthetic peptides. *Peptide Res.* **1,** 19-30.

Hodges, R. S., Sodek, J., Smillie, L. B., and Jurasek, L. (1972) Tropomyosin: amino acid sequence and coiled-coil structure. *Cold Spring Harbor Symp. Quant. Biol.* **37,** 299-310.

Hodges, R. S., Zhou, N. E., Kay, C. M., and Semchuk, P. D. (1990) Synthetic model proteins: contribution of hydrophobic residues and disulfide bonds to protein stability. *Peptide Res.* **3,** 123-137.

Hodges, R. S., Zhu, B. Y., Zhou, N. E., and Mant, C. T. (1994) Reversed-phase chromatography: a useful probe of hydrophobic interactions involved in protein folding and stability. *J. Chromatogr.* **676,** 3-15.

Hol, W. G. J., Halie, L. M., and Sander, C. (1981) Dipoles of the α-helix and β-sheet: their role in protein folding. *Nature* **294,** 532-536.

Hol, W. G. J., Van Duijnen, P. T., and Berendsen, H. J. C. (1978) The α-helix dipole and the properties of proteins. *Nature* **273,** 443-446.

Holtzer, M. E., Lovett, E. G., d'Avignon, D. A., and Holtzer, A. (1997) Thermal unfolding in a GCN4-like leucine zipper: $^{13}C^{\alpha}$ NMR chemical shifts and local unfolding curves. *Biophys. J.* **73,** 1031-1041.

Honig, B. & Nicholls, A. (1995) Classical electrostatics in biology and chemistry. *Science* **268,** 1144-1149.

Honig, B. & Yang, A. S. (1995) Free energy balance in protein folding. *Adv. Protein Chem.* **46,** 27-58.

Horovitz, A. & Fersht, A. R. (1990) Strategy for analysing the co-operativity of intramolecular interactions in peptides and proteins. *J. Mol. Biol.* **214,** 613-617.

Horovitz, A., Matthews, J. M., and Fersht, A. R. (1992) α-Helix stability in proteins. II. Factors that influence stability at an internal position. *J. Mol. Biol.* **227,** 560-658.

Horovitz, A., Serrano, L., Avron, B., Bycroft, M., and Fersht, A. R. (1990) Strength and cooperativity of contributions of surface salt bridges to protein stability. *J. Mol. Biol.* **216,** 1031-1044.

Hoshino, M., Yumoto, N., Yoshikawa, S., and Goto, Y. (1997) Design and characterization of the anion-sensitive coiled-coil peptide. *Protein Sci.* **6,** 1396-1404.

Houston, M. E., Jr, Wallace, A., Bianchi, E., Pessi, A., and Hodges, R. S. (1996) Use of a conformationally restricted secondary structural element to display peptide libraries: a two-stranded α-helical coiled-coil stabilized by lactam bridges. *J. Mol. Biol.* **262,** 270-282.

Hu, J. C., Newell, N. E., Tidor, B., and Sauer, R. T. (1993) Probing the roles of residues at the **e** and **g** positions of the GCN4 leucine zipper by combinatorial mutagenesis. *Protein Sci.* **2,** 1072-1084.

Hu, J. C., O'Shea, E. K., Kim, P. S., and Sauer, R. T. (1990) Sequence requirements for coiled-coils: analysis with λ-repressor-GCN4 leucine zipper fusions. *Science* **250,** 1400-1403.

Hu, J. C. & Sauer, R. T. (1992) The basic-region leucine-zipper family of DNA binding proteins. *Nucleic Acids Mol. Biol.* **6,** 82-101.

Huheey, J. E. (1983) *Inorganic Chemistry Principles of Structure and Reactivity, 3rd edit.*, p. 577 and 805, Harper and Row, New York.

Huyghues-Despointes, B. M. P., Klingler, T. M., and Baldwin, R. L. (1995) Measuring the strength of side-chain hydrogen bonds in peptide helices: the Gln•Asp (i,i+4) interaction. *Biochemistry* **34,** 13267-13271.

Huyghues-Despointes, B. M. P., Scholtz, J. M., and Baldwin, R. L. (1993a) Effect of a single aspartate on helix stability at different positions in a neutral alanine-based peptide. *Protein Sci.* **2,** 1604-1611.

Huyghues-Despointes, B. M. P., Scholtz, J. M., and Baldwin, R. L. (1993b) Helical peptides with three pairs of Asp-Arg and Glu-Arg residues in different orientations and spacings. *Protein Sci.* **2,** 80-85.

Ihara, S., Ooi, T., and Takahashi, S. (1982) Effects of salts on the nonequivalent stability of the α-helices of isomeric block copolypeptides. *Biopolymers* **21,** 131-145.

Ikura, M. (1996) Calcium binding and conformational response in EF-hand proteins. *Trends Bioch. Sci.* **21,** 14-17.

Ingraham, R. H., Lau, S. Y. M., Taneja, A. K., and Hodges, R. S. (1985) Denaturation and the effects of temperature on hydrophobic-interaction and reversed-phase high performance liquid chromatography of proteins. *J. Chromatogr.* **327,** 77-92.

Iverson, B. L., Iverson, S. A., Roberts, V. A., Getzoff, E. D., Tainer, J. A., Benkovic, S. J., and Lerner, R. A. (1990) Metalloantibodies. *Science* **249,** 659-662.

Jaenicke, R. (1991) Protein stability and molecular adaptation to extreme conditions. *Eur. J. Biochem.* **202,** 715-728.

Janin, J. & Wodak, S. (1978) Conformation of amino acid side-chains in proteins. *J. Mol. Biol.* **125,** 357-386.

Jelesarov, I. & Bosshard, H. R. (1996) Thermodynamic characterization of the coupled folding and association of heterodimeric coiled-coils (leucine zippers). *J. Mol. Biol.* **263,** 344-358.

Jelesarov, I., Dürr, E., Thomas, R. M., and Bosshard, H. R. (1998) Salt effects on hydrophobic interaction and charge screening in the folding of a negatively charged peptide to a coiled coil (leucine zipper). *Biochemistry* **37,** 7539-7550.

Jones, N. (1990) Transcriptional regulation by dimerization: two sides to an incestuous relationship. *Cell* **61,** 9-11.

Junius, F. K., O'Donoghue, S. I., Nilges, M., Weiss, A. S., and King, G. F. (1996) High resolution NMR solution structure of the leucine zipper domain of the c-Jun homodimer. *J. Biol. Chem.* **271,** 13663-13667.

Kaiser, E., Colescot, R. L., Bossinger, C. D., and Cook, P. I. (1970) Color test for detection of free terminal amino groups in the solid-phase synthesis of peptides. *Anal. Biochem.* **34,** 595-598.

Kaiser, E. T. & Kezdy, F. J. (1983) Secondary structures of proteins and peptides in amphiphilic environments (A Review). *Proc. Natl. Acad. Sci. U.S.A.* **80,** 1137-1143.

Kammerer, R. A., Schulthess, T., Landwehr, R., Lustig, A., and Engl, J. (1998) Tenascin-C hexabrachion assembly is a sequential two-step process initiated by coiled-coil α-helices. *J. Biol. Chem.* **in press**

Kamtekar, S. & Hecht, M. H. (1995) The four-helix bundle: what determines a fold? *FASEB J.* **9,** 1013-1022.

Kamtekar, S., Schiffer, J. M., Xiong, H., Babik, J. M., and Hecht, M. H. (1993) Protein design by binary patterning of polar and non-polar amino acids. *Science* **262,** 1680-1685.

Karplus, P. A. (1997) Hydrophobicity regained. *Protein Sci.* **6,** 1302-1307.

Kauzmann, W. (1959) Some factors in the interpretation of protein denaturation. *Adv. Protein Chem.* **14,** 1-63.

Kay, L. E., Forman-Kay, J. D., McCubbin, W. D., and Kay, C. M. (1991) Solution structure of a polypeptide dimer comprising the fourth Ca^{2+} binding site of troponin C by nuclear magnetic resonance. *Biochemistry* **30,** 4323-4333.

Kellis, J. T., Jr., Nyberg, K., and Fersht, A. R. (1989) Energetics of complimentary side-chain packing in a protein hydrophobic core. *Biochemistry* **28,** 4914-4922.

Kellis, J. T., Todd, R. J., and Arnold, F. H. (1991) Protein stabilization by engineered metal chelation. *Bio/technology* **9,** 994-995.

Kendrew, J. C., Bodo, G., M., D. H., Parrish, R. G., Wyckoff, H., and Phillips, D. C. (1958) A three-dimensional model of the myoglobin molecule obtained by x-ray analysis. *Nature* **181,** 662-666.

King, G. F. (1996) NMR spectroscopy and X-ray crystallography provide complementary information on the structure and dynamics of leucine zippers. *Biophys. J.* **71,** 1152-1154.

Kippen, A. D., Arcus, V. L., and Fersht, A. R. (1994) Structural studies on peptides corresponding to mutants of the major α-helix of barnase. *Biochemistry* **33,** 10013-10021.

Klemba, M., Gardner, K. H., Marino, S., Clarke, N. D., and Regan, L. (1995) Novel metal-binding proteins by design. *Nature Struct. Biol.* **2,** 368-373.

Knowles, J. R. (1987) Tinkering with enzymes: what are we learning? *Science* **236,** 1252-1258.

Kohn, W. D., Kay, C. M., and Hodges, R. S. (1995a) Protein destabilization by electrostatic repulsions in the two-stranded α-helical coiled-coil/leucine zipper. *Protein Sci.* 4, 237-250.

Kohn, W. D., Monera, O. D., Kay, C. M., and Hodges, R. S. (1995b) The effects of interhelical repulsions between glutamic acid residues in controlling the dimerization and stability of two-stranded α-helical coiled-coils. *J. Biol. Chem.* 270, 25495-25506.

Kohn, W. D., Mant, C. T., and Hodges, R. S. (1997a) α-Helical protein assembly motifs. *J. Biol. Chem.* **272,** 2583-2586.

Kohn, W. D., Kay, C. M., and Hodges, R. S. (1997b) Positional dependence of the effects of negatively charged Glu side-chains on the stability of two-stranded α-helical coiled-coils. *J. Pept. Sci.* 3, 209-223.

Kohn, W. D., Kay, C. M., and Hodges, R. S. (1997c) Salt effects on protein stability: two-stranded α-helical coiled-coils containing inter- or intrahelical ion pairs. *J. Mol. Biol.* 267, 1039-1052.

Kohn, W. D. & Hodges, R. S. (1998) *De novo* design of α-helical coiled-coils and bundles: models for development of protein design principles. *Trends Biotech.* **in press**

Kohn, W. D., Kay, C. M., and Hodges, R. S. (1998a) Effects of lanthanide binding on the stability of *de novo* designed α-helical coiled-coils. *J. Pept. Res.* 51, 9-18.

Kohn, W. D., Kay, C. M., Sykes, B. D., and Hodges, R. S. (1998b) Metal ion induced folding of a *de novo* designed coiled-coil peptide. *J. Am. Chem. Soc.* 120, 1124-1132.

Kohn, W. D., Kay, C. M., and Hodges, R. S. (1998c) Orientation, positional, additivity and oligomerization-state effects of interhelical ion pairs in α-helical coiled-coils. *J. Mol. Biol.* submitted

König, P. & Richmond, T. J. (1993) The X-ray structure of the GCN4-bZIP bound to ATF/CREB site DNA shows the complex depends on DNA flexibility. *J. Mol. Biol.* **233,** 139-154.

Krylov, D, Barchi, J, and Vinson, C. (1998) Inter-helical interactions in the leucine zipper coiled coil dimer: pH and salt dependence of coupling energy between charged amino acids. *J. Mol. Biol.* **279,** 959-972.

Krylov, D., Mikhailenko, I., and Vinson, C. (1994) A thermodynamic scale for leucine zipper stability and dimerization specificity: e and g interhelical interactions. *EMBO J.* **13,** 2849-2861.

Kuroda, Y., Hamada, D., Tanaka, T., and Goto, Y. (1996) High helicity of peptide fragments corresponding to β-strand regions of β-lactoglobulin observed by 2D-NMR spectroscopy. *Folding and Design* **1,** 255-263.

Lanyi, J. K. (1974) Salt-dependent properties of proteins from extremely halophilic bacteria. *Bacteriol. Rev.* **38,** 272-290.

Lau, S. Y. M., Taneja, A. K., and Hodges, R. S. (1984a) Effects of high performance liquid chromatographic solvents and hydrophobic matrices on the secondary and quaternary structure of a model protein. *J. Chromatogr.* **317,** 129-140.

Lau, S. Y. M., Taneja, A. K., and Hodges, R. S. (1984b) Synthesis of a model protein of defined secondary and quaternary structure. Effect of chain length on the stabilization and formation of two-stranded α-helical coiled-coils. *J. Biol. Chem.* **259,** 13253-13261.

Lavigne, P., Kondejewski, L. H., Houston, M. E., Jr, Sönnichsen, F. D., Lix, B., Sykes, B. D., Hodges, R. S., and Kay, C. M. (1995) Preferential heterodimeric parallel coiled-coil formation by synthetic Max and c-Myc leucine zippers: a description of putative electrostatic interactions responsible for the specificity of heterodimerization. *J. Mol. Biol.* **254,** 505-520.

Lavigne, P., Sönnichsen, F. D., Kay, C. M., and Hodges, R. S. (1996) Interhelical salt bridges, coiled-coil stability, and specificity of dimerization. *Science* **271,** 1136-1137.

Lazaridis, T., Archontis, G., and Karplus, M. (1995) Enthalpic contribution to protein stability: insights from atom-based calculations and statistical mechanics. *Adv. Protein Chem.* **47,** 231-306.

Lear, J. D., Wasserman, Z. R., and DeGrado, W. F. (1988) Synthetic amphiphilic peptide models for protein ion channels. *Science* **240,** 1177-1181.

Leberman, R. & Soper, A. K. (1995) Effect of high salt concentrations on water structure. *Nature* **378,** 364-366.

Lee, K. K., Black, J. A., and Hodges, R. S. (1991) Separation of intrachain disulfide bridged peptides from their reduced forms by reversed-phase chromatography. In *High-Performance Liquid Chromatography of Peptides and Proteins: Separation, Analysis, and Conformation* (Mant, C. T. & Hodges, R. S., eds), pp. 783-791, CRC Press, Baca Raton, Florida.

Lee, L. & Sykes, B. D. (1980) Strategies for the use of lanthanide NMR shift probes in the determination of protein structure in solution. Application to the EF calcium binding site of carp parvalbumin. *Biophys. J.* **32,** 193-210.

Lehrer, S. S., Qian, Y., and Hvidt, S. (1989) Assembly of the native heterodimer of *Rana esculenta* tropomyosin by chain exchange. *Science* **246,** 926-928.

Lehrer, S. S. & Stafford, W. F., III (1991) Preferential assembly of the tropomyosin heterodimer: equilibrium studies. *Biochemistry* **30,** 5682-5688.

Lieberman, M. & Sasaki, T. (1991) Iron(II) organizes a synthetic peptide into three-helix bundles. *J. Am. Chem. Soc.* **113,** 1470-1471.

Lin, T.-Y. & Timasheff, S. N. (1996) On the role of surface tension in the stabilization of globular proteins. *Protein Sci.* **5,** 372-381.

Linderstrom-Lang, K. (1924) On the ionization of proteins. *Compt. Rend. Trav. Lab. Carlsberg* **15,** 1-29.

Livingstone, J. R., Spolar, R. S., and Record, M. T., Jr. (1991) Contribution to the thermodynamics of protein folding from the reduction in water-accessible nonpolar surface area. *Biochemistry* **30,** 4237-4244.

Lockhart, D. J. & Kim, P. S. (1993) Electrostatic screening of charge and dipole interactions with the helix backbone. *Science* **260,** 198-202.

Lounnas, V. & Wade, R. C. (1997) Exceptionally stable salt bridges in cytochrome P450cam have functional roles. *Biochemistry* **36,** 5402-5417.

Lovejoy, B., Choe, S., Cascio, D., McRorie, D. K., DeGrado, W. F., and Eisenberg, D. (1993) Crystal structure of a synthetic triple-stranded alpha-helical bundle. *Science* **259,** 1288-1293.

Lovett, E. G., D'Avignon, D. A., Holtzer, M. E., Braswell, E. H., Zhu, D., and Holtzer, A. (1996) Observation via one-dimensional $^{13}C^{\alpha}$ NMR of local conformational substates in thermal unfolding equilibria of a synthetic analog of the GCN4 leucine zipper. *Proc. Natl. Acad. Sci. USA* **93,** 1781-1785.

Lowey, S. (1965) Comparative study of the α-helical muscle proteins. Tyrosyl titration and effect of pH on conformation. *J. Biol. Chem.* **240,** 2421-2427.

Lu, Y. & Valentine, J. S. (1997) Engineering metal-binding sites in proteins. *Curr. Opin. Struct. Biol.* **7,** 495-500.

Lumb, K. J., Carr, C. M., and Kim, P. S. (1994) Subdomain folding of the coiled-coil leucine zipper from the bZIP transcriptional activator GCN4. *Biochemistry* **33,** 7361-7367.

Lumb, K. J. & Kim, P. S. (1995a) A buried polar interaction imparts structural uniqueness in a designed heterodimeric coiled-coil. *Biochemistry* **34,** 8642-8648.

Lumb, K. J. & Kim, P. S. (1995b) Measurement of interhelical electrostatic interactions in the GCN4 leucine zipper. *Science* **268,** 436-439.

Lumb, K. J. & Kim, P. S. (1996) Interhelical salt bridges, coiled-coil stability, and specificity of dimerization. *Science* **271,** 1137-1138.

Lupas, A. (1996) Coiled-coils: new structures and new functions. *Trends Biochem. Sci.* **21,** 375-382.

Lupas, A., Van Dyke, M., and Stock, J. (1991) Predicting coiled-coils from protein sequences. *Science* **252,** 1162-1164.

Lyu, P. C., Gans, P. J., and Kallenbach, N. R. (1992) Energetic contribution of solvent-exposed ion pairs to alpha-helix structure. *J. Mol. Biol.* **223,** 343-350.

Lyu, P. C., Wemmer, D. E., Zhou, H. X., Pinker, R. J., and Kallenbach, N. R. (1993) Capping interactions in isolated α-helices: position-dependent substitution effects and structure of a serine-capped peptide helix. *Biochemistry* **32,** 421-425.

Mackay, J. P., Shaw, G. L., and King, G. F. (1996) Backbone dynamics of the c-Jun leucine zipper: ^{15}N NMR relaxation studies. *Biochemistry* **35,** 4867-4877.

Mainfroid, V., Terpstra, P., Beauregard, M., Frere, J.-M., Mande, S. C., Hol, W. G. J., Martial, J. A., and Goraj, K. (1996) Three hTIM mutants that provide new insights on why TIM is a dimer. *J. Mol. Biol.* **257,** 441-456.

Makhatadze, G. I. & Privalov, P. L. (1992) Protein interactions with urea and guanidinium chloride. A calorimetric study. *J. Mol. Biol.* **226,** 491-505.

Makhatadze, G. I. & Privalov, P. L. (1993) Contribution of hydration to protein folding thermodynamics. I. The enthalpy of hydration. *J. Mol. Biol.* **232,** 639-659.

Makhatadze, G. I. & Privalov, P. L. (1995) Energetics of protein structure. *Adv. Protein Chem.* **47,** 307-425.

Manning, G. S. (1972) On the application of polyelectrolyte "limiting laws" to the helix-coil transitions of DNA. I. excess univalent cations. *Biopolymers* **11,** 937-949.

Manning, G. S. (1978) The molecular theory of polyelectrolyte solutions with applications to the electrostatic properties of polynucleotides. *Quart. Rev. Biophys.* **11,** 179-246.

Märki, W., Oppliger, M., and Schwyzer, R. (1977a) Chemical synthesis, proton NMR parameters, hydrogen- and calcium-ion complexation of L-γ-carboxyglutamyl-L-γ-carboxyglutamic acid and D-γ-carboxyglutamyl-L-leucine. *Helv. Chim. Acta* **60,** 807-815.

Märki, W., Oppliger, M., Thanei, P., and Schwyzer, R. (1977b) D(-)- and L(+)-γ-carboxyglutamic acid (Gla): resolution of synthetic Gla derivatives. *Helv. Chim. Acta* **60,** 798-806.

Marko, I., Giles, P. R., Tsukazaki, M., Brown, S. M., and Urch, C. J. (1996) Copper-catalyzed oxidation of alcohols to aldehydes and ketones: an efficient, aerobic alternative. *Science* **274,** 2044-2046.

Marmorstein, R., Carey, M., Ptashne, M., and Harrison, S. C. (1992) DNA recognition by GAL4: structure of a protein DNA complex. *Nature* **356,** 408-414.

Marmorstein, R. & Harrison, S. C. (1994) Crystal structure of a PPR1-DNA complex: DNA recognition by proteins containing a Zn_2Cys_6 binuclear cluster. *Genes Dev.* **8,** 2504-2512.

Matthews, B. W. (1995a) Studies on protein stability with T4 lysozyme. *Adv. Protein Chem.* **46,** 249-278.

Matthews, B. W. (1996) Structural and genetic analysis of the folding and function of T4 lysozyme. *FASEB J.* **10,** 35-41.

Matthews, D. J. (1995b) Interfacial metal-binding site design. *Curr. Opin. Biotechnol.* **6,** 419-424.

Matthews, D. J. & Wells, J. A. (1994) Engineering an interfacial zinc site to increase hormone-receptor affinity. *Chem. Biol.* **1,** 25-30.

Mayo, S. L. & Baldwin, R. L. (1993) Guanidinium chloride induction of partial unfolding in amide proton exchange in RNAse A. *Science* **262,** 873-876.

Mayr, L. M. & Schmid, F. X. (1993) Stabilization of a protein by guanidinium chloride. *Biochemistry* **32,** 7994-7998.

McDevit, W. F. & Long, F. A. (1952) The activity coefficient of benzene in aqueous salt solutions. *J. Am. Chem. Soc.* **74,** 1773-1777.

McGrath, M. E., Haymore, B. L., Summers, N. L., Craik, C. S., and Fletterick, R. J. (1993) Structure of an engineered, metal-actuated switch in trypsin. *Biochemistry* **32,** 1914-1919.

McKnight, S. L. (1991) Molecular zippers in gene regulation. *Sci. Am.* **264,** 54-64.

McLachlan, A. D. & Stewart, M. (1975) Tropomyosin coiled-coil interactions: evidence for an unstaggered structure. *J. Mol. Biol.* **98,** 293-304.

McLachlan, A. D. & Stewart, M. (1976) The 14-fold periodicity in α-tropomyosin and the interaction with actin. *J. Mol. Biol.* **103,** 271-298.

McRorie, D. K. & Voelker, P. J. (1993) *Self-associating Systems in the Analytical Ultracentrifuge,* Beckman Instruments Inc., Fullerton, California.

Merrifield, R. B. (1963) Solid-phase peptide synthesis I. The synthesis of a tetrapeptide. *J. Am. Chem. Soc.* **85,** 2149-2154.

Merutka, G., Lipton, W., Shalongo, W., Park, S.-H., and Stellwagen, E. (1990) Effect of central residue replacements on the helical stability of a monomeric peptide. *Biochemistry* **29,** 7511-7515.

Meyer, M., Schreck, R., and Baeuerle, P. A. (1993) H_2O_2 and antioxidants have opposite effects on activation of NF-κB and AP-1 in intact cells: AP-1 as secondary antioxidant-responsive factor. *EMBO J.* **12,** 2005-2015.

Miceli, R., Myszka, D., Mao, J., Sathe, G., and Chaiken, I. (1996) The coiled-coil stem loop miniprotein as a presentation scaffold. *Drug Design and Discovery* **13,** 95-105.

Mo, J., Holtzer, M. E., and Holtzer, A. (1990) The thermal denaturation of nonpolymerizable αα-tropomyosin and its segments as a function of ionic strength. *Biopolymers* **30,** 921-927.

Moitra, J., Szilak, L., Krylov, D., and Vinson, C. (1997) Leucine is the most stabilizing aliphatic amino acid in the **d** position of a dimeric leucine zipper coiled-coil. *Biochemistry* **36,** 12567-12573.

Monera, O. D., Kay, C. M., and Hodges, R. S. (1994a) Electrostatic interactions control the parallel and antiparallel orientation of α-helical chains in two-stranded α-helical coiled-coils. *Biochemistry* **33,** 3862-3871.

Monera, O. D., Kay, C. M., and Hodges, R. S. (1994b) Protein denaturation with guanidine hydrochloride or urea provides a different estimate of stability depending on the contributions of electrostatic interactions. *Protein Sci.* **3,** 1984-1991.

Monera, O. D., Sereda, T. J., Zhou, N. E., Kay, C. M., and Hodges, R. S. (1995) Relationship of sidechain hydrophobicity and α-helical propensity on the stability of the single-stranded amphipathic α helix. *J. Pept. Sci.* **1,** 319-329.

Monera, O. D., Sonnichsen, F. D., Hicks, L., Kay, C. M., and Hodges, R. S. (1996) The relative positions of alanine residues in the hydrophobic core control the formation of two-stranded or four-stranded α-helical coiled-coils. *Protein Eng.* **9,** 353-363.

Monera, O. D., Zhou, N. E., Kay, C. M., and Hodges, R. S. (1993) Comparison of antiparallel and parallel two-stranded α-helical coiled-coils: design, synthesis, and characterization. *J. Biol. Chem.* **268,** 19218-19227.

Morjana, N. A., McKeone, B. J., and Gilbert, H. F. (1993) Guanidine hydrochloride stabilization of a partially unfolded intermediate during the reversible denaturation of protein disulfide isomerase. *Proc. Natl. Acad. Sci. USA* **90,** 2107-2111.

Morrow, J. R., Buttrey, L. A., Shelton, V. M., and Berback, K. A. (1992) Efficient catalytic cleavage of RNA by lanthanide(III) macrocyclic complexes: toward synthetic nucleases for *in vivo* applications. *J. Am. Chem. Soc.* **114,** 1903-1905.

Muegge, I., Schweins, T., and Warshel, A. (1998) Electrostatic contributions to protein-protein binding affinities: application to Rap/Raf interaction. *Proteins: Struct. Funct. Genet.* **30,** 407-423.

Munoz, V. & Serrano, L. (1994) Intrinsic secondary structure propensities of the amino acids, using statistical Φ-Ψ matrices: comparison with experimental scales. *Proteins: Struct. Funct. Genet.* **20,** 301-311.

Murphy, K. P., Privalov, P. L., and Gill, S. J. (1990) Common features of protein unfolding and dissolution of hydrophobic compounds. *Science* **247,** 559-561.

Murre, C., Schonleber McCaw, P., and Baltimore, D. (1989) A new DNA binding and dimerization motif in immunoglobulin enhancer binding, daughterless, MyoD, and myc proteins. *Cell* **56,** 777-783.

Mutter, M., Gassmann, R., Buttkus, U., and Altmann, K.-H. (1991) Switch peptides: pH-induced α-helix to β-sheet transitions of bis-amphiphilic oligopeptides. *Angew. Chem. Int. Ed. Engl.* **30,** 1514-1516.

Myers, J. K. & Pace, C. N. (1996) Hydrogen bonding stabilizes globular proteins. *Biophys. J.* **71,** 2033-2039.

Myers, J. K., Pace, C. N., and Scholtz, J. M. (1995) Denaturant *m* values and heat capacity changes: relation to changes in accessible surface areas of protein unfolding. *Protein Sci.* **4,** 2138-2148.

Myers, J. K., Pace, C. N., and Scholtz, J. M. (1997) Helix propensities are identical in proteins and peptides. *Biochemistry* **36,** 10923-10929.

Nakamura, H. (1996) Roles of electrostatic interaction in proteins. *Quart. Rev. Biophys.* **29,** 1-90.

Nandi, P. K. & Robinson, D. R. (1972a) The effects of salts on the free energies of nonpolar groups in model peptides. *J. Am. Chem. Soc.* **94,** 1308-1315.

Nandi, P. K. & Robinson, D. R. (1972b) The effects of salts on the free energy of the peptide group. *J. Am. Chem. Soc.* **94,** 1299-1308.

Nautiyal, S., Woolfson, D. N., King, D. S., and Alber, T. (1995) A designed heterotrimeric coiled-coil. *Biochemistry* **34,** 11645-11651.

Nicholson, H., Anderson, D. E., Dao-pin, S., and Matthews, B. W. (1991) Analysis of the interaction between charged side chains and the α-helix dipole using designed thermostable mutants of phage T4 lysozyme. *Biochemistry* **30,** 9816-9828.

Nicholson, H., Becktel, W. J., and Matthews, B. W. (1988) Enhanced protein thermostability from designed mutations that interact with α-helix dipoles. *Nature* **336,** 651-656.

Nilges, M. & Brunger, A. T. (1993) Successful prediction of the coiled-coil geometry of the GCN4 leucine zipper domain by simulated annealing: comparison to the X-ray structure. *Proteins Struct. Funct. Genet.* **15,** 133-146.

Noelken, M. & Holtzer, A. (1964) The denaturation of paramyosin and tropomyosin by guanidine hydrochloride. In *Biochemistry of Muscle Contraction* (Gergely, J., ed.), pp. 374-378, Little, Brown, and Co., Boston, MA.

Novabiochem (1997) *Novabiochem Catalog and Peptide Synthesis Handbook '97/98,* Novabiochem, San Diego, CA.

O'Neil, K. T. & DeGrado, W. F. (1990) A thermodynamic scale for the helix-forming tendencies of the commonly occurring amino acids. *Science* **250,** 646-651.

O'Shea, E. K., Klemm, J. D., Kim, P. S., and Alber, T. (1991) X-ray structure of the GCN4 leucine zipper, a two-stranded, parallel coiled-coil. *Science* **254,** 539-544.

O'Shea, E. K., Lumb, K. J., and Kim, P. S. (1993) Peptide "velcro": design of a heterodimeric coiled-coil. *Curr. Biol.* **3,** 658-667.

O'Shea, E. K., Rutkowski, R., and Kim, P. S. (1989a) Evidence that the leucine zipper is a coiled-coil. *Science* **243,** 538-542.

O'Shea, E. K., Rutkowski, R., and Kim, P. S. (1992) Mechanism of specificity in the Fos-Jun oncoprotein heterodimer. *Cell* **68,** 699-708.

O'Shea, E. K., Rutkowski, R., Stafford, W. F. I., and Kim, P. S. (1989b) Preferential heterodimer formation by isolated leucine zippers from Fos and Jun. *Science* **245,** 646-648.

Oas, T. G., McIntosh, L. P., O'Shea, E. K., Dahlquist, F. W., and Kim, P. S. (1990) Secondary structure of a leucine zipper determined by nuclear magnetic resonance spectroscopy. *Biochemistry* **29,** 2891-2894.

Ogihara, N. L., Weiss, M. S., DeGrado, W. F., and Eisenberg, D. (1997) The crystal structure of the designed trimeric coiled-coil-V_aL_d: implications for engineering crystals and supramolecular assemblies. *Protein Sci.* **6,** 80-88.

Pace, C. N. (1986) Determination and analysis of urea and guanidine hydrochloride denaturation curves. *Methods Enzymol.* **131,** 266-280.

Pace, C. N., Shirley, B. A., McNutt, M., and Gajiwala, K. (1996) Forces contributing to the conformational stability of proteins. *FASEB J.* **10,** 75-83.

Pack, P. & Pluckthun, A. (1992) Miniantibodies: use of amphipathic helices to produce functional, flexibly linked dimeric F_v fragments with high avidity in *Escherichia coli. Biochemistry* **31,** 1579-1584.

Patel, L. R., Curran, T., and Kerppola, T. K. (1994) Energy transfer analysis of Fos-Jun dimerization and DNA binding. *Proc. Natl. Acad. Sci. USA* **91,** 7360-7364.

Pauling, L. & Corey, R. B. (1953) Compound helical configurations of polypeptide chains: structure of proteins of the α-keratin type. *Nature* **171,** 59-61.

Pearson, R. G. (1963) Hard and soft acids and bases. *J. Am. Chem. Soc.* **85,** 3533-3539.

Pertsemlidis, A., Saxena, A. M., Soper, A. K., and Head-Gordon, T. (1996) Direct evidence for modified solvent structure within the hydration shell of a hydrophobic amino acid. *Proc. Natl. Acad. Sci. USA* **93,** 10769-10774.

Perutz, M. F. (1978) Electrostatic effects in proteins. *Science* **201,** 1187-1191.

Perutz, M. F., Gronenborn, G. M. C., Fogg, J. H., and Shih, D. T. (1985) The pK_a values of two histidine residues in human haemoglobin, the Bohr effect, and the dipole moments of α-helices. *J. Mol. Biol.* **183,** 491-498.

Pflugrath, J. W. & Quiocho, F. A. (1985) Sulphate sequestered in the sulphate-binding protein of *Salmonella typhimurium* is bound solely by hydrogen bonds. *Nature* **314,** 257-260.

Phillips, G. N., Jr. (1992) What is the pitch of the α-helical coiled-coil? *Proteins: Struct. Funct. Genet.* **14,** 425-429.

Phillips, G. N., Jr., Fillers, J. P., and Cohen, C. (1986) Tropomyosin crystal structure and muscle regulation. *J. Mol. Biol.* **192,** 111-131.

Pognonec, P., Rato, H., and Roeder, R. G. (1992) The helix-loop-helix/leucine repeat transcription factor USF can be functionally regulated in a redox-dependent manner. *J. Biol. Chem.* **267,** 24563-24567.

Potekhin, S. A., Medvedkin, V. N., Kashparov, I. A., and Venyaminov, S. Y. (1994) Synthesis and properties of the peptide corresponding to the mutant form of the leucine zipper of the transcriptional activator GCN4 from yeast. *Protein Eng.* **7,** 1097-1101.

Presta, L. G. & Rose, G. D. (1988) Helix signals in proteins. *Science* **240,** 1632-1641.

Privalov, P. L., Ptitsyn, O. B., and Birshtein, T. M. (1969) Determination of stability of the DNA double helix in an aqueous medium. *Biopolymers* **8,** 559-571.

Prorok, M., Warder, S. E., Blandl, T., and Castellino, F. J. (1996) Calcium binding properties of synthetic γ-carboxyglutamic acid-containing marine cone snail "sleeper" peptides, Conantokin-G and Conantokin-T. *Biochemistry* **35,** 16528-16534.

Ptitsyn, O. B. (1995) Molten globule and protein folding. *Adv. Protein Chem.* **47,** 83-229.

Pu, W. T. & Struhl, K. (1993) Dimerization of leucine zippers analyzed by random selection. *Nucl. Acids Res.* **21,** 4348-4355.

Qian, H. (1994) A thermodynamic model for the helix-coil transition coupled to dimerization of short coiled-coil peptides. *Biophys. J.* **67,** 349-355.

Ramalingam, K., Aimoto, S., and Bello, J. (1992) Conformational studies of anionic melittin analogues: effect of peptide concentration, pH, ionic strength, and temperature - models for protein folding and halophilic proteins. *Biopolymers* **32,** 981-992.

Reddy, B. A., Etkin, L. D., and Freemont, P. S. (1992) A novel zinc finger coiled-coil domain in a family of nuclear proteins. *Trends Bioch. Sci.* **17,** 344-345.

Regan, L. (1993) The design of metal-binding sites in proteins. *Annu. Rev. Biophys. Biomol. Struct.* **22,** 257-281.

Regan, L. (1995) Protein design: novel metal-binding sites. *Trends Biochem. Sci.* **20,** 280-285.

Regan, L. & Clarke, N. D. (1990) A tetrahedral zinc(II)-binding site introduced into a designed protein. *Biochemistry* **29,** 10878-10883.

Regan, L., Rockwell, A., Wasserman, Z., and Degrado, W. (1994) Disulfide crosslinks to probe the structure and flexibility of a designed four-helix bundle protein. *Protein Sci.* **3,** 2419-2427.

Richardson, J. S. & Richardson, D. C. (1988) Amino acid preferences for specific locations at the ends of α-helices. *Science* **240,** 1648-1652.

Roberts, V. A. & Getzoff, E. D. (1995) Metalloantibody design. *FASEB J.* **9,** 94-100.

Robinson, C. R. & Sligar, S. G. (1993) Electrostatic stabilization in four-helix bundle proteins. *Protein Sci.* **2,** 826-837.

Rogers, N. K. & Sternberg, M. J. E. (1984) Electrostatic interactions in globular proteins: different dielectric models applied to the packing of α-helices. *J. Mol. Biol.* **174,** 527-542.

Rohl, C. A., Chakrabartty, A., and Baldwin, R. L. (1996) Helix propagation and N-cap propensities of the amino acids measured in alanine-based peptides in 40 volume percent trifluoroethanol. *Protein Sci.* **5,** 2623-2637.

Ruan, F., Chen, Y., and Hopkins, P. B. (1990) Metal ion enhanced helicity in synthetic peptides containing unnatural, metal-ligating residues. *J. Am. Chem. Soc.* **112,** 9403-9404.

Russo, M. J., Bayley, H., and Toner, M. (1997) Reversible permeabilization of plasma membranes with an engineered switchable pore. *Nature Biotechnol.* **15,** 278-282.

Saiki, R. K., Gelfand, D. H., Stoffel, S., Scharf, S. J., Higuchi, R., Horn, G. T., Mullis, K. B., and Erlich, H. A. (1988) Primer-directed enzymatic amplification of DNA with a thermostable DNA polymerase. *Science* **239,** 487-491.

Sali, D., Baycroft, M., and Fersht, A. R. (1991) Surface electrostatic interactions contribute little to stability of barnase. *J. Mol. Biol.* **220,** 779-788.

Sali, D., Bycroft, M., and Fersht, A. R. (1988) Stabilization of protein structure by interaction of α-helix dipole with a charged side chain. *Nature* **335,** 740-743.

Sancho, J., Serrano, L., and Fersht, A. R. (1992) Histidine residues at the N- and C-termini of α-helices: perturbed pK_as and protein stability. *Biochemistry* **31,** 2253-2258.

Saudek, V., Pastore, A., Castiglione Morelli, M. A., Frank, R., Gausepohl, H., and Gibson, T. (1991) The solution structure of a leucine-zipper motif peptide. *Protein Eng.* **4,** 519-529.

Schmidt-Dörr, T., Oertel-Buchheit, P., Pernelle, C., Bracco, L., Schnarr, M., and Granger-Schnarr, M. (1991) Construction, purification, and characterization of a hybrid protein comprising the DNA binding domain of the LexA repressor and the Jun leucine zipper: a circular dichroism and mutagenesis study. *Biochemistry* **30,** 9657-9664.

Schneider, J. P. & Kelly, J. W. (1995) Synthesis and efficacy of square planar copper complexes designed to nucleate β-sheet structure. *J. Am. Chem. Soc.* **117,** 2533-2546.

Schneider, J. P., Lear, J. D., and DeGrado, W. F. (1997) A designed buried salt bridge in a heterodimeric coiled-coil. *J. Am. Chem. Soc.* **119,** 5742-5743.

Scholtz, J. M., Qian, H., Robbins, V. H., and Baldwin, R. L. (1993) The energetics of ion-pair and hydrogen-bonding interactions in a helical peptide. *Biochemistry* **32,** 9668-9676.

Schreck, R., Rieber, P., and Baeuerle, P. A. (1991) Reactive oxygen intermediates as apparently widely used messengers in the activation of the NF-κB transcription factor and HIV-1. *EMBO J.* **10,** 2247-2258.

Schuermann, M., Hunter, J. B., Hennig, G., and Muller, R. (1991) Non-leucine residues in the leucine repeats of Fos and Jun contribute to the stability and determine the specificity of dimerization. *Nucl. Acids Res.* **19,** 739-746.

Schulz, G. E. & Schirmer, R. H. (1979) Chapter 3: Noncovalent forces determining protein structure. In *Principles of Protein Structure,* pp. 27-45, Springer-Verlag, New York.

Seo, J. & Cohen, C. (1993) Pitch diversity in α-helical coiled-coils. *Proteins: Struct. Funct. Genet.* **15,** 223-234.

Sereda, T. J., Mant, C. T., Sönnichsen, F. D., and Hodges, R. S. (1994) Reversed-phase chromatography of synthetic amphipathic α-helical peptides as a model for ligand/receptor interactions: effect of changing hydrophobic environment on the relative hydrophilicity/hydrophobicity of amino acid side-chains. *J. Chromatogr.* **676,** 139-153.

Serrano, L. & Fersht, A. R. (1989) Capping and α-helix stability. *Nature* **342,** 296-299.

Serrano, L., Horovitz, A., Avron, B., Bycroft, M., and Fersht, A. R. (1990) Estimating the contribution of engineered surface electrostatic interactions to protein stability by using double-mutant cycles. *Biochemistry* **29,** 9343-9352.

Sessa, G., Morelli, G., and Ruberti, I. (1993) The Athb-1 and -2 HD-Zip domains homodimerize forming complexes of different DNA binding specificities. *EMBO J.* **12,** 3507-3517.

Shoemaker, K. R., Kim, P. S., Brems, D. N., Marqusee, S., York, E. J., Chaiken, I. M., Stewart, J. M., and Baldwin, R. L. (1985) Nature of the charged-group effect on the stability of the C-peptide helix. *Proc. Natl. Acad. Sci. USA* **82,** 2349-2353.

Shoemaker, K. R., Kim, P. S., York, E. J., Stewart, J. M., and Baldwin, R. L. (1987) Tests of the helix dipole model for stabilization of α-helices. *Nature* **326,** 563-567.

Shortle, D. (1995) Staphylococcal nuclease: a showcase of *m-* value effects. *Adv. Protein Chem.* **46,** 217-247.

Skolnick, J. & Holtzer, A. (1985) Theory of α-helix to random coil transition of two-chain coiled-coils. Application of the augmented theory to thermal denaturation of α-tropomyosin. *Macromolecules* **18,** 1549-1559.

Skolnick, J. & Holtzer, A. (1986) α-Helix to random-coil transitions of two-chain coiled-coils: a theoretical model for the "pretransition" in cysteine-190-cross-linked tropomyosin. *Biochemistry* **25,** 6192-6202.

Smillie, L. B. (1979) Structure and functions of tropomyosins from muscle and non-muscle sources. *Trends Bioch. Sci.* **4,** 151-155.

Songster, M. F. & Barany, G. (1997) Handles for solid-phase peptide synthesis. *Methods Enzymol.* **289,** 126-174.

Sonnichsen, F. D., Van Eyk, J. E., Hodges, R. S., and Sykes, B. D. (1992) Effect of trifluoroethanol on protein secondary structure: an NMR and CD study using a synthetic actin peptide. *Biochemistry* **31,** 8790-8798.

Soriano-Garcia, M., Padmanabhan, K., de Vos, A. M., and Tulinsky, A. (1992) The Ca^{2+} ion and membrane binding structure of the Gla domain of Ca-prothrombin Fragment 1. *Biochemistry* **31,** 2554-2566.

Sosnick, T. R., Jackson, S., Wilk, R. R., Englander, S. W., and DeGrado, W. F. (1996) The role of helix formation in the folding of a fully α-helical coiled-coil. *Proteins: Struct. Funct. Genet.* **24,** 427-432.

Sperling, R., Furie, B. C., Blumenstein, M., Keyt, B., and Furie, B. (1978) Metal binding properties of γ-carboxyglutamic acid. *J. Biol. Chem.* **253,** 3898-3906.

Spolar, R. S., Ha, J.-H., and Record, M. T., Jr. (1989) Hydrophobic effect in protein folding and other noncovalent processes involving proteins. *Proc. Natl. Acad. Sci. USA* **86,** 8382-8385.

Stellwagen, E., Park, S. H., Shalongo, W., and Jain, A. (1992) The contribution of residue ion pairs to the helical stability of a model peptide. *Biopolymers* **32,** 1193-1200.

Stewart, J. & Young, J. (1984) *Solid Phase Peptide Synthesis,* Pierce Chemical Co., Rockford, Illinois.

Stewart, J. D., Roberts, V. A., Crowder, M. W., Getzoff, E. D., and Benkovic, S. J. (1994) Creation of a novel biosensor for Zn(II). *J. Am. Chem. Soc.* **116,** 415-416.

Stewart, M. (1993) Intermediate filament structure and assembly. *Curr. Opin. Cell Biol.* **5,** 3-11.

Stigter, D. & Dill, K. A. (1990) Charge effects on folded and unfolded proteins. *Biochemistry* **29,** 1262-1271.

Stone, D., Sodek, J., Johnson, P., and Smillie, L. B. (1975) Tropomyosin: correlation of amino acid sequence and structure. In *Proceedings of the IX Federation of European Biochemical Societies Meeting, Proteins of Contractile Systems* (Biro, E. N. A., ed.), pp. 125-136, North Holland Publishing, Amsterdam.

Strehlow, K. G. & Baldwin, R. L. (1989) Effect of the substitution Ala-Gly at each of five residue positions in the C-peptide helix. *Biochemistry* **28,** 2130-2133.

Strynadka, N. C. J. & James, M. N. G. (1989) Crystal structures of the helix-loop-helix calcium-binding proteins. *Annu. Rev. Biochem.* **58,** 951-998.

Su, J. Y., Hodges, R. S., and Kay, C. M. (1994) Effect of chain length on the formation and stability of synthetic α-helical coiled-coils. *Biochemistry* **33,** 15501-15510.

Sunnerhagen, M., Forsen, S., Hoffren, A.-M., Drakenberg, T., Teleman, O., and Stenflo, J. (1995) Structure of the Ca^{2+}-free Gla domain sheds light on membrane binding of blood coagulation proteins. *Nature Struct. Biol.* **2,** 504-509.

Szilak, L., Moitra, J., Krylov, D., and Vinson, C. (1997a) Phosphorylation destabilizes α-helices. *Nature Struct. Biol.* **4,** 112-114.

Szilak, L., Moitra, J., and Vinson, C. (1997b) Design of a leucine zipper coiled-coil stabilized 1.4 kcal/mol by phosphorylation of a serine in the **e** position. *Protein Sci.* **6,** 1273-1283.

Takahashi, S., Kim, E.-H., Hibino, T., and Ooi, T. (1989) Comparison of α-helix stability in peptides having a negatively or positively charged residue block attached either to the N- or C-terminus of an α-helix: the electrostatic contribution and anisotropic stability of the α-helix. *Biopolymers* **28,** 995-1009.

Talbot, J. A. & Hodges, R. S. (1982) Tropomyosin: a model protein for studying coiled-coil and α-helix stabilization. *Acc. Chem. Res.* **15,** 224-230.

Tam, J. P., Wu, C.-R., Liu, W., and Zhang, J.-W. (1991) Disulfide bond formation in peptides by dimethyl sulfoxide. Scope and applications. *J. Am. Chem. Soc.* **113,** 6657-6662.

Tanford, C. (1970) Protein Denaturation. Part C. Theoretical models for the mechanism of denaturation. *Adv. Protein Chem.* **24,** 1-95.

Taylor, R. & Kennard, O. (1984) Hydrogen-bond geometry in organic crystals. *Acc. Chem. Res.* **17,** 320-326.

Thompson, K. S., Vinson, C. R., and Freire, E. (1993) Thermodynamic characterization of the structural stability of the coiled-coil region of the bZIP transcription factor GCN4. *Biochemistry* **32,** 5491-5496.

Thompson-Kenar, K., García-Moreno, B., and Freire, E. (1995) A calorimetric characterization of the salt dependence of the stability of the GCN4 leucine zipper. *Protein Sci.* **4,** 1934-1938.

Tian, Z.-Q. & Bartlett, P. A. (1996) Metal coordination as a method for templating peptide conformation. *J. Am. Chem. Soc.* **118,** 943-949.

Tidor, B. (1994) Helix-capping interaction in λ cro protein: a free energy simulation analysis. *Proteins: Struct. Funct. Genet.* **19,** 310-323.

Titus, M. A. (1993) Myosins. *Curr. Opin. Cell Biol.* **5,** 77-81.

Tripet, B., Yu, L., Bautista, D. L., Wong, W. Y., Irvin, R. T., and Hodges, R. S. (1996) Engineering a *de novo* designed coiled-coil heterodimerization domain for the rapid detection, purification and characterization of recombinantly expressed peptides and proteins. *Protein Eng.* **9,** 1029-1042.

Tripet, B., Zhou, N., Sönnichsen, F., and Hodges, R. S. (1995) Hybritein 1: a *de novo* designed protein displaying cooperative interactions between a metal-ion binding loop and a helix-helix dimerization motif. In *Peptides 1994: Proceedings of the 23rd European Peptide Symposium.* (Maia, H.L.S., ed.), pp. 79-80, ESCOM, Leiden, The Netherlands.

Tsong, T. Y. (1975) An acid induced conformational transition of denatured cytochrome c in urea and guanidine hydrochloride solutions. *Biochemistry* **14,** 1542-1547.

Villegas, V., Viguera, A. R., Aviles, F. X., and Serrano, L. (1996) Stabilization of proteins by rational design of α-helix stability using helix-coil transition theory. *Folding and Design* **1,** 29-34.

Vinson, C. R., Hai, T., and Boyd, S. M. (1993) Dimerization specificity of the leucine zipper-containing bZIP motif on DNA binding: prediction and rational design. *Genes Dev.* **7**, 1047-1058.

Volbeda, A., Fontecilla-Camps, J. C., and Frey, M. (1996) Novel metal sites in protein structures. *Curr. Opin. Struct. Biol.* **6**, 804-812.

Von Hippel, P. H. & Wong, K. Y. (1965) On the conformational stability of globular proteins: the effects of various electrolytes and non-electrolytes on the thermal ribonuclease transition. *J. Biol. Chem.* **240**, 3909-3923.

Voyer, N. & Lamothe, J. (1995) The use of peptidic frameworks for the construction of molecular receptors and devices. *Tetrahedron* **51**, 9241-9284.

Wada, A. (1976) The α-helix as an electric macro-dipole. *Adv. Biophys.* **9**, 1-63.

Wade, W. S., Ashley, J. A., Jahangiri, G. K., McElhaney, G., Janda, K. D., and Lerner, R. A. (1993) A highly specific metal-activated catalytic antibody. *J. Am. Chem. Soc.* **115**, 4906-4907.

Wagner, G. (1995) The importance of being floppy. *Nature Struct. Biol.* **2**, 255-257.

Waldburger, C. D., Schildbach, J. F., and Sauer, R. T. (1995) Are buried salt bridges important for protein stability and conformational specificity? *Nature Struct. Biol.* **2**, 122-128.

Walkup, G. K. & Imperiali, B. (1996) Design and evaluation of a peptidyl fluorescent chemosensor for divalent zinc. *J. Am. Chem. Soc.* **118**, 3053-3054.

Waltho, J. P., Feher, V. A., Merutka, G., Dyson, H. J., and Wright, P. E. (1993) Peptide models of protein folding initiation sites. 1. Secondary structure formation by peptides corresponding to the G- and H- helices of myoglobin. *Biochemistry* **32**, 6337-6347.

Wang, C.-L. A., Leavis, P. C., Horrocks, W. D., Jr., and Gergely, J. (1981) Binding of lanthanide ions to troponin C. *Biochemistry* **20**, 2439-2444.

Wang, Y., DuBois, J. L., Hedman, B., Hodgson, K. O., and Stack, T. D. P. (1998) Catalytic galactose oxidase models: biomimetic Cu(II)-phenoxyl-radical reactivity. *Science* **279**, 537-540.

Warshel, A. & Russell, S. T. (1984) Calculations of electrostatic interactions in biological systems and in solutions. *Quart. Rev. Biophys.* **17**, 283-422.

Weast, R. C. (1971) Editor of *Handbook of Chemistry and Physics*, 52nd edit., CRC, Cleveland, Ohio.

Wells, J. A. (1990) Additivity of mutational effects in proteins. *Biochemistry* **29**, 8509-8517.

Wendt, H., Berger, C., Baici, A., Thomas, R. M., and Bosshard, H. R. (1995) Kinetics of folding of leucine zipper domains. *Biochemistry* **34**, 4097-4107.

Wendt, H., Leder, L., Härmä, H., Jelesarov, I., Baici, A., and Bosshard, H. R. (1997) Very rapid, ionic strength-dependent association and folding of a heterodimeric leucine zipper. *Biochemistry* **36,** 204-213.

Willett, W. S., Gillmor, S. A., Perona, J. J., Fletterick, R. J., and Craik, C. S. (1995) Engineered metal regulation of trypsin specificity. *Biochemistry* **34,** 2172-2180.

Williams, R. J. P. (1995) Energised (entatic) states of groups and of secondary structures in proteins and metalloproteins. *Eur. J. Biochem.* **234,** 363-381.

Williams, T. C., Corson, D. C., and Sykes, B. D. (1984) Calcium-binding proteins: calcium(II)-lanthanide(III) exchange in carp parvalbumin. *J. Am. Chem. Soc.* **106,** 5698-5702.

Wimley, W. C., Gawrisch, K., Creamer, T. P., and White, S. H. (1996) Direct measurement of salt-bridge solvation energies using a peptide model system: implications for protein stability. *Proc. Natl. Acad. Sci. USA* **93,** 2985-2990.

Wishart, D. S., Sykes, B. D., and Richards, F. M. (1991) Relationship between nuclear magnetic resonance chemical shift and protein secondary structure. *J. Mol. Biol.* **222,** 311-333.

Wójcik, J., Altmann, K.-H., and Scheraga, H. A. (1990) Helix-coil stability constants for the naturally occurring amino acids in water. XXIV. Half-cystine parameters from random poly(hydroxybutylglutamine-co-S-methylthio-L-cysteine). *Biopolymers* **30,** 121-134.

Wong, C.-H. (1989) Enzymatic catalysts in organic synthesis. *Science* **244,** 1145-1152.

Wu, Z., Johnson, K. W., Goldstein, B., Choi, Y., Eaton, S. F., Laue, T. M., and Ciardelli, T. L. (1995) Solution assembly of a soluble, heteromeric, high affinity interleukin-2 receptor complex. *J. Biol. Chem.* **270,** 16039-16044.

Xiong, H., Buckwalter, B. L., Shieh, H.-M., and Hecht, M. H. (1995) Periodicity of polar and nonpolar amino acids is the major determinant of secondary structure in self-assembling oligomeric peptides. *Proc. Natl. Acad. Sci. U.S.A.* **92,** 6349-6353.

Xu, D., Lin, S. L., and Nussinov, R. (1997) Protein binding *versus* protein folding: the role of hydrophilic bridges in protein associations. *J. Mol. Biol.* **265,** 68-84.

Yang, A.-S. & Honig, B. (1993) On the pH dependence of protein stability. *J. Mol. Biol.* **231,** 459-474.

Yang, J., Spek, E. J., Gong, Y., Zhou, H., and Kallenbach, N. R. (1997) The role of context on α-helix stabilization: host-guest analysis in a mixed background peptide model. *Protein Sci.* **6,** 1264-1272.

Yao, S., Ghosh, I., Zutshi, R., and Chmielewski, J. (1997) A pH-modulated, self-replicating peptide. *J. Am. Chem. Soc.* **119,** 10559-10560.

Yellen, G., Sodickson, D., Chen, T.-Y., and Jurman, M. E. (1994) An engineered cysteine in the external mouth of a K^+ channel allows inactivation to be modulated by metal binding. *Biophys. J.* **66,** 1068-1075.

Yip, K. S. P., Stillman, T. J., Britton, K. L., Artymiuk, P. J., Baker, P. J., Sedelnikova, S. E., Engel, P. C., Pasquo, A., Chiaraluce, R., Consalvi, V., Scandurra, R., and Rice, D. W. (1995) The structure of *Pyrococcus furiosus* glutamate dehydrogenase reveals a key role for ion-pair networks in maintaining enzyme stability at extreme temperatures. *Structure* **3,** 1147-1158.

Yu, Y. (1996) Investigation of electrostatic interactions in two-stranded α-helical coiled-coils through residue shuffling. PhD Dissertation, The Johns Hopkins University

Yu, Y., Monera, O. D., Hodges, R. S., and Privalov, P. L. (1996) Ion pairs significantly stabilize coiled-coils in the absence of electrolyte. *J. Mol. Biol.* **255,** 367-372.

Zaccai, G. & Eisenberg, H. (1990) Halophilic proteins and the influence of solvent on protein stabilization. *Trends Bioch. Sci.* **15,** 333-337.

Zell, A., Einspahr, H., and Bugg, C. E. (1985) Model for calcium binding to γ-carboxyglutamic acid residues of proteins: crystal structure of calcium α-ethylmalonate. *Biochemistry* **24,** 533-537.

Zeng, X., Zhu, H., Lashuel, H. A., and Hu, J. C. (1997) Oligomerization properties of GCN4 leucine zipper *e* and *g* position mutants. *Protein Sci.* **6,** 2218-2226.

Zhou, H. X., Lyu, P., Wemmer, D. E., and Kallenbach, N. R. (1994a) Alpha helix capping in synthetic model peptides by reciprocal side chain-main chain interactions: evidence for an N terminal "capping box". *Proteins: Struct. Funct. Genet.* **18,** 1-7.

Zhou, N. E., Kay, C. M., and Hodges, R. S. (1992a) Synthetic model proteins: positional effects of interchain hydrophobic interactions on stability of two-stranded α-helical coiled-coils. *J. Biol. Chem.* **267,** 2664-2670.

Zhou, N. E., Kay, C. M., and Hodges, R. S. (1992b) Synthetic model proteins: the relative contribution of leucine residues at the non-equivalent positions of the 3-4 hydrophobic repeat to the stability of the two-stranded α-helical coiled-coil. *Biochemistry* **31,** 5739-5746.

Zhou, N. E., Kay, C. M., and Hodges, R. S. (1993a) Disulfide bond contribution to protein stability: positional effects of substitution in the hydrophobic core of the two-stranded α-helical coiled-coil. *Biochemistry* **32,** 3178-3187.

Zhou, N. E., Kay, C. M., and Hodges, R. S. (1994b) The net energetic contribution of interhelical electrostatic attractions to coiled-coil stability. *Protein Eng.* **7,** 1365-1372.

Zhou, N. E., Kay, C. M., and Hodges, R. S. (1994c) The role of interhelical ionic interactions in controlling protein folding and stability: *de novo* designed synthetic two-stranded α-helical coiled-coils. *J. Mol. Biol.* **237,** 500-512.

Zhou, N. E., Kay, C. M., Sykes, B. D., and Hodges, R. S. (1993b) A single-stranded amphipathic α-helix in aqueous solution: design, structural characterization, and its application for determining α-helical propensities of amino acids. *Biochemistry* **32,** 6190-6197.

Zhou, N. E., Mant, C. T., and Hodges, R. S. (1990) Effect of preferred binding domains on peptide retention behavior in reversed-phase chromatography: amphipathic α-helices. *Peptide Res.* **3,** 8-20.

Zhou, N. E., Monera, O. D., Kay, C. M., and Hodges, R. S. (1994d) α-Helical propensities of amino acids in the hydrophobic face of an amphipathic α-helix. *Protein Pept. Lett.* **1,** 114-119.

Zhou, N. E., Zhu, B.-Y., Kay, C. M., and Hodges, R. S. (1992c) The two-stranded α-helical coiled-coil is an ideal model for studying protein stability and subunit interactions. *Biopolymers* **32,** 419-426.

Zhou, N. E., Zhu, B.-Y., Sykes, B. D., and Hodges, R. S. (1992d) Relationship between amide proton chemical shifts and hydrogen bonding in amphipathic α-helical peptides. *J. Am. Chem. Soc.* **114,** 4320-4326.

Zhou, N. E., Zhu, B. Y., Kay, C. M., and Hodges, R. S. (1993c) Importance of intrachain ionic interactions in stabilizing α-helices in proteins. In *Peptides, Biology and Chemistry: Proceedings of the 1992 Chinese Peptide Symposium* (Du, Y. C., Tam, J. P. & Zhang, Y. S., eds), pp. 217-220, ESCOM, Leiden, The Netherlands.

Zhu, B. Y., Zhou, N. E., Kay, C. M., and Hodges, R. S. (1993) Packing and hydrophobicity effects on protein folding and stability: effects of β-branched amino acids, valine and isoleucine, on the formation and stability of two-stranded α-helical coiled-coils/leucine zippers. *Protein Sci.* **2,** 383-394.

Zhu, B. Y., Zhou, N. E., Semchuk, P. D., Kay, C., and Hodges, R. S. (1992) Design, synthesis and structural characterization of model heterodimeric coiled-coil proteins. *Int. J. Peptide Protein Res.* **40,** 171-179.

Zhukovsky, E. A., Mulkerrin, M. G., and Presta, L. G. (1994) Contribution to global protein stabilization of the N-capping box in human growth hormone. *Biochemistry* **33,** 9856-9864.

Zitzewitz, J. A., Bilsel, O., Luo, J., Jones, B. E., and Matthews, C. R. (1995) Probing the folding mechanism of a leucine zipper peptide by stopped-flow circular dichroism spectroscopy. *Biochemistry* **34,** 12812-12819.

Zou, Q., Habermann-Rottinghaus, S. M., and Murphy, K. P. (1998) Urea effects on protein stability: hydrogen bonding and the hydrophobic effect. *Proteins: Struct. Funct. Genet.* **31,** 107-115.

APPENDIX I

DE NOVO DESIGN OF α-HELICAL COILED-COILS AND BUNDLES: MODELS FOR DEVELOPMENT OF PROTEIN-DESIGN PRINCIPLES[9]

Abstract

The *de novo* design of model α-helical proteins from first principles has proved to be a useful approach to studying the short- and long-range noncovalent interactions that control the folding, stability, conformational changes and biological functions of proteins. These synthetic proteins are also pointing the way towards a host of potential applications. Here, we review recent progress in the development of design principles with model proteins and briefly discuss some of the potential applications for this technology.

Introduction

De novo protein design is a relatively new field of scientific endeavour that has two major objectives. Since Anfinsen's experiments demonstrating reversible unfolding of ribonuclease A (Anfinsen, 1973), it has been recognized that the three-dimensional structure of proteins is encoded within the primary sequence; the unknown relationship between primary and tertiary structure is the protein-folding problem. The design of artificial proteins is a method of trying to unravel the protein-folding problem by predicting a protein sequence that will adopt a particular structure and then experimentally testing the prediction. The second, and perhaps ultimately more important, reason for protein design is for obtaining novel molecules with useful functional activities for medical or industrial applications (Voyer & Lamothe, 1995).

---

[9] A version of this review paper has been accepted for publication: Kohn, W. D. and Hodges, R. S. (1998) *Trends Biotech.* (in press)

However, before *de novo* design of proteins with desired activities can be consistently achieved, a strong understanding of the short- and long-range noncovalent interactions that affect protein folding, stability and activity is needed (Hodges, 1996). In particular, the relative contributions of different noncovalent forces must be understood. Thus, much of the *de novo* design effort has been devoted to measuring the effects of various noncovalent forces in simple model-protein systems. For several reasons, most of the *de novo* design efforts to date have used the α-helix (Box 1) as the secondary structural unit (Zhou *et al.*, 1992b): (1) the α-helix is the most common secondary structure, comprising on average approximately one third of all residues in globular proteins; (2) proteins containing only one form of secondary structure, particularly α-helix, are simpler to analyse by techniques such as circular-dichroism spectroscopy; (3) α-helical-bundle proteins can be fairly simple in terms of having high degrees of symmetry, and yet they can accurately represent the various types of interhelical side-chain interactions that are the major force responsible for the folding of all α-helical proteins and of proteins in general. This article is a brief but comprehensive overview of the progress made in *de novo* design of α-helical proteins and, in particular, what has been learned from these systems about the forces that control protein folding and structure.

Aspects of *de novo* design

Protein synthesis

The *de novo* design of proteins has been made possible by two techniques: solid-phase peptide synthesis invented by Merrifield (Erickson & Merrifield, 1976; Fields & Noble, 1990) and bacterial protein expression via recombinant DNA technology (Gilbert & Villa-Komaroff, 1980). The strengths of peptide chemistry include its ease of use and high level of refinement, and also the ability to incorporate unnatural amino acids and special constraints such as lactam bridges (Houston *et al.*, 1996). However, the synthesis of polypeptides of more than 50 residues still remains a challenge with this technique. The greatest advantage of bacterial expression is that longer proteins can be made and, once an expression system and purification protocol are established, the generation of a large

---

Box 1: General characteristics of an α-helix

The α-helix is one of two regularly repeating conformations that the polypeptide backbone can adopt, the other being β sheet. The polypeptide is covalently held together by amide bonds between the amino acid building blocks, which are planar (indicated by a box around the four atoms which lie in a plane) and around which rotation is severely limited, owing to partial double bond character **(a)**. In contrast, the bonds between the α carbon and the nitrogen and between the α carbon and the carbonyl carbon of each amino acid are pure single bonds with a large degree of rotational freedom as specified by the conformational angles phi (ϕ) and psi (ψ), respectively **(a)**. In an α-helix composed of naturally-occurring *l*- amino acids, the ϕ and ψ angles are near -63° and -42°, respectively, and the helix has a clockwise or right-handed *screw sense* . A left-handed helix is sterically disallowed with *l*- amino acids but can occur in a peptide composed exclusively of the enantiomeric *d*- amino acids.

The major stabilizing feature of the α-helix is hydrogen bonds between the backbone carbonyl oxygen of each residue and the backbone NH proton of the fourth residue downchain (toward the carboxy terminus). Hydrogen bonds are denoted by dotted lines in the ball and stick representation below **(b)**. Each main chain CO and NH group is hydrogen bonded except the first four NH groups and the last four CO groups of the helix.

The helix is a rod-like structure from which the side chains, denoted R, point out in a pin wheel-like array **(b)**. On average, one residue corresponds to a 100° rotation and a translation along the helix axis of 1.5 Å. Accordingly, there are 3.6 residues per complete turn of the helix and a pitch (distance along the helix axis per turn) of 5.4 Å.

a

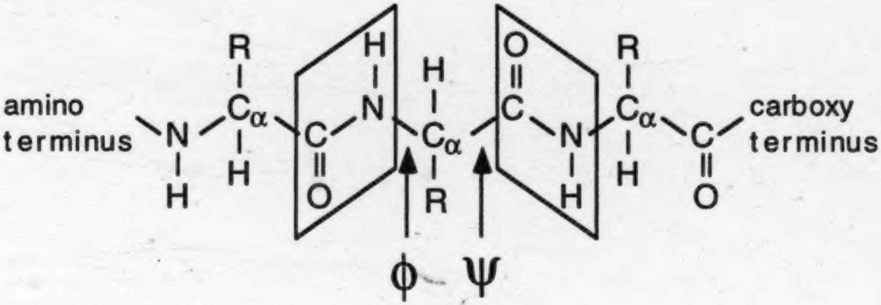
amino terminus
carboxy terminus
R
H
Cα
N
C
O
φ
ψ

b

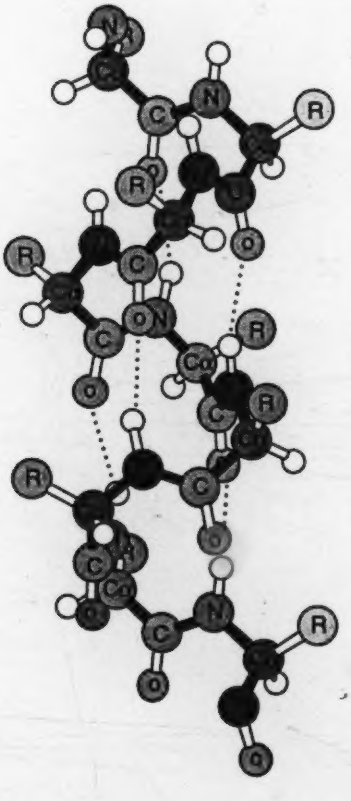

number of analogues can be rapidly achieved. However, the initial development of the expression and purification procedures is often difficult.

Sequence design

Sequence design can be approached in a number of ways. Because the object of *de novo* design is to obtain a particular folded structure, it is common for researchers to use the knowledge obtained from studying naturally-occurring examples of a folding motif as a guideline for their designs; for example, the study of the protein tropomyosin aided the synthesis of the first *de novo* designed α-helical coiled-coil protein (Hodges *et al.*, 1981; Talbot & Hodges, 1982). Traditionally, *de novo* design has been approached from a minimalist view (DeGrado *et al.*, 1989): by studying small proteins containing a limited number of noncovalent interactions and with highly repetitive sequences, uniform secondary structure and high symmetry, it was hoped that the rules that govern protein folding could be discerned. However, a purely minimalist design approach has led to synthetic proteins that lack some of the thermodynamic characteristics of native proteins (Box 2). Thus, it has become clear that, rather than a minimalist approach, design of proteins with native-like character requires a hierarchic design strategy (Bryson *et al.*, 1995). In essence, it is important to build in specific hydrophobic packing and/or hydrogen-bonding and electrostatic interactions to favour a particular folded structure (Handel *et al.*, 1993; Raleigh *et al.*, 1995; Raleigh & DeGrado, 1992). Another important aspect of a successful design strategy is the concept of negative design, through which a unique design can be favoured by destabilizing alternative structures. Because of the complexity of protein folding, even with small model proteins, new proteins will generally be obtained only through considerable trial and error. The design of artificial proteins therefore involves an iterative process in which an initial design is conceived and synthesized, then structurally and biophysically characterized (Box 3). The protein is then modified in further design cycles to optimize the desired characteristics (Fig. 1).

Box 2: Native-like versus molten globule-like structure

Naturally-occurring globular proteins fold under native conditions into a unique structure stabilized by hydrophobic interactions, specific packing (van der Waals) interactions, hydrogen-bonding, and electrostatic interactions. A number of biophysical criteria for a native-like structure have been identified, which include:

- a well-defined oligomeric state
- chemical-shift dispersion in the NMR spectrum, indicating a unique chemical environment for each atom
- a tightly packed hydrophobic core with no solvent access, as indicated by protection from amide-hydrogen exchange for portions of the backbone buried in the core and an inability to bind the hydrophobic dye ANS (see Box 3).
- a highly cooperative (sigmoidal) denaturation profile
- a large, positive ΔC_p (heat capacity change) of unfolding, indicative of the exposure of hydrophobic surface area to water

In contrast, the 'molten globule' has been described as a partially folded or intermediate state, in which secondary structure is essentially completely formed but the discrete packing interactions of the native state are absent. Thus, the protein core is loosely held together and may populate a number of rapidly interconverting conformations. The initial *de novo* designed helical bundles failed to meet all the criteria for a native-like structure and therefore exhibit some of the properties of molten globules. The energy-level diagram below illustrates the difference between the folding of a native and a molten globule-like protein. A native protein folds from the unfolded state, which is a large ensemble of conformations with similar energies, to folding intermediates such as the molten globule with fewer possible conformations to a single conformation in the fully folded state. The folded state of a molten globule-like protein resembles the intermediate states of a native protein, as both have a number of conformations, all with similar energies. However, the stability of the molten globule-like folded state can be quite high. One approach to obtaining a more native-like folded state is to destabilize the intermediate-like folded ensemble while, hopefully, specifying one particular conformation out of the ensemble that will have higher stability (lower free energy) than the rest. This may be accomplished through incorporation of interactions between buried polar side chains but could also be simply a result of specific steric complementarity of the core-packing interactions.

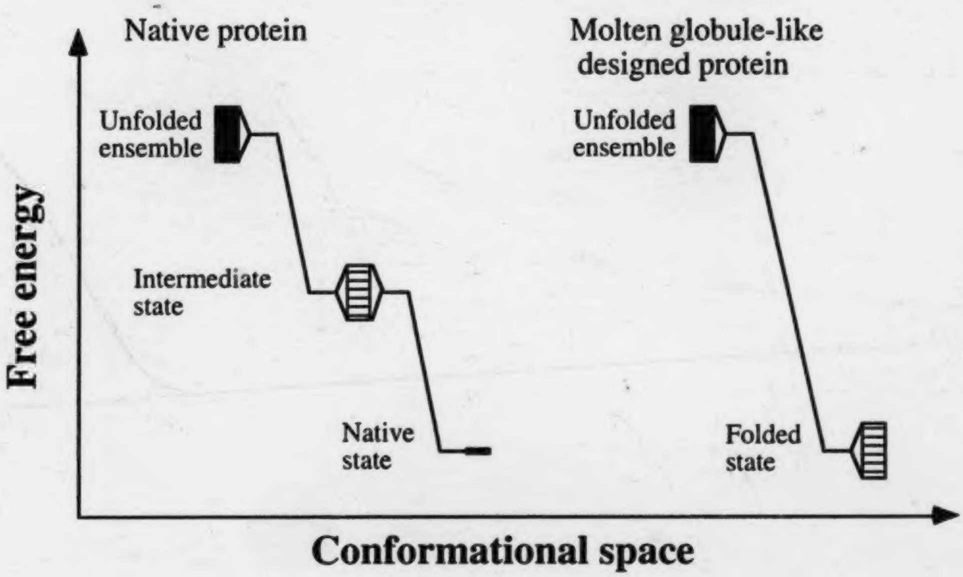
Native protein
Molten globule-like designed protein
Free energy
Unfolded ensemble
Intermediate state
Native state
Unfolded ensemble
Folded state
Conformational space

Box 3: Biophysical characterization techniques

Thorough characterization at each step of the design process is critical in *de novo* design. A number of biophysical methods are used for analysing the properties of designed coiled-coils and helical bundles. Far-UV circular-dichroism (CD) spectroscopy is an easy and effective way of measuring α-helical content and is the standard technique for monitoring the unfolding process during thermal or chemical denaturation. Stability measurements can also be made with differential scanning microcalorimetry, which has the advantage of being a direct measurement of the unfolding enthalpy rather than an indirect measurement, as is spectroscopy. For proteins containing aromatic residues, fluorescence spectroscopy and near-UV CD spectroscopy can also serve as useful probes of tertiary structure and dynamics. Fluorescence spectroscopy is also applied to measuring the binding of the hydrophobic dye 8-anilino-1-naphthalenesulfonate (ANS) to proteins, which is evidence for poor packing in the hydrophobic core. Size-exclusion (gel-filtration) chromatography and analytical ultracentrifugation are vital for studying oligomerization states. Nuclear-magnetic-resonance (NMR) spectroscopy has been extensively used to study the secondary and tertiary structures of synthetic proteins, and can also give qualitative information on native-like protein structure (Box 2). The use of NMR for structural determination of α-helical coiled-coils and bundles is difficult, particularly with repetitive (minimalist) designs, due to spectral overlap. X-ray crystallography has yielded a number of high-resolution structures of naturally-occurring and designed coiled-coils and bundles.

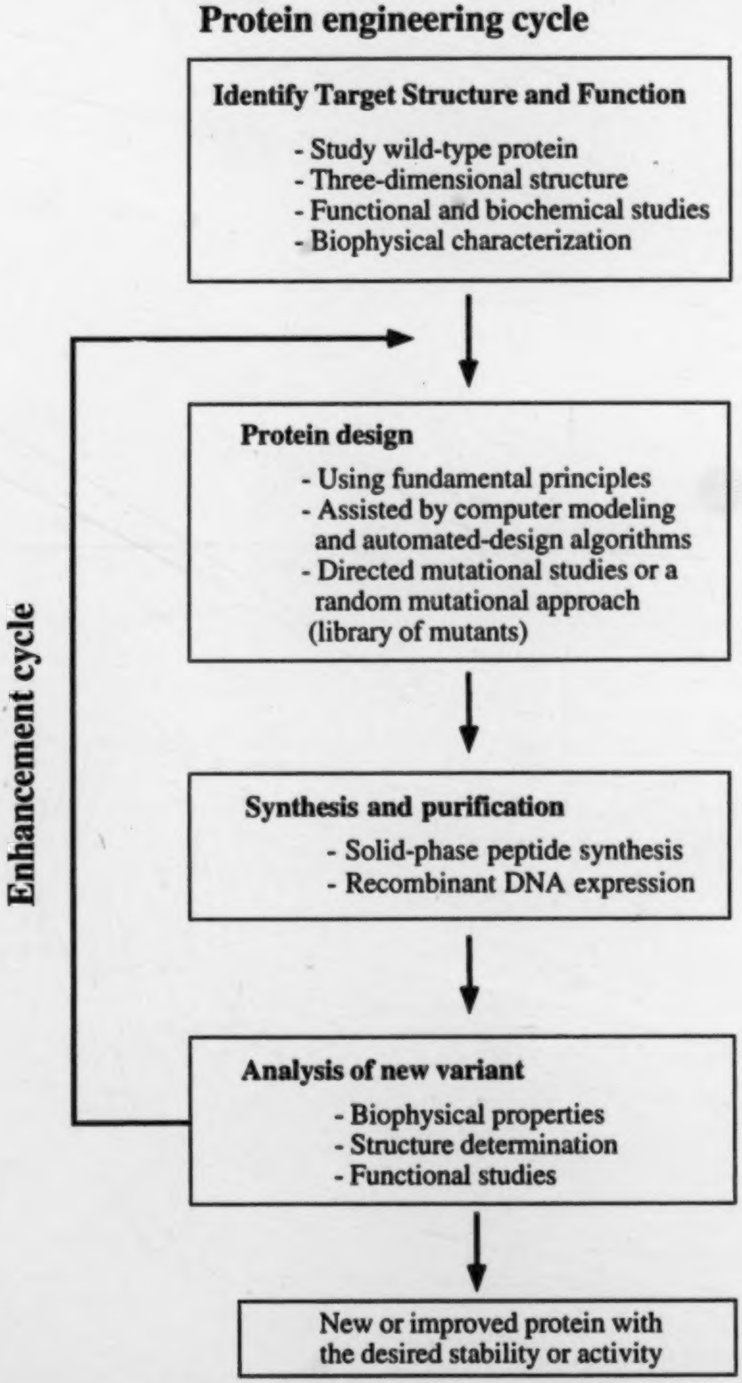
Protein engineering cycle
Identify Target Structure and Function
- Study wild-type protein
- Three-dimensional structure
- Functional and biochemical studies
- Biophysical characterization
Enhancement cycle
Protein design
- Using fundamental principles
- Assisted by computer modeling and automated-design algorithms
- Directed mutational studies or a random mutational approach (library of mutants)
Synthesis and purification
- Solid-phase peptide synthesis
- Recombinant DNA expression
Analysis of new variant
- Biophysical properties
- Structure determination
- Functional studies
New or improved protein with the desired stability or activity

Figure 1 General schematic of a *de novo* protein design or protein-engineering cycle.

In contrast to the standard, semi-rational trial-and-error approach to *de novo* design, some researchers are developing computer algorithms to automate the design process. Owing to its importance in the folded state of proteins, the hydrophobic core is a common target for automated design and structure prediction (Bowie *et al.*, 1991; Harbury *et al.*, 1995). For example, a computerized approach was used successfully to redesign the hydrophobic core of the phage 434 cro protein (Desjarlais & Handel, 1995), and a more ambitious example of automated design was recently demonstrated by Mayo and co-workers, who developed an algorithm that took into account residues in all parts of a protein: the buried core, the fully solvent-exposed surface and the transition region between the core and the surface. They were able to obtain a 28-residue sequence that mimics the zinc-finger fold with a well-packed hydrophobic core but requires no zinc for folding (Dahiyat *et al.*, 1997). Despite isolated successes in automated design of sequences to give a desired fold and in the prediction of structure from sequence, the development of a universal structure-prediction program is not likely to occur soon.

Another approach to protein design is the isolation of folded proteins from random sequence libraries, in which α-helical bundles displaying cooperative unfolding transitions and specific oligomeric states can make up as much as 1% of the total sequences (Davidson *et al.*, 1995; Roy *et al.*, 1997). This technique may offer promise for design, particularly in cases where some initial criteria are employed in library design (Kamtekar *et al.*, 1993). Ultimately, a combination of combinatorial and rational design strategies may prove most successful in obtaining new functional proteins.

General principles of coiled-coil and helical-bundle structures

Coiled-coils and helical bundles are two common α-helical motifs found in native proteins (Kohn *et al.*, 1997b). Coiled-coils are assemblies of two to four α-helices that pack either parallel or antiparallel to each other with a helix crossing angle near 20°. α-Helical bundles most commonly contain four helices and can be grouped into two major types - those in which the helix crossing angles are all the same and near 20° and those in which larger helix crossing angles occur - but we will discuss only the former type here. These helical bundles and coiled-coils are very similar, but some important differences are discussed below.

Observations of native and designed proteins have allowed some general principles for folding of α-helical assemblies to be elucidated. In particular, the major factor that controls the formation of helical proteins is the periodicity of hydrophobic (nonpolar) and hydrophilic (polar) residues within the sequence, which can be considered as a type of binary pattern (Fig. 2). Because a protein will fold in aqueous solution in such a way as to bury the hydrophobic side chains in the core (Dill, 1990), the type(s) of secondary structure present will be that most compatible with burying the most hydrophobicity, as shown in early studies (DeGrado *et al.*, 1989; Kaiser & Kezdy, 1983) and more recently by Hecht and co-workers (Kamtekar *et al.*, 1993; Xiong *et al.*, 1995). Basically, if hydrophobic and hydrophilic residues alternate, amphipathic β-sheet structure is formed preferentially (Fig. 2A), while a spacing of hydrophobic residues 3 or 4 residues apart leads to the formation of an amphipathic α-helix (Fig. 2B). The amphipathic α-helices or β-strands can then associate, with the hydrophobic face of each helix or strand buried in the subunit interface. Secondary structure in proteins is also influenced by the intrinsic conformational propensities of individual side chains (Munoz & Serrano, 1994). These propensities have been shown experimentally to impart only modest effects on stability; for example, a substitution in the solvent-exposed face of a coiled-coil (O'Neil & DeGrado, 1990) or a monomeric amphipathic α-helix (Monera *et al.*, 1995) affected stability by less than 1 kcal/mol, so intrinsic secondary-structure preferences only will affect structure if summed over a significant stretch of residues. If a conflict occurs between intrinsic secondary-structure propensities and the binary pattern of hydrophilic and hydrophobic residues (Fig. 2), the binary pattern is more likely to dictate the structure because the burial of hydrophobic surface area will generally contribute more to the stability of the folded state

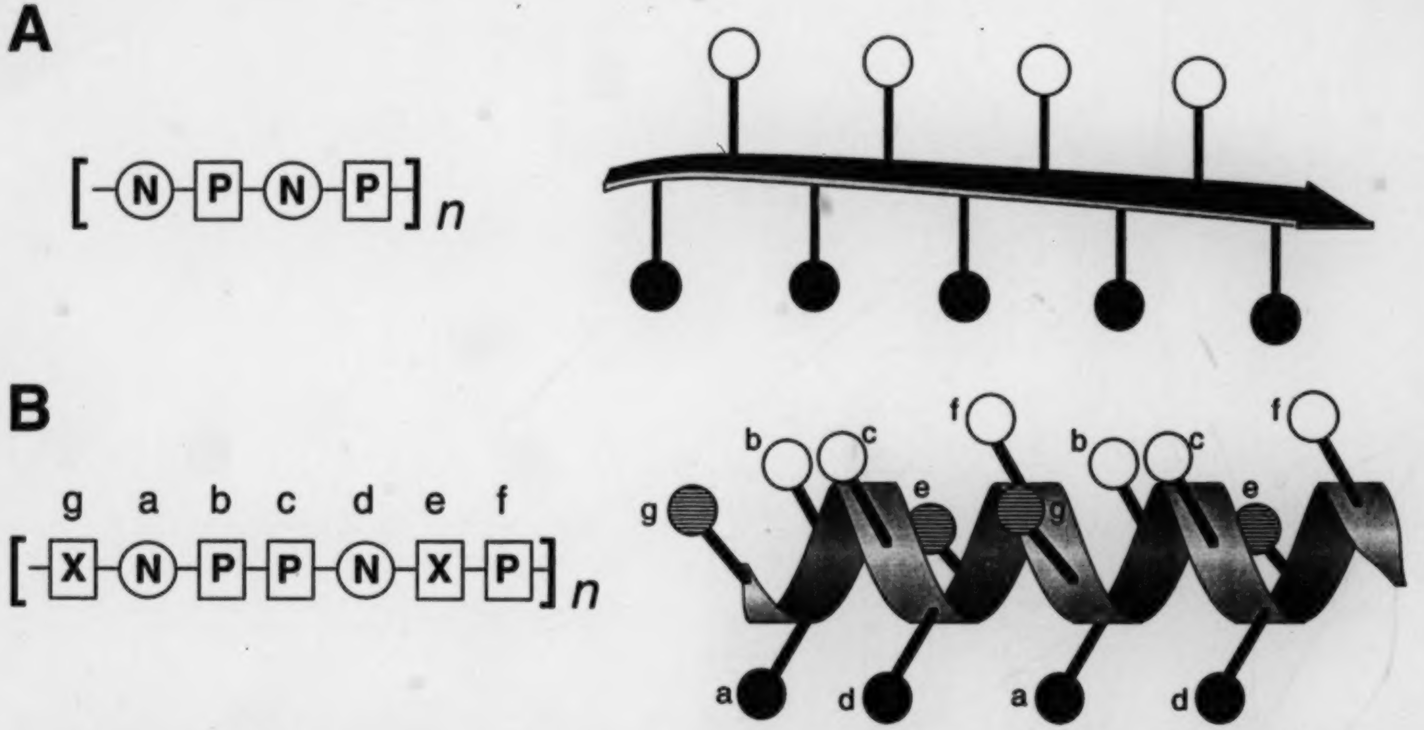

Figure 2 Patterns of polar (P) and nonpolar (N) amino acid residues that promote amphipathic β-sheet (**A**) or α-helical (**B**) secondary structure. The term binary pattern can be used here because there are two alternatives: a polar (hydrophilic) or a nonpolar (hydrophobic) side chain at each position. Open balls represent polar side chains, closed balls represent nonpolar side chains and hatched balls represent side chains that could be polar or nonpolar. In an amphipathic α helix, the **[gabcdef]**$_n$ nomenclature is used to label the various positions of the seven-residue sequence repeat, as explained in the text. Placement of hydrophobic residues only at positions **a** and **d** leads to the so-called 3-4 (or 4-3) hydrophobic repeat, in which the spacing between hydrophobes is three (**d** is three positions down from **a**) followed by four (**a** is four positions down from **d**). The **e** and **g** positions (hatched balls) are able to contribute to either the polar or the nonpolar face of the helix and may contain polar or nonpolar residues. In general, the position at which the heptad sequence starts is arbitrary since it is a repeating sequence, but in *de novo* designed coiled coils it is generally started at position **g**, which allows the N-terminal **g** residue to participate in a stabilizing **g-e'** interhelical interaction (Lumb & Kim, 1994).

(Xiong *et al.*, 1995). A dramatic recent result in which a primarily β-sheet domain was converted to an α-helical bundle through less than 50% sequence change (Dalal *et al.*, 1997) illustrates the importance of the burial of hydrophobic side chains and emphasizes the fact that only some of the residues in a protein sequence are critical for dictating the fold.

The formation of amphipathic α-helices is generally indicated by a heptad sequence repeat denoted **[abcdefg]**$_n$, in which positions **a** and **d** are occupied mostly by hydrophobic residues and form the hydrophobic face required for helix-helix interaction (Fig. 2B). Positions **e** and **g** flank the hydrophobic face and can also participate in interhelical interactions (Fig. 2B). These positions often contain charged residues, which may participate in interhelical attractions or repulsions (Kohn *et al.*, 1995; Zhou *et al.*, 1994). The remaining heptad positions (**b**, **c**, and **f**) are solvent exposed. Helical-wheel diagrams (Figs 4 and 5) offer a cross-sectional (end-on) view of coiled-coils and bundles, and are a common way of illustrating the interhelical interactions that occur in these molecules.

One of the major differences between helical bundles and coiled-coils is that a coiled-coil contains a narrow hydrophobic face (hydrophobic residues primarily at the **a** and **d** heptad positions) while bundles tend to contain a wider hydrophobic face, owing to a greater incidence of hydrophobes at the **e** and **g** positions (Mant *et al.*, 1993). The wider hydrophobic face naturally promotes higher oligomerization states in which more surface area can be buried, and so the four-helix bundle is the most common. However, even coiled-coils with all polar residues at the **e** and **g** positions can prefer a four-stranded structure (Monera *et al.*, 1996a, 1996b). Coiled-coils are characterized by left-handed supercoiling (twisting) of the helices around one another like the strands of a rope, which changes the effective number of residues per turn (along the coiled-coil axis) from 3.6 to 3.5 and allows the helices to stay in continuous contact over long distances (Cohen & Parry, 1990) (Fig. 3). By contrast, the helices of a bundle diverge at the ends due to the

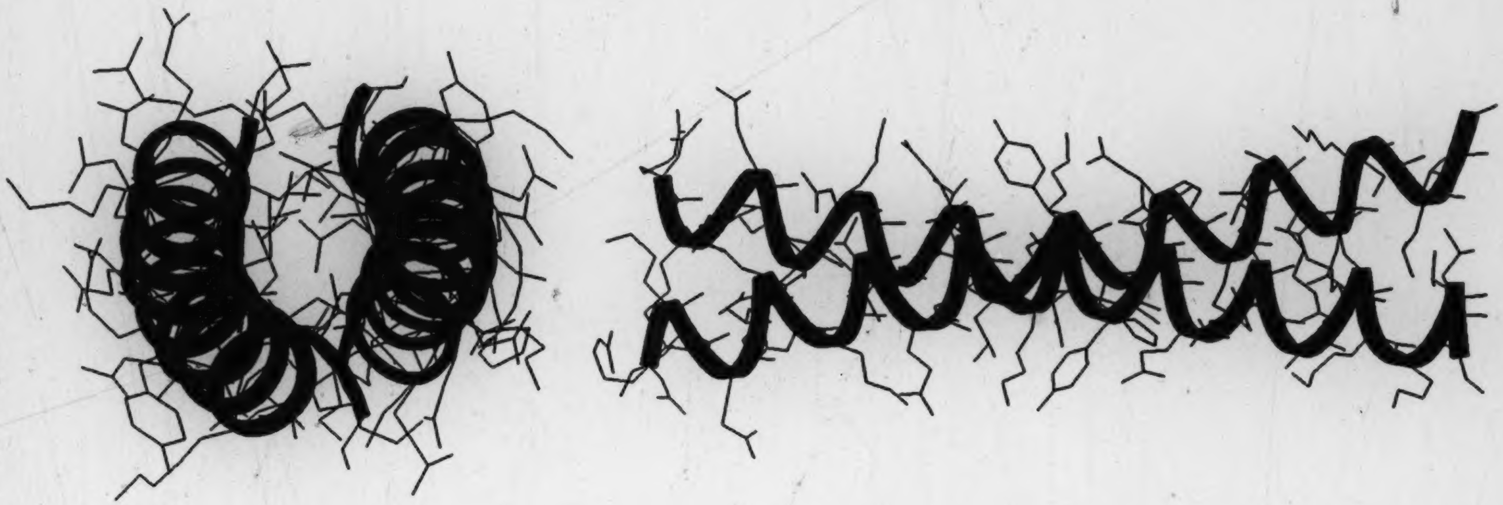

Figure 3 Two views of a two-stranded α-helical coiled coil, in which the helical peptide backbone is highlighted by a ribbon. A view along the superhelix axis from the N terminus (left) illustrates the curved nature and left-handed supercoiling of the helices. The pitch of the superhelical twist of a two-stranded coiled coil is generally 140-150Å (there are about 100 residues per repeat of the superhelix). The side view (right) clearly shows the 18° crossing angle of the helices. (adapted from the crystal structure coordinates of the GCN4 leucine zipper (O'Shea *et al.*, 1991))

absence of significant supercoiling. This divergence can be important for function by allowing the formation of cavities that can bind cofactors, such as in haem-binding proteins like cytochrome b562 (Kamtekar & Hecht, 1995). Independently of interhelical-packing interactions, amphipathic helices are inherently curved, such that the hydrophobic face is concave and the hydrophilic face is convex (Barlow & Thornton, 1988; Zhou *et al.*, 1992c), resulting in backbone hydrogen bonds that are shorter and more linear (the donor-hydrogen-acceptor angle is near zero) in the hydrophobic face and longer in the hydrophilic face (O'Shea *et al.*, 1991; Zhou *et al.*, 1992c).

Hydrophobic-core interactions

Although the hydrophobic effect is well accepted as the driving force for protein folding and stability (Dill, 1990), it is also clear that the precise packing of residues in the hydrophobic core is the major determinant for specifying the native-like properties of natural proteins (Box 2). Much work has been focussed on understanding the stability and structural effects of hydrophobic-core mutations in both natural and designed proteins. The native four-stranded coiled-coil protein Rop has been a good model for *de novo* hydrophobic core design (Betz *et al.*, 1997; Munson *et al.*, 1994, 1996). Munson *et al.* (1994) created a repacked, simplified core containing only Leu and Ala in Rop, resulting in increased thermal stability while maintaining the structural and native-like physical properties of the wild-type protein. Later work on Rop showed that the packing requirements for stability and native-like character are related but different (Munson *et al.*, 1996), allowing the creation of native-like variants with higher or lower stability.

In the *de novo* design of proteins from first principles, a native-like structure has been difficult to achieve. The first minimalist four-helix bundle, produced by DeGrado and co-workers (Regan & DeGrado, 1988), contained Leu residues at all **a** and **d** positions and formed a 'molten globule-like' structure (Box 2), as did the four-helix bundle 'Felix' which, unlike DeGrado's peptide, was designed with a nonuniform hydrophobic core (Hecht *et al.*, 1990). Subsequently, DeGrado's group were able to improve their design by making mutations of different hydrophobic residues to improve the steric complementarity of the helix-helix interface (Raleigh & DeGrado, 1992). The addition of several hydrophilic residues to the core of the redesigned helical bundle further increased the native-like properties (Raleigh *et al.*, 1995), apparently by introducing interactions between the hydrophilic side chains that are more specific than interactions between hydrophobic side chains, thereby limiting the protein to a more well-defined (less dynamic) folded state.

Synthetic coiled-coils have proved to be very good models for studying hydrophobic-core-packing effects. For example, we have employed a minimalist model with Leu residues at the hydrophobic **a** and **d** positions of the heptad repeat (Hodges *et al.*, 1981; Zhou *et al.*, 1992b) to demonstrate the inequivalence of positions **a** and **d**. Substitutions of Ala for Leu were found to be more destabilizing at position **a** than at position **d** if the chains were linked by a disulfide bridge (Zhou *et al.*, 1992a); without the interchain disulfide bridge, the Ala substitutions were equally destabilizing at positions **a** and **d**, suggesting a repacking of the hydrophobic core to compensate (see below) (Zhou *et al.*, 1992a). The effect of the β-branched amino acids Val and Ile on stability was also different at positions **a** and **d**, with position **a** being favoured energetically (Zhu *et al.*, 1993). This agreed with studies of the GCN4 leucine zipper, a naturally-occurring coiled-coil that controls dimerization of a yeast transcriptional factor, which showed that the highly conserved leucine residues at position **d** were less tolerant of substitution than were hydrophobic residues at position **a** (Hu *et al.*, 1990). The high resolution X-ray structure of the GCN4 leucine zipper confirmed that the packing environments of positions **a** and **d** are different (O'Shea *et al.*, 1991). As shown in Figure 4, there are two types of packing in a parallel two-stranded coiled-coil. The **a** positions exhibit 'parallel packing', so named because the C_α-C_β vector is roughly parallel to the C_α-C_α vector between position **a'** on the opposite chain (against which it packs) and the preceding residue **g'** (Fig. 4A). The **d** positions, on the other hand, show perpendicular packing (Fig. 4B). A β-branched side chain can pack efficiently at position **a** with the γ-methyl group pointing into the interface

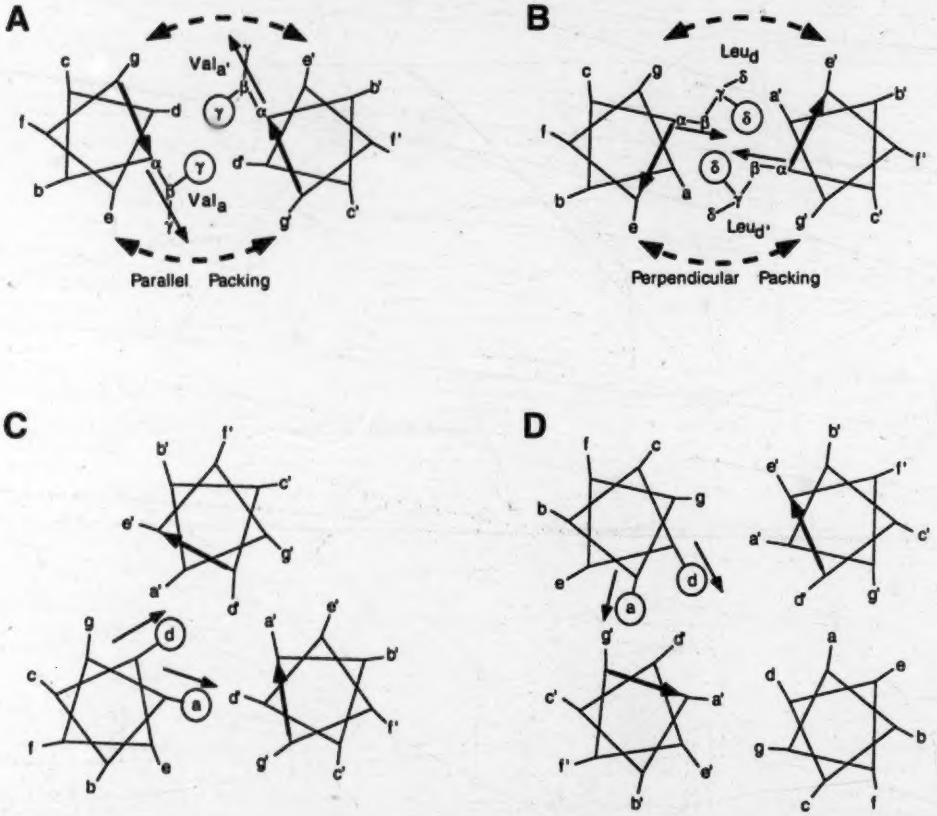

Figure 4 Comparison of the canonical hydrophobic-core-packing interactions in dimeric, trimeric and tetrameric parallel coiled-coils. In the dimer, residues at position **a** display parallel packing (**A**), in which the C_α-C_β vectors (light arrows) are parallel to the C_α-C_α vectors (heavy arrows) between position **a'** and the preceding residue **g'** on the other helix. Residues at position **d** adopt perpendicular packing (**B**), in which the C_α-C_β vectors (light arrows) are nearly perpendicular to the C_α-C_α vectors (heavy arrows) between position **d'** and the following residue **e'** on the other helix. The dashed arrows represent interhelical electrostatic i to i'+5 (**g**-**e'** or **g'**-**e**) interactions. In the tetramer (**D**) the C_α-C_β vector of position **a** (light arrow) packs roughly perpendicular to the C_α-C_α vector (heavy arrow) between position **a'** and the preceding residue **g'** on the adjacent helix; and the C_α-C_β vector of position **d** (light arrow) packs parallel to the C_α-C_α vector (heavy arrow) between position **d'** and the following residue **e'** on the adjacent helix. The packing geometry for positions **a** and **d** is thus reversed from that observed in the dimer. In the trimer (**C**) acute packing occurs, in which the C_α-C_β vectors (light arrows) of both positions **a** and **d** pack at an angle of less than 90° to the respective **g'**-**a'** or **d'**-**e'** C_α-C_α vector (heavy arrows) on the adjacent helix.

(Fig. 4A) while at position **d**, a strong geometric complementarity exists for the γ-branched Leu side chain, with one of the δ-methyl groups from each Leu residue filling the central cavity (Fig. 4B). By contrast, for a β-branched amino acid to be accommodated at position **d**, it would need to adopt a thermodynamically unfavourable rotamer for the χ_1 side-chain conformational angle or a steric clash between γ-methyl groups would result (Betz *et al.*, 1995; Moitra *et al.*, 1997). Various substitutions in the core positions of two-stranded coiled-coils have been studied (Hodges *et al.*, 1990; Moitra *et al.*, 1997), and the results agree with others obtained from mutations of T4 lysozyme (Eriksson *et al.*, 1992), which showed that the energetic effects of hydrophobic-core substitutions are felt not only in the alteration of the amount of buried nonpolar surface area, but also in the effects on van der Waals interactions that result from close packing arrangements. Thus, cavities caused by substituting Ala for large hydrophobes are destabilizing, particularly if the protein is unable to repack its core to compensate and to some degree avoid having a cavity present (Eriksson *et al.*, 1992). Likewise, the substitution of very large hydrophobes like Phe, which are too big to fit the available space, is also destabilizing (Hodges *et al.*, 1990). Eriksson *et al.* (1992) estimated that a Leu-to-Ala mutation in the core of T4 lysozyme led to a 2 kcal/mol destabilization if the resulting cavity size was extrapolated to zero and a 5 kcal/mol destabilization if no repacking took place. A recent coiled-coil study found that a Leu-to-Ala mutation at position **d** of the VBP leucine zipper, another naturally-occurring coiled-coil dimerization domain, led to a 4.6 kcal/mol destabilization and concluded that no repacking of the coiled-coil took place (Moitra *et al.*, 1997). However, other evidence suggests that coiled-coils may be able to repack their interfaces in response to mutations, but that a disulfide bridge between the chains can 'lock in' the structure and reduce the ability for repacking to occur (Hodges *et al.*, 1990; Zhou *et al.*, 1992a). Thus, the different effects on stability of an Ala substitution at positions **a** and **d** were observed only when the disulfide bridge was present. The nature of such 'repacking' in coiled-coils is as yet unclear.

Effects on oligomerization state

One of the most important aspects of the design of an α-helical assembly is controlling the number of helices in the assembly. Coiled-coils are known to be composed of two to four helices, and so the coiled-coil motif illustrates that a simple periodicity of hydrophobic residues (3-4 hydrophobic repeat, Fig. 2B) is compatible with different global structures that may lie close to one another in terms of energy. For example, the DeGrado group designed a minimalist coiled-coil protein, 'coil-Ser', which contained Leu at all **a** and **d** positions and displayed a mixture of dimer and trimer formation in solution (Betz *et al.*, 1995). By contrast, a unique oligomerization state is a requirement for a native-like *de novo* design. Recent studies of mutants of the GCN4 coiled-coil have shown that the packing preferences of the hydrophobic core **a** and **d** residues can favour one oligomerization state over others and are therefore a primary determinant of overall structure (Betz *et al.*, 1995; Harbury *et al.*, 1993, 1994). For example, a GCN4 mutant (p-LI) with Leu at the **a** positions and Ile at the **d** positions formed a tetramer, while switching the Leu and Ile residues (p-IL) led to dimer formation (Harbury *et al.*, 1993). Because β-branched residues are preferred at position **a** and Leu is preferred at position **d** in a parallel dimer (Figs 4A and 4B), the results of p-IL are as expected. However, in a parallel tetramer, residues at position **a** display perpendicular packing and residues at position **d** display parallel packing; the exact opposite of what occurs in the dimer (Fig. 4D) (Betz *et al.*, 1995). Thus, the oligomerization state of p-LI switches to maintain the preferred packing, in which β-branched residues are involved in parallel packing and Leu residues are involved in perpendicular packing. If p-LI formed a dimer, the Ile side chains would need to adopt an unfavourable conformation to avoid a steric clash. Trimer formation results in 'acute packing', in which the angles between the C_α-C_β vectors of both positions **a** and **d** and the corresponding C_α-C_α vectors against which they pack are under 90° (Fig. 4C). For the peptide p-II (in which Ile occurs at all **a** and **d** positions) the dimeric and tetrameric states would both be unfavourable because some Ile residues would need to engage in unfavourable perpendicular packing in either state. Thus, it was found that p-II formed a trimer (Harbury *et al.*, 1993, 1994), in which the Ile side chain was found to adopt the most preferred conformation at positions **a** and **d** (Harbury *et al.*, 1994). Trimers appear to be a more permissive state and may, in some cases, represent a default structure when dimer and tetramer formation is disfavoured. The coil-Ser structure displayed packing geometries of the Leu side chains ranging from parallel to perpendicular packing, but was mostly acute. Therefore, the canonical packing interactions observed in the GCN4 mutants are an ideal case but nonetheless offer important insights into how side-chain shape and packing affect global structure.

Hydrophobic-core mutations that control structure

Like four-helix bundles, synthetic coiled-coils have been used to study the effects of certain hydrophobic-core substitutions on structure. For example, the GCN4 coiled-coil dimer has an Asn residue at an **a** position (Asn 16) in the middle of the coiled-coil, which, when mutated to Val, led to formation of a trimer with higher stability than the wild-type dimer (Potekhin *et al.*, 1994). Engineering a uniform hydrophobic core in GCN4 with Val at all **a** positions led to a mixture of the dimeric and trimeric forms (Harbury *et al.*, 1993). Subsequently, two designed peptides containing Leu at all **a** and **d** positions were found to form a heterotetramer, while substitution of a single Asn at an **a** position in each peptide resulted in heterodimer formation instead (Lumb & Kim, 1995). These results suggest that the Asn substitution specifies dimer formation, probably through a specific interhelical hydrogen bond between Asn side chains. Such an interaction has, in fact, been observed in the X-ray structure of GCN4 (O'Shea *et al.*, 1991). Alber's group recently showed that the interaction between the Asn16 residues is critical for promoting dimer formation in GCN4 since a mutant with Gln at position 16 forms a mixture of dimer and trimer (Gonzalez *et al.*, 1996b). Crystal structures of the dimeric and trimeric forms of the Gln16 mutant showed that no hydrogen bonds occur between Gln side chains in either structure. Instead, the Gln residues formed hydrogen bonds to buried water molecules and were in different, but apparently energetically similar, environments in the two states. In the same study, a Lys substitution for Asn favoured dimer formation but, in this case, it was probably because the charged ε-amino group of the Lys side chain is more exposed in the dimer than in the trimer. Therefore, simply introducing a break in the hydrophobic repeat is not enough to specify a unique structure unless the substituted hydrophilic residues contribute energetically different interactions to the alternative states.

The presence of a cavity resulting from Ala substitutions in the core can also affect the oligomerization state. Disulfide-bridged coiled-coils were used to show that if four Ala residues are at the same packing plane of a potential four-stranded coiled-coil, the cavity created would be so destabilizing as to favour the two-stranded form (Monera *et al.*, 1996a). If the four Ala residues are spread over two adjacent packing planes, the cavity is spread out and can be accommodated by the four-stranded state. Similarly, substitution of Ala for Asn16 in GCN4 resulted in retention of the dimer state because a larger cavity would be present in the trimer (Gonzalez *et al.*, 1996a). Addition of benzene or cyclohexane caused the peptide to form a trimer, because the cavity caused by the Ala16 residues in the trimeric form was just the right size to bind these hydrophobic molecules (Gonzalez *et al.*, 1996a).

Antiparallel chain orientation

Another important issue in coiled-coil and helical-bundle folding and design is parallel versus antiparallel chain orientation. In most four-helix bundles, the helices are antiparallel to the nearest neighbour helices (Kohn *et al.*, 1997b), partly because it allows for favourable interactions of the helix macrodipole moments (Robinson & Sligar, 1993). Another factor that may affect chain orientation is the difference in hydrophobic-packing interactions between the two orientations. In the parallel orientation, position **a** packs against the symmetry-related position **a'** and position **d** packs against the symmetry-related position **d'**, resulting in two different types of layers that alternate in the hydrophobic interface (Figs 4A and 4B). In an antiparallel coiled-coil, position **a** packs against position

d' and position **d** packs against position **a'**, resulting in all identical packing layers. It has been shown that antiparallel packing is intrinsically more stable in a model two-stranded coiled-coil containing homogenous Leu-Leu packing interactions (Monera *et al.*, 1994). Thus, the fact that most two-stranded coiled-coils in nature are parallel is probably due mostly to interhelical hydrogen-bonding and electrostatic interactions, such as the Asn16-Asn16' hydrogen bond in GCN4, that favour the parallel orientation. Such interactions can be used as a negative design principle to promote parallel coiled-coil assembly. By contrast, negative design principles can be incorporated in the hydrophobic core to favour antiparallel assembly. For example, it has been shown recently that the placement of Ala residues in the core could be used to switch between parallel and antiparallel chain orientation in four-stranded coiled-coils because the Ala residues avoid the formation of large cavities (Fig. 5A) by segregating themselves amongst different layers of the core (Fig. 5B) (Monera *et al.*, 1996b). The principle also appears to be critical in the structure of the four-stranded antiparallel coiled-coil protein Rop, which alternates large and small hydrophobes in its core (Betz *et al.*, 1997).

While design principles can be used to specify a parallel or antiparallel chain orientation, it is often still necessary to distinguish which of the two a particular coiled-coil design adopts. The chain orientation in dimeric coiled-coils can be verified by the attachment of the self-quenching fluorescent moiety fluorescein to either the N- or the C-terminus. A parallel orientation causes two fluorescein groups to come into close proximity and quench each other's fluorescence, while no quenching occurs in an antiparallel chain orientation (Wendt *et al.*, 1994). The chain orientation can be fixed by an interchain disulfide bridge (Monera *et al.*, 1994), and antiparallel coiled-coils can be designed in the form of a helical hairpin with a covalent linkage between the helices (Myszka & Chaiken, 1994).

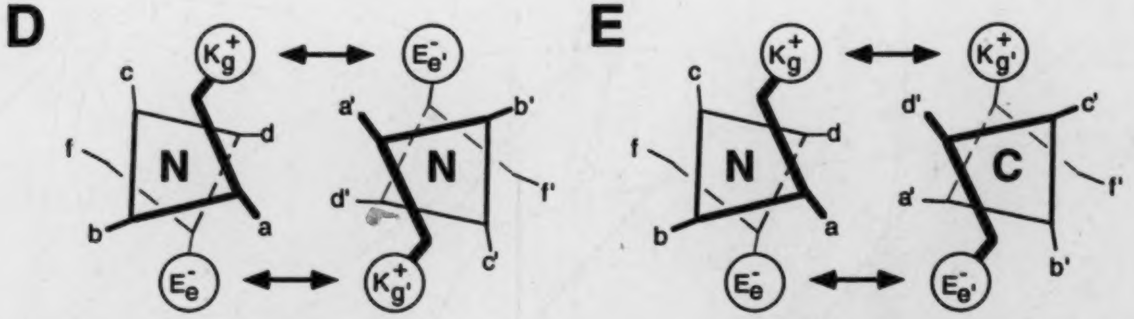

Parallel - attractions

Antiparallel - repulsions

Figure 5 Examples of negative design principles that can specify one structure over an alternate structure. Alternation of large (Leu) and small (Ala) side chains within the hydrophobic core strongly favours antiparallel chain orientation, because packing of the helices in the parallel orientation (A) causes the small Ala side chains (here at position **d**) to occupy individual layers in the hydrophobic core and form large destabilizing cavities. With antiparallel packing (B), each layer of the core contains two Ala and two Leu residues (at positions **d** and **a**, respectively), which can pack efficiently (Monera *et al.*, 1996a, 1996b; Betz *et al.*, 1997) . (C) Heterodimerization is highly favoured by interhelical **g-e'** (and **g'-e**) ionic repulsions that destabilize the respective homodimers and interhelical **g-e'** (and **g'-e**) ionic attractions that may stabilize the heterodimer (right) (O'Shea *et al.*, 1993). The parallel chain orientation (D) of a homodimer is highly favoured by the formation of **g-e'** (and **g'-e**) ionic attractions, while the antiparallel orientation (E) is highly destabilized by interhelical **e-e'** and **g-g'** ionic repulsions. In (A), (B), (D) and (E), helices labelled 'N' are being viewed from the N terminus and those labelled 'C' are being viewed from the C terminus.

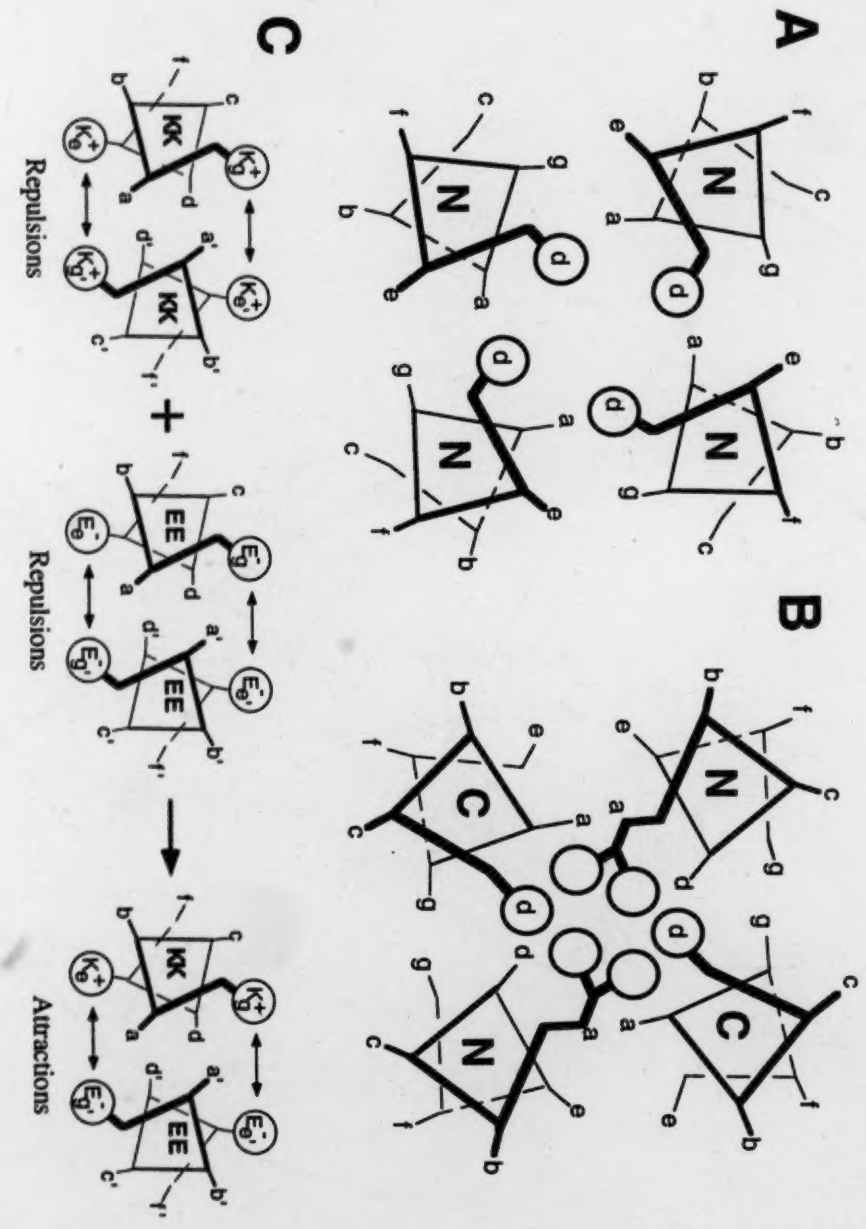
A
B
C
N
C
d
a
b
c
e
f
g
KK
EE
K_g^+
K_e^+
E_g^-
E_e^-
+
Repulsions
Repulsions
Attractions

Ionic interactions and metal binding

One of the most controversial aspects of protein-design research has been deciphering the role of electrostatic interactions in protein folding and stability (Hendsch & Tidor, 1994). X-ray structures, such as that of the GCN4 coiled-coil (O'Shea *et al.*, 1991), show the formation of interhelical **g-e'** ion pairs between oppositely charged residues in position **g** of one helix and position **e'** of the other helix five residues downchain (also denoted i to i'+5). These ion-pairing interactions appear to assist the folding of the **e** and **g** side chains across the hydrophobic core formed by the **a** and **d** residues (Fig. 4A) and may increase stability through a synergy between ionic attraction and increased burial of hydrophobicity (Kohn *et al.*, 1997a). Mutational analyses have shown that the proposed **g-e'** ion pairs account for about 0.5 to 1 kcal/mol of stabilization (Krylov *et al.*, 1994; Zhou *et al.*, 1994), which is similar to the stabilization observed for ion pairs on the surface of globular proteins (Hendsch & Tidor, 1994). Similarly, **g-e'** repulsions between like-charged residues destabilize coiled-coils by about 0.5 kcal/mol (Kohn *et al.*, 1995; Krylov *et al.*, 1994). The formation of ionic attractions versus repulsions is an effective design principle for controlling hetero- versus homodimerization (Fig. 5C) (O'Shea *et al.*, 1993), where the number of repulsions are maximized in the homodimer and the number of attractions are maximized in the heterodimer. This principle is believed to be crucial in the dimerization specificity of naturally-occurring coiled-coils (Baxevanis & Vinson, 1993) and has also been extended to the *de novo* design of heterotrimeric (Nautiyal *et al.*, 1995) and heterotetrameric (Fairman *et al.*, 1996) coiled-coils (although, interestingly, the heterotetramer was specified through ionic interactions involving the **b** and **c** positions rather than the **e** and **g** positions (Fairman *et al.*, 1996)). Similarly, ionic and hydrogen-bond interactions are effective in specifying parallel versus antiparallel chain orientation (Betz & DeGrado, 1996; Monera *et al.*, 1994) (Figs 5D and 5E). An ionic interaction was recently designed into the core of the GCN4 coiled-coil by replacing the Asn16-Asn16' hydrogen bond with an ion pair between Asp and Dab (2,4-diaminobutyric acid) in a heterodimer (Schneider *et al.*, 1997); a 22-fold preference for heterodimer formation was observed. Ionic interactions between charged residues at core positions also play a role in heterodimerization of some native coiled-coils (Lavigne *et al.*, 1995).

Electrostatic interactions are also being studied for their effects on reversibly regulating folding, stability and dynamics. A coiled-coil was recently designed that, when phosphorylated on a Ser residue at position **e**, was stabilized by 1.4 kcal/mol, owing to inter- and intrahelical ionic interactions between the phospho-Ser group and three Arg residues (Szilak *et al.*, 1997). Metal-binding sites engineered into designed proteins have been used to control folding and stability. In one case, a tetrahedral Zn(II)-binding site was introduced into a four-helix bundle (Regan & Clarke, 1990), resulting in a significant dependence of the protein's stability on metal binding. A later design also illustrated the ability of engineered metal-binding sites to increase the native-like character by replacing relatively nonspecific hydrophobic interactions with highly specific metal-ligand interactions (Handel *et al.*, 1993). A dramatic example of metal-induced folding of a coiled-coil has been recently demonstrated, in which the apo-peptide is a random coil prevented from folding by **g-e'** repulsions between γ-carboxyglutamic acid side chains that chelate a metal ion in the folded form (Kohn *et al.*, 1998). Metal-ion chelation has also been used to tether peptides into helical bundles (Ghadiri *et al.*, 1992a, 1992b) by attaching a metal-binding group at one of their ends. Another approach to tethering helices into bundles is covalent attachment to a topological template (Tuchscherer & Mutter, 1995). Such template-assembled synthetic proteins (TASP) are useful in aiding the design process towards a desired result, but they can not be bacterially expressed, and so are less desirable as a final product.

Applications and functional proteins

As was stated above, the ultimate goal of *de novo* protein design is to obtain proteins with useful functions and applications. However, to date, researchers have primarily been struggling to design for structure, without even considering function.

Nevertheless, our growing knowledge of the principles of protein structure is allowing a shift towards function as a focus of design. A number of potential applications originating from research on coiled-coils have been identified and are being pursued, as previously outlined (Hodges, 1996). Several of these applications involve the heterodimerization concept, including: detection and purification of recombinantly expressed proteins by affinity chromatography; a dimerization domain for use with biosensors; two-stage drug targeting and delivery; and peptide vaccine carriers. The use of a coiled-coil as a conformationally defined template for combinatorial-library display is a particularly promising area (Houston *et al.*, 1996). Coiled-coils have also been applied to the generation of miniantibodies by fusion to the F_V fragment (Pack *et al.*, 1995), or for solution assembly of receptor complexes by fusion with the extracellular portions of the receptor subunits (Wu *et al.*, 1995). The identification of coiled-coils in disease processes, such as fusion of the HIV membrane with host cells and overactivity of certain transcription factors in cancerous cells, has led to the possibility of blocking these coiled-coil interactions with peptide or peptidomimetic inhibitors (Chan *et al.*, 1997; Olive *et al.*, 1997).

Several attempts at functional design have involved helical bundles. Dutton and co-workers designed a four-helix bundle that bound four haem groups, and redox titrations showed that the haems were coupled to allow long-range electron transfer (Robertson *et al.*, 1994); such proteins may act as models for the redox proteins that catalyse electron tranfer in biological systems. Several groups have dealt with membrane-interacting α-helical proteins, such as transmembrane ion channels and conductors. For example, minimalized amphipathic α-helices were used to demonstrate the role of the α-helical macrodipole in the asymmetry of ion conduction through an ion channel (Kienker *et al.*, 1994). Studies with predicted transmembrane segments of a voltage-gated calcium channel led to functional calcium channels, which have helped to elucidate the functional determinants of the intact protein (Grove *et al.*, 1993). Toward the design of multispanning membrane-bound receptors, a four-helix bundle with three connecting loops has been designed and inserted into a membrane with the desired overall topology (Whitley *et al.*, 1994). A very interesting recent design was of a 69 amino acid four-helix bundle in which one hydrophobic helix was surrounded by three amphipathic helices, forming a soluble native-like structure in solution with the ability to insert into membranes (Lee *et al.*, 1997). The insertion mechanism was proposed to resemble that of some bacterial toxins, in which the protein unfolds like an umbrella to expose the central hydrophobic helix, which can then insert into the membrane. In a different twist on this theme, a 24 amino acid amphipathic helix has been designed that acts as a 'detergent' for keeping integral membrane proteins soluble by interaction of its hydrophobic face with the hydrophobic membrane-spanning portions of the protein (Schafmeister *et al.*, 1993).

One area where little progress has been made is the design of artificial enzymes. This is not surprising, considering that enzymes tend to have complex tertiary structures and active sites. Two α-helical peptides have been designed that have modest catalytic activities: a self-associating Leu-Lys-rich peptide has been shown to catalyse oxaloacetate decarboxylation (Johnsson *et al.*, 1993), and a four-helix bundle displayed weak hydrolytic activity against 4-nitrophenyl esters (Hahn *et al.*, 1990). More recent efforts by Baltzer and co-workers have yielded the largest reaction rate enhancements yet observed for 4-nitrophenyl ester hydrolysis or transesterification by a *de novo* designed α-helical bundle catalyst (Broo *et al.*, 1997). It was suggested that these catalysts may have only low activity partly because they behave as molten globules and thus may be in an active conformation only part of the time (Bryson *et al.*, 1995). The incorporation through some selection technique of mutations that stabilize the catalytically active form may be useful for generating more-effective catalysts.

Future Prospects

The past ten years have seen the growth of *de novo* protein design from its roots in the minimalist approach to a number of examples of native-like structures. With many of the design principles having been determined in simple model systems, *de novo* design has turned more towards functional studies. It is also clear that there is still much to be learned from basic research into short- and long-range protein-folding interactions. A major issue that still needs clarification is the extent to which additivity principles apply to the stabilization of protein structure (Dill, 1997). In other words, can the overall stability of a protein be predicted from adding up the effects of all the noncovalent interactions present, or is there cooperativity between the various interactions that precludes an easy interpretation?

We predict that the near future should see a further emphasis on the design of proteins for particular functions and applications, which will undoubtedly involve the design of more elaborate structures in some cases and the continued development of computer-assisted-design protocols. The use of combinatorial methods as a way of generating diversity within the framework of a particular structural motif will probably also play a role in the development of useful proteins, particularly in cases where a library can be screened for a desired binding or functional activity.

References

Anfinsen, C. B. (1973) Principles that govern the folding of protein chains. *Science* **181,** 223-230.

Barlow, D. J. & Thornton, J. M. (1988) Helix geometry in proteins *J. Mol. Biol.* **201,** 601-619.

Baxevanis, A. D. & Vinson, C. R. (1993) Interaction of coiled-coils in transcription factors: where is the specificity? *Curr. Opin. Genet. Dev.* **3,** 278-285.

Betz, S. F., Bryson, J. W., and DeGrado, W. F. (1995) Native-like and structurally characterized designed α-helical bundles. *Curr. Opin. Struct. Biol.* **5,** 457-463.

Betz, S. F. & DeGrado, W. F. (1996) Controlling topology and native-like behavior of *de novo* designed peptides: design and characterization of antiparallel four-stranded coiled-coils. *Biochemistry* **35,** 6955-6962.

Betz, S. F., Liebman, P. A., and DeGrado, W. F. (1997) *De novo* design of native proteins: characterization of proteins intended to fold into antiparallel, Rop-like, four-helix bundles. *Biochemistry* **36,** 2450-2458.

Bowie, J. U., Lüthy, R., and Eisenberg, D. (1991) A method to identify protein sequences that fold into a known three-dimensional structure. *Science* **253,** 164-170.

Broo, K. S., Brive, L., Ahlberg, P., and Baltzer, L. (1997) Catalysis of hydrolysis and transesterification reactions of p-nitrophenyl esters by a designed helix-loop-helix dimer. *J. Am. Chem. Soc.* **119,** 11362-11372.

Bryson, J. W., Betz, S. F., Lu, H. S., Suich, D. J., Zhou, H. X., O'Neil, K. T., and DeGrado, W. F. (1995) Protein design: a hierarchic approach. *Science* **270,** 935-941.

Chan, D. C., Fass, D., Berger, J. M., and Kim, P. S. (1997) Core structure of gp41 from the HIV envelope glycoprotein. *Cell* **89,** 263-273.

Cohen, C. & Parry, D. A. D. (1990) α-Helical coiled-coils and bundles: how to design an α-helical protein. *Proteins: Struct. Funct. Genet.* **7,** 1-15.

Dahiyat, B. I., Sarisky, C. A., and Mayo, S. L. (1997) *De novo* protein design: towards fully automated sequence selection. *J. Mol. Biol.* **273,** 789-796.

Dalal, S., Balasubramanian, S., and Regan, L. (1997) Protein alchemy: changing β-sheet into α-helix. *Nature Struct. Biol.* **4,** 548-552.

Davidson, A. R., Lumb, K. J., and Sauer, R. T. (1995) Cooperatively folded proteins in random sequence libraries. *Nature Struct. Biol.* **2,** 856-864.

DeGrado, W. F., Wasserman, Z. R., and Lear, J. D. (1989) Protein design, a minimalist approach. *Science* **243,** 622-628.

Desjarlais, J. R. & Handel, T. M. (1995) *De novo* design of the hydrophobic cores of proteins. *Protein Sci.* **4,** 2006-2018.

Dill, K. (1990) Dominant forces in protein folding. *Biochemistry* **29,** 7133-7135.

Dill, K. A. (1997) Additivity principles in biochemistry. *J. Biol. Chem.* **272,** 701-704.

Erickson, B. W. & Merrifield, R. B. (1976) Solid-phase peptide synthesis. In *The Proteins, vol. 2* (Neurath, H. and Hill, R. L., eds), pp. 255-527, Academic Press, New York.

Eriksson, A. E., Baase, W. A., Zhang, X.-J., Heinz, D. W., Blaber, M., Baldwin, E. P., and Matthews, B. W. (1992) Response of a protein structure to cavity-creating mutations and its relation to the hydrophobic effect. *Science* **255,** 178-183.

Fairman, R., Chao, H.-G., Lavoie, T. B., Villafranca, J. J., Matsueda, G. R., and Novotny, J. (1996) Design of heterotetrameric coiled-coils: evidence for increased stabilization by Glu-Lys ion pair interactions. *Biochemistry* **35,** 2824-2829.

Fields, G. B. & Noble, R. L. (1990) Solid phase peptide synthesis utilizing 9-fluorenylmethoxycarbonyl amino acids. *Int. J. Peptide Protein Res.* **35,** 161-214.

Ghadiri, M. R., Soares, C., and Choi, C. (1992a) A convergent approach to protein design. Metal ion-assisted spontaneous self-assembly of a polypeptide into a triple-helix bundle protein. *J. Am. Chem. Soc.* **114,** 825-831.

Ghadiri, M. R., Soares, C., and Choi, C. (1992b) Design of an artificial four-helix bundle metalloprotein via a novel ruthenium(II)-assisted self-assembly process. *J. Am. Chem. Soc.* **114,** 4000-4002.

Gilbert, W. & Villa-Komaroff, L. (1980) Useful proteins from recombinant bacteria. *Sci. Am.* **242,** 74-94.

Gonzalez, L., Jr , Plecs, J. J., and Alber, T. (1996a) An engineered allosteric switch in leucine-zipper oligomerization. *Nature Struct. Biol.* **3,** 510-515.

Gonzalez, L., Jr, Woolfson, D. N., and Alber, T. (1996b) Buried polar residues and structural specificity in the GCN4 leucine zipper. *Nature Struct. Biol.* **3,** 1011-1018.

Grove, A., Tomich, J. M., Iwamoto, T., and Montal, M. (1993) Design of a functional calcium channel protein: inferences about an ion channel-forming motif derived from the primary structure of voltage-gated calcium channels. *Protein Sci.* **2,** 1918-1930.

Hahn, K. W., Klis, W. A., and Stewart, J. M. (1990) Design and synthesis of a peptide having chymotrypsin-like esterase activity. *Science* **248,** 1544-1547.

Handel, T. M., Williams, S. A., and DeGrado, W. F. (1993) Metal ion-dependent modulation of the dynamics of a designed protein. *Science* **261,** 879-885.

Harbury, P. B., Kim, P. S., and Alber, T. (1994) Crystal structure of an isoleucine-zipper trimer. *Nature* **371,** 80-83.

Harbury, P. B., Tidor, B., and Kim, P. S. (1995) Repacking protein cores with backbone freedom: structure prediction for coiled-coils. *Proc. Natl. Acad. Sci. U.S.A.* **92,** 8408-8412.

Harbury, P. B., Zhang, T., Kim, P. S., and Alber, T. (1993) A switch between two-, three-, and four-stranded coiled-coils in GCN4 leucine zipper mutants. *Science* **262,** 1401-1407.

Hecht, M. H., Richardson, J. S., Richardson, D. C., and Ogden, R. C. (1990) *De novo* design, expression, and characterization of Felix: a four-helix bundle protein of native-like sequence. *Science* **249,** 884-891.

Hendsch, Z. S. & Tidor, B. (1994) Do salt bridges stabilize proteins? A continuum electrostatic analysis. *Protein Sci.* **3,** 211-226.

Hodges, R. S. (1996) *De novo* design of α-helical proteins: basic research to medical applications. *Biochem. Cell Biol.* **74,** 133-154.

Hodges, R. S., Saund, A. K., Chong, P. C. S., St.-Pierre, S. A., and Reid, R. E. (1981) Synthetic model for two-stranded α-helical coiled-coils. Design, synthesis, and characterization of an 86-residue analog of tropomyosin. *J. Biol. Chem.* **256,** 1214-1224.

Hodges, R. S., Zhou, N. E., Kay, C. M., and Semchuk, P. D. (1990) Synthetic model proteins: contribution of hydrophobic residues and disulfide bonds to protein stability. *Peptide Res.* **3,** 123-137.

Houston, M. E., Jr, Wallace, A., Bianchi, E., Pessi, A., and Hodges, R. S. (1996) Use of a conformationally restricted secondary structural element to display peptide libraries: a two-stranded α-helical coiled-coil stabilized by lactam bridges. *J. Mol. Biol.* **262,** 270-282.

Hu, J. C., O'Shea, E. K., Kim, P. S., and Sauer, R. T. (1990) Sequence requirements for coiled-coils: analysis with λ-repressor-GCN4 leucine zipper fusions. *Science* **250,** 1400-1403.

Johnsson, K., Allemann, R. K., Widmer, H., and Benner, S. A. (1993) Synthesis, structure and activity of artificial, rationally designed catalytic polypeptides. *Nature* **365,** 530-532.

Kaiser, E. T. & Kezdy, F. J. (1983) Secondary structures of proteins and peptides in amphiphilic environments (A Review). *Proc. Natl. Acad. Sci. U.S.A.* **80,** 1137-1143.

Kamtekar, S. & Hecht, M. H. (1995) The four-helix bundle: what determines a fold? *FASEB J.* **9,** 1013-1022.

Kamtekar, S., Schiffer, J. M., Xiong, H., Babik, J. M., and Hecht, M. H. (1993) Protein design by binary patterning of polar and nonpolar amino acids. *Science* **262,** 1680-1685.

Kienker, P. K., DeGrado, W. F., and Lear, J. D. (1994) A helical-dipole model describes the single-channel current rectification of an uncharged peptide ion channel. *Proc. Natl. Acad. Sci. U.S.A.* **91,** 4859-4863.

Kohn, W. D., Kay, C. M., and Hodges, R. S. (1995) Protein destabilization by electrostatic repulsions in the two-stranded α-helical coiled-coil. *Protein Sci.* **4,** 237-250.

Kohn, W. D., Kay, C. M., and Hodges, R. S. (1997a) Salt effects on protein stability: two-stranded α-helical coiled-coils containing inter- or intrahelical ion-pairs. *J. Mol. Biol.* **267,** 1039-1052.

Kohn, W. D., Kay, C. M., Sykes, B. D., and Hodges, R. S. (1998) Metal ion-induced folding of a *de novo* designed coiled-coil peptide. *J. Am. Chem. Soc.* **120,** 1124-1132.

Kohn, W. D., Mant, C. T., and Hodges, R. S. (1997b) α-Helical protein assembly motifs. *J. Biol. Chem.* **272,** 2583-2586.

Krylov, D., Mikhailenko, I., and Vinson, C. (1994) A thermodynamic scale for leucine zipper stability and dimerization specificity: e and g interhelical interactions. *EMBO J.* **13,** 2849-2861.

Lavigne, P., Kondejewski, L. H., Houston, M. E., Jr, Sönnichsen, F. D., Lix, B., Sykes, B. D., Hodges, R. S., and Kay, C. M. (1995) Preferential heterodimeric parallel coiled-coil formation by synthetic Max and c-Myc leucine zippers: a description of putative electrostatic interactions responsible for the specificity of heterodimerization. *J. Mol. Biol.* **254,** 505-520.

Lee, S., Kiyota, T., Kunitake, T., Matsumoto, E., Yamashita, S., Anzai, K., and Sugihara, G. (1997) *De novo* design, synthesis, and characterization of a pore-forming small globular protein and its insertion into lipid bilayers. *Biochemistry* **36,** 3782-3791.

Lumb, K. J., Carr, C. M., and Kim, P. S. (1994) Subdomain folding of the coiled-coil leucine zipper from the bZIP transcriptional activator GCN4. *Biochemistry* **33,** 7361-7367.

Lumb, K. J. & Kim, P. S. (1995) A buried polar interaction imparts structural uniqueness in a designed heterodimeric coiled-coil. *Biochemistry* **34,** 8642-8648.

Mant, C. T., Zhou, N. E., and Hodges, R. S. (1993) The role of amphipathic helices in stabilizing peptide and protein structure. In *The Amphipathic Helix* (Epand, R. M., ed.), pp. 39-64, CRC Press, Inc., Boca Raton, Florida.

Moitra, J., Szilak, L., Krylov, D., and Vinson, C. (1997) Leucine is the most stabilizing aliphatic amino acid in the **d** position of a dimeric leucine zipper coiled-coil. *Biochemistry* **36,** 12567-12573.

Monera, O. D., Kay, C. M., and Hodges, R. S. (1994) Electrostatic interactions control the parallel and antiparallel orientation of α-helical chains in two-stranded α-helical coiled-coils. *Biochemistry* **33,** 3862-3871.

Monera, O. D., Sereda, T. J., Zhou, N. E., Kay, C. M., and Hodges, R. S. (1995) Relationship of sidechain hydrophobicity and α-helical propensity on the stability of the single-stranded amphipathic α-helix. *J. Pept. Sci.* **1,** 319-329.

Monera, O. D., Sönnichsen, F. D., Hicks, L., Kay, C. M., and Hodges, R. S. (1996a) The relative positions of alanine residues in the hydrophobic core control the formation of two-stranded or four-stranded α-helical coiled-coils. *Protein Eng.* **9,** 353-363.

Monera, O. D., Zhou, N. E., Lavigne, P., Kay, C. M., and Hodges, R. S. (1996b) Formation of parallel and antiparallel coiled-coils controlled by the relative positions of alanine residues in the hydrophobic core. *J. Biol. Chem.* **271,** 3995-4001.

Munoz, V. & Serrano, L. (1994) Intrinsic secondary structure propensities of the amino acids, using statistical Φ-Ψ matrices: comparison with experimental scales. *Proteins: Struct. Funct. Genet.* **20,** 301-311.

Munson, M., Balasubramanian, S., Fleming, K. G., Nagi, A. D., O'Brien, R., Sturtevant, J. M., and Regan, L. (1996) What makes a protein a protein? Hydrophobic core designs that specify stability and structural properties. *Protein Sci.* **5,** 1584-1593.

Munson, M., O'Brien, R., Sturtevant, J. M., and Regan, L. (1994) Redesigning the hydrophobic core of a four-helix-bundle protein. *Protein Sci.* **3,** 2015-2022.

Myszka, D. G. & Chaiken, I. M. (1994) Design and characterization of an intramolecular antiparallel coiled-coil peptide. *Biochemistry* **33,** 2363-2372.

Nautiyal, S., Woolfson, D. N., King, D. S., and Alber, T. (1995) A designed heterotrimeric coiled-coil. *Biochemistry* **34,** 11645-11651.

O'Neil, K. T. & DeGrado, W. F. (1990) A thermodynamic scale for the helix-forming tendencies of the commonly occurring amino acids. *Science* **250,** 646-651.

O'Shea, E. K., Klemm, J. D., Kim, P. S., and Alber, T. (1991) X-ray structure of the GCN4 leucine zipper, a two-stranded, parallel coiled-coil. *Science* **254,** 539-544.

O'Shea, E. K., Lumb, K. J., and Kim, P. S. (1993) Peptide "velcro": design of a heterodimeric coiled-coil. *Curr. Biol.* **3,** 658-667.

Olive, M., Krylov, D., Echlin, D. R., Gardner, K., Taparowsky, E., and Vinson, C. (1997) A dominant negative to activation protein-1 (AP1) that abolishes DNA binding and inhibits oncogenesis. *J. Biol. Chem.* **272,** 18586-18594.

Pack, P., Müller, K., Zahn, R., and Plückthun, A. (1995) Tetravalent miniantibodies with high avidity assembling in Escherichia coli. *J. Mol. Biol.* **246,** 28-34.

Potekhin, S. A., Medvedkin, V. N., Kashparov, I. A., and Venyaminov, S. Y. (1994) Synthesis and properties of the peptide corresponding to the mutant form of the leucine zipper of the transcriptional activator GCN4 from yeast. *Protein Eng.* **7,** 1097-1101.

Raleigh, D. P., Betz, S. F., and DeGrado, W. F. (1995) A *de novo* designed protein mimics the native state of natural proteins. *J. Am. Chem. Soc.* **117,** 7558-7559.

Raleigh, D. P. & DeGrado, W. F. (1992) A *de novo* designed protein shows a thermally induced transition from a native to a molten globule-like state. *J. Am. Chem. Soc.* **114,** 10079-10081.

Regan, L. & Clarke, N. D. (1990) A tetrahedral zinc(II)-binding site introduced into a designed protein. *Biochemistry* **29,** 10878-10883.

Regan, L. & DeGrado, W. F. (1988) Characterization of a helical protein designed from first principles. *Science* **241,** 976-978.

Robertson, D. E., Farid, R. S., Moser, C. C., Urbauer, J. L., Mulholland, S. E., Pidikiti, R., Lear, J. D., Wand, A. J., DeGrado, W. F., and Dutton, P. L. (1994) Design and synthesis of multi-haem proteins. *Nature* **368,** 425-432.

Robinson, C. R. & Sligar, S. G. (1993) Electrostatic stabilization in four-helix bundle proteins. *Protein Sci.* **2,** 826-837.

Roy, S., Helmer, K. J., and Hecht, M. H. (1997) Detecting native-like properties in combinatorial libraries of *de novo* proteins. *Folding & Design* **2,** 89-92.

Schafmeister, C. E., Miercke, L. J. W., and Stroud, R. M. (1993) Structure at 2.5 Å of a designed peptide that maintains solubility of membrane proteins. *Science* **262,** 734-738.

Schneider, J. P., Lear, J. D., and DeGrado, W. F. (1997) A designed buried salt bridge in a heterodimeric coiled-coil. *J. Am. Chem. Soc.* **119,** 5742-5743.

Szilak, L., Moitra, J., and Vinson, C. (1997) Design of a leucine zipper coiled-coil stabilized 1.4 kcal/mol by phosphorylation of a serine in the **e** position. *Protein Sci.* **6,** 1273-1283.

Talbot, J. A. & Hodges, R. S. (1982) Tropomyosin: A model protein for studying coiled-coil and α-helix stabilization. *Acc. Chem. Res.* **15,** 224-230.

Tuchscherer, G. & Mutter, M. (1995) Protein design as a challenge for peptide chemists. *J. Pept. Sci.* **1,** 3-10.

Voyer, N. & Lamothe, J. (1995) The use of peptidic frameworks for the construction of molecular receptors and devices. *Tetrahedron* **51,** 9241-9284.

Wendt, H., Baici, A., and Bosshard, R. (1994) Mechanism of assembly of a leucine zipper domain. *J. Am. Chem. Soc.* **116,** 6973-6974.

Whitley, P., Nilsson, I., and von Heijne, G. (1994) *De novo* design of integral membrane proteins. *Nature Struct. Biol.* **1,** 858-862.

Wu, Z., Johnson, K. W., Goldstein, B., Choi, Y., Eaton, S. F., Laue, T. M., and Ciardelli, T. L. (1995) Solution assembly of a soluble, heteromeric, high affinity interleukin-2 receptor complex. *J. Biol. Chem.* **270,** 16039-16044.

Xiong, H., Buckwalter, B. L., Shieh, H.-M., and Hecht, M. H. (1995) Periodicity of polar and nonpolar amino acids is the major determinant of secondary structure in self-assembling oligomeric peptides. *Proc. Natl. Acad. Sci. U.S.A.* **92,** 6349-6353.

Zhou, N. E., Kay, C. M., and Hodges, R. S. (1992a) Synthetic model proteins: The relative contribution of leucine residues at the non-equivalent positions of the 3-4 hydrophobic repeat to the stability of the two-stranded α-helical coiled-coil. *Biochemistry* **31,** 5739-5746.

Zhou, N. E., Kay, C. M., and Hodges, R. S. (1994) The net energetic contribution of interhelical electrostatic attractions to coiled-coil stability. *Protein Eng.* **7,** 1365-1372.

Zhou, N. E., Zhu, B.-Y., Kay, C. M., and Hodges, R. S. (1992b) The two-stranded α-helical coiled-coil is an ideal model for studying protein stability and subunit interactions. *Biopolymers* **32,** 419-426.

Zhou, N. E., Zhu, B.-Y., Sykes, B. D., and Hodges, R. S. (1992c) Relationship between amide proton chemical shifts and hydrogen bonding in amphipathic α-helical peptides. *J. Am. Chem. Soc.* **114,** 4320-4326.

Zhu, B. Y., Zhou, N. E., Kay, C. M., and Hodges, R. S. (1993) Packing and hydrophobicity effects on protein folding and stability: Effects of β-branched amino acids, valine and isoleucine, on the formation and stability of two-stranded α-helical coiled-coils / leucine zippers. *Protein Sci.* **2,** 383-394.